UNIVERSITY OF CALIFORNIA

Santa Barbara

Development of Renewable and Recyclable Epoxy Thermosets Based on Lignin Derived Phenols

A dissertation submitted in partial satisfaction of the

requirements for the degree Doctor of Philosophy

in Chemistry

by

Shou Zhao

Committee in charge:

Professor Mahdi M. Abu−Omar, Chair

Professor Susannah L. Scott

Professor Christopher M. Bates

Professor Steven K. Buratto

September 2018

The dissertation of Shou Zhao is approved.

_____

Susannah L. Scott

_____

Christopher M. Bates

_____

Steven K. Buratto

_____

Mahdi M. Abu−Omar, Committee Chair

June 2018

Development of Renewable and Recyclable Epoxy Thermosets

Based on Lignin Derived Phenols

by

Shou Zhao

Dedicated to my family.

ACKNOWLEDGEMENTS

After seven years of undergraduate and master study in the area of environmental engineering, it is challenging to enter a new filed working at the interface of chemistry and material. This transition could not have been happened without the help and support of the following people.

First and foremost, I would like to thank my advisor, Professor Mahdi Abu−Omar for his guidance, support and encouragement throughout my Ph.D. study. In my mind, Mahdi is always energetic and enthusiastic for research, which encourages me to pursuit higher quality in academics. He is also very supportive and open−minded, which gives me sufficient opportunities to try new things. It has been an honor to work with and learn from him. He has set a good model for me in my future academic career.

I would also like to thank my committee members: Professor Susannah Scott, Christopher Bates and Steven Buratto. Your constructive advices and comments improve the quality of this thesis and inspire me to think about the wider applications of the materials I have synthesized. Special thank goes to Professor Andrew Whelton in Purdue University. He substantially expanded the applications of my compounds for environmental purposes. Meanwhile, he generously provided mechanical tests for my samples, which made this thesis complete.

I am also indebted to all former and current members of the Abu−Omar Group for their valuable help and companion, which made my graduate study joyful and colorful. Special thanks go to Shuo Liu, Ian Klein, Hao Luo, Baoyuan Liu, Manxi Xiong, Curt Bougher, Thilina Gunasekara, Chan Park and Jun Hee Jang.

Graduate study without a hobby would be monotonous. I am extremely grateful to have many soccer buddies to play with. Special thanks go to Taotao He, Xiangyu Zhang, Chipeng Zhang, Kai Miao, Xing Fei and Chengpeng Gong in CDFC at Purdue. It has been a pleasure to play with your guys and I will never forget the time we spent together in Purdue. When I moved to UCSB, I am lucky to meet new soccer buddies including Yu Chen, Yonghao Zheng, Ming Wang, Zhuofan Zhang, Song Gao, Yizhou Liu, Runsheng Song, Chunqing Liu, Cuefeng Peng, Maohua Zhu and Ziming Qi. The soccer time of every Saturday is one of the most joyful time I have had in UCSB.

I am greatly blessed with a beautiful family that gives me unconditional love and constant encouragement. My parents, Ms. Lili Cai and Mr. Bin Zhao are given special appreciation for their steadfast support of my academic endeavors. I am also grateful to my parents−in−law, Ms. Xiuqin Ma and Mr. Chao Huang for their care and support. I cannot thank them enough.

My deepest gratitude goes to my wife, Ms. Xiangning Huang, who is the impetus for what I have done. Having her in my life is always pleased and satisfied. Her love and support enable me to complete the long journey of graduate life. Without her sacrifices and waiting, all my efforts would have been vain.

VITA OF SHOU ZHAO

June 2018

EDUCATION

B.S. Environmental Engineering, Tianjin Polytechnic University, China, July 2010

M.S. Environmental Engineering, Beijing Normal University, China, July 2013

Ph.D. Chemistry, University of California, Santa Barbara, June 2018

PROFESSIONAL EMPLOYMENT

2016−2018: Research Assistant, Department of Chemistry and Biochemistry, University of California, Santa Barbara

2014−2016: Research Assistant, Department of Chemistry, Purdue University

2013−2014: Research Assistant, Purdue University Interdisciplinary Life Science Program (PULSe), Purdue University

2010−2013: Research Assistant, School of Environment, Beijing Normal University

2008−2010: Undergraduate Student Researcher, School of Environmental and Chemical Engineering, Tianjin Polytechnic University

AWARDS

- Mellichamp Summer Fellowship, Mellichamp Academic Initiative in Sustainability, University of California, Santa Barbara (2016, 2017)
- Graduate Student with Honor, Beijing Municipal Education Commission (2013)
- Zhou Tingru Scholarship, Beijing Normal University (2013)
- National Graduate Scholarship, Ministry of Education, China (2012)
- Liyun Graduate Scholarship, First Award, Beijing Normal University (2012)
- Yutu Graduate Scholarship, First Award, Beijing Normal University (2012)
- Graduate Academic Award, Beijing Normal University (2011)
- Graduate Student with Honor, Tianjin Polytechnic University (2010)

PUBLICATIONS

1. Peer-reviewed journal (published)

- **Shou Zhao** and Mahdi M. Abu−Omar. Biobased epoxy nanocomposites derived from lignin−based monomers. *Biomacromolecules*, **2015**, *16*, 2025−2031.
- **Shou Zhao** and Mahdi M. Abu−Omar. Renewable epoxy networks derived from lignin−based monomers: effect of cross−linking density. *ACS Sustain. Chem. Eng.*, **2016**, *4*, 6082−6089.
- **Shou Zhao** and Mahdi M. Abu−Omar. Renewable thermoplastics based on lignin−derived polyphenols. *Macromolecules*, **2017**, *50*, 3573−3581.
- **Shou Zhao** and Mahdi M. Abu−Omar. Synthesis of renewable thermoset polymers through successive lignin modification using lignin−derived phenols. *ACS Sustain. Chem. Eng.* **2017**, *5*, 5059−5066.
- Xiangning Huang, **Shou Zhao**, Mahdi M. Abu−Omar and Andrew J. Whelton. In−situ cleaning of heavy metal contaminated plastic water pipes using a biomass derived ligand. *J. Environ. Chem. Eng.* **2017**, *5*, 3622−3631.
- Yuan Jiang, Duanchen Ding, **Shou Zhao**, Hanyu Zhu, Hilkka I. Kenttamaa and Mahdi M. Abu−Omar. Renewable thermoset polymers based on lignin and carbohydrate derived monomers. *Green Chem.* **2018**, DOI: 10.1039/C7GC03552G .
- Jonathan G. Mehtala, Dmitry Y. Zemlyanov, Joann P. Max, Naveen Kadasala, **Shou Zhao** and Alexander Wei. Citrate−stabilized gold nanorods. *Langmuir*, **2014**, *30*, 13727−13730.

2. Peer-reviewed journal (submitted or in preparation)

- **Shou Zhao** and Mahdi M. Abu−Omar. Universal modifications of lignin−derived phenols to make renewable epoxy thermosets.
- **Shou Zhao**, Xiangning Huang, Andrew J. Whelton, and Mahdi M. Abu−Omar. Renewable epoxy thermosets from fully lignin−derived triphenols.
- **Shou Zhao**, Xiangning Huang, Andrew J. Whelton, and Mahdi M. Abu−Omar. Method for incorporating lignin into epoxy thermosets.
- **Shou Zhao** and Mahdi M. Abu−Omar. Degradable and recyclable epoxy thermoset bearing aromatic imine bonds.

3. Peer-reviewed journal (during master study in BNU)

- **Shou Zhao**, Chenghong Feng, Xiangning Huang, Baohua Li, Junfeng Niu, Zhenyao Shen. Role of uniform pore structure and high positive charges in the arsenate adsorption performance of Al_{13}–modified montmorillonite. *J. Hazard. Mater.* **2012**, *203*, 317–325.
- **Shou Zhao**, Chenghong Feng, Yiru Yang, Junfeng Niu, Zhenyao Shen. Risk assessment of sediment metals in the Yangtze Estuary: New evidence of the substitution relations between two typical index methods. *J. Hazard. Mater.* **2012**, *241*, 164–172.
- **Shou Zhao**, Chenghong Feng, Dongxin Wang, Yanzhen Liu, Zhenyao Shen. Salinity increases the mobility of Cd, Cu, Mn, and Pb in the sediments of Yangtze Estuary: Relative role of sediments properties and metal speciation. *Chemosphere* **2013**, *91*, 977–984.
- **Shou Zhao**, Chenghong Feng, Dongxin Wang, Chenhao Tian, Zhenyao Shen. Relationship of metal enrichment with adverse biological effect in the Yangtze Estuary sediments: Role of metal background values, *Environ. Sci. Pollut. Res.* **2014**, *21*, 464−472.
- **Shou Zhao**, Chenghong Feng, Weimin Quan, Xiaofeng Chen, Junfeng Niu, Zhenyao Shen. Role of living environments in the accumulation characteristics of heavy metals in fishes and crabs in the Yangtze River Estuary, China. *Marine Pollut. Bull.* **2012**, *64*, 1163–1171.
- **Shou Zhao**, Dongxin Wang, Chenghong Feng, Zhenyao Shen. Sequence of the main geochemical controls on the Cu and Zn fractions in the Yangtze River estuarine sediments. *Front. Environ. Sci. Eng*. **2016**, *10*, 19−27.
- Chenghong Feng, **Shou Zhao**, Dongxin Wang, Junfeng Niu, Zhenyao Shen. Sedimentary records of metal speciation in the Yangtze Estuary: Role of hydrological events. *Chemosphere*, **2014**, *107*, 415−422.
- Chenghong Feng, **Shou Zhao**, Zhe Bi, Dongsheng Wang, Hongxiao Tang. Speciation of prehydrolyzed Al salt coagulants with electrospray ionization time–of–flight mass spectrometry and ^{27}Al NMR spectroscopy. *Colloid Surf. A: Physicochem. Eng. Asp.* **2011**, *392*, 95–102.
- Chenghong Feng, Zhe Bi, **Shou Zhao**, Ning Li, Dongsheng Wang, Hongxiao Tang. Quantification analysis of polymeric Al species in solutions with electrospray ionization time–of–flight mass spectrometry (ESI–TOF–MS). *Int. J. Mass Spectrom.* **2012**, *309*, 22–29.

PRESENTATIONS

- Shou Zhao and Chenghong Feng. Categories of Al species existed in polymeric aluminum solutions. The 11th International Hydrocolloids Conference, Purdue University, IN, 2012.
- Shou Zhao and Mahdi M. Abu−Omar. Fabrication and characterization of a lignin−derived epoxy resin montmorillonite nanocomposite. PINDU Inorganic Symposium, Indiana University, IN, 2014.
- Shou Zhao and Mahdi M. Abu−Omar. Synthesis of renewable epoxy resins based on fully lignin−derived triphenylmethane−type polyphenols. Renewable Carbon Workshop, Mellichamp Academic Initiative in Sustainability, University of California, Santa Barbara, CA, 2016.

ABSTRACT

Development of Renewable and Recyclable Epoxy Thermosets

Based on Lignin Derived Phenols

by

Shou Zhao

Epoxy thermoset represents one of the most versatile thermosetting materials that has been used as coatings, adhesives, electronic materials and structural composites. However, by far more than 90% of the epoxy cross−linked polymers involve the use of petroleum−based bisphenol A (BPA). Lignin is an abundant, low−cost and renewable source that can provide building blocks for epoxy thermosets. Lignin−derived monomers, oligomers and bulk lignin were modified through methods including demethylation, phenolation and condensation to make renewable BPA analogs. Glycidylation of these analogs followed by cross−linking process yielded renewable thermosets with marked thermomechanical properties that could replace or supplement the BPA−based counterparts. While most of the traditional epoxy thermosets cannot be reprocessed after cross−linking, incorporating reversible bonds into the backbone of thermosets can achieve stress relaxation and reversible depolymerization through cross−link exchange and bonds cleavage−reformation. This affords malleability, weldability and recyclability to the renewable thermosets.

Table of Contents

List of Figures

List of Tables

Chapter 1

Introduction

1.1 Motivation

Epoxy thermoset represents one of the most versatile thermosetting materials that has been used as coatings, adhesives, electronic materials and structural composites. By far, more than 90% of epoxy cross−linked polymers involve the use of bisphenol A (BPA). However, considering the foreseeable depletion of fossil fuel, it is advantageous to replace petroleum−derived chemicals (e.g., BPA) with sustainable and environmentally friendly building blocks. Lignin has been widely viewed as a promising renewable material because it is abundant, low−cost and the sole large−volume aromatic feedstock. It is especially reasonable to use lignin−derived chemicals to synthesize thermosetting materials, as the aromatic structure provides good thermal and mechanical performance. Thus, one motivation of this thesis is to synthesize renewable lignin−based epoxy thermosets and investigate their potential to replace or supplement BPA−based materials. Meanwhile, epoxy thermosets are highly cross−linked networks that are most infusible and insoluble, which makes them nondegradable and nonrecyclable. Thus, another motivation of this thesis is to eliminate the inertness of renewable thermosets by incorporating reversible bonds into the networks to make covalent adaptable networks (CANs). Malleability, processability and recyclability of obtained materials are evaluated.

1.2 Epoxy Chemistry

Since it was first discovered in 1909 by Prileschajew,[1] epoxy thermosets have been rapidly evolved and applied in various applications requiring superior strength, excellent adhesion,

good chemical resistance, and excellent performance at elevated temperatures (Figure 1.1). According to a recent report, the global epoxy market accounted for USD 7.54 billion in 2015 and is expected to increase to USD 11.22 billion by 2021.[2] Epoxy thermosets are generally prepared by contacting at least one epoxy prepolymer and at least one hardener to form a cross−linked polymer with the aid of heat or other action of energy. Epoxy prepolymer is referred to as a low−molecular−weight molecule containing more than one epoxide group. The most popular epoxy prepolymers are those prepared from the reaction of BPA and epichlorohydrin, in the presence of a base. The structure of the major product, bisphenol A diglycidyl ether (DGEBA or BADGE) and its condensed forms, depends on the stoichiometry of the reactants (Figure 1.2 and 1.3a). Other common commercial epoxy prepolymers include bisphenol F diglycidyl ether (DGEBF) and epoxidized novolac oligomer (Figure 1.3b and 1.3c).

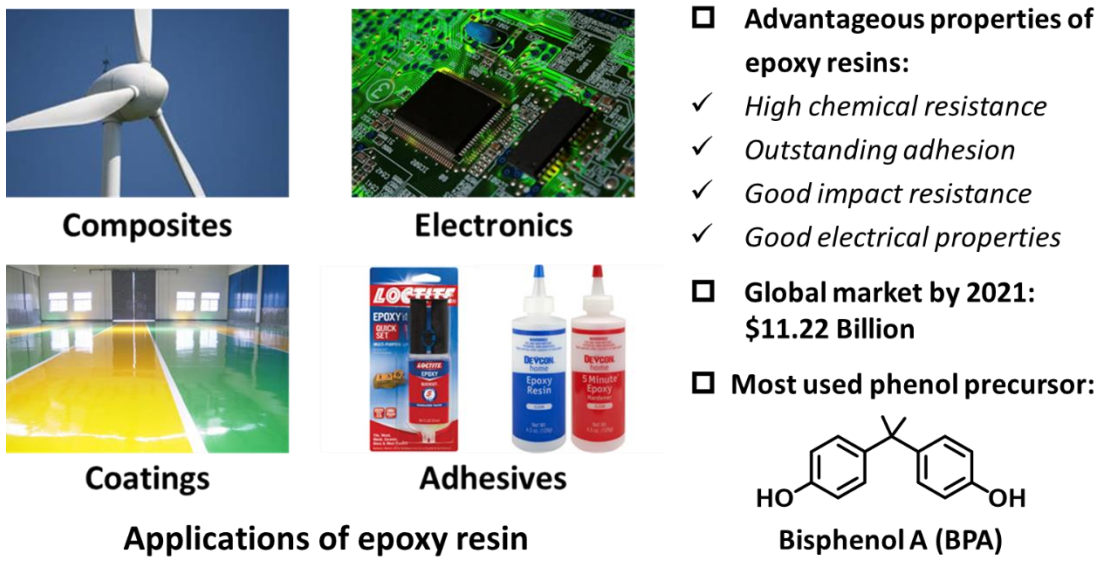

Figure 1.1 Properties and applications of epoxy thermosets.

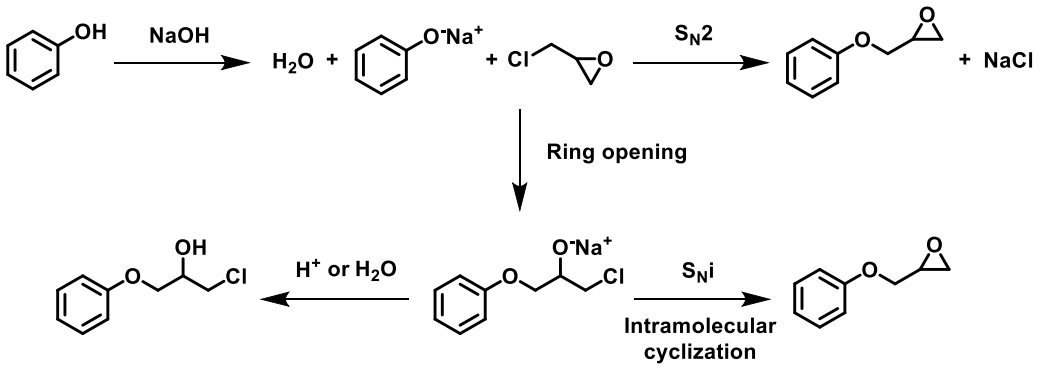

Figure 1.2 Mechanism of O−glycidylation of phenolic compounds.

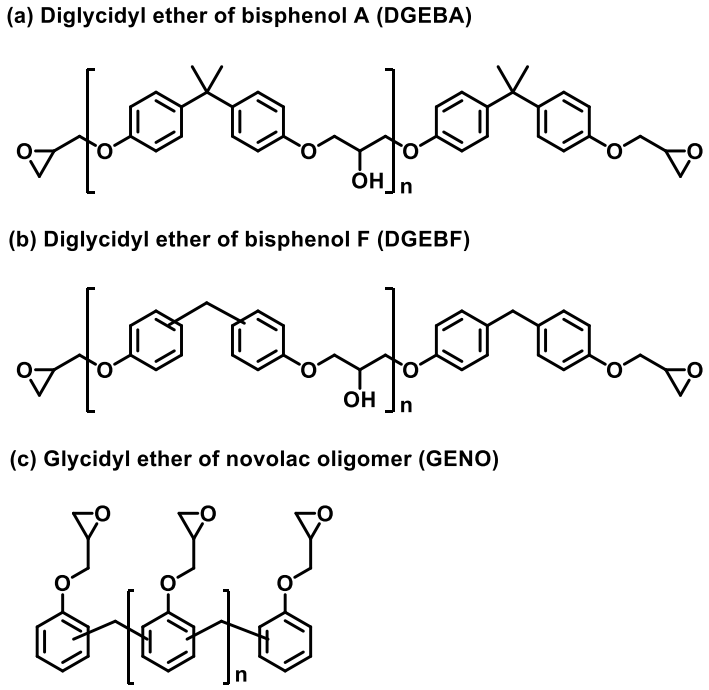

Figure 1.3 Main commercial phenolic epoxy prepolymers.

Properties of epoxy thermoset depend on the selection of appropriate epoxy precursors, curing agents, reagent stoichiometry and the addition of organic or inorganic fillers and components. These factors determine the components and cross−link density of the network, which affect the thermomechanical properties (e.g., glass transition temperature, modulus, strength and onset degradation temperature etc.) of epoxy thermosets. Curing chemistry of an epoxy prepolymer with an amine hardener is illustrated in Figure 1.4. When one epoxy is reacted with one −NH group of the amine, one hydroxyl group is generated simultaneously.

Initial epoxy−amine reaction builds linear molecular weight, which gives low viscosity increase. The next step in the curing process is the cross−linking of the chains with each other. For this to occur, amine hardener should have more than two reactive −NH groups. The cross−linking of larger molecules causes a rapid increase of the observed viscosity. Steric hindrance can lead to incomplete curing, which can be remedied by means of post−cure or the use of plasticizers. Except amine, other curing agents including polyfunctional acids, anhydrides, phenols, alcohols and thiols can also be used for various applications.

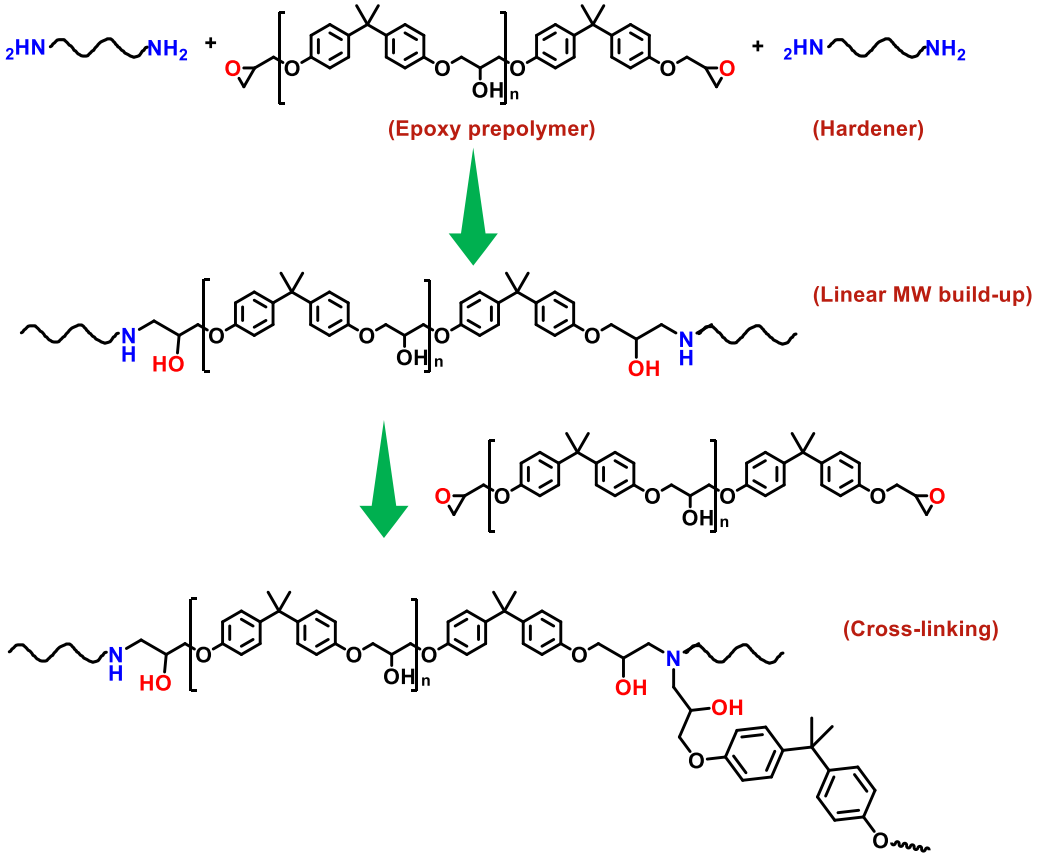

Figure 1.4 Curing reactions between epoxy prepolymer and amine hardener.

1.3 Lignin−Based Epoxy Thermosets

Lignin constitutes one of the three major components of lignocellulosic biomass, of which the other two components include cellulose and hemicellulose. Lignin is a three−dimensional amorphous polymer comprising methoxylated phenylpropane structures. It fills the spaces

between cellulose and hemicellulose in plant cell walls and behaves as a resin that keeps the lignocellulose matrix together. Figure 1.5 demonstrates a schematic representation of lignin in biomass. There are three types of monolignols (*p*−coumaryl alcohol, coniferyl alcohol and sinapyl alcohol) making up the lignin backbone (Figure 1.6), which form *p*−hydroxyphenyl (H), guaiacyl (G) and syringyl (S), with varying number of methoxy groups.[3, 4] These monolignols are connected by linkages like *β*−O−4, *β*−5, 4−O−5, 5−5, *β*−1, dibenzodioxocin and *β*−*β*, of which the *β*−O−4 linkage is dominant, comprising more than 50% of the lignin linkage structures. To prepare lignin−derived epoxy thermosets, the following starting phenolic compounds are usually employed: 1) lignin−derived phenol monomers (LDPMs), 2) partially depolymerized lignin (PDL) and 3) bulk lignin.

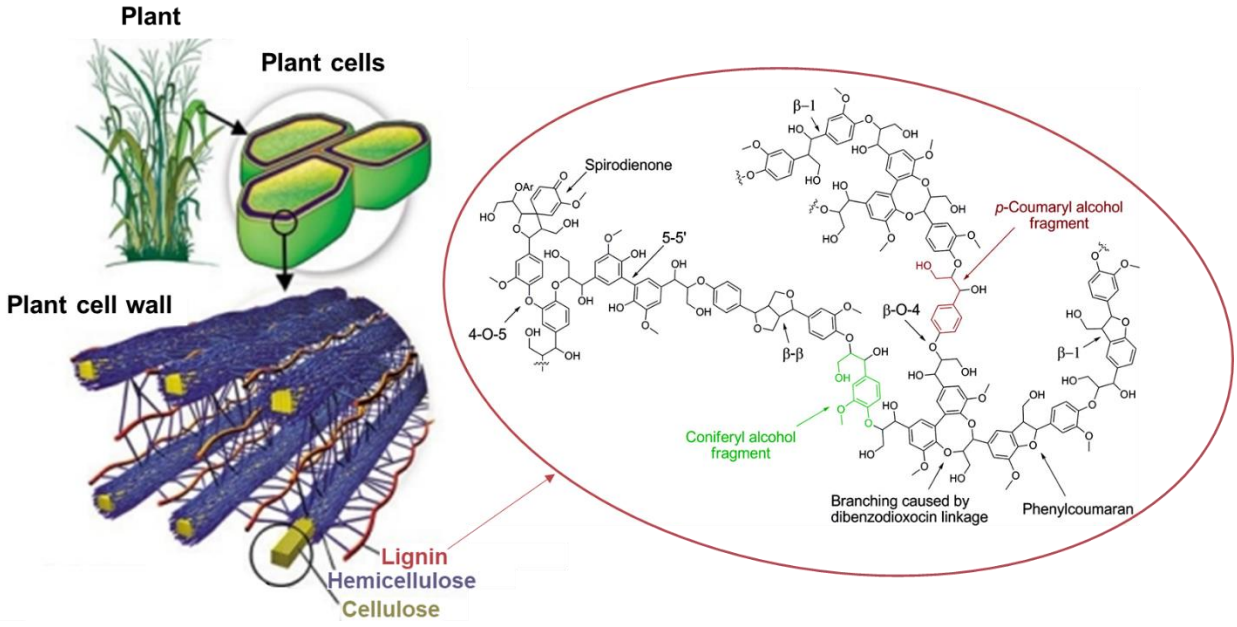

Figure 1.5 Schematic representation of lignin structure in lignocellulosic material. Adapted from Weckhuysen *et al.*[5]

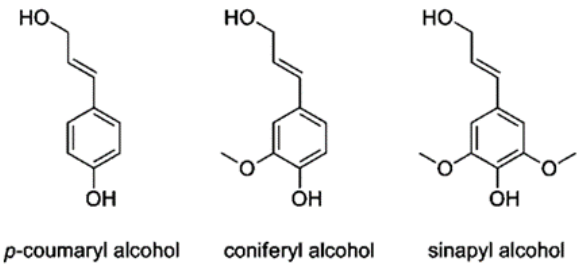

Figure 1.6 Three monolignols building blocks of lignin.

1.3.1 LDPM−Based Epoxy Thermosets.

Recent catalytic depolymerization techniques can convert lignin to various value−added phenolic monomers including phenols and aldehydes. Because of their straightforward structure, LDPMs are often used as phenolic precursors to make epoxy thermosets with predictable properties. Since cross−linkable epoxy monomers require at least two epoxides per molecule, special efforts have been taken to increase the number of functional hydroxyl groups through (1) conversion of other reactive groups like methoxy, double bond, or aldehyde to hydroxyl groups.[6–10] For example, vanillin is an industrially available, non−toxic and lignin−derived building block. On the one hand, oxidation of vanillin leads to vanillic acid or methoxyhydroquinone resulting from decarboxylation under alkaline conditions. On the other hand, reduction of vanillin results in vanillyl alcohol. All these modified compounds possess two functional hydroxyl groups, which makes them feasible to make epoxy prepolymers. Diglycidyl ethers of vanillin derivatives were formulated to make epoxy thermosets, which possess comparable properties to their BPA−based counterparts.[6, 8] (2) Coupling repeated LDPMs using bridging reagents. [11–20] For example, guaiacol novolac and wood−tar creosote novolac were synthesized by reacting lignin−derived guaiacol and creosote with formaldehyde, respectively.[11] Synthesized novolac oligomers have improved hydroxyl groups, which can be used to cure the sorbitol polyglycidyl ether. The obtained thermosets exhibited comparable

properties to phenol novolac based materials.

1.3.2 PDL−Based Epoxy Thermosets.

Compared to the production of LDPM that is often associated with intensive energy consumption as well as several separation and purification steps, partially depolymerized lignin is more cost−effective. Unlike LDPMs, PDL already have multiple functional hydroxyl groups, which requires no additional modification processing to increase hydroxyl groups. van de Pas and Torr recently reported a partially deconstructed native softwood lignin using mild hydrogenolysis.[21] Mild hydrogenolysis selectively cleaves the *β*−O−4 and *α*−O−4 ether linkages, while stabilizes the lignin fragments against repolymerization through catalytic reduction. The treated product contained a mixture of phenolic monomers, dimers and oligomers. Glycidylation of the mixture with epichlorohydrin yielded an epoxy prepolymer that can lead to thermosets with marked properties. In another study, Sasaki *et al.* reported a partially depolymerized lignin extracted from steam−exploded bamboo.[22] Steam explosion has recently been widely applied to lignocellulosic materials.[23, 24] During steam explosion, lignocellulosic matrix is exposed to pressurized steam, prior to a rapid pressure reduction. This treatment typically leads to substantial breakdown of the lignocellulosic structure and depolymerization of the lignin components. After several solvent−extraction processes, the depolymerized lignin exhibited potential to replace petroleum−based BPA for making thermosets. PDL is also available for making epoxy hardener. According to Zhang *et al.*,[25] Kraft lignin was partially depolymerized through base catalyzed depolymerization in supercritical methanol. The PDL was then converted to polyfunctional carboxylic acid by treating with succinic anhydride. By reacting the lignin−based acid with DGEBA, they claimed that lignin

could serve as a feedstock in the preparation of curing agent and be used for epoxy applications.

1.3.3 Bulk Lignin−Based Epoxy Thermosets.

Compared to LDPM and PDL, bulk lignin is more abundant and cheaper. It is reported that the total availability of technical grade lignin in the biosphere exceeds 300 billion tons,[26] while its price is 20 times cheaper than phenol.[27] Thus, it would be advantageous to replace BPA with lignin as prepolymers for thermosets. However, only 2% of lignin is being used for value−added products,[3] which is limited by its low reactivity and incompatibility with polymeric compounds. By far, methods of incorporating bulk lignin into epoxy thermosets can be summarized into three categories:[28] (1) using lignin derivatives as fillers to directly blend into general epoxy thermosets; (2) modifying lignin by direct epoxidation; and (3) modifying lignin derivatives to improve its reactivity, followed by epoxidation. Most of reported lignin and epoxidized lignin are infusible solids, which cannot be directly cured by hardeners and at least one epoxy co−prepolymer needs to be introduced for making thermosets.[29−32] Thus, lignin should be modified to increase its reactivity and compatibility before glycidylation. Glycidylation of pre−modified lignin could produce simultaneously solid and liquid phase epoxy prepolymers.[33] For example, Hofmann *et al*. prepared epoxy prepolymers using hydroxyalkyl lignin derivatives.[34] Hydroxyalkylation was conducted by reacting lignin first with propylene oxide and then with ethylene oxide. Glycidylation of hydroxyalkylated lignin produced an epoxy prepolymer mixture, while the curable liquid prepolymer had to be collected after several fractionation processes. By making a methylolated lignin, Mansouri *et al.* synthesized solid and liquid phase of epoxidized lignin simultaneously.[35] Even though the liquid phase could be separated by filtration, its epoxy content only accounted for < 20% in the

mixture. By far, there has been no report on the preparation of exclusive liquid bulk−lignin containing epoxy prepolymer. In their liquid phase, lignin−containing epoxy prepolymers would find much wider applications compared to their solid phase counterparts.

1.4 Covalent Adaptable Networks (CANs)

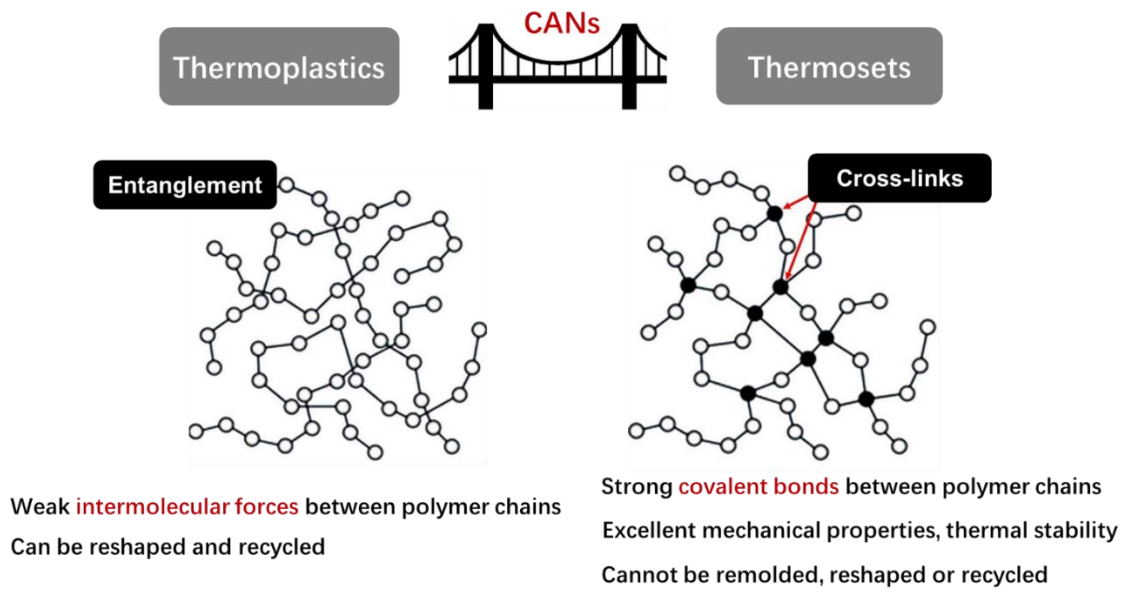

Figure 1.7 Covalent adaptable networks, new polymers that combine the advantages of thermosets and thermoplastics.

Synthetic polymer materials are generally classified into two categories: thermosets and thermoplastics. Thermosets are composed of small molecules that are covalently linked to each other. Thus, thermoset can also be viewed as a single molecule that has infinite molecular weight. The highly cross−linked structure renders thermoset excellent mechanical and thermal properties. However, because of these covalent bonds, thermosets are most intractable and cannot be remolded, reprocessed or recycled after cross−linking. By comparison, thermoplastics are composed of polymer chains that are connected by weak intermolecular forces. The lack of cross−links in thermoplastics significantly alter the characteristics and behavior as compared to thermosets. Thermoplastic materials may have a glass transition

and/or a crystalline transition. When temperature is above these transitions, the materials can undergo a macroscopic flow that permanently changes the equilibrium shape of the material when the molecular structure keeps intact. Thus, thermoplastics can often be reprocessed and recycled.

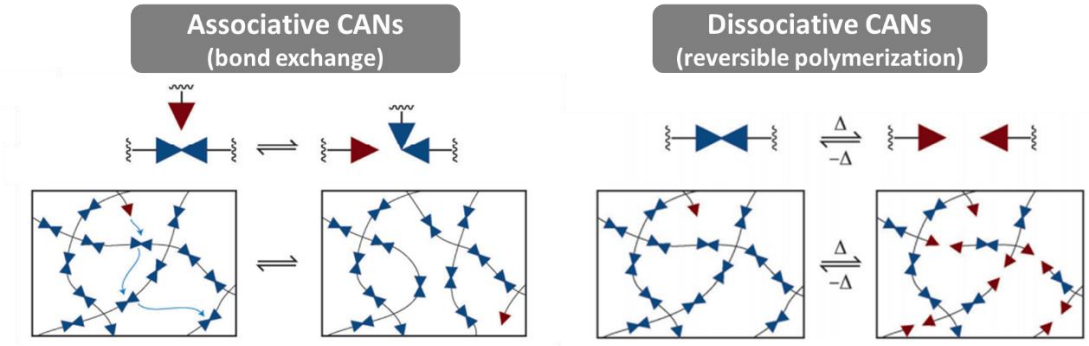

Figure 1.8 Mechanisms of the associative CANs and dissociative CANs. Adapted from Bowman and Kloxin.[36]

To combine the advantages of thermosets and thermoplastics, the concept of covalent adaptable networks (CANs) has recently been proposed (Figure 1.7). By introducing dynamic covalent bonds into thermoset backbones or cross−linking points, CANs could retain the stiffness and strength, while also exhibit stress relaxation, malleability and recyclability through bond breakage and reformation.[36−39] CANs can be divided into two categories: associative CANs and dissociative CANs (Figure 1.8). For associative CANs, bonds exchange within the polymer network. An active species undergoes an exchange reaction that leads to bond exchange and formation of a new active species, which can then undergo additional exchange reactions. One example of associative CANs is the work of Leibler *et al*. (Figure 1.9).[40] First, DGEBA was reacted with polyfunctional carboxylic acid to achieve an epoxy thermoset cross−linked by ester bonds. Then the free hydroxyl group of another chain reacted with the ester bond with the help of a metal catalyst to undergo transesterification reaction.

When the rate of this reaction was fast enough (at elevated temperature), the thermoset was a viscoelastic liquid that could be reprocessed.

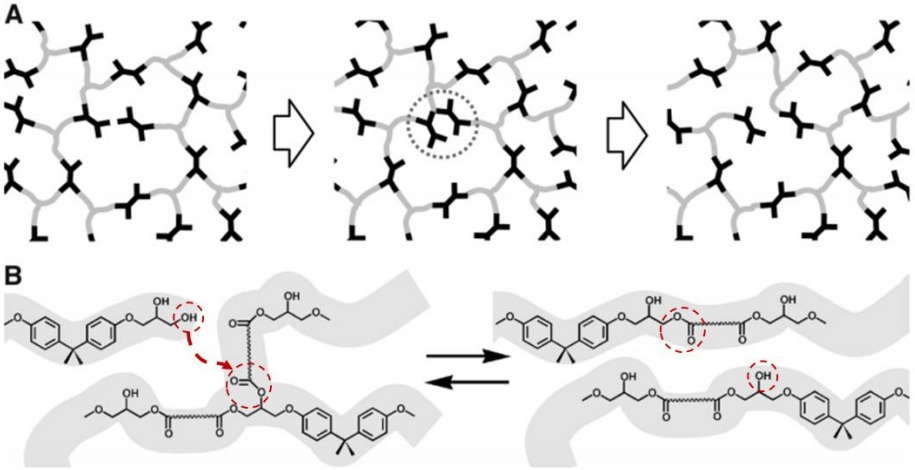

Figure 1.9 Associative CANs that is achieved by metal−catalyzed transesterification reactions. Adapted from Leilber *et al*.[40]

As for dissociative CANs, reversible polymerization takes place. When a stimulus is applied, the covalent bonds break. When the stimulus is removed, the covalent bond reform. During the bond breaking−reformation process, the thermoset can be decomposed or reshaped. One example of dissociative CANs is thermoset connected by Diels–Alder reaction.[41] The difference between the two CANs is, for associative CANs, the number of cross−links is constant, while for dissociative CANs this number changes.[39] Dynamic covalent motifs, including Diels−Alder (DA) cycloaddition,[41, 42] ester bonds,[40, 43, 44] imine bonds,[45−48] hindered urea bonds,[49, 50] Ru−catalyzed olefin metathesis,[51, 52] boronic ester linkages,[53] disulfide exchange,[54−56] trans−amination of vinyl urethanes[57] and silicon−oxygen bond exchange[58] have been recently utilized for thermoset syntheses, which substantially expands the applications of CANs. Among these bonds, it is noteworthy that imine bonds exhibit both associative and dissociative behaviors, which can afford CANs with interesting properties.

1.5 Scope and Outline of This Thesis

The objective of this thesis is to develop novel sustainable and recyclable thermosetting materials. To achieve this objective, several chemical modifications of lignin−derived compounds were conducted to increase their functional hydroxyl groups, improve their compatibility with polymeric materials and incorporate reversible bonds into polymer networks. Synthesized polyfunctional phenols were glycidylated to epoxy prepolymers and cured with appropriate hardeners to make thermosets. Thermal and mechanical properties of these thermosets were subsequently characterized to determine their potential for replacing or supplementing the conventional BPA−based counterparts

In Chapter 2, using dihydroeugenol (DHE) as the same phenol precursor, it is found that different modification methods (e.g., o−demethylation and phenol–formaldehyde reactions) yield polyphenol precursors with different molecular weight, orientation and number of functional groups, whose improvement increases the cross−link density of resulting epoxy networks. Cross−linking densities of cured networks were calculated using rubber elasticity theory from dynamic mechanical analysis (DMA). Networks with higher cross−link density are found to exhibit greater mechanical and thermal performance as measured by DMA and thermogravimetric analysis. Above results provide insights in designing high−performance thermosets. As inspired by these results, Chapter 3 demonstrates universal synthetic routes to lignin−based epoxy thermosets with tunable thermomechanical properties, which require no need to separate pure compounds from the lignin−based bio−oil mixture.

In Chapter 4, a series of fully renewable triphenylmethane−type polyphenols (TPs) are synthesized from lignin−derived aldehydes (4−hydroxybenzaldehyde, vanillin, and

syringaldehyde) and *para*−substituted guaiacols (methylguaiacol and propylguaiacol) in the first section. By converting guaiacols to catechols through o−demethylation, yields of TPs are remarkably increased. Compared to conventional bisphenolic compounds, the TP−based thermosets have significantly improved thermomechanical properties due to the rigid triphenylmethane framework, high functionality, and high cross−link density.

Lignin is characterized by methoxy substitution of its aromatic rings. As a result, lignin−based thermosets often have methoxy groups, which could affect thermomechanical properties of the resulting thermosets. Thus, Chapter 5 investigates the impacts of methoxy substituents on the properties of thermosets, while TP structure allows for a way to manipulate the number of methoxy substituents by using different starting aldehydes and *para*−unsubstituted phenols. Methoxy groups have different impacts on the mechanical, thermal and yield of the resulting thermosets. The different effects of methoxy substitution can guide the selection and/or modification (e.g. deoxygenation) of lignin−derived monomers for making epoxy polymers with desirable properties.

In Chapter 6, bulk lignin, instead of lignin−derived phenolic monomers, is incorporated into thermosets. An approach to lignin−based epoxy networks from both organosolv lignin and lignin−derived phenol (DHE) are developed using successive chemical modifications including demethylation, phenolation, and phenol−formaldehyde reaction. Compared to a conventional synthesis route in which lignin was epoxidized prior to blending with comonomers, the proposed approach can yield thermosets with improved cross−link density, α−relaxation temperature, storage modulus in a glassy region and increased thermal stability.

While the Chapter 6 describes an attractive way to make lignin−incorporated thermoset,

it suffers from low lignin content and the use of unfavorable chemicals including formaldehyde and hydrobromic acid. In Chapter 7, we describe greener chemistry for functionalizing bulk lignin. Bio−based salicyl alcohol (SA) is used to condense with phenolated lignin (PL) before glycidylation. It is found that SA has higher affinity for PL, while lignin content in starting polyphenol can approach 27 wt %, which is two times higher than the earlier approach. SA bears both hydroxymethyl group and reactive phenolic *para*/*ortho* sites. Thus, it could simultaneously react with the *para*/*ortho* sites of phenolics in PL and undergo self−condensation without the need for coupling agents like formaldehyde.

Finally, by embedding imine bonds into epoxy cross−linked networks as intermolecular linkages, we describe in Chapter 8 a novel epoxy thermoset that exhibits controlled degradation, recyclability, malleability and weldability, which require no additional ingredient such as catalyst or additional monomer, or complicated processing. The described recyclable thermoset makes use of lignin−derived monomers like vanillin.

1.6 References

1. Resins, E. Chemistry and Technology. *May, CA, Ed* **1988**, 656.
2. Lacal−Arántegui, R. 2012 JRC Wind Status Report. **2013**.
3. Laurichesse, S.; Avérous, L. *Prog. Polym. Sci.* **2014,** *39* (7), 1266−1290.
4. Upton, B. M.; Kasko, A. M. *Chem.l Rev.* **2015,** *116* (4), 2275−2306.
5. Zakzeski, J.; Bruijnincx, P. C.; Jongerius, A. L.; Weckhuysen, B. M. *Chem. Rev.* **2010,** *110* (6), 3552−3599.
6. Fache, M.; Darroman, E.; Besse, V.; Auvergne, R.; Caillol, S.; Boutevin, B. *Green Chem.* **2014,** *16* (4), 1987−1998.

7. Qin, J.; Liu, H.; Zhang, P.; Wolcott, M.; Zhang, J. *Polym. Int.* **2014,** *63* (4), 760−765.

8. Fache, M.; Auvergne, R.; Boutevin, B.; Caillol, S. *Eur. Polym. J.* **2015,** *67*, 527−538.

9. François, C.; Pourchet, S.; Boni, G.; Fontaine, S.; Gaillard, Y.; Placet, V.; Galkin, M. V.; Orebom, A.; Samec, J.; Plasseraud, L. *RSC Adv.* **2016,** *6* (73), 68732−68738.

10. Guzmán, D.; Ramis, X.; Fernández−Francos, X.; De la Flor, S.; Serra, A. *Prog. Org. Coat.* **2018,** *114*, 259−267.

11. Enjoji, M.; Yamamoto, A.; Shibata, M. *J. Appl. Polym. Sci.* **2015,** *132* (4).

12. Schutyser, W.; Koelewijn, S.−F.; Dusselier, M.; Van de Vyver, S.; Thomas, J.; Yu, F.; Carbone, M. J.; Smet, M.; Van Puyvelde, P.; Dehaen, W. *Green Chem.* **2014,** *16* (4), 1999−2007.

13. Meylemans, H. A.; Groshens, T. J.; Harvey, B. G. *ChemSusChem* **2012,** *5* (1), 206−210.

14. Ménard, R.; Caillol, S.; Allais, F. *Ind. Crops Prod.* **2017,** *95*, 83−95.

15. Maiorana, A.; Reano, A. F.; Centore, R.; Grimaldi, M.; Balaguer, P.; Allais, F.; Gross, R. A. *Green Chem.* **2016,** *18* (18), 4961−4973.

16. Wang, S.; Ma, S.; Xu, C.; Liu, Y.; Dai, J.; Wang, Z.; Liu, X.; Chen, J.; Shen, X.; Wei, J. *Macromolecules* **2017,** *50* (5), 1892−1901.

17. Hitce, J.; Crutizat, M.; Bourdon, C.; Vivès, A.; Marat, X.; Dalko−Csiba, M. *Green Chem.* **2015,** *17* (7), 3756−3761.

18. Shibata, M.; Tetramoto, N.; Imada, A.; Neda, M.; Sugimoto, S. *React. Funct. Polym.* **2013,** *73* (8), 1086−1095.

19. Liu, T.; Hao, C.; Wang, L.; Li, Y.; Liu, W.; Xin, J.; Zhang, J. *Macromolecules* **2017,** *50* (21), 8588−8597.

20. Wan, J.; Zhao, J.; Gan, B.; Li, C.; Molina−Aldareguia, J.; Zhao, Y.; Pan, Y.−T.; Wang,

D.−Y. *ACS Sustain. Chem. Eng.* **2016,** *4* (5), 2869−2880.

21. van de Pas, D. J.; Torr, K. M. *Biomacromolecules* **2017,** *18* (8), 2640−2648.

22. Sasaki, C.; Wanaka, M.; Takagi, H.; Tamura, S.; Asada, C.; Nakamura, Y. *Ind. Crops Prod.* **2013,** *43*, 757−761.

23. Chen, W.−H.; Pen, B.−L.; Yu, C.−T.; Hwang, W.−S. *Bioresour. Technol.* **2011,** *102* (3), 2916−2924.

24. Rocha, G.; Gonçalves, A. R.; Oliveira, B.; Olivares, E.; Rossell, C. *Ind.Crops Prod.* **2012,** *35* (1), 274−279.

25. Qin, J.; Woloctt, M.; Zhang, J. *ACS Sustain. Chem. Eng.* **2013,** *2* (2), 188−193.

26. Smolarski, N. *Frost & Sullivan, Paris* **2012,** 15.

27. Strassberger, Z.; Tanase, S.; Rothenberg, G. *RSC Adv.* **2014,** *4* (48), 25310−25318.

28. Xu, C.; Ferdosian, F., Conversion of Lignin into Bio−Based Chemicals and Materials. Springer: 2017.

29. Malutan, T.; Nicu, R.; Popa, V. I. *BioResources* **2008,** *3* (4), 1371−13767.

30. Hirose, S.; Hatakeyama, H. *Mem. Fukui Univ. Technol.* **2000**, *30*, 255–262.

31. Holsopple, D. B.; Kurple, W. W.; Kurple, W. M.; Kurple, K. R., Method of making epoxide−lignin resins. Patent US4265809, 1981.

32. Simionescu, C. I.; Rusan, V.; Macoveanu, M. M.; Cazacu, G.; Lipsa, R.; Vasile, C.; Stoleriu, A.; Ioanid, A. Lignin/epoxy composites. *Compos. Sci. Technol.* **1993,** *48* (1−4), 317−323.

33. Koike, T. *Polym. Eng. Sci.* **2012,** *52* (4), 701−717.

34. Hofmann, K.; Glasser, W. G. *J. Wood Chem. Technol.* **1993,** *13* (1), 73−95.

35. El Mansouri, N.−E.; Yuan, Q.; Huang, F. *BioResources,* **2011***, 6, (3),* 2492−2503.

36. Bowman, C. N.; Kloxin, C. J. *Angew. Chem. Int. Ed.* **2012,** *51* (18), 4272−4274.

37. Kloxin, C. J.; Scott, T. F.; Adzima, B. J.; Bowman, C. N. *Macromolecules* **2010,** *43* (6), 2643−2653.

38. Kloxin, C. J.; Bowman, C. N. *Chem Soc. Rev.* **2013,** *42* (17), 7161−7173.

39. Denissen, W.; Winne, J. M.; Du Prez, F. E. *Chem. Sci.* **2016,** *7* (1), 30−38.

40. Montarnal, D.; Capelot, M.; Tournilhac, F.; Leibler, L. *Science* **2011,** *334* (6058), 965−968.

41. Chen, X.; Dam, M. A.; Ono, K.; Mal, A.; Shen, H.; Nutt, S. R.; Sheran, K.; Wudl, F. *Science* **2002,** *295* (5560), 1698−1702.

42. Min, Y.; Huang, S.; Wang, Y.; Zhang, Z.; Du, B.; Zhang, X.; Fan, Z. *Macromolecules* **2015,** *48* (2), 316−322.

43. Capelot, M.; Montarnal, D.; Tournilhac, F. o.; Leibler, L. *J. Am. Chem. Soc.* **2012,** *134* (18), 7664−7667.

44. Capelot, M.; Unterlass, M. M.; Tournilhac, F.; Leibler, L. *ACS Macro Lett.* **2012,** *1* (7), 789−792.

45. Taynton, P.; Zhu, C.; Loob, S.; Shoemaker, R.; Pritchard, J.; Jin, Y.; Zhang, W. *Polym. Chem.* **2016,** *7* (46), 7052−7056.

46. Taynton, P.; Yu, K.; Shoemaker, R. K.; Jin, Y.; Qi, H. J.; Zhang, W. *Adv. Mater.* **2014,** *26* (23), 3938−3942.

47. Lei, X.; Jin, Y.; Sun, H.; Zhang, W. *J. Mater. Chem. A* **2017,** *5* (40), 21140−21145.

48. Taynton, P.; Ni, H.; Zhu, C.; Yu, K.; Loob, S.; Jin, Y.; Qi, H. J.; Zhang, W. *Adv. Mater.* **2016,** *28* (15), 2904−2909.

49. Ying, H.; Zhang, Y.; Cheng, J. *Nature Commun.* **2014,** *5*, 3218.

50. Zhang, Y.; Ying, H.; Hart, K. R.; Wu, Y.; Hsu, A. J.; Coppola, A. M.; Kim, T. A.; Yang, K.; Sottos, N. R.; White, S. R. *Adv. Mater.* **2016,** *28* (35), 7646−7651.

51. Lu, Y.−X.; Tournilhac, F.; Leibler, L.; Guan, Z. *J. Am. Chem. Soc.* **2012,** *134* (20), 8424−8427.

52. Lu, Y.−X.; Guan, Z. *J. Am. Chem. Soc.* **2012,** *134* (34), 14226−14231.

53. Cromwell, O. R.; Chung, J.; Guan, Z. *J. Am. Chem. Soc.* **2015,** 137 (20), 6492−6495.

54. Pepels, M.; Filot, I.; Klumperman, B.; Goossens, H. *Polym. Chem.* **2013,** *4* (18), 4955−4965.

55. Rekondo, A.; Martin, R.; de Luzuriaga, A. R.; Cabañero, G.; Grande, H. J.; Odriozola, I. *Mater. Hor.* **2014,** *1* (2), 237−240.

56. Lei, Z. Q.; Xiang, H. P.; Yuan, Y. J.; Rong, M. Z.; Zhang, M. Q. *Chem. Mater.* **2014,** *26* (6), 2038−2046.

57. Denissen, W.; Rivero, G.; Nicolaÿ, R.; Leibler, L.; Winne, J. M.; Du Prez, F. E. *Adv. Funct. Mater.* **2015,** *25* (16), 2451−2457.

58. Zheng, P.; McCarthy, T. J. *J. Am. Chem. Soc.* **2012,** *134* (4), 2024−2027.

Chapter 2

Renewable Epoxy Thermosets from Lignin−Derived Phenol Monomers (LDPMs): Effect of Cross−link Density

ABSTRACT: Three modification methods, which either improved molecular weight, orientation or the number of functional groups, were employed to increase the cross−link density of biobased epoxy networks based on 2−methoxy−4−propylphenol (or dihydroeugenol, DHE). The modifications were realized through o−demethylation and phenol−formaldehyde reactions. Structures of DHE−based monomers and cured networks were characterized by NMR and FTIR spectroscopy. Cross−link densities of cured networks were calculated using rubber elasticity theory from dynamic mechanical analysis (DMA). Networks with higher cross−link density were found to exhibit greater mechanical and thermal performance as measured by DMA and thermogravimetric analysis (TGA). GEDHEO−NOVO, an epoxy monomer featuring all three modification processes, exhibited significant improvements in cross−link density (0.39 to 9.77 mol/dm^3), α−relaxation temperature (T_α, 40 to 139 °C) and statistic heat−resistant index temperature (T_s, 125 to 153 °C) compared to the unmodified DHEO−based networks.

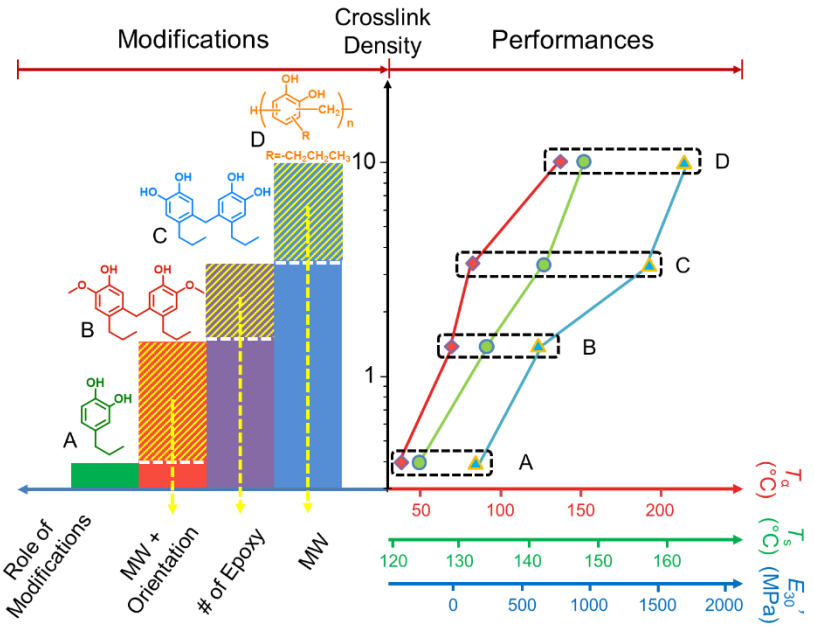

This section is partially adapted from: Shou Zhao and Mahdi M. Abu−Omar, *Biomacromolecules*, **2015**, *16* (7), 2025–2031, and Shou Zhao and Mahdi M. Abu−Omar, *ACS Sustain. Chem. Eng.* **2016,** *4* (11), 6082−6089.

2.1 Introduction

The use of lignin−derived phenols to replace aromatics derived from petroleum for making thermoset materials has attracted increasing attention over the last decade.[1,2] The merit of this replacement is often attributed to the sustainability of lignin over nonrenewable chemicals. Furthermore, the aromatic nature of lignin provides for high performance thermosets with desirable mechanical properties and thermal stability.[3]

To obtain lignin−based thermosets, two strategies have been employed. The first focuses on integrating functionalized bulk lignin with other natural or synthetic monomers to achieve copolymers or blends. For example, carboxylic acid−functionalized lignin obtained by reacting alkali lignin with acid anhydride acts as a curing agent for epoxy networks.[4] The use of bulk

lignin without deconstruction into its phenolic components has certain economic advantages. However, limitations of this strategy have become evident. The reactivity of lignin is low because the majority of its phenolic hydroxyl groups are etherified and all *para* as well as some *ortho* positions of the phenolic rings are occupied.[5] Also cross−link density of the resulting thermosets is often compromised because of the steric hindrance introduced by bulk lignin.[6,7]

Because of the above−mentioned limitations associated with the use of bulk lignin, use of well characterized lignin−derived monomers for thermosets design is most appealing and has received extensive attention. Thermosets including epoxy resins, polybenzoxazines, vinyl ester resins and cyanate ester resins developed from lignin−derived building blocks like eugenol,[8,9] vanillin,[10,11] guaiacol[12] and creosol[13] have been recently reported. Improved reactivity of lignin−derived monomers rather than bulk lignin provides thermosets which exhibit more satisfactory mechanical and thermal properties. Moreover, reactivity of lignin−derived monomers can be further increased through molecular reaction design such as demethylation,[14] methacrylation[15] or bridging monomers into oligomers through formaldehyde chemistry.[16]

From the viewpoint of "structure determines property," even if slightly varying monomer's chemical structure, e.g. *ortho*−, *meta*− and *para*−substituted bisphenols, the obtained polymers exhibit markedly different properties.[17] Even though significant work has been done on lignin−based thermosets,[1,2,18] differences in properties caused by various structural designs have not been explored systematically. In fact, if lignin−derived molecules can be shown to undergo reasonable structural design to achieve optimal properties, their sustainability and viability would become more meaningful. Previous laboratory experiments[19] and molecular modeling[20] studies have identified cross−link density as a key structural

parameter that determines thermomechanical properties of thermosets. To investigate the effects of cross−link density on fully cured thermosets from the same precursor, we employed the following methods: (1) variation of monomer molecular weight,[21] (2) alteration in number of functional groups on monomer[22] and (3) adjustment of chain orientation.[23,24]

In a recent report we described a bimetallic Zn/Pd/C catalytic system to convert lignin in intact lignocellulosic biomass directly into two methoxyphenol products.[25] One of the major products, 2−methoxy−4−propylphenol (or dihydroeugenol, DHE), exhibited potential as a building block for epoxy networks (Figure 2.1, Route 1),[26] in which DHE was o−demethylated to yield propylcatechol (DHEO), and subsequently glycidylated to epoxy monomer (glycidylated ether of DHEO, GEDHEO). Route 1 creates two hydroxyl groups per DHE molecule to make it a viable epoxy monomer. However, its properties are impaired due to the appearance of benzodioxane byproducts and decrease in extension caused by the *ortho* hydroxyls and three carbon propyl tail.

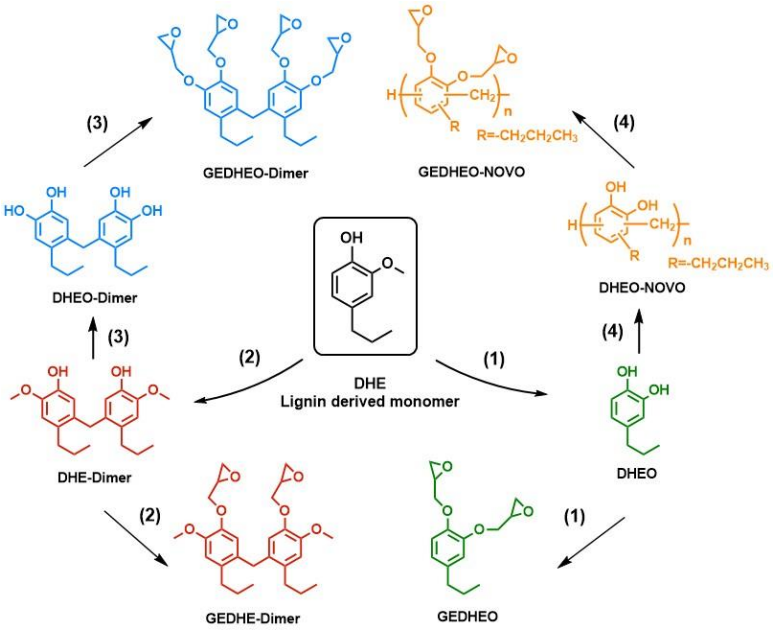

Figure 2.1 Modifications of DHE−based epoxy networks through: improving molecular weight

and adjusting orientation of functional group from DHE to DHE−Dimer in Route (2); increasing number of functional group from DHE−Dimer to DHEO−Dimer via o−demethylation in Route (3); and increasing molecular weight from DHEO to DHEO−NOVO via phenol−formaldehyde reaction in Route (4). Benzodioxane derivatives produced during the glycidylation of DHEO, DHEO−Dimer and DHEO−NOVO are not shown.

In this study, with the aim to improve the performance of the epoxy networks obtained from Route 1, three modified DHE−based epoxy networks with enhanced cross−link density were prepared by varying (a) the molecular weight and orientation of functional group by dimerization of DHE (DHE−Dimer) via Route 2; (b) the number of functional hydroxyl groups by demethylation (DHEO−Dimer) in Route 3; and (c) the molecular weight through phenol−formaldehyde reaction (DHEO−NOVO) in Route 4. The proposed DHE−based epoxy networks provide insight into thermoset syntheses using lignin−derived monomers, the majority of which possess similar structural characteristics with DHE. More importantly, this study highlights how the thermomechanical properties of epoxy networks can be improved through varying the cross−link density from the same precursor.

2.2 Results and Discussion

2.2.1 Characterization of DHE−Based Polyphenols and Epoxy Monomers

^{1}H NMR spectroscopy.

Structures of DHE−derived polyphenols are illustrated in Figure 2.2. The resonance peak at δ 3.9 is assigned to $-OCH_3$ proton of DHE (Figure 2.2, panel a). After DHE was demethylated in aqueous HBr, DHEO (Figure 2.2, panel b) exhibits no peak at δ 3.9 while two hydroxyl peaks are apparent at δ 5.3 and 5.4, indicating complete removal of methoxy group.

In another route, DHE−based polyphenol is achieved by dimerization of DHE through formaldehyde chemistry. Previous study reported Brønsted acid catalyzed formaldehyde coupling occurred exclusively at the position *meta* to the hydroxyl group with a selectivity of 97%.[27] The obtained bisphenol, DHE−Dimer, exhibits a methylene linkage at δ 3.8 (Figure 2.2, panel c). DHE−Dimer is further demethylated to DHEO−Dimer in HBr solution. Figure 2.2, panel d shows the disappearance of DHE−Dimer methoxy groups at δ 3.9 and doubling of the integration of hydroxyl groups at δ 5.7. NMR spectra of DHEO−NOVO (Figure 2.2, panel e), which is achieved through the DHEO−formaldehyde reaction, reveals a methylene linkage in the region of δ 3.5−4.1. The integration ratio of H4/H2 in Figure 2.2, panel e is around 0.57, indicating the novolac oligomer contains mainly dimers and trimers, which is consistent with a reported novolac product from wood−tar creosote.[16]

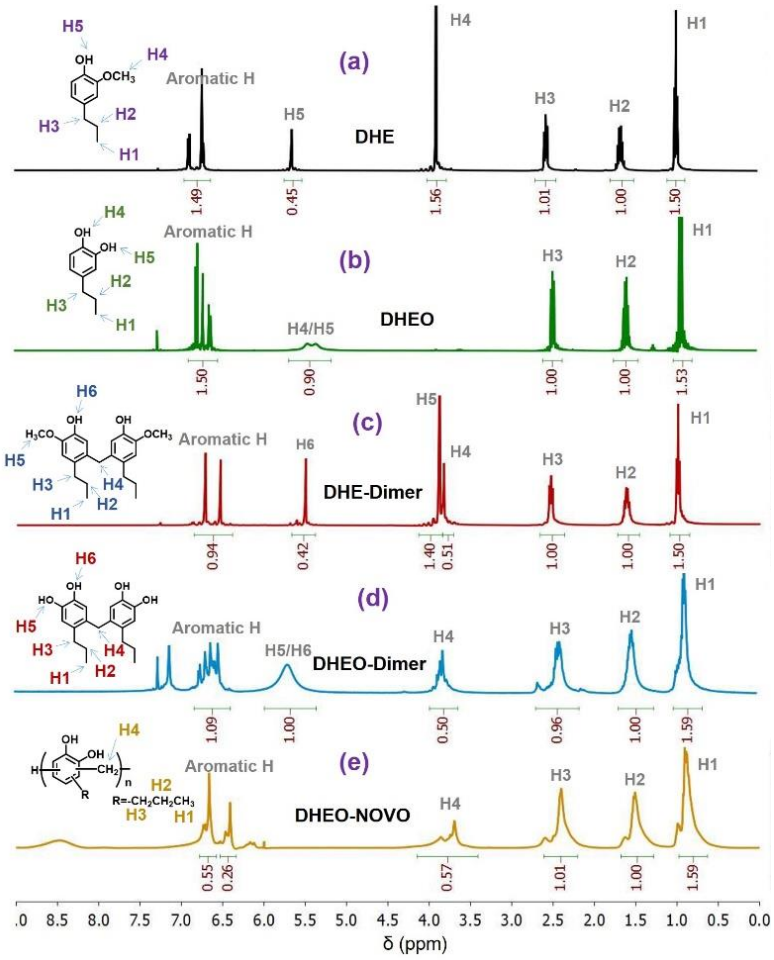

Figure 2.2 ^{1}H NMR spectra of (a) DHE, (b) DHE o−demethylated product (DHEO), (c) DHE−Dimer, (d) DHEO−Dimer and (e) DHEO−NOVO.

NMR spectra of glycidyl ethers of polyphenols are demonstrated in Figure 2.3. Glycidylation of DHEO with epichlorohydrin results in two products GEDHEO and benzodioxane with a molar ratio of *ca*. 2:1. GEDHEO exhibits epoxy protons H6a, H6b and H5 at δ 2.75, 2.88 and 3.37, while benzodioxane shows characteristic protons H4a, H5 and H4b at δ 3.99, 4.07 and 4.23 (Figure 2.3, panel a). Figure 2.3, panel b reveals glycidylation of DHE−Dimer lead to only one product (GEDHE−Dimer) with characteristic epoxy protons H8a, H8b and H7 at δ 2.6, 2.8 and 3.3, respectively. As for the spectra of GEDHEO−Dimer (Figure 2.3, panel c) and GEDHEO−NOVO (Figure 2.3, panel d), it is difficult to assign each peak

because DHEO−NOVO have different methylene linkage positions, while the intramolecular cyclization between two adjacent hydroxyls (benzodioxane products) could occur in both. Thus, NMR patterns of GEDHEO and GEDHE−Dimer in Figure 2.3, panels a and b are tentatively used to define the regions of characteristic epoxy (δ 2.6−3.0 and δ 3.2−3.5) and benzodioxane (δ 3.7−4.4) protons. Figure 2.3, panels c and d depict that there are peaks showing up in both regions, which indicates DHEO−Dimer and DHEO−NOVO are epoxidized.

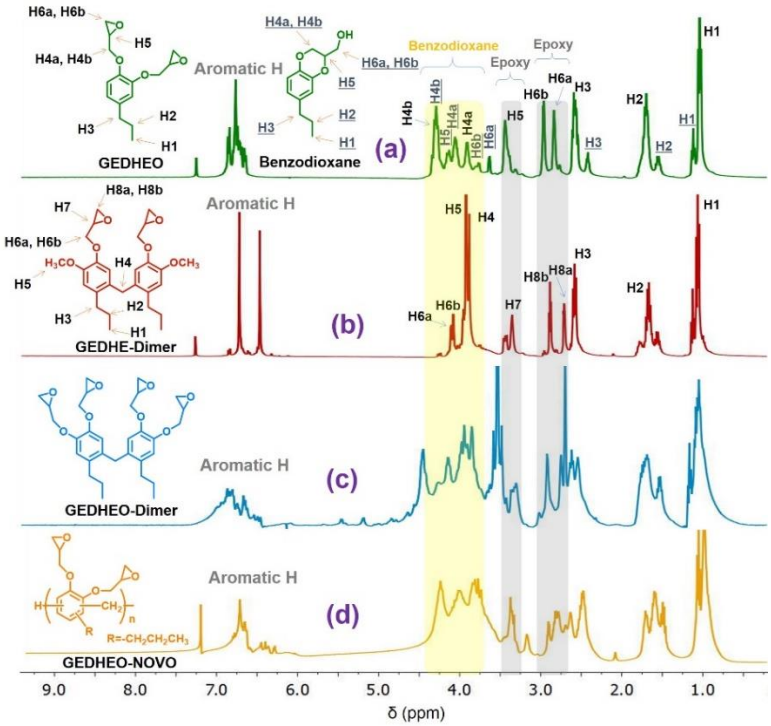

Figure 2.3 ^{1}H NMR spectra of glycidylation products of DHE−based polyphenols. (a) GEDHEO, (b) GEDHE−Dimer, (c) GEDHEO−Dimer and (d) GEDHEO−NOVO. Regions of characteristic epoxy (δ 2.6−3.0 and δ 3.2−3.5) and benzodioxane protons (δ 3.7−4.4) are highlighted. Benzodioxane derivatives of (c) and (d) are not shown in the figure.

FTIR spectroscopy.

The structures of polyphenols and corresponding epoxy monomers are further supported by FTIR analysis. Figure S2.1, panel A reveals characteristic absorption bands of DHEO,

DHE−Dimer, DHEO−Dimer and DHEO−NOVO appear at around 3355 cm^{-1} (O−H stretching), 2864 cm^{-1}, 2936 cm^{-1} and 2960 cm^{-1} (alkyl C−H stretch), and 1604 cm^{-1}, 1516 cm^{-1}, and 1445 cm^{-1} (aromatic C−C bond). After glycidylation of polyphenols with epichlorohydrin, an epoxy ring band at 912 cm^{-1} and a C−O−C ether linkage at 1028 cm^{-1} are observed (Figure 2.4). Meanwhile, OH bands of the glycidyl ethers decrease, indicating the hydroxyl groups are consumed in the glycidylation process. The FTIR results are consistent with the ^{1}H NMR analysis confirming formation of the epoxy ring. This conclusion is further supported by the FTIR spectra of the cured epoxy networks in Figure S2.1, panel B. When epoxy monomers are cured with DETA, epoxy peaks are opened while hydroxyl groups are generated concurrently. This process is reflected by the IR results, in which the epoxy band at 912 cm^{-1} of all cured networks disappear while the intensity of OH bands at around 3355 cm^{-1} increases.

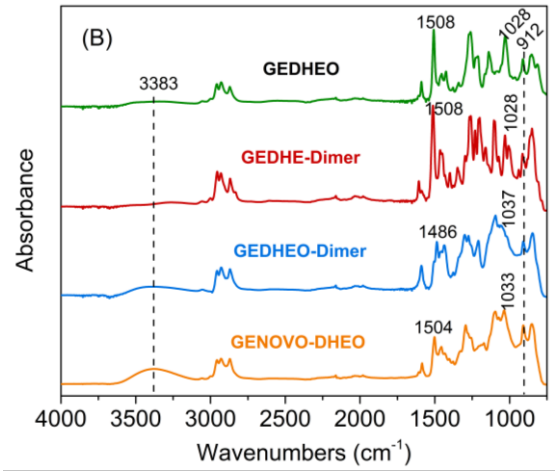

Figure 2.4 FTIR spectra of GEDHEO, (b) GEDHE−Dimer, (c) GEDHEO−Dimer and (d) GEDHEO−NOVO. FTIR bands corresponding to 912 cm^{-1} are attributed to epoxy groups.

2.2.2 Determination of Cross−link Density Using Rubber Elasticity Theory

Table 2.1. Dynamic mechanical properties and cross−link density (ν_e) of DHE−based epoxy networks. T_α is α−relaxation temperature and E_{30}' is the storage modulus at 30 °C.

Epoxy networks from	T_α (°C)	E_{30}' (MPa)	*E'* at T_α+30 °C (MPa)	ν_e (mol/dm^3)
GEDHEO	40	159	1.13	0.39
GEDHE−Dimer	70	551	4.31	1.39
GEDHEO−Dimer	84	1441	10.56	3.28
GEDHEO−NOVO	139	1703	35.91	9.77

Cross−link density (ν_e) is one of the major factors that determines the performance of an epoxy thermoset.[28] Table 2.1 reveals the cross−link density follows the order: DHEO < DHE−Dimer < DHEO−Dimer < DHEO−NOVO, which could be attributed to the variations of molecular weight, orientation and number of epoxy groups. The cross−link density of DHE−Dimer based network (1.39 mol/dm^3) is more than 3.5 times higher than that of DHEO (0.39 mol/dm^3). This evident improvement can be attributed to the following three reasons: (1) Molecular weight is increased. Increasing the molecular weight (e.g., dimerization) can provide higher cross−link density because the bonds between the iterative units are considered as *apriori* cross−links.[21] (2) The benzodioxane byproduct is avoided. As can be seen from the NMR spectra in Figure 2.3, DHEO−based epoxy monomer (panel a) contains around 20 mol% of benzodioxane byproducts that are not curable and would occupy certain free volume that impairs the cross−link density of the network, while there is no byproduct observed for the GEDHE−Dimer (panel b). (3) Orientation of functional group becomes more stretched from DHEO to DHE−Dimer. Figure S2.2 lists the simulated 3−D models of GEDHEO and GEDHE−Dimer. The two epoxy groups of GEDHEO are in *ortho* positions, which could form closed looping with DETA and limit the direction of network development. By comparison, GEDHE−Dimer has more stretched configuration of epoxy groups that can promote cross−link density.[29]

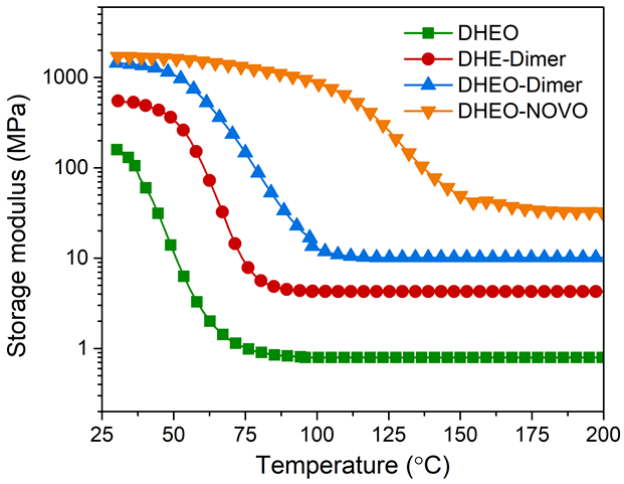

Figure 2.5 Storage modulus values of DHE−based epoxy networks as a function of temperature.

Increasing the number of functional groups is also able to improve cross−link density.[30] When methoxys of DHE−Dimer are demethylated to yield additional two hydroxyls per molecule, the obtained DHEO−Dimer based network exhibits further enhanced cross−link density of 3.28 mol/dm^3. It is evident that GEDHEO−Dimer is a dimer of GEDHEO, however, the cross−link density of GEDHEO−Dimer is around 8 times to that of GEDHEO, which also highlights the role of molecular weight. In fact, both DHEO and DHEO−Dimer would give rise to certain amounts of benzodioxane derivatives, but the negative influence of benzodioxane on cross−link density is reduced when molecular weight goes up. This is evident from the fact that DHEO−based benzodioxane is not curable while as for the epoxy mixture from DHEO−Dimer, even if the benzodioxane occurs in one benzene ring, another ring is still available for cross−link. The effect of molecular weight on cross−link density is further supported when DHEO−NOVO based network is scrutinized. As stated above, DHEO−formaldehyde reaction produces DHEO−NOVO as oligomers with average molecular weight between dimer and trimer. Even though the increase of molecular weight from DHEO−Dimer to DHEO−NOVO is not significant (less than 50% increase), DHEO−NOVO

based network exhibits significant improvement in cross−link density (from 3.28 to 9.77 mol/dm^3, around 200% increase).

Cross−link density can also be reflected from the α−relaxation temperature (T_α) because increased covalent cross−links restricts the mobility of polymer segments, which leads to higher T_α.[28,31] Table 2.1 and Figure 2.5 reveal T_α of the biobased networks follows the order: DHEO (40 °C) < DHE−Dimer (70 °C) < DHEO−Dimer (84 °C) < DHEO−NOVO (139 °C), which is in accordance with the cross−link density. The increment in T_α is significant after the modification like increasing molecular weight, adjusting orientation and improving epoxy groups. Moreover, T_α of DHEO−NOVO based network is 139 °C, which is slightly higher than the 137 °C of traditional DGEBA/DETA epoxy resins.[32] This finding highlights renewable DHE−based epoxy network has the potential to replace petroleum−based resins in terms of T_α. The storage modulus at 30 °C (E_{30}') of DHEO−NOVO based network (1703 MPa, Table 2.2) is lower than that of the DGEBA/DETA resin (3600 MPa),[32] which could be attributed to the structural disadvantages of DHEO with *ortho* epoxide and three carbon propyl tail, and the appearance of benzodioxane in the epoxy mixtures. Temperature dependence of the storage modulus of other cured DHE−based networks are also shown in Figure 2.5 and enhanced storage modulus is attributed to the increased cross−link density.

2.2.3 Effect of Modification Strategies on Curing Behaviors

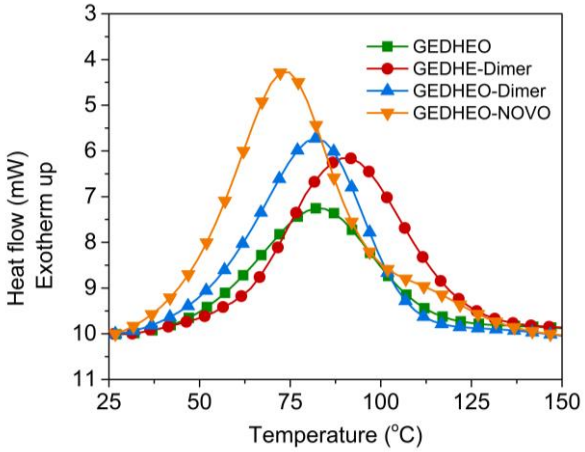

Figure 2.6 DSC temperature scans of heat release during nonisothermal cures of different DHE−based epoxy monomers/DETA curing systems at 10 °C/min.

Figure 2.6 and Table 2.2 demonstrate peak temperatures of epoxy/amine systems follow the trend: GEDHE−Dimer (91.7 °C) > GEDHEO (84.2 °C) > GEDHEO−Dimer (82.1 °C) > GEDHEO−NOVO (72.9 °C). The shift of DSC exothermic peak to lower temperature indicates increased overall activity of epoxy groups, which is derived from catalytic effects or favorable configuration.[33] GEDHE−Dimer has the highest peak temperature, which could be caused by the phenomenon that no catalytic benzodioxane byproduct is observed for GEDHE−Dimer from the NMR spectra in Figure 2.3, panel b. As for GEDHEO, GEDHEO−Dimer and GEDHEO−NOVO, certain amounts of benzodioxane with hydroxyls that can catalyze the curing reactions in these mixtures, resulting in decreased peak temperatures compared to GEDHE−Dimer. Meanwhile, the activation energy (E_a) decreases from DHEO to DHEO−NOVO, which may be attributed to improved configuration of the modified monomers.

Table 2.2. DSC curing data for DHE−based epoxy monomers/DETA systems exhibiting onset curing temperature (T_i), peak curing temperature (T_p) and activation energy (E_a).

Sample	T_i (°C)	T_p (°C)	E_a (kJ/mol)
GEDHEO	34.5	84.1	54.9
GEDHE−Dimer	51.4	91.7	45.9
GEDHEO−Dimer	42.7	82.1	44.0
GEDHEO−NOVO	39.6	72.9	41.9

2.2.4 Effect of Cross−link Density on Thermal Stability

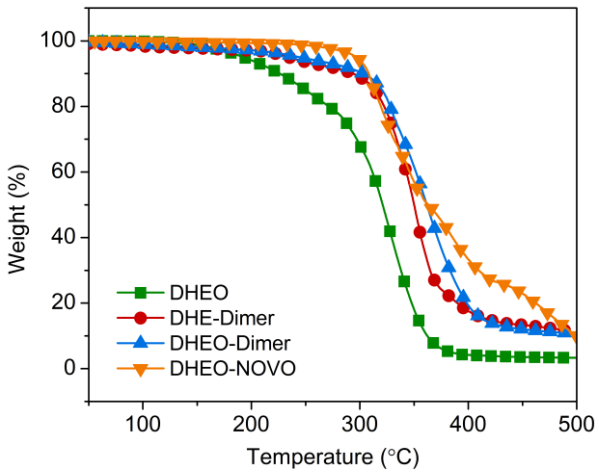

Figure 2.7 Thermogravimetric analysis thermograms of DHE−based epoxy networks as a function of temperature.

Figure 2.7 demonstrates all epoxy networks show a one−step degradation profile, which is attributed to the decomposition of cross−linked polymer network.[34] Thermal stability of the networks improves with increased cross−link density. This is reflected in the change of onset degradation temperature (expressed as T_{d5}, temperature at 5% weight loss) from 193 °C of GEDHEO based networks to 235, 245 and 297 °C of networks from DHE−Dimer, DHEO−Dimer and DHEO−NOVO, respectively. This phenomenon is explained by that polymer chains in highly−cross−linked networks are more constrained, leading to lower mobility during thermal expansion.[20] Meanwhile, the more tortuous pathway in the highly−cross−linked network postpones the decomposed products to diffuse out and heat to

flow into the underlying materials. The statistic heat−resistant index temperature (T_s),[35,36] which is calculated based on T_{d5} and T_{d30} (temperature at 30% weight loss), is characteristic of the thermal stability of cured resins. As can be seen in Table 2.3, T_s and T_{d50} (temperature at 50% weight loss) increase from DHEO to DHEO−NOVO based networks, supporting the positive role of cross−link density on thermal stability. Besides, $Char_{500}$ (char formed at 500 °C) of modified networks is also observed to be higher than the DHEO−based resin.

Table 2.3. Thermogravimetric data of T_{d5}, T_{d30}, T_{d50} (temperature at 5%, 30% and 50% weight loss), T_s (statistic heat−resistant index temperature) and $Char_{500}$ (char residue at 500 °C) of DHE−based epoxy networks.

Epoxy networks from	T_{d5} (°C)	T_{d30} (°C)	T_{d50} (°C)	T_s (°C)	$Char_{500}$ (%)
GEDHEO	193	296	321	125	3.3
GEDHE−Dimer	235	334	351	144	10.9
GEDHEO−Dimer	245	338	361	147	10.6
GEDHEO−NOVO	297	331	362	153	10.1

2.2.5 Effect of Cross−link Density on the Overall Performance of DHE−Based Epoxy Networks

To describe more clearly the role of molecular weight, orientation and number of functional groups on cross−link density, and further investigate the influence of cross−link density on the overall performance, T_α, E_{30}', T_s and ΔH of DHE−based epoxy networks are compared in Figure 2.8. Highlighted (in yellow) areas corresponding to cross−link densities of 0.39, 1.39, 3.28 and 9.77 mol/dm^3 represent the performances (T_α, E_{30}', T_s and ΔH) of networks from DHEO, DHE−Dimer, DHEO−Dimer and DHEO−NOVO, respectively. Dotted boxes (A, B and C) between the highlighted areas reflect related modification methods.

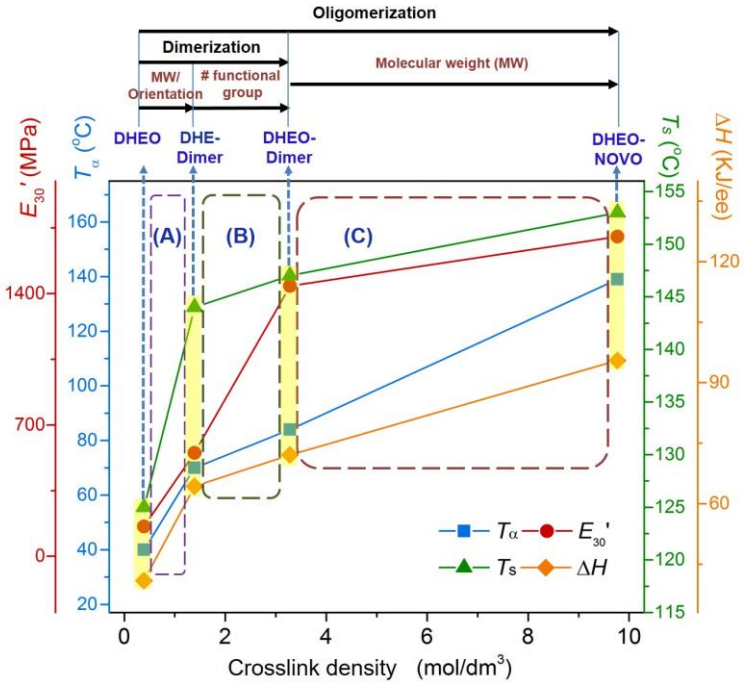

Figure 2.8 Performances (T_α, E_{30}', T_s and ΔH) of DHE−based epoxy networks as a function of cross−link density as modified through adjusting molecular weight, orientation and number of epoxy group. Highlighted areas correspond to the performances of DHE−based networks while dotted boxes between the highlighted areas reflect related modification methods.

Figure 2.8 reveals mechanical and thermal performances of DHE−based networks improve with increased cross−link density. It is important to note that performances increase proportionally with cross−link density, except a relatively higher slope in box (A) which is attributed to the role of molecular weight and orientation. The improvement in molecular weight and orientation can be easily realized by reacting DHE and aqueous HBr at ambient temperature and it is an effective way to increase cross−link density (around 256% increase and 57% increase in ΔH), mechanical (75% and 247% increase in T_α and E_{30}') and thermal (15% increase in T_s) properties as demonstrated in Figure 2.8. As stated above, for DHE−Dimer, the methylene bonds between two DHE molecules are considered as *apriori* cross−links. In

another word, by making DHE−Dimer, 50% of DHE molecules has already been linked even before the curing reaction. Moreover, the advantages of DHE−Dimer especially evident in the case of DHE−based monomer, because the undesired benzodioxane byproduct in GEDHEO is avoided and the obtained GEDHE−Dimer is more stretched.

The number of epoxy groups increases from GEDHE−Dimer to GEDHEO−Dimer. This modification, even though brings about certain amount of benzodioxane derivatives, still provides evident improvement for the networks as seen in Figure 2.8, box (B). For example, the cross−link density exhibits a 136% increase compared to the DHE−Dimer counterparts. The effect of dimerization reaction can also be evident when DHEO and DHEO−Dimer based networks are compared. As depicted in Figure 2.8, the dimerization of DHEO to DHEO−Dimer essentially consists of improvements of molecular weight, orientation and number of functional group. All these improvements contribute to the significant increase (741%) of cross−link density from DHEO to DHEO−Dimer based networks.

DHEO−NOVO based network is also featured with continuous improvements of molecular weight, orientation and number of functional group. After the phenol−formaldehyde oligomerization reaction, the molecular weight of DHEO−NOVO (average molecular weight between dimer and trimer) is slightly higher than DHEO−Dimer as mentioned above. The effect of molecular weight increase from DHEO−Dimer to DHEO−NOVO based networks can be estimated through the comparison in Figure 2.8, box (C). A 198% increase in cross−link density from DHEO−Dimer to DHEO−NOVO is observed. This might imply that a slight increase in the molecular weight can evidently promote cross−link density. Overall, it can be concluded that performance parameters of DHE−based epoxy networks improve with

increased cross−link density. Oligomerization of DHEO can create simultaneous modifications of molecular weight, orientation and number of functional groups, which lead to the highest performance parameters among all investigated networks.

2.3 Conclusions

Renewable biobased epoxy networks become more relevant if the mechanical and thermal properties are improved. DHE, a renewable building block monomer derived from lignin, has unfavorable structural characteristics if used without modification. However, modifications of DHE−based epoxy monomers through improving (1) molecular weight, (2) orientation and (3) number of epoxy groups via dimerization and oligomerization reactions are found to increase the cross−link density of cured thermosets, while enhanced cross−link density improves thermal and mechanical properties. Oligomerization of DHEO is an effective way of improving performances due to its simultaneous modifications of molecular weight, orientation and number of functional groups. The modified renewable DHE−based epoxy networks exhibit sufficiently desirable performance parameters to potentially replace petroleum−based thermosets.

2.4 Experimental Section

General. 2−methoxy−4−propylphenol, epichlorohydrin, 48% aqueous hydrobromic acid, tetrabutylammonium bromide and diethylenetriamine (DETA) were purchased from Aldrich Chemical Co. Formaldehyde solution (37%) was obtained from Macron Fine Chemicals. All chemicals were used without further purification.

2.4.1 Preparation of Polyphenols from DHE.

2.4.1.1 O–demethylation of DHE to Make Propylcatechol (DHEO).

2–methoxy–4–propylphenol (16.6 g, 0.1 mol) was added to 83 g 48% aqueous hydrobromic acid. The reaction mixture was magnetically stirred at 115 °C for 19 h, cooled to ambient temperature, saturated with NaCl and extracted 3 times with diethyl ether. The organic layer was dried over $MgSO_4$ and concentrated using rotary evaporation. The obtained DHE o–demethylated product (DHEO) (yield = 94%) was used as a dihydroxyl starting compound for epoxy monomer synthesis.

2.4.1.2 Synthesis of *6, 6′−methylenebis (2−methoxy−4−propylphenol)* (DHE−Dimer).

DHE (3.32 g, 0.02 mol), 37% formaldehyde solution (0.81 g, 0.01 mol), 48% hydrobromic acid (15 mL) and H_2O (8 mL) were stirred at room temperature for 24 h. Viscous oil was formed in the upper layer, while the lower aqueous layer was carefully removed. The oil product was washed with water 3 times and dried under vacuum overnight to yield DHE−Dimer as a viscous oil (2.86 g, 83% yield). ^{1}H NMR ($CDCl_3$, 400 MHz) δ: 6.72 (s, 2H), 6.53 (s, 2H), 5.50 (s, 2H), 3.88 (s, 6H), 3.83 (s, 2H), 2.53 (t, 4H, J =7.6 Hz), 1.62 (sex, 4H, J =7.3 Hz), 1.01 (t, 6H, J =7.6 Hz). ^{13}C NMR ($CDCl_3$, 400 MHz) δ: 144.7, 143.4, 132.3, 131.4, 119.2, 115.9, 55.9, 34.8, 34.1, 24.2, 14.1.

2.4.1.3 Synthesis of *6, 6′−methylenebis (4−propylbenzene−1, 2−diol)* (DHEO−Dimer).

DHEO−Dimer was prepared through o−demethylation of DHE−Dimer. In detail, DHE−Dimer (3.44 g, 0.01 mol) was added to 12 mL 48% aqueous hydrobromic acid. The reaction mixture was refluxed at 120 °C for 20 h, cooled to ambient temperature, saturated with NaCl and extracted 3 times with diethyl ether. The organic layer was dried over $MgSO_4$ and concentrated using rotary evaporation to obtain DHEO−Dimer as a viscous oil (2.54 g, 80% yield). ^{1}H NMR ($CDCl_3$, 400 MHz) δ: 6.68 (m, 4H), 5.69 (s, 4H), 3.81 (m, 2H), 2.44 (t, 4H, J

=6.6 Hz), 1.52 (sex, 4H, J =7.1 Hz), 0.89 (t, 6H, J =7.1 Hz). ^{13}C NMR ($CDCl_3$, 400 MHz) δ: 143.2, 141.1, 138.4, 135.9, 121.9, 115.2, 37.3, 37.2, 24.5, 13.7.

2.4.1.4 Synthesis of DHEO Novolac Oligomer (DHEO−NOVO).

DHEO (1.52 g, 0.01 mol), 37% formaldehyde solution (0.81 g, 0.01 mol), concentrated hydrochloric acid (4 mg) and H_2O (8 mL) were mixed and refluxed at 100 °C for 6 h. Water and hydrogen chloride were then evaporated under reduced pressure at 80 °C. The unreacted DHEO was removed by washing with toluene 3 times and evaporating the toluene at 40 °C under vacuum overnight to yield DHEO−NOVO as a viscous oil (1.46 g, 89% yield, based on an assumption that the novolac with an infinite molecular weight was obtained).

2.4.2 Preparation of Glycidylated Ether of DHEO, DHE−Dimer (GEDHE−Dimer), DHEO−Dimer (GEDHEO−Dimer) and DHEO−NOVO (GEDHEO−NOVO).

GEDHE−Dimer was prepared by reaction of DHE−Dimer (1.72 g, 0.005 mol) and epichlorohydrin (17 g, 0.18 mol). Tetrabutylammonium bromide (0.16 g) was used as a phase transfer catalyst. The mixture was heated at 60 °C for 3 h and followed by a dropwise addition of 0.8 g of 50% w/w NaOH solution. The reaction was kept for another 3 h and the mixture was washed with acetone, filtered to remove salt and concentrated with a rotary evaporator. GEDHEO, GEDHEO−Dimer and GEDHEO−NOVO were obtained according to the same procedure as GEDHE−Dimer.

2.4.3 Formation of DHE−Based Epoxy Networks.

DHE−based epoxy monomers, i.e., GEDHEO, GEDHE−Dimer, GEDHEO−Dimer and GEDHEO−NOVO were respectively introduced to diethylenetriamine (DETA) with stoichiometric ratio of epoxy vs. −NH for curing. The mixtures were stirred for 10 min,

degassed under vacuum to remove entrapped air and poured into molds for curing according to the profile: 55 °C for 2 h, 75 °C for 2 h and 95 °C for 2 h.

2.4.4 Analysis methods.

The structural evolution from DHE to final cured epoxy was examined using ^{1}H NMR and FTIR. The NMR spectra were performed on a Bruker Avance ARX–400 spectrometer using deuterated chloroform as solvent. FTIR analyses were conducted using a Thermo–Nicolet Nexus 470 FTIR Spectrometer equipped with an ultra–high–performance, versatile Attenuated Total Reflectance (ATR) sampling accessory. The spectra were scanned over a wavenumber range of 400–4000 cm^{-1} with a resolution of 4 cm^{-1}.

Curing profiles and catalytic curing behaviors were determined using a differential scanning calorimetry (Perkin Elmer Jade DSC 4000) under dry nitrogen atmosphere. Samples of 5–10 mg were placed in sealed aluminum pans for all DSC runs.

Dynamic mechanical properties were characterized using a DMA 2980 (TA Instruments). Rectangular specimens with dimensions of 30 mm length, 10 mm width and 2 mm thickness were measured in a single–cantilever mode. The measurements were conducted from 25 °C to 100 °C at a heating rate of 3.00 °C/min and a frequency of 1 Hz. Cross−link densities (ν_e) for cured DHE−based networks were calculated from the equilibrium storage modulus in the rubber region over the α−relaxation temperature (T_α) according to the rubber elasticity theory in Equation 1,[29–31]

$$ve = E'/(\Phi RT) \qquad (1)$$

where E' is the storage modulus at T_α+30 °C. ϕ is the front factor (approximated to 1 in the Flory theory[30,32]), while R and T are the gas constant and absolute temperature at T_α+30 °C,

respectively.

Thermal stability studies were carried out on a TGA Q500 (TA Instruments) under a nitrogen flow of 40 mL/min. Samples (15–20 mg) were placed in a platinum pan and scanned from 30 to 500 °C at a ramp rate of 20 °C/min. The statistic heat−resistant index temperature (T_s) is calculated based on T_{d5} and T_{d30} (temperature at 5% and 30% weight loss) in Equation 2:

$$T_s = 0.49\left[T_{d5} + 0.6(T_{d30} - T_{d5})\right] \qquad (2)$$

2.5 References

(1) Auvergne, R. M.; Caillol, S.; David, G.; Boutevin, B.; Pascault, J. P. *Chem. Rev.* **2013,** *114* (2), 1082−1115.

(2) Raquez, J. M.; Deléglise, M.; Lacrampe, M. F.; Krawczak, P. *Prog. Polym. Sci.* **2010,** *35* (4), 487−509.

(3) Griffini, G.; Passoni, V.; Suriano, R.; Levi, M.; Turri, S. *ACS Sustain. Chem. Eng.* **2015,** *3* (6), 1145−1154.

(4) Liu, W.; Zhou, R.; Goh, H. L. S.; Huang, S.; Lu, X. *ACS Appl. Mat. Interfaces* **2014,** *6* (8), 5810−5817.

(5) Podschun, J.; Saake, B.; Lehnen, R. *Eur. Polym. J.* **2015,** *67*, 1−11.

(6) Sen, S.; Patil, S.; Argyropoulos, D. S. *Green Chem.* **2015,** *17*, 1077−1087.

(7) Yuan, Z.; Cheng, S.; Leitch, M.; Xu, C. C. *Bioresour. Technol.* **2010,** *101* (23), 9308−9313.

(8) Thirukumaran, P.; Shakila Parveen, A.; Sarojadevi, M. *ACS Sustain. Chem. Eng.* **2014,** *2* (12), 2790−2801.

(9) Stanzione, J. F.; Sadler, J. M.; La Scala, J. J.; Wool, R. P. *ChemSusChem* **2012,** *5* (7), 1291−1297.

(10) Kaya, İ.; Doğan, F.; Gül, M. *J. Appl. Polym. Sci.* **2011,** *121* (6), 3211−3222.

(11) Sini, N. K.; Bijwe, J.; Varma, I. K. *J. Polym. Sci. Part A: Polym. Chem.* **2014,** *52* (1), 7−11.

(12) Wang, C.; Sun, J.; Liu, X.; Sudo, A.; Endo, T. *Green Chem.* **2012,** *14* (10), 2799−2806.

(13) Meylemans, H. A.; Harvey, B. G.; Reams, J. T.; Guenthner, A. J.; Cambrea, L. R.; Groshens, T. J.; Baldwin, L. C.; Garrison, M. D.; Mabry, J. M. *Biomacromolecules* **2013,** *14* (3), 771−780.

(14) Harvey, B. G.; Guenthner, A. J.; Lai, W. W.; Meylemans, H. A.; Davis, M. C.; Cambrea, L. R.; Reams, J. T.; Lamison, K. R. *Macromolecules* **2015,** *48* (10), 3173–3179.

(15) Stanzione III, J. F.; Giangiulio, P. A.; Sadler, J. M.; La Scala, J. J.; Wool, R. P. *ACS Sustain. Chem. Eng.* **2013,** *1* (4), 419−426.

(16) Enjoji, M.; Yamamoto, A.; Shibata, M. *J. Appl. Polym. Sci.* **2015,** *132* (4), 41347.

(17) Liu, J.; Ishida, H. *Macromolecules* **2014,** *47* (16), 5682−5690.

(18) Delidovich, I.; Hausoul, P. J.; Deng, L.; Pfützenreuter, R.; Rose, M.; Palkovits, R. *Chem. Rev.* **2016**, *116*, 1540−1599.

(19) Becker, O.; Cheng, Y. B.; Varley, R. J.; Simon, G. P. *Macromolecules* **2003,** *36* (5), 1616−1625.

(20) Bandyopadhyay, A.; Valavala, P. K.; Clancy, T. C.; Wise, K. E.; Odegard, G. M. *Polymer* **2011,** *52* (11), 2445−2452.

(21) Ogata, M.; Kinjo, N.; Kawata, T. *J. Appl. Polym. Sci.* **1993,** *48* (4), 583−601.

(22) Chung, H.; Washburn, N. R. *ACS Appl. Mat. Interfaces* **2012,** *4* (6), 2840−2846.

(23) Dingemans, T. J.; Mendes, E.; Hinkley, J. J.; Weiser, E. S.; StClair, T. L. *Macromolecules* **2008,** *41* (7), 2474−2483.

(24) Guenthner, A. J.; Lamison, K. R.; Vij, V.; Reams, J. T.; Yandek, G. R.; Mabry, J. M. *Macromolecules* **2011,** *45* (1), 211−220.

(25) Parsell, T.; Yohe, S.; Degenstein, J.; Jarrell, T.; Klein, I.; Gencer, E.; Hewetson, B.; Hurt, M.; Im Kim, J.; Choudhari, H.; Saha, B.; Meilan, R.; Mosier, N.; Ribeiro, F.; Delgass, W. N.; Chapple, C.; Kenttämaa, H.I.; Agrawal, R.; Abu−Omar, M. M. *Green Chem.* **2015,** *17*, 1492−1499.

(26) Zhao, S.; Abu−Omar, M. M. *Biomacromolecules* **2015,** *16* (7), 2025−2031.

(27) Meylemans, H. A.; Groshens, T. J.; Harvey, B. G. *ChemSusChem* **2012,** *5* (1), 206−210.

(28) Putz, K. W.; Palmeri, M. J.; Cohn, R. B.; Andrews, R.; Brinson, L. C. *Macromolecules* **2008,** *41* (18), 6752−6756.

(29) Van Krevelen, D. W.; Te Nijenhuis, K., *Properties of Polymers,* 4th ed; Elsevier: Amsterdam, 2009.

(30) Pan, X.; Sengupta, P.; Webster, D. C. *Biomacromolecules* **2011,** *12* (6), 2416−2428.

(31) Wu, S.; Guo, Q.; Kraska, M.; Stühn, B.; Mai, Y. W. *Macromolecules* **2013,** *46* (20), 8190−8202.

(32) Garcia, F. G.; Soares, B. G.; Pita, V. J. R. R.; Sánchez, R.; Rieumont, J. *J. Appl. Polym. Sci.* **2007,** *106* (3), 2047−2055.

(33) Alzina, C.; Mija, A.; Vincent, L.; Sbirrazzuoli, N. *J. Phys. Chem. B* **2012,** *116* (19), 5786−5794.

(34) Lligadas, G.; Ronda, J. C.; Galià, M.; Cádiz, V. *Biomacromolecules* **2006,** *7* (12), 3521−3526.

(35) Benyahya, S.; Aouf, C.; Caillol, S.; Boutevin, B.; Pascault, J. P.; Fulcrand, H. *Ind. Crop.*

Prod. **2014,** *53*, 296−307.

(36) Chiu, Y. C.; Tsai, H. C.; Imae, T. *J. Appl. Polym. Sci.* **2012,** *124* (2), 1234−1240.

(37) Iijima, T.; Yoshioka, N.; Tomoi, M. *Eur. Polym. J.* **1992,** *28* (6), 573−581.

(38) Nouailhas, H.; Aouf, C.; Le Guerneve, C.; Caillol, S.; Boutevin, B.; Fulcrand, H. *J. Polym. Sci. Part A: Polym. Chem.* **2011,** *49* (10), 2261−2270.

(39) Cook, W. D.; Schiller, T. L.; Chen, F.; Moorhoff, C.; Thang, S. H.; Bowman, C. N.; Scott, T. F. *Macromolecules* **2012,** *45* (24), 9734−9741.

(40) Flory, P. J. Molecular theory of rubber elasticity. *Polymer* **1979,** *20* (11), 1317−1320.

Chapter 3

Universal Modifications of LDPMs to Make Epoxy Thermosets

ABSTRACT: The development of thermosets from lignin−derived phenol monomers (LDPMs) is often impeded by deficiency in hydroxyl functional groups and the need for complex separations. Three modifications are described herein, which improve greatly the feasibility of LDP−based thermosets: 1) o−demethylation of methoxy substituents, 2) oligomerization of guaiacol derivatives, and 3) oligomerization of catechol derivatives. A synthetic lignin−based bio−oil containing featured LDPMs is used to confirm the feasibility of the described approaches. Structural evolution from bio−oil to epoxy thermosets is followed by high−performance liquid chromatography, nuclear magnetic resonance and Fourier transform infrared spectroscopic characterizations. The described modifications (deployed individually or collectively) provide universal routes to LDPMs−based epoxy thermosets. Meanwhile, the resulting thermosets exhibit markedly wide range of glass transition temperature (55−116 °C) and glassy modulus (364−3553 MPa), making them suitable for various applications.

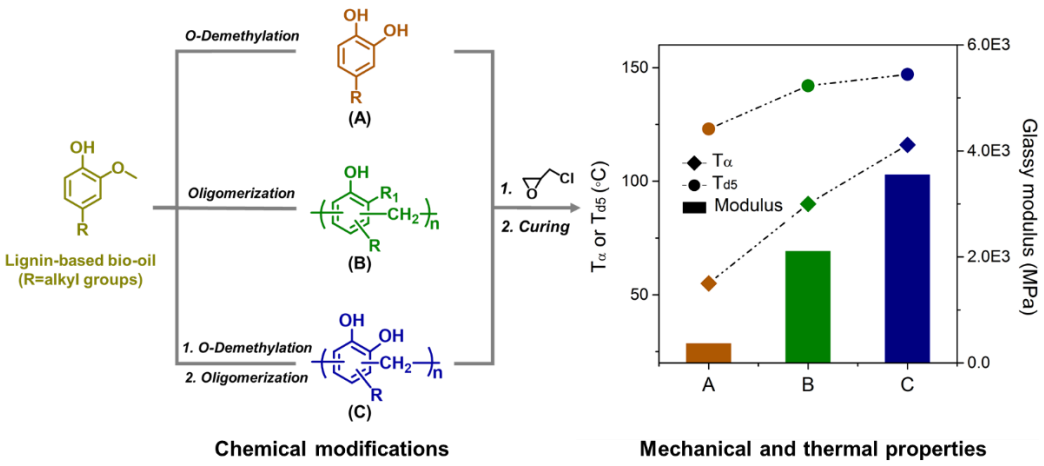

3.1 Introduction

Epoxy thermosets are highly versatile polymers that are used in adhesives, composites, electronics and coatings. By far, petroleum−based bisphenol A (BPA) is still the most extensively used epoxy thermoset precursor because its aromatic structure provides a polymer matrix with high rigidity and thermal stability.[1] However, renewable resources have recently gained increasing interest in polymer applications.[2,3] Among these, lignin is considered as the most reasonable feedstock for thermoset synthesis, as it is the sole large−volume sustainable source composed of an aromatic skeleton.[4] The rapid development of lignin depolymerization and valorization has augmented the feasibility of lignin−based polymers.[5]

Valorization of lignin through pyrolysis, oxidation, hydroprocessing, and catalytic approaches yields a bio−oil mixture of lignin−derived phenol monomers (LDPMs).[6–12] Conversion of LDPMs to thermoset materials is limited by deficiency of functional hydroxyl groups and the need for pure monomer, which would require expensive separations of a complex mixture.[13,14] On one hand, LDPMs generally possess a structural characteristic of phenol substituted by inert methoxy at *ortho* sites and alkyl groups at *para* sites (structures resembling creosol).[15] Such structures makes LDPMs especially difficult to be directly employed as epoxy thermoset precursor, as cross−linkable precursor must have at least two functional OH groups per molecule. On the other hand, most lignin−based polymers reported in literature involve the use of high−purity individual LDPMs.[16–18] Furthermore, modifications that work for one type of monomer do not necessarily apply to LDPM mixtures. For example, vanillin has been widely studied as a renewable building block.[19] Most modifications of vanillin involve: 1) converting the aldehyde group to carboxylic acid or alcohol via oxidation

or reduction,[20,21] or 2) dimerization through acetalization[22] and amine/aldehyde reactions.[23] While these approaches uniformly functionalize vanillin at the *para* aldehyde group, most LDPMs are more inert as their *para* site is substituted by unreactive alkyl group. The appearance of these unreactive species in bio−oil evidently dilutes the content of modifiable sites. Besides, because of the structural similarity of LDPMs, sophisticated separation processes are often needed to isolate monomers, and such processes are energy intensive.[24]

In this study, the feasibility of lignin−based bio−oil as epoxy thermoset precursor is developed. A synthetic bio−oil mixture proposed by Wool *et al*. is used to simulate LDP mixtures.[25] According to Wool *et al.*, this bio−oil mimic was adopted from the aromatic products of pyrolysis of Kraft pine lignin (Indulin AT) at 400 °C for 7.5 min in a nitrogen atmosphere.[26] Composition of this bio−oil mimic is representative as the selected phenolic compounds account for ~ 84 wt % of pyrolysis products. From the aspect of structure, most of these compounds are creosol derivatives, which is consistent with the characteristic structure of LDPMs mentioned above. For LDPMs that possess reactive *para* site like aldehyde and unsaturated bonds, they can be readily converted to alkyl group (characteristic structure), or hydroxyl or carboxylic acid (functional groups) through reduction/oxidation in preliminary treatments of the bio−oil mixture. Three chemical modifications of LDPMs (Scheme 3.1) are described: 1) o−demethylation of the methoxy group. This is the most straightforward approach that yields catechol derivatives with two OHs. 2) Oligomerization through the *ortho* and/or *para* site. As LDPMs in bio−oil have unoccupied phenolic *ortho* and/or *para* sites. Thus, phenol−formaldehyde reaction can be used to make oligomers with increased molecular weight and number of hydroxyl groups. 3) Oligomerization of demethylated bio−oil (catechol

derivatives, enhanced content of *para* site compared to 2). Compared to guaiacols, catechol derivatives have enhanced number of *para* and *ortho* site for oligomerization. These newly formed sites, especially the *para* site, improve the reactivity of LDPMs that could yield oligomers with high molecular weights.[18] While the proposed modifications are especially suitable for guaiacyl−derived phenols (which are most abundant in LDPMs), they also apply to phenols derived from *p*−hydroxyphenyl and syringyl units of lignin, which makes these modifications universal to all lignin types. The proposed phenol precursors are then converted to the corresponding glycidyl ethers and cured to epoxy thermosets. Compared to epoxy materials based on petroleum− or lignin−derived pure monomers, this work provides a synthetic route to renewable materials that are environmentally and economically attractive.

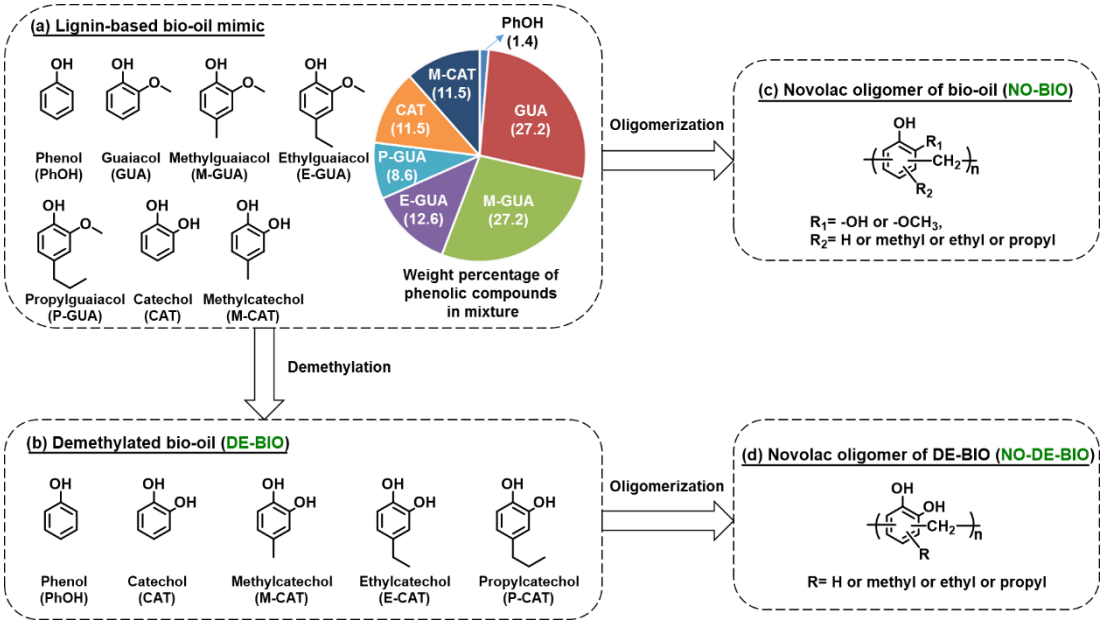

Scheme 3.1. Chemical composition of (a) lignin−based bio−oil mimic, (b) o−demethylated bio−oil (DE−BIO), and derived novolac oligomers (c) NO−BIO and (d) NO−DE−BIO.

3.2 Results and Discussion

3.2.1 Structure of Demethylated Phenolics and Glycidyl Ethers

O−demethylation of lignin−based bio−oil yields catechol derivatives with two hydroxyls, which makes them suitable as epoxy thermoset precursors. To confirm the resulting structure, proton NMR spectra of individual starting guaiacols (guaiacol, 4−methylguaiacol, 4−ethylguaiacol and 4−propylguaiacol), obtained catechols and corresponding glycidyl ethers are shown in Figures S3.1−S3.5. NMR spectra of guaiacols show the $-OCH_3$ group at around δ 3.8 ppm (panel a). After o−demethylation reaction, the peak for $-OCH_3$ group vanished while OH peaks became evident at δ 4.9−6.1 ppm, which suggested complete o−demethylation (panel b). Glycidylation of catechols with epichlorohydrin yielded two products (panel c). Protons of the desired methyloxirane product were observed at δ 2.78 (H1a), 2.89 (H1b) and 3.36 (H2). Because the adjacent OHs could form intramolecular ring with epichlorohydrin, protons of benzodioxane byproduct were also observed at δ 3.95 (H3a), 4.03 (H2), and 4.25 (H3b).

After confirming the structure of individual compounds, components in bio−oil mixture were identified through HPLC analysis. Figure S3.6, panel a, illustrates the components in starting bio−oil. After o−demethylation, Figure S3.6, panel b, shows all starting guaiacols are demethylated to the corresponding catechols. The measured molar ratio of catechols is similar with theoretical values, which confirms the composition of DE−BIO (Table 3.1). Products of glycidylation of DE−BIO are listed in Figure S3.6, panel c. In accordance with the NMR results, both methyloxirane and benzodioxane products are observed, with an approximate molar ratio of 60:40, respectively.

Table 3.1. Molar ratio of compounds in bio−oil before and after o−demethylation.

Phenolic compound	*Prepared*[a] *(mol %)*	*Theoretical*[b] *(mol %)*	*Measured*[b] *(mol %)*
Phenol	2	2	2
Guaiacol	29	0	0
Methylguaiacol	25	0	0
Ethylguaiacol	11	0	0
Propylguaiacol	7	0	0
Catechol	14	47	41
Methylcatechol	12	33	34
Ethylcatechol	0	11	12
Propylcatechol	0	7	11

[a] As initially prepared. [b] After demethylation.

Oligomers of bio−oil and DE−BIO were prepared through the phenol−formaldehyde condensation reaction. NMR spectra of NO−BIO and NO−DE−BIO are illustrated in Figure S3.7, panels a and b. Compared to the starting monomers, NO−BIO and NO−DE−BIO exhibit new peaks at 3.4−4.2 ppm, which is attributed to the methylene linkage. Other characteristic peaks observed are at 0.8−2.6 ppm (aliphatic protons), 5.8−7.3 ppm (aromatic protons) and 7.7−9.1 ppm (aromatic OH). When NO−BIO and NO−DE−BIO are converted to glycidyl ethers (Figure S3.7, panels c and d), peaks of aromatic OH disappear, while new peaks are observed at 2.6−2.9 ppm and 3.2−3.4 ppm for methyloxirane and 3.7−4.4 for benzodioxane derivatives.

Structures of DE−BIO, NO−BIO and NO−DE−BIO are further confirmed by IR. Figure 3.1, panels a, d, and g exhibit characteristic absorption bands of DE−BIO, NO−BIO and NO−DE−BIO at 3064−3595 cm^{-1} (O−H stretching), 2871, 2942 and 2965 cm^{-1} (alkyl C−H stretch) and 1608, 1510 and 1437 cm^{-1} (aromatic C−C bond). When polyphenols are converted to glycidyl ethers, the broad hydroxyl band diminishes significantly, while a C−O−C ether

linkage at around 1028 cm^{-1} and an oxirane band at 912 cm^{-1} appear (Figure 3.1, panels b, e and h). This is in accordance with the NMR results confirming the formation of epoxide group. When epoxy monomers are reacted with DETA, epoxy groups are opened by the NH− group while OH groups are formed concurrently. This process is confirmed by the IR spectra of cured networks (Figure 3.1, panels c, f and i), in which the oxirane band at 912 cm^{-1} decreases while the OH band grows.

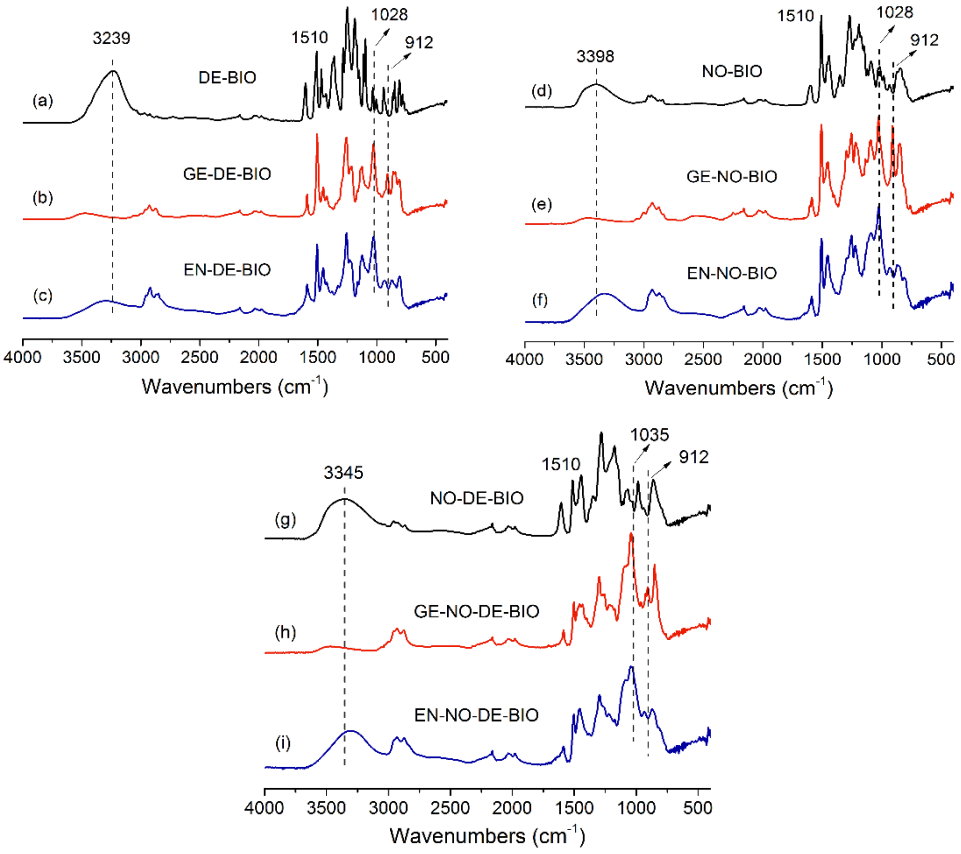

Figure 3.1 FTIR spectra of lignin−based polyphenols (a, d and g), their glycidylation products (b, e and h) and cured epoxy networks (c, f and i).

3.2.2 Differential Scanning Calorimetry Analysis

Table 3.2. DSC curing data for epoxy monomer/DETA systems exhibiting peak curing temperature (T_p), enthalpy of reaction (ΔH) and activation energy (E_a).

Epoxy monomer	T_p (°C)	ΔH (kJ/ee)	E_a (kJ/mol)
GE−DE−BIO	77	93	50
GE−NO−BIO	80	95	54
GE−NO−DE−BIO	69	96	43

Table 3.2 and Figure 3.2 illustrate peak temperatures of epoxy/amine curing system, which follow the order: GE−NO−DE−BIO (69 °C) < GE−DE−BIO (77 °C) < GE−NO−BIO (80 °C). The shift of exothermic peak to lower temperature suggests improved reactivity of epoxy groups, which could be associated with a catalytic effect. As mentioned above, glycidylation of catechol yields certain amount of benzodioxane byproduct. The hydroxyl group of benzodioxane could catalyze the epoxy/amine reaction,[4] which explains the lower peak temperature of GE−NO−DE−BIO and GE−DE−BIO. By comparison, since NO−BIO was prepared from non−demethylated bio−oil, there are large portion of guaiacol derivatives existing in NO−BIO. Glycidylation of guaiacol with epichlorohydrin does not yield benzodioxane byproduct, which explains the highest peak temperature of GE−NO−BIO curing system. Activation energy (E_a) of these systems exhibits the same trend as peak temperature, which confirms the catalytic effect of benzodioxane. Enthalpy (ΔH) values of all curing systems fall in the range of 93 to 96 kJ/ee, which is consistent with the typical value of 90−100 kJ/ee for epoxy/amine reactions.

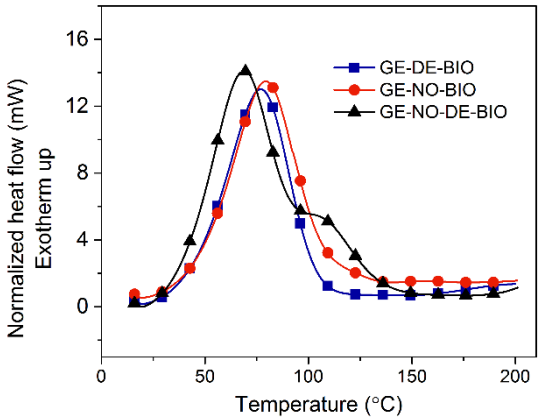

Figure 3.2 DSC temperature scans of heat release during nonisothermal cures of different epoxy monomers/DETA curing systems at 10 °C/min.

3.2.3 Dynamic Mechanical Analysis

Cross−link density (ν_e) is one of the fundamental parameters that determines the mechanical performance of epoxy thermosets.[32] ν_e is often related to the glass transition temperature (T_g), as improved covalent cross−links restrict the mobility of polymer chain segments, leading to higher T_g. Figure 3.3 reveals T_α (α−relaxation temperature, peak temperature of tan delta curve, also related to T_g) of epoxy networks that follow the order: EN−DE−BIO (55 °C) < EN−NO−BIO (90 °C) < EN−NO−DE−BIO (116 °C). Starting with the same bio−oil, DE−BIO and NO−BIO were obtained from respective demethylation and oligomerization. Oligomerization of bio−oil results in greater increment in T_α, which can be rationalized as follows. Compared to catechol monomers in DE−BIO, increased molecular weight of NO−BIO confers higher cross−link density since the covalent bonds between oligomer iterative units have already been linked before curing.[28] On the other hand, catechol derivatives in DE−BIO have hydroxyls in adjacent positions. This configuration often restricts the branching of networks and generates close loop with curing agent. By comparison, NO−BIO contains majority of iterative guaiacol units connecting by methylene linkages at

ortho sites. Methylene linkages can effectively enhance the space between OH groups, which improve the branching and cross−links. It is noteworthy that the number of hydroxyl groups can also affect the cross−links.[29] However, although catechol units have higher number of hydroxyls than guaiacol units, around 40 mol% of catechols end up being benzodioxane derivatives when reacted with epichlorohydrin (see HPLC results), making epoxy contents (EEW) of GE−DE−BIO and GE−NO−BIO roughly the same.

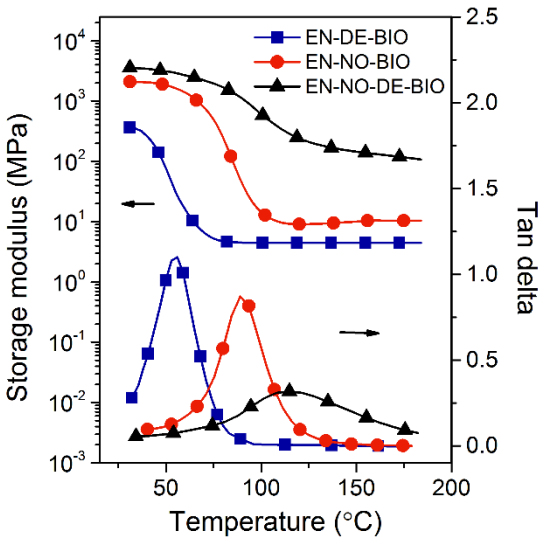

Figure 3.3 DMA curves of epoxy networks derived from lignin−based bio−oil after various chemical modifications. Temperature at the maximum in tan δ curve is taken as T_α (related to glass transition).

Compared to individual modification, when bio−oil was modified successively with o−demethylation and oligomerization, the resulting network EN−NO−DE−BIO exhibits the highest T_α. This increment is related to molecular weight and orientation of epoxy monomers. It is known that aromatic *para* sites have higher reactivity over *ortho* sites towards the phenol−formaldehyde reaction. For lignin−based guaiacols, the phenolic *para* site is often substituted by alkyl group. Thus, oligomerization of guaiacol derivatives (NO−BIO approach)

mainly occurs at the *ortho* site of iterative units. This *ortho*−specific coupling reduces the molecular weight of oligomers due to steric. By comparison, when guaiacol derivatives were demethylated to the corresponding catechols, a *para* site corresponding to the newly−formed hydroxyl is generated. As reported by previous studies, this *para* site can improve the reactivity and thus yield NO−DE−BIO with higher molecular weight.[18] Meanwhile, coupling at the *para* site makes hydroxyls have more stretched orientation compared to *ortho*−linked guaiacol derivatives in NO−BIO. Improved orientation further increases the cross−link density of the resulting network.[30,31]

Besides T_α, cross−link density of epoxy networks can also be reflected by the storage modulus and equilibrium modulus in the rubber region. As seen in Figure 3.3, storage modulus follows the order: EN−DE−BIO < EN−NO−BIO < EN−NO−DE−BIO in the temperature range of 30 to 180 °C (spanning both glassy and equilibrium regions), which is consistent with T_α. Since EN−DE−BIO, EN−NO−BIO and EN−NO−DE−BIO have the same monomers (they are derived from the same starting bio−oil), the network with higher cross−link density generally possesses enhanced modulus.[32,33] It is noteworthy that the glassy modulus E_{30}' (storage modulus at 30 °C) of EN−NO−BIO and EN−NO−DE−BIO are 2.10 and 3.55 GPa, while their T_α are 90 and 116 °C, respectively. To compare the mechanical properties of these networks with BPA–based materials, diglycidyl ether of BPA (DGEBA) and DETA were cured using the same curing profile. E_{30}' and T_α of DGEBA/DETA network were found to be 2.04 GPa and 100 °C, which are comparable to the networks prepared in this work. This phenomenon demonstrates that lignin−based epoxy networks have noticeable rigidity and strength that can compete with BPA−based materials. By comparison, EN−DE−BIO exhibits more

elastomer−like properties (T_α of 55 °C and E_{30}' of 364 MPa). This significant difference makes lignin−based thermosets with tunable mechanical properties, which widens their applications.

Mechanical performance of networks prepared from demethylated individual monomers (i.e., catechol, methylcatechol and propylcatechol) were also characterized and summarized in Figure 3.4. Generally, networks prepared from demethylated individual monomers exhibit similar properties to those from the bio−oil mixture such as EN−DE−BIO (T_α of 40−62 °C vs. 55 °C, and E_{30}' of 158−371 MPa vs. 364 MPa). Meanwhile, mechanical performance decreases as the alkyl chain of catechols increases: EN−P−CAT < EN−M−CAT < EN−CAT. This is attributed to the steric effect of the alkyl side chain, which creates certain amount of void volume and impedes the epoxy/amine cross−link reaction.

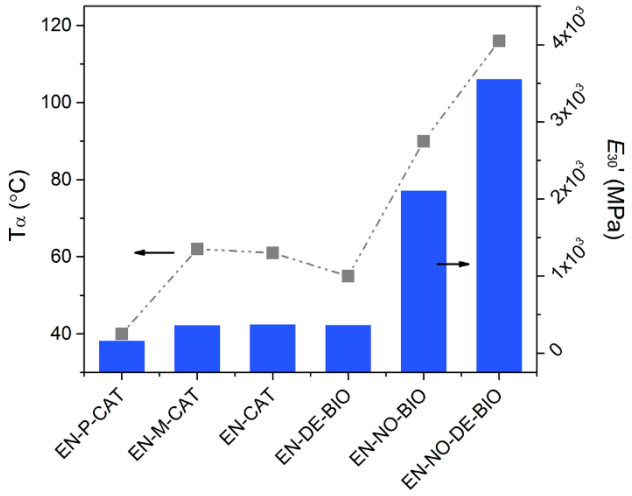

Figure 3.4 Mechanical properties of lignin−derived epoxy networks. T_α is α−relaxation temperature and E_{30}' is the glassy storage modulus at 30 °C.

3.2.4 Thermogravimetric Analysis

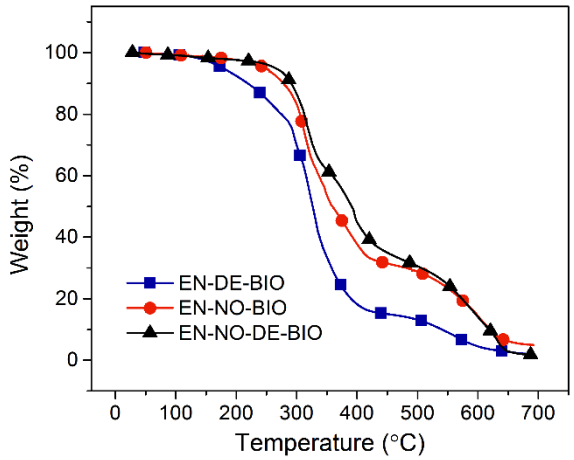

Figure 3.5 Thermogravimetric analysis thermograms of lignin−derived epoxy networks.

Table 3.3. Thermogravimetric data of T_{d5}, T_{d30}, T_{d50} (temperature at 5%, 30% and 50% weight loss), T_s (statistic heat−resistant index temperature) and $Char_{500}$ (char residue at 500 °C) of lignin−derived epoxy networks.

Epoxy networks	T_{d5} (°C)	T_{d30} (°C)	T_{d50} (°C)	T_s (°C)	$Char_{500}$ (%)
EN−DE−BIO	181	299	326	123	13
EN−NO−BIO	251	318	361	142	28
EN−NO−DE−BIO	264	326	392	147	31
EN−P−CAT	193	295	321	124	3
EN−M−CAT	184	309	330	127	11
EN−CAT	195	310	333	129	13

Figure 3.5 reveals degradation curves of lignin−derived epoxy networks. Figure 3.5 and Table 3.3 demonstrate thermal stability increases with enhanced cross−link density (i.e., EN−DE−BIO < EN−NO−BIO < EN−NO−DE−BIO). This is reflected from the shift of onset degradation temperature (defined as T_{d5}, temperature at 5% weight loss) from EN−DE−BIO (181 °C) to EN−NO−BIO (251 °C) and EN−NO−DE−BIO (264 °C). This trend can be attributed to the more constrained structure of networks with higher cross−link density, which results in lower chain mobility during thermal expansion. Meanwhile, mass exchange is more

likely to be postponed in the tortuous pathway of high−cross−linked networks. T_{d30}, T_{d50} (temperature at 30% and 50% weight loss), and T_s (statistic heat−resistant index temperature) demonstrate the same trend with T_{d5}, which confirms the role of cross−link density. Table 3.3 also illustrates thermal parameters of networks prepared from individual monomers (EN−P−CAT, EN−M−CAT and EN−CAT). These networks exhibit similar performance to EN−DE−BIO, which is in accordance with the mechanical properties. When the temperature reaches 500 °C, the majority of polymer mass has been burned out, with 3−31% weight of char formed.

3.3 Conclusions

Lignin−derived phenols typically possess unfavorable structural characteristics if they are employed directly as epoxy thermoset precursors. Modifications of LDP mixtures through o−demethylation and/or oligomerization have proved their universality and feasibility in making lignin−based epoxy thermosets. O−demethylation and oligomerization, while employed individually or collectively, can yield polyphenols with different molecular weights, number of functional hydroxyl groups (−OH) and hydroxyl orientations, whose enhancement results in increased cross−link density, and thus improved mechanical and thermal performance of obtained thermosets. Simple o−demethylation provides thermoset with elastomer−like properties (low modulus and T_g), while oligomerization of o−demethylated LDP mixtures lead to rigid thermoset that is comparable to BPA−based analogs. The tunable properties of renewable lignin−based thermosets may widen their applications. Meanwhile, utilization of LDP mixtures minimizes the number of sepatation steps, making the proposed approaches environmetnally and economically attractive.

3.4 Experimental Section

General. Phenol (PhOH), guaiacol (GUA), 4−methylguaiacol (M−GUA), 4−ethylguaiacol (E−GUA), 4−propylguaiacol (P−GUA), catechol (CAT), 4−methylcatechol (M−CAT), 48% aqueous hydrobromic acid, epichlorohydrin, tetrabutylammonium bromide, diglycidyl ether of bisphenol A (DGEBA) and diethylenetriamine (DETA) were purchased from Aldrich Chemical Co. Formaldehyde solution (37%) was obtained from Macron Fine Chemicals. All chemicals were used as received without further purification. Composition of phenolics in bio−oil mimic is given in Scheme 3.1. According to Wool *et al.*, this composition represented ~ 84 wt% of phenolic compounds derived from pyrolysis of Kraft pine lignin (Indulin AT) at 400 °C for 7.5 min in a nitrogen atmosphere.

3.4.1 Preparation of Demethylated Bio−Oil (DE−BIO).

Bio−oil (5.0 g, 38.2 mmol of phenolic compounds) was added to 30 g of 48% aqueous hydrobromic acid. The reaction mixture was vigorously stirred and refluxed at 120 °C for 24 h, cooled to ambient temperature, saturated with NaCl, and extracted 3 times with ethyl acetate. The organic layer was dried with $MgSO_4$ and concentrated using rotary evaporation to yield demethylated bio−oil as a brownish oil (94% yield based on mass). Individual compounds, i.e., guaiacol, 4−methylguaiacol, 4−ethylguaiacol and 4−propylguaiacol were demethylated to corresponding catechols using the same method as bio−oil. Retention time of obtained catechols was recorded by HPLC, and HPLC analysis of bio−oil and DE−BIO confirmed the consistency of molar ratio of compounds before and after demethylation (Table 3.1).

3.4.2 Preparation of Novolac Oligomers of Bio−Oil (NO−BIO) and DE−BIO (NO−DE−BIO).

Bio−oil (2.0 g, 15.3 mmol of phenolic compounds), 37% formaldehyde solution (1.24 g,

15.3 mol), concentrated hydrochloric acid (6 mg) and H_2O (10 mL) were added to a 50 mL round−bottomed flask, and the solution was refluxed at 100 °C for 6 h. Water and hydrogen chloride were then evaporated under reduced pressure at 80 °C. Unreacted compounds were removed by washing with toluene 3 times. Removing the toluene under vacuum overnight yielded NO−BIO as a brownish solid (89% yield based on mass). NO−DE−BIO (91% yield) was prepared from DE−BIO and formaldehyde using the same procedure as that described for NO−BIO.

3.4.3 Preparation of Glycidyl Ethers of DE−BIO, NO−BIO and NO−DE−BIO.

Glycidyl ether of DE−BIO (GE−DE−BIO) was prepared by reaction of DE−BIO (2.0 g, 16.5 mmol) and epichlorohydrin (20 g, 213.3 mmol). Tetrabutylammonium bromide (0.25 g, 0.8 mmol) was used as a phase transfer catalyst. The mixture was heated at 75 °C for 3 h and followed by a dropwise addition of 6 g of 20% w/w NaOH solution. The reaction was kept for another 2.0 h, and the mixture was washed with acetone, filtered to remove formed NaCl and concentrated with a rotary evaporator to yield GE−DE−BIO as a brownish oil (2.97 g). Other glycidyl ethers (GE−NO−BIO and GE−NO−DE−BIO) were prepared using the same method as GE−DE−BIO, with similar yields. Epoxy equivalent weight (EEW) was determined to be 198, 206 and 195 g/eq. for GE−DE−BIO, GE−NO−BIO and GE−NO−DE−BIO, respectively, by the HCl/acetone titration method.

3.4.4 Formation of Epoxy Networks.

Bio−oil based epoxy monomers, i.e., GE−DE−BIO, GE−NO−BIO and GE−NO−DE−BIO, were respectively mixed with diethylenetriamine (DETA) with stoichiometric ratio of epoxy vs. −NH for curing. The mixtures were stirred for 10 min, degassed under vacuum to remove

entrapped air and poured into silicone molds for curing with the profile: 65 °C for 8 h, 90 °C for 2 h and 120 °C for 2 h. Cured epoxy networks were expressed as EN−DE−BIO, EN−NO−BIO and EN−NO−DE−BIO, respectively. Epoxy networks based on pure monomers, i.e., propylcatechol, methylcatechol and catechol, were also prepared for comparison and expressed as EN−P−CAT, EN−M−CAT and EN−CAT, respectively.

3.4.5 Analysis Methods.

Analysis methods are similar to Chapter 2.

3.5 References

(1) Auvergne, R. M.; Caillol, S.; David, G.; Boutevin, B.; Pascault, J. P. *Chem. Rev.* **2013**, *114*, 1082−1115.

(2) Gandini, A. *Macromolecules* **2008**, *41*, 9491−9504.

(3) Schneiderman, D. K.; Hillmyer, M. A. *Macromolecules* **2017**, *50*, 3733−3749.

(4) Zhao, S.; Abu−Omar, M. M. *ACS Sustainable Chem. Eng.* **2017**, *5*, 5059−5066.

(5) Kaiho, A.; Mazzarella, D.; Satake, M.; Kogo, M.; Sakai, R.; Watanabe, T. *Green Chem.* **2016**, *18*, 6526−6535.

(6) Zakzeski, J.; Bruijnincx, P. C. A.; Jongerius, A. L.; Weckhuysen, B. M. *Chem. Rev.* **2010**, *110*, 3552−3599.

(7) Upton, B. M.; Kasko, A. M. *Chem. Rev.* **2015**, *116*, 2275−2306.

(8) Song, Q.; Wang, F.; Cai, J.; Wang, Y.; Zhang, J.; Yu, W.; Xu, J. *Energy & Environ. Sci.* **2013**, *6*, 994−1007.

(9) Lange, H.; Decina, S.; Crestini, C. *Eur. Polym. J.* **2013**, *49*, 1151−1173.

(10) Parsell, T.; Yohe, S.; Degenstein, J.; Jarrell, T.; Klein, I.; Gencer, E.; Hewetson, B.; Hurt,

M.; Im Kim, J.; Choudhari, H.; Saha, H.; Meilan, R.; Mosier, N.; Ribeiro, F.; Delgass, W. N.; Chapple, C.; Kenttämaa, H. I.; Agrawal, R.; Abu−Omar, M. M. *Green Chem.* **2015**, *17*, 1492−1499.

(11) Luo, H.; Klein, I. M.; Jiang, Y.; Zhu, H.; Liu, B.; Kenttämaa, H. I.; Abu−Omar, M. M. *ACS Sustainable Chem. Eng.* **2016**, *4*, 2316−2322.

(12) F. De Gregorio, G.; Prado, R.; Vriamont, C.; Erdocia, X.; Labidi, J.; Hallett, J. P.; Welton, T. *ACS Sustainable Chem. Eng.* **2016**, *4*, 6031−6036.

(13) Zhao, S.; Abu−Omar, M. M. *Biomacromolecules* **2015**, *16*, 2025−2031.

(14) Holmberg, A. L.; Karavolias, M. G.; Epps, T. H. *Polym. Chem.* **2015**, *6*, 5728−5739.

(15) Pandey, M. P.; Kim, C. S. *Chem. Eng. Technol.* **2011**, *34*, 29−41.

(16) Thirukumaran, P.; Shakila Parveen, A.; Sarojadevi, M. *ACS Sustainable Chem. Eng.* **2014**, *2*, 2790−2801.

(17) Meylemans, H. A.; Harvey, B. G.; Reams, J. T.; Guenthner, A. J.; Cambrea, L. R.; Groshens, T. J.; Baldwin, L. C.; Garrison, M. D.; Mabry, J. M. *Biomacromolecules* **2013**, *14*, 771−780.

(18) Zhao, S.; Abu−Omar, M. M. *Macromolecules* **2017**, *50*, 3573−3581.

(19) Fache, M.; Boutevin, B.; Caillol, S. *ACS Sustainable Chem. Eng.* **2015**, *4*, 35−46.

(20) Fache, M.; Darroman, E.; Besse, V.; Auvergne, R.; Caillol, S.; Boutevin, B. *Green Chem.* **2014**, *16*, 1987−1998.

(21) Fache, M.; Boutevin, B.; Caillol, S. *Eur. Polym. J.* **2015**, *68*, 488−502.

(22) Koike, T. *Polym. Eng. Sci.* **2012**, *52*, 701−717.

(23) Gu, L.; Chen, G.; Yao, Y. *Polym. Degrad. Stab.* **2014**, *108*, 68−75.

(24) Mülhaupt, R. *Macromol. Chem. Phys.* **2013**, *214*, 159−174.

(25) Stanzione III, J. F.; Giangiulio, P. A.; Sadler, J. M.; La Scala, J. J.; Wool, R. P. *ACS Sustainable Chem. Eng.* **2013**, *1*, 419−426.

(26) Jegers, H. E.; Klein, M. T. *Ind. Eng. Chem. Process Des. Dev.* **1985**, *24*, 173−183.

(27) Kissinger, H. E. *Anal. Chem.* **1957**, *29*, 1702−1706.

(28) Ogata, M.; Kinjo, N.; Kawata, T. *J. Appl. Polym. Sci.* **1993**, *48*, 583−601.

(29) Chung, H.; Washburn, N. R. *ACS Appl. Mater. Interfaces* **2012**, *4*, 2840−2846.

(30) Dingemans, T. J.; Mendes, E.; Hinkley, J. J.; Weiser, E. S.; StClair, T. L. *Macromolecules* **2008**, *41*, 2474−2483.

(31) Guenthner, A. J.; Lamison, K. R.; Vij, V.; Reams, J. T.; Yandek, G. R.; Mabry, J. M. *Macromolecules* **2011**, *45*, 211−220.

(32) Becker, O.; Cheng, Y. B.; Varley, R. J.; Simon, G. P. *Macromolecules* **2003**, *36*, 1616−1625.

(33) Bandyopadhyay, A.; Valavala, P. K.; Clancy, T. C.; Wise, K. E.; Odegard, G. M. *Polymer* **2011**, *52*, 2445−2452.

Chapter 4

Synthesis of Triphenol−Based Epoxy Thermoset from *para*−Substituted LDPMs

ABSTRACT: A series of renewable triphenylmethane−type polyphenols (TPs) were synthesized from lignin derived *para*−substituted guaiacols (methylguaiacol and propylguaiacol) and aldehydes (4−hydroxybenzaldehyde, vanillin and syringaldehyde). By converting guaiacols to catechols through o−demethylation, the newly−formed phenolic *para* site remarkably improved the reactivity as reflected by conversion of TPs. Optimized reagent molar ratios were: aldehyde/catechol (1:4) and aldehyde/H_2SO_4 (1:3). A typical TP (VAN−M−CAT) was converted to glycidyl ether (GE−VAN−M−CAT) to examine its feasibility as precursor to epoxy thermosets. The resulting network exhibited excellent glassy modulus (12.3 GPa), glass transition temperature (167 °C) and thermal stability, which were attributed to the rigid triphenylmethane framework, high functionality (n = 5) and high cross−link density. A fully biobased epoxy comonomer (VAN−LIN−EPO), which was prepared by esterification of VAN−M−CAT with linoleic acid followed by epoxidation could tune the material properties.

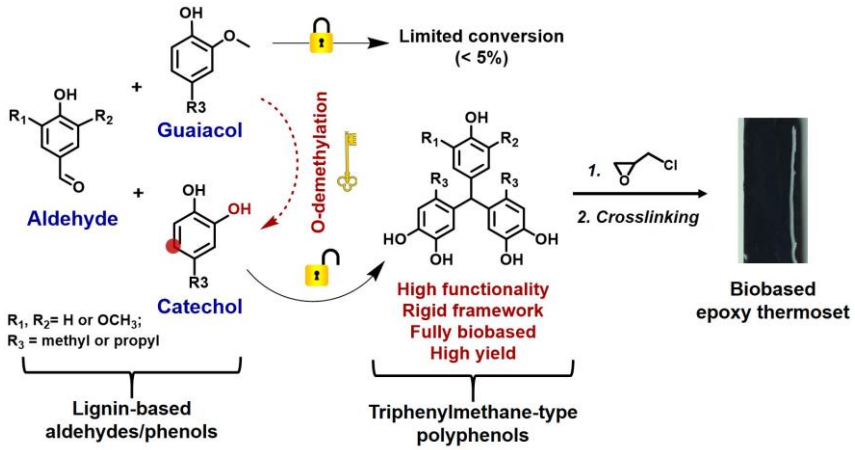

This section is partially adapted from: Shou Zhao and Mahdi M. Abu−Omar, *Macromolecules* **2017**, *50* (9), 3573−3581

4.1 Introduction

Polyphenols are important precursors to polymers like epoxy thermosets. As development of renewable materials has become increasingly important, partially− or fully−biobased polyphenols have been prepared with the purpose to replace or supplement petroleum−based bisphenol A (BPA).[1–3] Polyphenols are generally produced by condensation of phenol with ketone or aldehyde in the presence of an acid.[4] Using this approach, several biobased polyphenols have recently been reported: 1) diphenolic acid based on cellulose−derived levulinic acid;[5] 2) bisphenol obtained from cellulose−based 2,3−pentanedione;[6] 3) bisphenol based on lignin−derived creosol[7] and 4) triphenol prepared from lignin−based vanillin and guaiacol.[8]

For phenol−aldehyde condensation, the phenolic *para* position is the preferred coupling site due to its higher reactivity over the *ortho* site.[9,10] However, lignin−derived phenols are often characterized as *para* site occupied by alkyl groups, while partial *ortho* sites are substituted by methoxy groups,[11,12] which makes them especially difficult to couple to

aldehydes. Because of this obstruction, either *para*−available phenols like guaiacol[8] or *ortho*−specified coupling catalysts like zinc acetate[7] has been used as alternative methodologies, even though these approaches are frequently associated with limitations such as insufficient phenol candidates and limited orientation and stretch of functional hydroxyls obtained via *ortho* coupling.[13]

To increase the applications of lignin based phenols, creating a *para* site on *para*−substituted phenol could be a more universal and straightforward methodology. This improvement can be realized through o−demethylation of *ortho* methoxy, a characteristic group of lignin−derived phenols.[14,15] As illustrated in Scheme 4.1, o−demethylation of typical lignin−based guaiacols leads to new *para* and *ortho* sites. These newly−formed sites, especially the *para* site, could enhance reactivity. Meanwhile, demethylation also increases the number of functional OH groups. TPs with higher OH content have the potential to further improve the cross−link density and mechanical properties of subsequently formed polymers.[13,16,17]

Recent development in catalytic lignin depolymerization techniques is capable of converting bulk lignin into various smaller aromatic molecules including aldehydes, e.g. 4−hydroxybenzaldehyde (HBA), vanillin (VAN) and syringaldehyde (SYA)[18,19] and guaiacols such as 4−methylguaiacol (M−GUA) and 4−propylguaiacol (P−GUA).[20,21] Condensation between aromatic aldehyde and phenol yields triphenylmethane−type phenol (TP). TP−based materials are supposed to be highly rigid due to the triphenylmethane framework and highly functional (n = 5). To tune the rigidity, vegetable oils with flexible carbon chains may represent a renewable modifier.[22,23] Especially, unsaturated fatty acids (e.g. linoleic acid, LA) are often used as plasticizer or copolymer adjusting the rigidity of thermoplastics.[24,25] The integration of

lignin−based TPs and unsaturated fatty acids would yield renewable polymers with tunable mechanical properties.

In this study, we first describe the effective synthesis of fully−renewable polyphenols from the above−mentioned aldehydes and *para*−substituted guaiacols. By creating a *para* site on *para*−substituted guaiacols through o−demethylation, reactivity of the afforded catechols significantly improves. The proposed TPs have unique molecular architecture, three aromatic rings and five functional OH groups. To explore their potential as precursors to epoxy resin, a typical TP (VAN−M−CAT, prepared from condensation of vanillin and methylcatechol) is then reacted with epichlorohydrin to produce glycidyl ether prepolymer (GE−VAN−M−CAT). VAN−M−CAT was selected since it was easily separated from the reaction mixture, while it had relatively high yield (88 %) among all TPs. Meanwhile, VAN−M−CAT is reacted with chlorinated linoleic acid via esterification followed by epoxidation to make an epoxy comonomer (VAN−LIN−EPO), which acts as a plasticizer that tunes the rigidity of the resulting thermosets. The mixture of GE−VAN−M−CAT and VAN−LIN−EPO with different mass ratios is cured with a hardener (diethylenetriamine, DETA) to make epoxy networks. Thermal and mechanical performances of biobased thermosets are characterized to evaluate their potential for replacing BPA−based counterparts.

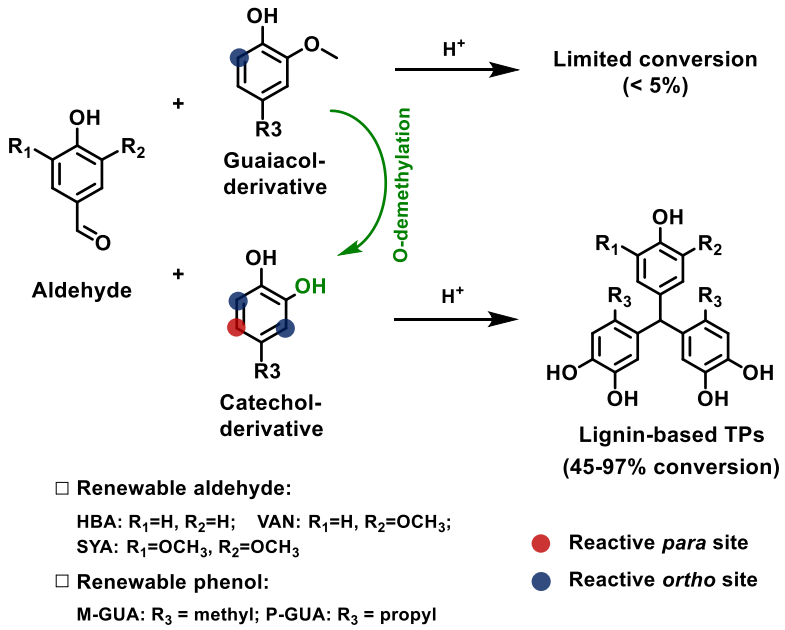

Scheme 4.1. Synthesis route of fully−renewable triphenylmethane−type polyphenols from lignin−derived aldehydes and *para*−substituted guaiacols. Condensation reactions between aldehydes and guaiacols give conversions below 5%. O−demethylation of guaiacols to corresponding catechols significantly improve the reactivity. The conversions of methylcatechol (M−CAT) based TPs are more than 90%, while propylcatechol (P−CAT) based TPs are more than 45%. Reaction condition: molar ratio of aldehyde: phenol=1:4, aldehyde: H_2SO_4 =1:3, room temperature for 2 d. Absolute ethanol is used as solvent. Conversions and isolated yields of different lignin−based TPs are listed in Table 4.2.

4.2 Results and Discussion

4.2.1 Synthesis of Renewable TPs under Optimized Conditions

Molar ratios of aldehyde/phenol and aldehyde/H_2SO_4 are capable of affecting the yield of TPs. To obtain optimal conditions, reaction between vanillin and methylcatechol was studied as an example due to the facile isolation and purification of the product VAN−M−CAT. Isolated yields of VAN−M−CAT under various synthesis conditions are listed in Table 4.1. Effect of

vanillin/methylcatechol molar ratio was studied first. For entry 1, condensation of one equivalent vanillin with two equivalents of methylcatechol gave a yield of 72%. Increasing methylcatechol/vanillin ratio to 3:1 (entry 2) readily improved isolated yield to 83%. As the ratio raises to 4:1, the yield increased further to 88% (entry 3). The effect of catalyst amount was then investigated (entries 3, 4 and 5). The amount of H_2SO_4 was insufficient when equal mole of H_2SO_4 and vanillin were used (entry 4, 75% isolated yield). After increasing the H_2SO_4/vanillin ratio to 3:1 (entry 3), the yield increased to 88%. It is noteworthy that the yields of entry 5 (89%) and entry 3 are similar, even though the H_2SO_4/vanillin ratio is increased to 5:1. Thus, H_2SO_4/vanillin ratio of 3:1 is effective at catalyzing the coupling reaction and considered optimal.

Amount of solvent ethanol was also found to impact product yields (compare entries 3 and 6). In entry 3, to fully dissolve 1 equivalent vanillin and 4 equivalents methylcatechol, the weight ratio of ethanol/vanillin had to be at least 3. For production of VAN−M−CAT, using the least amount of solvent is advantageous since it minimizes the product dissolved in solvent and facilitates isolation of product. This was confirmed when weight ratio of ethanol/vanillin increased to 6 in entry 6. Even though increasing solvent could facilitate mixing of reactants, the yield in entry 6 (83%) was still slightly lower than that in entry 3. Therefore, overall evaluation of the above−mentioned conditions revealed entry 3 as the optimal synthesis condition (molar ratio of vanillin/M−CAT = 1:4, vanillin/H_2SO_4 = 1:3), which produced high isolated yield while consuming relatively less H_2SO_4 and ethanol.

Table 4.1. Effect of stoichiometric ratio of reactants, amount of catalyst and solvent on the isolated yield of VAN−M−CAT.

Entry	Vanillin/ M−CAT[a]	Vanillin/ H_2SO_4[a]	Vanillin/ EtOH[b]	Isolated yield (%)
1	1:2	1:3	1:3	72
2	1:3	1:3	1:3	83
3	1:4	1:3	1:3	88
4	1:4	1:1	1:3	75
5	1:4	1:5	1:3	89
6	1:4	1:3	1:6	83

[a] Molar ratio; [b] Weight ratio. Condensation was conducted at room temperature for 2 d.

The optimized condition was subsequently used for condensation of other lignin−based aldehydes and phenols. Initially, direct condensation of aldehydes (HBA, VAN or SYA) with *para*−substituted guaiacols (M−GUA or P−GUA) was studied using HPLC to measure the conversion. However, it turned out that conversions of all reactions were negligible (< 5%). In an effort to increase the conversion, reaction time was increased up to 7 days, but with no enhancement in conversion. As *ortho* site of M−GUA and P−GUA is the only available position for condensation, low reactivity due to steric effect of the *ortho* sites significantly decreased the reactivity of guaiacols. To increase the reactivity, M−GUA and P−GUA were demethylated to the corresponding catechols (M−CAT and P−CAT).

Compared to the negligible conversions of *para*−substituted guaiacols, Table 4.2 shows significant increase in conversion and yield when the corresponding catechols are used. For example, TPs based on M−CAT have conversions in the range of 90−97%, with isolated yields of 71−88%. By comparison, P−CAT based TPs have lower conversion (45−50%) and isolated yields (33−42%), which might be attributed to the greater steric effect of the propyl group. Structure of aldehydes also has impact on conversion. Generally, conversion follows the order: HBA > VAN > SYA. As the number of electron−donating (methoxy) groups increases from

HBA to SYA, the electrophilicity decreases, which reduces their reactivity in electrophilic substitution reactions.

Table 4.2. Conversions and isolated yields of TPs derived from lignin−based aldehydes and catechols. Reaction condition: molar ratio of aldehyde: phenol = 1:4, aldehyde: H_2SO_4 = 1:3, room temperature for 2 d. Absolute ethanol is used as solvent.

Entry	Aldehyde	Catechol	Polyphenol	Conversion (%)	Isolated yield (%)
1	HBA	M−CAT	HBA−M−CAT	97	84
2	HBA	P−CAT	HBA−P−CAT	50	42
3	VAN	M−CAT	VAN−M−CAT	95	88
4	VAN	P−CAT	VAN−P−CAT	48	35
5	SYA	M−CAT	SYA−M−CAT	90	71
6	SYA	P−CAT	SYA−P−CAT	45	33

4.2.2 Structure of TPs

Proton and carbon NMR spectra of VAN−M−CAT are shown in Figure 4.1. The proton peak at 5.39 ppm corresponds to the triphenyl methyl group, which indicates successful coupling of vanillin with methylcatechol. Aromatic protons are found at 6.74, 6.69, 6.65, 6.42 and 6.23 ppm. The methoxy group is observed at 3.69 ppm while the methyl peak at 2.00 ppm. As for the carbon NMR, the methoxy, triphenyl methyl and methyl groups are observed at 56.13, 49.70 and 18.80 ppm, respectively. The characteristic triphenyl methyl peak is also observed for other lignin−based TPs (as depicted in Figure S4.3−S4.7), which confirms the formation of triphenylmethane framework. The structure of M−CAT and P−CAT based TPs are also confirmed by IR and mass spectra in Figure S4.8−S4.14.

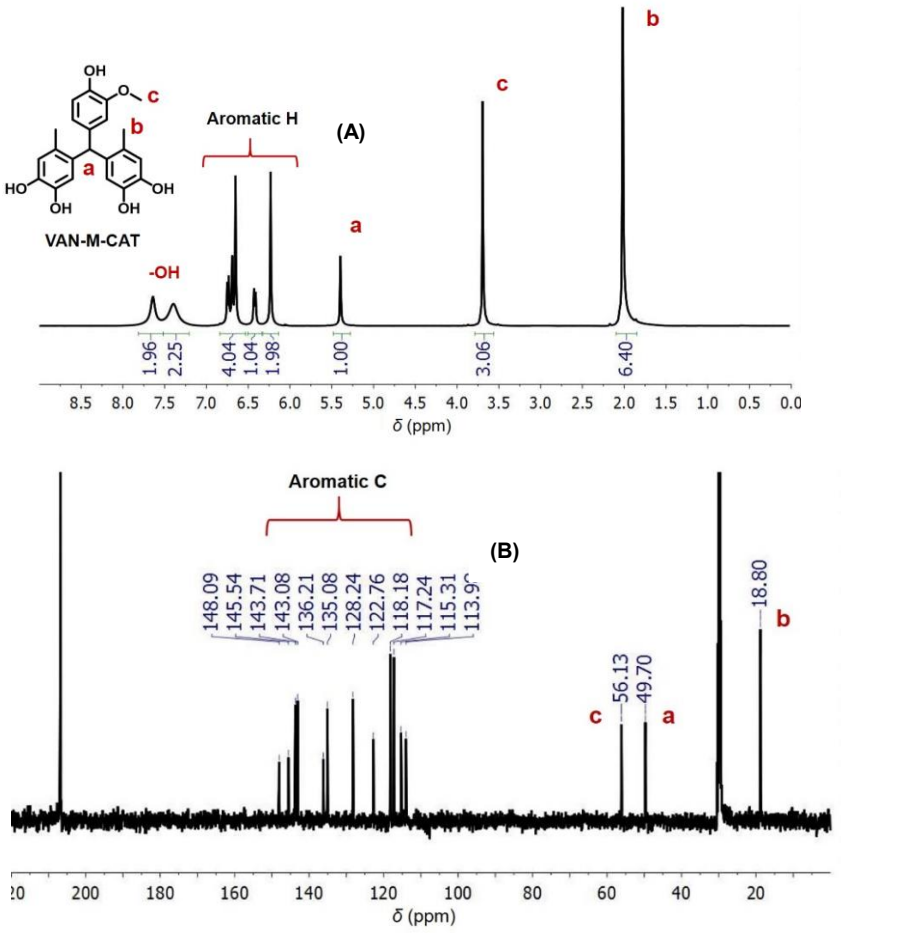

Figure 4.1 Proton (A) and carbon (B) NMR spectra of VAN−M−CAT. Solvent: acetone−d_6.

X−ray structure of VAN−M−CAT is also measured to confirm the structure and determine the coupling site. It is observed in Figure 4.2 that vanillin couples exclusively at the *para* sites of both methylcatechol molecules. This can be explained by higher reactivity of the *para* site. Meanwhile, the *para* site has less steric hindrance compared to *ortho* sites when subjected to condensation. The high reactivity of phenolic *para* position highlights the role of demethylation, which could be an effective way of modifying lignin−derived phenols, especially for those with *para* substituted and *ortho* occupied by methoxy group. Besides, the stretched orientation of functional hydroxyls of TPs is also advantageous for making polymers with desirable properties.

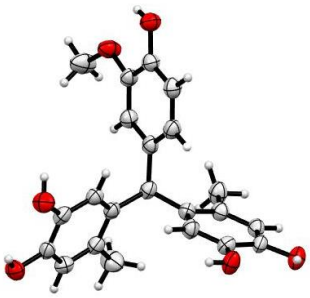

Figure 4.2 X−ray structure of VAN−M−CAT. Crystal was obtained from the slow evaporation of an ether solution at room temperature.

4.2.3 Epoxy Monomers from VAN−M−CAT and Fatty Acid

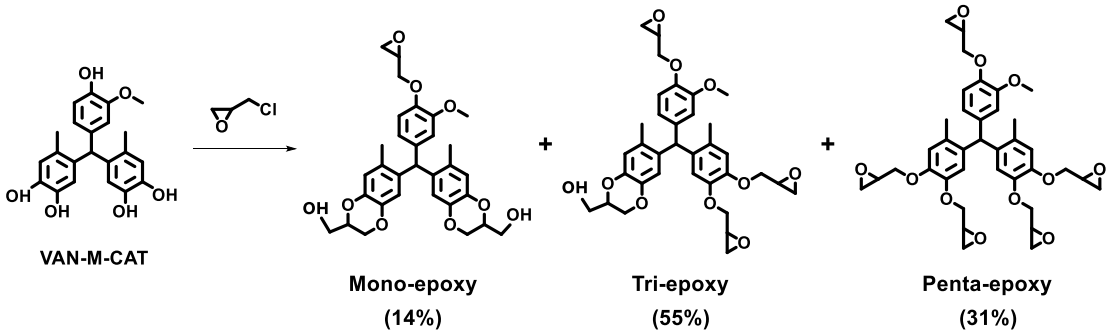

Scheme 4.2. Glycidylation of VAN−M−CAT with epichlorohydrin. Three major products with mono−epoxy substituted (GE−VAN−M−CAT−1), tri−epoxy substituted (GEVAN−M−CAT−3) and penta−epoxy substituted (GEVAN−M−CAT−5) were isolated using a preparative HPLC and their molar ratio was measured to be 14: 55: 31 using an analytical HPLC spectra.

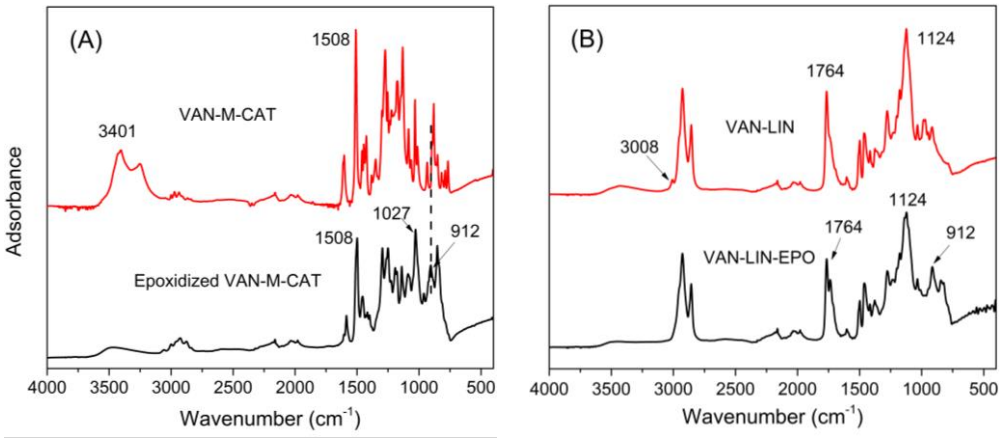

Figure 4.3 FTIR spectra of (A) VAN−M−CAT and its epoxidized product GE−VAN−M−CAT,

and (B) VAN−LIN and its epoxidized product VAN−LIN−EPO.

Glycidylation of VAN−M−CAT with epichlorohydrin yields three products with different substitution of oxirane groups (Scheme 4.2). Proton, carbon, HMQC NMR spectra and mass spectra of each product are illustrated in Figure S4.15−S4.21. Formation of epoxy groups is also confirmed using IR spectra. As seen in Figure 4.3, panel A, after VAN−M−CAT is glycidylated to GE−VAN−M−CAT, its broad hydroxyl band at 3401 cm^{-1} decreases significantly, and it is accompanied by the presence of an epoxy ring band at 912 cm^{-1} and a C−O−C ether linkage at 1027 cm^{-1}. The catechol groups of VAN−M−CAT make it inevitable to cause side reactions like intramolecular cyclization between two adjacent oxiranes. Benzodioxane derivative can occur in either one or both catechols to form mono−epoxy substituted (GE−VAN−M−CAT−1) or tri−epoxy substituted (GE−VAN−M−CAT−3) products. From the viewpoint of functionality, the appearance of benzodioxane derivative is unfavorable since it is unreactive with amine hardener/cross−linker and is likely to create dangling chain ends that impair cross−link of the resulting polymers.[28] However, if the penta−epoxy substituted (GE−VAN−M−CAT−5) is the only glycidylation product, the formed network could be highly brittle due to the high rigidity and functionality (related to cross−link density) of VAN−M−CAT.[29] Therefore, from the viewpoint of processing and application, the presence of certain amount of benzodioxane byproducts is favorable since it helps adjust the rigidity of cured networks. As the major product, tri−epoxy substituted product (55%) could effectively reduce the rigidity while still keep cross−linked within the network. Meanwhile, hydroxyl groups of benzodioxane can also catalyze the reaction between monomer and cross−linker.[30,31]

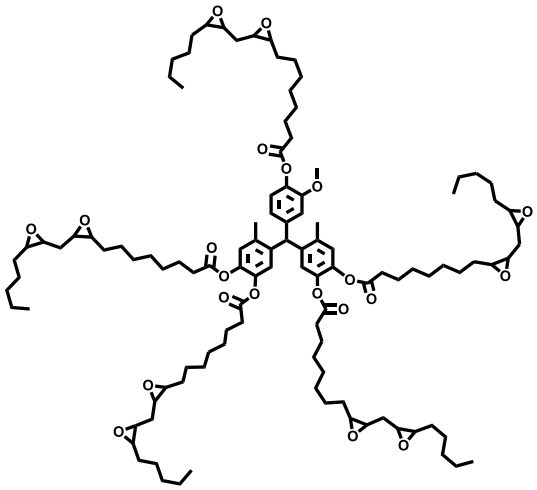

Figure 4.4 Structure of fully biobased epoxy prepolymer VAN−LIN−EPO, which is synthesized via esterification between VAN−M−CAT and linoleic acid, and followed by epoxidation.

Introduction of flexible components is another way of adjusting rigidity. By esterifying VAN−M−CAT and linoleic acid, followed by epoxidation, a fully biobased epoxy monomer with rigid core and flexible branches was synthesized (VAN−LIN−EPO) as shown in Figure 4.4. Figure 4.5, panel A exhibits the NMR spectra of linoleic acid. The peak at δ 5.4 corresponds to C=C double bonds, while peaks at δ 0.9−2.8 are related to the saturated part of the carbon chain. After linoleic acid is esterified with VAN−M−CAT to yield VAN−M−CAT−LIN (VAN−LIN), characteristic peaks of both linoleic acid and VAN−M−CAT (δ 6.5−6.9, aromatic H; δ 5.5, Ar_3−CH; δ 3.7, $-OCH_3$ and δ 2.0, $-CH_3$) are evident (Figure 4.5, panel B). To produce epoxy comonomer, VAN−LIN is epoxidized using peracetic acid to yield VAN−LIN−EPO. As seen in Figure 4.5, panel C, the double bond peak of VAN−LIN−EPO disappears while a new epoxy peak at δ 2.9 appears. As for the FTIR spectra of VAN−LIN in Figure 4.3, panel B, it reveals a C=C stretching vibration band at 3008 cm^{-1} and an ester bond at 1764 cm^{-1}. When VAN−LIN is epoxidized with peracetic acid, the C=C band is gone while a new epoxy band at

912 cm^{-1} appears.

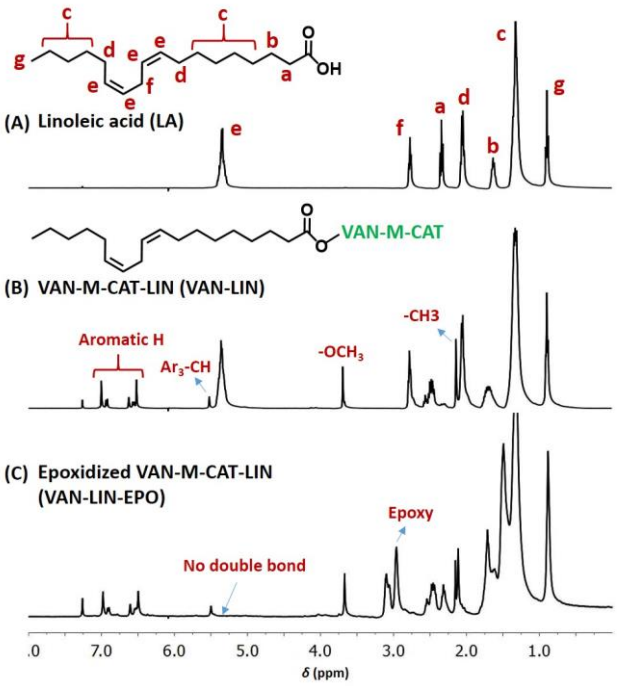

Figure 4.5 Proton NMR structure of (A) linoleic acid, (B) VAN−LIN, product of esterification between VAN−M−CAT and linoleoyl chloride and (C) epoxidized VAN−LIN (VAN−LIN−EPO). Solvent: $CDCl_3$.

4.2.4 Dynamic Mechanical Analysis

Cross−link density (ν_e) is a key parameter that determines performance of epoxy thermosets.[32] ν_e can be reflected from α−relaxation temperature (T_α, related to glass transition temperature) since increased covalent cross−links restricts the mobility of polymer segments, which leads to higher T_α. Inset of Figure 4.6 illustrates T_α of $VAN_{100}LIN_0$ (167 °C), $VAN_{75}LIN_{25}$ (111 °C) and $VAN_{50}LIN_{50}$ (82 °C), which gradually decreases as portion of VAN−LIN−EPO increases from 0 to 50 wt%. Even though GE−VAN−M−CAT mixture and VAN−LIN−EPO are calculated to have similar epoxy equivalent value (531 and 539 mmol epoxy/100 g, respectively), the flexible nature of VAN−LIN−EPO remarkably decreases cross−link density of the resulting polymer. On one hand, the saturated component of the

carbon side chain introduces void volume and yields a network that deforms more readily.[33] On the other hand, closed looping could be formed by the hardener and epoxies of VAN−LIN−EPO in adjacent carbon chains, which limits the direction of the resulting network. The plasticizer role of VAN−LIN−EPO can also be reflected through height of tan δ, which is the ratio of loss to storage modulus. As seen in Figure 4.6, height of tan δ decreases from $VAN_{50}LIN_{50}$ to $VAN_{100}LIN_0$, suggesting lower segmental mobility and fewer relaxing species in $VAN_{100}LIN_0$.[34,35]

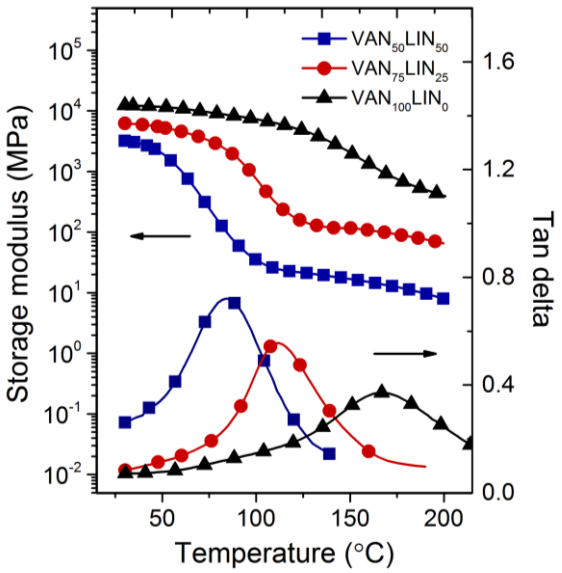

Figure 4.6 DMA curve of epoxy networks with different weight ratio of GE−VAN−M−CAT and VAN−LIN−EPO as a function of temperature. $VAN_{75}LIN_{25}$, for example, represents epoxy network with 75 wt% GE−VAN−M−CAT and 25 wt% VAN−LIN−EPO in prepolymer mixture. Temperature at the maximum in tan δ curve is taken as T_α (related to glass transition).

Storage modulus (E') values are also presented in Figure 4.6. Without addition of VAN−LIN−EPO, $VAN_{100}LIN_0$ exhibits a high glassy E' of 12.3 GPa, which could be attributed to the high rigidity and functionality of GE−VAN−M−CAT mixture. Addition of flexible VAN−LIN−EPO comonomer effectively decreases the modulus, as E' of $VAN_{75}LIN_{25}$ and

$VAN_{50}LIN_{50}$ decreases to 6.2 GPa and 3.2 GPa, respectively. This confirms the plasticizer nature of VAN−LIN−EPO. It is noteworthy that T_α and E' of BPA diglycidyl ether (DGEBA)/DETA network were reported to be 137 °C and 3.6 GPa,[36] which is lower than that of GE−VAN−M−CAT/DETA. This finding highlights renewable TP based epoxy networks possess marked mechanical performance to replace or supplement petroleum−based thermosets.

4.2.5 Thermogravimetric analysis

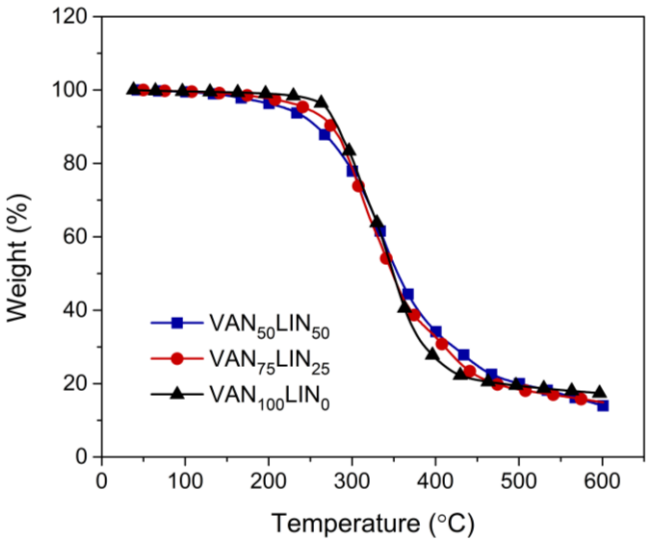

Figure 4.7 Thermogravimetric analysis thermograms of epoxy networks with different weight ratio of GE−VAN−M−CAT and VAN−LIN−EPO. $VAN_{75}LIN_{25}$, for example, represents epoxy network with 75 wt% GE−VAN−M−CAT and 25 wt% VAN−LIN−EPO in the prepolymer mixture.

Figure 4.7 exhibits a one−step degradation profile for all epoxy networks. Thermal stability of cured thermosets increases with cross−link density. This can be reflected from the shift of onset degradation temperature (expressed as T_{d5}, temperature at 5% weight loss) from 220 °C of $VAN_{50}LIN_{50}$ to 245 and 269 °C of $VAN_{75}LIN_{25}$ and $VAN_{100}LIN_0$. As cross−link

density increases, polymer chains become more constrained, which causes lower molecular mobility during thermal expansion. Meanwhile, the tortuous pathway in highly−cross−linked network postpones mass exchange. Statistic heat−resistant index temperature (T_s), which is calculated using T_{d5} and T_{d30} (temperature at 30% weight loss), reflects the thermal stability of cured networks.[37] Table 4.3 illustrates T_s increases slightly from $VAN_{50}LIN_{50}$ (136 °C) to $VAN_{75}LIN_{25}$ (140 °C) and $VAN_{100}LIN_0$ (146 °C), verifying the role of cross−link density on thermal stability. Besides, $Char_{600}$ (char formed at 600 °C) of networks is also observed to increase from $VAN_{50}LIN_{50}$ to $VAN_{100}LIN_0$.

Table 4.3. Thermogravimetric data of T_{d5}, T_{d30} (temperature at 5% and 30% weight loss), T_s (statistic heat−resistant index temperature) and $Char_{600}$ (char residue at 600 °C) of epoxy networks with different ratio of GE−VAN−M−CAT and VAN−LIN−EPO.

Epoxy networks	T_{d5} (°C)	T_{d30} (°C)	T_s (°C)	$Char_{600}$ (%)
$VAN_{50}LIN_{50}$	220	317	136	14.0
$VAN_{75}LIN_{25}$	245	313	140	14.9
$VAN_{100}LIN_0$	269	318	146	17.3

4.3 Conclusions

Synthetic routes to renewable triphenylmethane−type polyphenols were demonstrated, widening the applications of typical lignin−based *para*−substituted guaiacols. O−demethylation of *para*−substituted guaiacols to give the corresponding catechols was key in providing new and highly reactive *para* sites, which effectively improves the reactivity for aldehyde coupling. Under optimized conditions, M−CAT and P−CAT based TPs are obtained in high to moderate yields in the range 71−88% and 33−42%, respectively. Steric effect and electron−donating group influence the conversions and yields of TPs. The proposed TPs have

rigid triphenylmethane framework and high functionality (n = 5). These advantageous structural properties make renewable TPs excellent precursors to epoxy thermosets. As an example, VAN−M−CAT based network exhibits excellent glassy modulus (12.3 GPa) and glass transition temperature (167 °C), which is attributed to the high cross−link density of the obtained network. To adjust the brittleness of above−mentioned network, a fully biobased plasticizer and copolymer based on linoleic acid (VAN−LIN−EPO) was employed and found to effectively tune the storage modulus. With the advantages of moderate to high yields, excellent mechanical and thermal parameters, and tunable properties, the proposed renewable TP−based epoxy thermosets exhibit sufficient potential to replace or supplement petroleum−based materials.

4.4 Experimental Section

General. 4−hydroxybenzaldehyde, vanillin, syringaldehyde, 4−methylguaiacol, 4−propylguaiacol, 4−methylcatechol, 48% aqueous hydrobromic acid, epichlorohydrin, tetrabutylammonium bromide, diethylenetriamine (DETA), peracetic acid (32 wt% in dilute acetic acid), linoleic acid and oxalyl chloride were purchased from Aldrich Chemical Co. Ethanol (200 proof) was purchased from Decon Labs, Inc. Sulfuric acid (98%) was obtained from Fisher Scientific. All chemicals were used as received without further purification.

4.4.1 O−demethylation of 4−methylguaiacol and 4−propylguaiacol.

Lignin−based phenols were o−demethylated as previously reported.[14] Briefly, 4−propylguaiacol (P−GUA, 16.6 g, 0.1 mol) was added to 83 g of 48% aqueous hydrobromic acid. The reaction mixture was magnetically stirred at 120 °C for 20 h, cooled to ambient temperature, saturated with NaCl, and extracted three times with diethyl ether. The organic

layer was dried over $MgSO_4$ and concentrated using rotary evaporation to yield P−GUA derived catechol (P−CAT) as a yellow oil (94% yield). M−GUA demethylated product (M−CAT) was prepared using the same method with 92% yield. Proton NMR spectra of M−GUA, M−CAT, P−GUA and P−CAT are shown in Figure S4.1 and S4.2.

4.4.2 Synthesis of Lignin Based Triphenylmethane−Type Phenols (TP).

M−CAT based TPs.

Vanillin (VAN, 1.05 g, 7 mmol) and M−CAT (3.47 g, 28 mmol) were dissolved in 3 mL absolute ethanol. To this solution, 2.0 g of concentrated sulfuric acid, dissolved in 1.5 mL of absolute ethanol, were slowly added while stirred. An ice bath was used to control the temperature below 10 °C. After the addition of sulfuric acid, the temperature was increased to room temperature. The system was gently stirred for 2 days under room temperature. Then, 100 mL of H_2O and 15 mL of diethyl ether was successively added to precipitate flakes. The precipitate was then collected through filtration, washed with water three times and dried at 65 °C under vacuum for 2 days to obtain the TP product (VAN−M−CAT) as a white powder (2.35 g, 88% isolated yield).

^{1}H NMR (acetone−d_6, 400 MHz) δ: 7.64 (s, 2H, Ar−OH), 7.39 (s, 2H, Ar−OH), 6.74 (d, J = 8.1, 1H, Ar−H), 6.69 (s, 1H, Ar−H), 6.65 (s, 2H, Ar−H), 6.42 (d, J = 7.8, 1H, Ar−H), 6.23 (s, 2H, Ar−H), 5.39 (s, 1H, Ar_3−CH), 3.69 (s, 3H, −OCH_3), 2.00 (s, 6H, −CH_3). ^{13}C NMR (acetone−d_6, 400 MHz) δ: 148.09, 145.54, 143.71, 143.08, 136.21, 135.08, 128.24, 122.76, 118.18, 117.24, 115.31, 113.98, 56.13 (−OCH_3), 49.70 (Ar_3−CH), 18.80 (−CH_3). [$C_{22}H_{22}O_6$ − H^+]: 381.4.

SYA−M−CAT was obtained from M−CAT and syringaldehyde (SYA) using the

above−mentioned method (2.05 g, 71% isolated yield).

^{1}H NMR (acetone−d6, 400 MHz) δ: 7.65 (s, 2H, Ar−OH), 7.40 (s, 2H, Ar−OH), 7.08 (s, 1H, Ar−OH), 6.63 (s, 2H, Ar−H), 6.33 (s, 2H, Ar−H), 6.23 (s, 2H, Ar−H), 5.37 (s, 1H, Ar_3−CH), 3.67 (s, 6H, −OCH_3), 2.00 (s, 6H, −CH_3). ^{13}C NMR (acetone−d_6, 400 MHz) δ: 148.45, 143.75, 143.09, 135.30, 135.06, 134.93, 128.25, 118.15, 117.16, 108.10, 56.54 (−OCH_3), 50.03 (Ar_3−CH), 18.76 (−CH_3). [$C_{23}H_{24}O_7$ − H^+]: 411.4

For HBA−M−CAT that is derived from 4−hydroxybenzaldehyde (HBA) and M−CAT, only isolation method is different from the above. In detail, after the reaction was complete, 100 mL H_2O was poured into the mixture prior to the addition of 20 mL diethyl ether to extract the product. The ethereal extract was dried with $MgSO_4$ and the solvent allowed to evaporate slowly to yield colorless crystals, which were subsequently washed with cold ether and dried at 65 °C under vacuum for 2 days to yield a white powder (2.07 g, 84% isolated yield).

^{1}H NMR (acetone−d_6, 400 MHz) δ: 7.58 (s, 5H, Ar−OH), 6.84 (d, J = 8.4, 2H, Ar−H), 6.75 (d, J = 8.4, 2H, Ar−H), 6.64 (s, 2H, Ar−H), 6.20 (s, 2H, Ar−H), 5.38 (s, 1H, Ar_3−CH), 1.99 (s, 6H, −CH_3). ^{13}C NMR (acetone−d_6, 400 MHz) δ: 156.32, 143.68, 143.10, 135.34, 135.53, 135.15, 131.27, 128.17, 120.93, 118.18, 117.27, 116.85, 115.89, 115.72, 49.24 (Ar_3−CH), 18.74 (−CH_3). [$C_{21}H_{20}O_5$ − H^+]: 351.4

P−CAT based TPs.

P−CAT based TPs (HBA−P−CAT, VAN−P−CAT and SYA−P−CAT) were prepared using the same reaction conditions as VAN−M−CAT. The desired TPs were separated from unreacted phenols and aldehydes using silica gel chromatography (hexane/ethyl acetate, 3:1 to 1:1) to give:

HBA−P−CAT, orange solid, 1.20 g, 42% isolated yield. ^{1}H NMR (acetone−d_6, 400 MHz) δ: 7.53 (s, 4H, Ar−OH), 6.81 (d, J = 8.2, 2H, Ar−H), 6.73 (d, J = 8.1, 2H, Ar−H), 6.66 (s, 2H, Ar−H), 6.22 (s, 2H, Ar−H), 5.57 (s, 1H, Ar_3−CH), 2.35 (t. J =7.2, 4H, −CH_2−), 1.47 (dt, J = 15.0, 7.4, 4H, −CH_2−), 0.85 (t, J = 7.2, 6H, −CH_3). ^{13}C NMR (acetone−d_6, 400 MHz) δ: 156.27, 143.82, 143.04, 136.82, 134.81, 132.66, 131.07, 117.79, 117.34, 115.68, 47.99 (Ar_3−CH), 34.85 (−CH_2−), 24.84 (−CH_2−), 14.45 (−CH_3). [$C_{25}H_{28}O_5$ − H^+]: 407.4

VAN−P−CAT, orange solid, 1.07 g, 35% isolated yield. ^{1}H NMR (acetone−d_6, 400 MHz) δ: 7.66 (s, 2H, Ar−OH), 7.39 (s, 1H, Ar−OH), 7.37 (s, 2H, Ar−OH), 6.72 (d, J = 8.0, 1H, Ar−H), 6.66 (s, 2H, Ar−H), 6.63 (s, 1H, Ar−H), 6.41 (d, J = 7.2, 1H, Ar−H), 6.24 (s, 2H, Ar−H), 5.58 (s, 1H, Ar_3−CH), 3.68 (s, 3H, −OCH_3), 2.36 (t, J = 7.2, 4H, −CH_2−), 1.48 (dt, J = 15.0, 7.4, 4H, −CH_2−), 0.85 (t, J = 7.2, 6H, −CH_3). ^{13}C NMR (acetone−d_6, 400 MHz) δ: 148.06, 145.54, 143.85, 143.02, 137.48, 134.75, 132.71, 122.78, 117.52, 117.27, 115.33, 113.85, 107.64, 56.16 (−OCH_3), 48.44 (Ar_3−CH), 34.85 (−CH_2−), 24.78 (−CH_2−), 14.47 (−CH_3). [$C_{26}H_{30}O_6$ − H^+]: 437.4

SYA−P−CAT, orange solid, 1.08 g, 33% isolated yield. ^{1}H NMR (acetone−d6, 400 MHz) δ: 7.68 (s, 2H, Ar−OH), 7.36 (s, 2H, Ar−OH), 7.05 (s, 1H, Ar−OH), 6.66 (d, J = 1.8, 2H, Ar−H), 6.28 (dd, J = 15.7, 1.8, 4H, Ar−H), 5.57 (s, 1H, Ar_3−CH), 3.66 (s, 6H, −OCH_3), 2.36 (t, J = 7.2, 4H, −CH_2−), 1.45 (dt, J = 15.0, 7.4, 4H, −CH_2−), 0.85 (t, J = 7.2, 6H, −CH_3). ^{13}C NMR (acetone−d_6, 400 MHz) δ: 148.45, 143.89, 143.01, 136.58, 135.11, 134.64, 132.76, 117.68, 117.48, 108.11, 56.58 (−OCH_3), 48.81 (Ar_3−CH), 34.85 (−CH_2−), 24.75 (−CH_2−), 14.48 (−CH_3). [$C_{27}H_{32}O_7$ − H^+]: 467.6

4.4.3 Preparation of Glycidylated Ether of VAN−M−CAT (GE−VAN−M−CAT).

GE−VAN−M−CAT was prepared by reaction of VAN−M−CAT (2 g, 5.2 mmol) and epichlorohydrin (30 g, 320 mmol). Tetrabutylammonium bromide (0.84 g, 2.6 mmol) was used as a phase transfer catalyst. The mixture was heated at 95 °C for 1 h and followed by a dropwise addition of 10 g of 20% w/w NaOH solution. The reaction was kept for another 3 h and the mixture was washed with water, extracted with ethyl acetate and concentrated with a rotary evaporator to yield GE−VAN−M−CAT as a viscous oil (2.8 g). The catechol−like structure of VAN−M−CAT is likely to produce benzodioxane derivatives during glycidylation (Scheme 4.2). Using a preparative scale HPLC, three major glycidylated products, i.e., mono−epoxy substituted (GE−VAN−M−CAT−1), tri−epoxy substituted (GE−VAN−M−CAT−3) and penta−epoxy substituted (GE−VAN−M−CAT−5) were isolated. Structure of the major glycidylated products were measured by NMR and mass spectra. An analytical HPLC was used to detect peaks of each epoxidized product and determine their molar ratio in the mixture to be GE−VAN−M−CAT−1: GE−VAN−M−CAT−3: GE−VAN−M−CAT−5 = 14: 55: 31. Epoxy equivalent value of GE−VAN−M−CAT mixture was determined to be 495 mmol epoxy/100 g by the HCl/acetone chemical titration method. This is in accordance with the calculated value (531 mmol epoxy/100 g) using the above ratio.

GE−VAN−M−CAT−1, yellow oil, 14 mol % in epoxidized product mixture. ^{1}H NMR ($CDCl_3$, 400 MHz) δ: 6.27−6.80 (7H, Ar−H), 5.37 (1H, f), 4.13−4.28 (5H, c', g', h), 3.94−4.10 (3H, c, g), 3.82−3.87 (4H, i, i'), 3.76 (3H, d), 3.37 (1H, b), 2.89 (1H, a), 2.73 (1H, a'), 2.03 (6H, e). ^{13}C NMR ($CDCl_3$, 400 MHz) δ: 113.58−140.51 (Ar−C), 73.31 (h), 70.07 (c), 65.07 (g), 61.74 (i), 55.89 (d), 50.14 (f), 48.99 (b), 44.99 (a), 18.66 (e). [$C_{31}H_{34}O_9 + Na^+$]: 573.

GE−VAN−M−CAT−3, brown oil, 55 mol % in epoxidized product mixture. ^{1}H NMR

($CDCl_3$, 400 MHz) δ: 6.23−6.80 (7H, Ar−H), 5.37 (1H, f), 4.18−4.25 (5H, c', g', h), 3.92−4.07 (4H, c, g), 3.78−3.82 (2H, i, i'), 3.74 (3H, d), 3.22−3.37 (3H, b), 2.61−2.88 (6H, a, a'), 1.99−2.03 (6H, e). ^{13}C NMR ($CDCl_3$, 400 MHz) δ: 113.40−149.39 (Ar−C), 73.29 (h), 70.08 (c), 65.18 (g), 61.74 (i), 55.84 (d), 50.12 (f), 49.09 (b), 44.66 (a), 18.93 (e). [$C_{34}H_{38}O_{10} + Na^+$]: 629.

GE−VAN−M−CAT−5, brown oil, 31 mol % in epoxidized product mixture. ^1H NMR ($CDCl_3$, 400 MHz) δ: 6.32−6.80 (7H, Ar−H), 5.40 (1H, f), 4.09−4.25 (5H, c'), 3.88−4.99 (5H, c), 3.74 (3H, d), 3.22−3.36 (5H, b), 2.60−2.87 (10H, a, a'), 2.03 (6H, e). ^{13}C NMR ($CDCl_3$, 400 MHz) δ: 113.29−146.78 (Ar−C), 70.28 (c), 55.77 (d), 50.23 (b), 49.20 (f), 45.26 (a), 18.89 (e). [$C_{37}H_{42}O_{11} + Na^+$]: 686.

4.4.4 Esterification of VAN−M−CAT with Linoleic Acid and Epoxidation.

Linoleic acid was first converted to linoleoyl chloride (LC) to increase its reactivity.[26] To a solution of linoleic acid (4.2 g, 15 mmol) dissolved in 35 mL dry dichloromethane was added slowly 4.23g (33.3 mmol) of oxalyl chloride at 0 °C. The temperature was then raised to room temperature and stirred for 4 h. The reaction mixture was concentrated with rotary evaporator to yield LC as a yellowish oil (4.13 g, 92% isolated yield).

Esterification between VAN−M−CAT and LC was then performed by a solvent−free and catalyst−free condition as established by a previous study.[27] In detail, VAN−M−CAT (1 g, 2.6 mmol) and LC (8.97 g, 30 mmol) was introduced in a 50 mL reactor with a nitrogen−gas bubbling system and an outlet connected to a wash bottle holding a NaOH solution. The mixture was then stirred and heated at 130 °C for 15 h under a continuous nitrogen stream. The obtained esterified product, VAN−M−CAT−LIN, was washed using cold ethanol to remove the

excess acid chloride and further purified by a silica column using an eluent of hexane/ethyl acetate (10:1) to yield 2.79 g, 63% isolated yield.

VAN−M−CAT−LIN was then epoxidized using peracetic acid to make epoxy comonomer. 1.5 g (0.88 mmol, 8.8 mmol of double bond) of VAN−M−CAT−LIN was dissolved in 25 mL dichloromethane in a 50 mL round−bottomed flask. To this flask was added dropwise peracetic acid (4.2 g, 17.6 mmol). The reaction mixture was stirred at room temperature overnight, washed 3 times with brine and extracted with ethyl acetate. The ethyl acetate was removed using a rotary evaporator to yield epoxidized VAN−M−CAT−LIN (VAN−M−CAT−LIN−EPO) as a yellowish oil (1.4 g, 86% isolated yield).

4.4.5 Formation of Biobased Epoxy Networks.

Three epoxy monomer mixtures with weight ratio GE−VAN−M−CAT to VAN−M−CAT−LIN−EPO of 100:0, 75:25 and 50:50 are respectively mixed with diethylenetriamine (DETA) with stoichiometric ratio of epoxy vs. −NH for curing. The mixtures were stirred for 10 min, degassed under vacuum to remove entrapped air and poured into molds for curing. Given GE−VAN−M−CAT was highly reactive with DETA, the mixtures were cured at room temperature for 8 h, followed by 60 °C for 4 h and 80 °C for 4 h. The obtained cured epoxy thermosets, denoted as $VAN_{100}LIN_0$, $VAN_{75}LIN_{25}$ and $VAN_{50}LIN_{50}$, were subjected to mechanical and thermal analyses.

4.4.6 Analysis Methods.

Conversions of phenol−aldehyde condensation reaction were measured by high−performance liquid chromatography (HPLC, Agilent 1260 Infinity Quaternary), with a Zorbax Eclipse XDB−C_{18} Column (250 x 74.6mm). ESI−MS analyses in negative mode were

performed using a 7 Tesla Thermo Scientific LQIT/FT−ICR mass spectrometer. Waters Delta Prep 4000 HPLC was used to separate and collect each of the glycidylated products of VAN−M−CAT in 50 mg scale.

Crystal of VAN−M−CAT was obtained from slow evaporation of an ether solution at room temperature. Single crystals were mounted on Mitegen microloop mounts using a trace of mineral oil and cooled in−situ to 100(2) K for data collection on a Nonius KappaCCD diffractometer equipped with a graphite crystal, incident beam monochromator using Mo Kα radiation (λ = 0.71073 Å). Data were collected using the Nonius Collect software and processed using HKL3000 and corrected for absorption and scaled using Scalepack.

Other analysis methods are similar to Chapter 2.

4.5 References

(1) Laurichesse, S.; Avérous, L. *Prog. Polym. Sci.* **2014**, *39*, 1266−1290.

(2) Auvergne, R.; Caillol, S.; David, G.; Boutevin, B.; Pascault, J. P. *Chem. Rev.* **2013**, *114*, 1082−1115.

(3) Isikgor, F. H.; Becer, C. R. *Polym. Chem.* **2015**, *6*, 4497−4559.

(4) Wang, L.; Meng, Y. Z.; Wang, S. J.; Shang, X. Y.; Li, L.; Hay, A. S. *Macromolecules* **2004**, *37*, 3151−3158.

(5) Maiorana, A.; Spinella, S.; Gross, R. A. *Biomacromolecules* **2015**, *16*, 1021−1031.

(6) Schutyser, W.; Koelewijn, S. F.; Dusselier, M.; Van de Vyver, S.; Thomas, J.; Yu, F.; Carbone, M. J.; Smet, M.; Van Puyvelde, P.; Dehaen, W. *Green Chem.* **2014**, *16*, 1999−2007.

(7) Meylemans, H. A.; Groshens, T. J.; Harvey, B. G. *ChemSusChem* **2012**, *5*, 206−210.

(8) Zhang, L.; Zhu, Y.; Li, D.; Wang, M.; Chen, H.; Wu, J. *RSC Adv.* **2015**, *5*, 96879−96887.

(9) Zhou, Z.; Parr, R. G. *J. Am. Chem. Soc.* **1990**, *112*, 5720−5724.

(10) Hernandez, E. D.; Bassett, A. W.; Sadler, J. M.; La Scala, J. J.; Stanzione III, J. F. *ACS Sustain. Chem. & Eng.* **2016**, *4*, 4328−4339.

(11) Xu, J.; Jiang, J.; Hse, C.; Shupe, T. F. *Green Chem.* **2012**, *14*, 2821−2830.

(12) Liu, W. J.; Jiang, H.; Yu, H. Q. *Green Chem.* **2015**, *17*, 4888−4907.

(13) Zhao, S.; Abu−Omar, M. M. *ACS Sustain. Chem. & Eng.* **2016**, *4*, 6082−6089.

(14) Chung, H.; Washburn, N. R. *ACS Appl. Mater. & Inter.* **2012**, *4*, 2840−2846.

(15) Zhao, S.; Abu−Omar, M. M. *Biomacromolecules* **2015**, *16*, 2025−2031.

(16) Putz, K. W.; Palmeri, M. J.; Cohn, R. B.; Andrews, R.; Brinson, L. C. *Macromolecules* **2008**, *41*, 6752−6756.

(17) Pan, X.; Sengupta, P.; Webster, D. C. *Biomacromolecules* **2011**, *12*, 2416−2428.

(18) Stärk, K.; Taccardi, N.; Bösmann, A.; Wasserscheid, P. *ChemSusChem* **2010**, *3*, 719−723.

(19) Mialon, L.; Pemba, A. G.; Miller, S. A. *Green Chem.* **2010**, *12*, 1704−1706.

(20) Xu, W.; Miller, S. J.; Agrawal, P. K.; Jones, C. W. *ChemSusChem* **2012**, *5*, 667−675.

(21) Parsell, T. H.; Owen, B. C.; Klein, I.; Jarrell, T. M.; Marcum, C. L.; Haupert, L. J.; Amundson, L. M.; Kenttämaa, H. I.; Ribeiro, F.; Miller, J. T.; Abu−Omar M. M. *Chem. Sci.* **2013**, *4*, 806−813.

(22) Xia, Y.; Larock, R. C. *Green Chem.* **2010**, *12*, 1893−1909.

(23) Miyagawa, H.; Misra, M.; Drzal, L. T.; Mohanty, A. K. *Polymer* **2005**, *46*, 445−453.

(24) Meier, M. A. R.; Metzger, J. O.; Schubert, U. S. *Chem. Soc. Rev.* **2007**, *36*, 1788−1802.

(25) Pleissner, D.; Lau, K. Y.; Zhang, C.; Lin, C. S. K. *ChemSusChem* **2015**, *8*, 1686−1691.

(26) Wu, H.; Kelley, C. J.; Pino−Figueroa, A.; Vu, H. D.; Maher, T. J. *Bioorg. Med. Chem.* **2013**,

21, 5188−5197.

(27) Laurichesse, S.; Huillet, C.; Avérous, L. *Green Chem.* **2014**, *16*, 3958−3970.

(28) Nouailhas, H.; Aouf, C.; Le Guerneve, C.; Caillol, S.; Boutevin, B.; Fulcrand, H. *J. Polym. Sci. Part A: Polym. Chem.* **2011**, *49*, 2261−2270.

(29) Thompson, Z. J.; Hillmyer, M. A.; Liu, J.; Sue, H. J.; Dettloff, M.; Bates, F. S. *Macromolecules* **2009**, *42*, 2333−2335.

(30) Cole, K. C. *Macromolecules* **1991**, *24*, 3093−3097.

(31) Mezzenga, R.; Boogh, L.; Månson, J. A. E.; Pettersson, B. *Macromolecules* **2000**, *33*, 4373−4379.

(32) Wu, S.; Guo, Q.; Kraska, M.; Stühn, B.; Mai, Y. W. *Macromolecules* **2013**, *46*, 8190−8202.

(33) de Espinosa, L. M.; Ronda, J. C.; Galià, M.; Cádiz, V. *J. Polym. Sci. Part A: Polym. Chem.* **2009**, *47*, 1159−1167.

(34) Pan, Y.; Xu, Y.; An, L.; Lu, H.; Yang, Y.; Chen, W.; Nutt, S. *Macromolecules* **2008**, *41*, 9245−9258.

(35) Gu, H.; Tadakamalla, S.; Zhang, X.; Huang, Y.; Jiang, Y.; Colorado, H. A.; Luo, Z.; Wei, S.; Guo, Z. *J. Mater. Chem. C* **2013**, *1*, 729−743.

(36) Garcia, F. G.; Soares, B. G.; Pita, V. J. R. R.; Sánchez, R.; Rieumont, J. *J. Appl. Polym. Sci.* **2007**, *106*, 2047−2055.

(37) Chiu, Y. C.; Tsai, H. C.; Imae, T. *J. Appl. Polym. Sci.* **2012**, *124*, 1234−1240.

Chapter 5

Impacts of Methoxy Substituents on Properties of Lignin−Derived Epoxy Thermosets

ABSTRACT: Because lignin−derived compounds often have methoxy groups, a series of TPs with various number of methoxy group substituents (n= 0−6) were synthesized using *para*−unsubstituted lignin−derived phenols (guaiacol and 2,6−dimethoxyphenol) and aldehydes (4−hydroxybenzaldehyde, vanillin and syringaldehyde). Increasing the content of methoxy groups resulted in decreased glass transition temperature (132 to 118 °C) and glassy modulus (2.6 to 2.2 GPa). Thermal stability of high−methoxy−content thermosets was reduced due to electron−donating effects and higher oxygen content. Conversions and isolated yields of TPs significantly decreased as number of methoxy substituents increased, which markedly determined the feasibility of TPs as precursors to polymers. Evaluation of impacts of methoxy substitution provides insights in the selection of lignin−derived monomers.

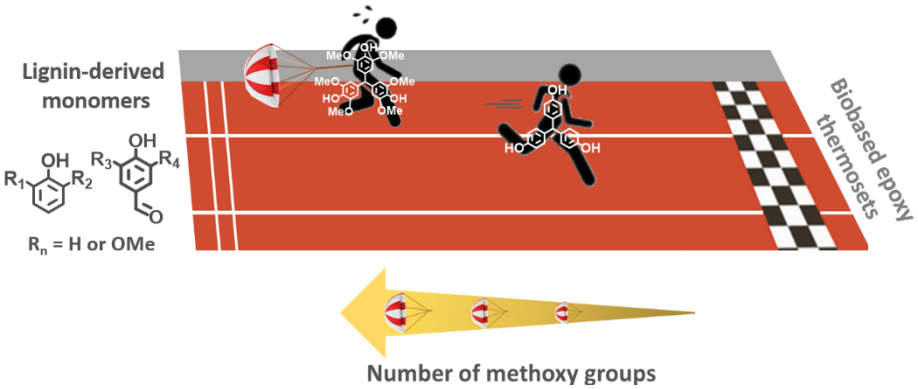

This section is partially adapted from: Shou Zhao, Xiangning Huang, Andrew J. Whelton, and Mahdi M. Abu−Omar, to be submitted.

5.1 Introduction

Epoxy thermosets have been extensively used as coatings, adhesives, electronic materials and structural composites because of their excellent thermal and mechanical performance. The most popular epoxy monomers are derived from bisphenol A (BPA), which accounts for more than 90 % of epoxy cross−linked polymers.[1] The suitability of BPA comes from its aromatic structure, which confers good mechanical and thermal properties on the resulting epoxy thermosets. However, as the development of renewable materials has received increased attention, numerous biomass derived molecules have been utilized to replace or supplement the petroleum−based BPA.[2–23] Among these feedstocks, lignin is the most promising candidate for making epoxy thermosets, since it is the sole large−volume sustainable source composed of an aromatic skeleton.[24, 25]

Recent catalytic depolymerization techniques can convert lignin to various value−added phenolic monomers including phenols and aldehydes.[26–31] Lignin−derived phenol monomers (LDPMs) have been extensively studied as BPA alternatives. Since cross−linkable epoxy monomers require at least two epoxides per molecule, special efforts have been taken to increase the number of functional hydroxyl groups of LDPMs through (1) conversion of other reactive groups like methoxy, double bond, or aldehyde to hydroxyl groups,[32–37] and (2) coupling repeated LDPMs using bridging reagents.[38–48] Despite the abundance of LDPMs and their coupling methods, lignin−derived aldehyde monomers (LDAMs) are often neglected as renewable bridging reagents (akin to acetone in the preparation of BPA). A few examples include the work of Foyer *et al*., in which a synthesis route of formaldehyde−free resol resin based on vanillin was reported.[49, 50] However, because alkaline catalyst preferentially

deprotonated the hydroxyl of vanillin over phenols in resol synthesis, the hydroxyl group of vanillin had to be protected prior to polymerization. Moreover, it is important to develop building blocks that can yield polymer with tunable properties permitting wider applications. For example, with the aid of an acid, LDAMs can condense with phenols at the *para* and/or *ortho* position to yield triphenols (TPs). The TP architecture improves the rigidity compared to conventional bisphenolic systems, while adjusting the number of functional hydroxyl could tune the cross−link density and therefore mechanical properties of the resulting networks.[51] Furthermore, functionalizing the hydroxyl groups to epoxy, olefin, or cyanate ester results in different types of materials.

Apart from the aromatic nature, lignin is characterized by methoxy substitution of its aromatic rings. There are three types of monolignols (*para*−coumaryl alcohol, coniferyl alcohol and sinapyl alcohol) existing in the lignin backbone, which form *p*−hydroxyphenyl (H), guaiacyl (G) and syringyl (S), with varying number of methoxy groups.[52,53] Methoxy substitution plays an important role in determining the physiochemical properties of lignin. For example, lignin with high methoxy groups (e.g., hardwood lignin) generally is less thermally stable and produces less char compared to the low methoxys counterparts (e.g., softwood lignin) during lignin pyrolysis.[54,55] Meanwhile, several experimental and theoretical studies have pointed out oxygen−carbon bond dissociation enthalpy was substantially decreased when *ortho* or *para* methoxy substituent was situated on the phenethyl phenyl ether model compounds for the dominant *β*−O−4 linkages.[56–58] Inspired by these studies, we set out to investigate the impact of methoxy substituents on the performance of lignin−derived polymers. Hernandez *et al.* recently reported a bio−based epoxy resin using bis−guaiacol (BG), which was synthesized

from vanillyl alcohol and guaiacol.[59] To investigate the impact of methoxy groups, BG−based resin was compared to bisphenol F (BPF) based counterpart. It was found that methoxy groups could lower the glass transition temperature (T_g) and thermal stability of the resulting resins. Harvey *et al.* reported similar results when making cyanate ester resins with lignin−based bis−creosol, while the significant decrease in thermal stability was attributed to the electron donating effect of methoxy.[60] While these studies provided important information on the impact of methoxy substitution, the following information is still missing: 1) The above studies only focused on guaiacyl type (e.g. guaiacol, one methoxy group substituted at *ortho* position of phenol), neglecting another important syringyl type that is abundant in hardwood lignin (e.g. 2,6−dimethoxyphenol, DMP, which bears two methoxys at *ortho* sites). The additional methoxy of DMP would affect the electron donating effect and symmetry of obtained polyphenols and merits investigation. 2) Literature studies thus far have compared bisphenols with only 0 vs. 2 methoxys. With the aid of triphenol architecture proposed in this work, triphenols with 0−6 methoxys can be achieved, which magnifies the effects of methoxy. 3) Guidance on the selection of lignin (e.g., low S vs. high S) as phenol sources for larger scale manufacturing would be of interest. Apart from the thermomechanical properties of thermosets, the feasibility and processability of thermoset precursors (e.g. bisphenol or triphenol) should also be considered. Effect of methoxy on properties of these precursors, including conversion, difficulty in isolation, yield and melting point needs to be discerned, especially when methoxy number reaches higher levels of 3−6 per molecule.

In the present work we report: 1) synthesis of fully lignin−derived TPs. The synthesis of TPs employs lignin−derived aromatic aldehydes as bridging reagents, which avoids the

carcinogenic and highly volatile molecules like formaldehyde and acetone. Meanwhile, TP architecture confers thermosets with improved rigidity compared to conventional bisphenolic systems; and 2) the impact of methoxy groups on performance of TP−based thermosets. TP structure allows for a way to manipulate the number of methoxy substituents. By controlling the starting LDAMs, i.e., 4−hydroxybenzaldehyde (HBA), vanillin (VAN), syringaldehyde (SYA), and LDPMs, i.e., phenol (PhOH), guaiacol (GUA) and 2,6−dimethoxyphenol (DMP), TPs with 0 to 6 methoxy substituents can be prepared. Selected TPs were converted to glycidyl ethers and cured to explore their feasibility as precursors to make renewable epoxy resins (Figure 5.1).

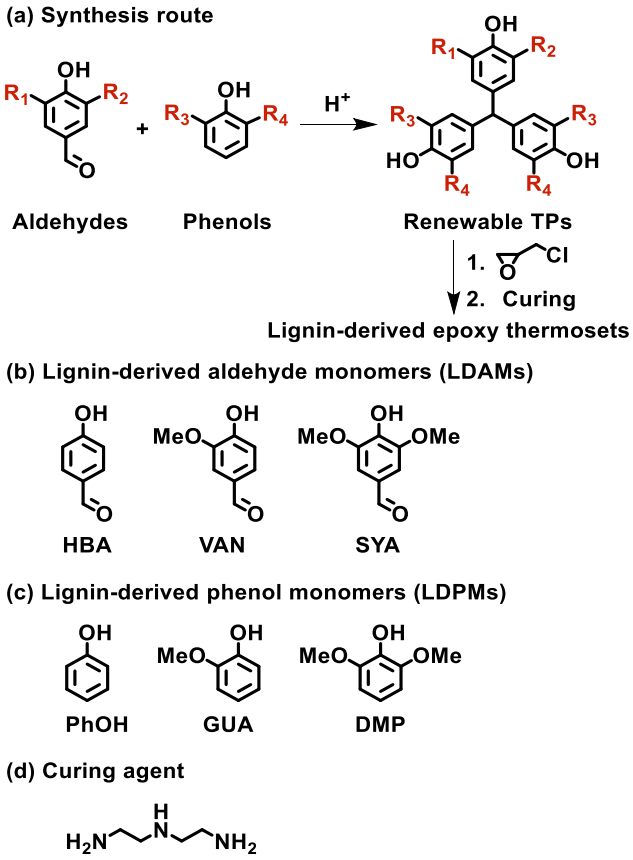

Figure 5.1 Synthesis route of epoxy networks from lignin−derived aldehydes and phenols.

5.2 Results and Discussion

5.2.1 Structure of TPs and Glycidyl Ethers

Triphenylmethane architecture provides an approach of manipulating the number of methoxy substituents by employing different starting aldehydes and phenols. To confirm the structure, proton and carbon NMR spectra of M_0 to M_6 are shown in Figure S5.1−S5.9. The proton peak at ~ 5.3 ppm corresponds to the triphenylmethyl group, which indicates successful condensation of aldehyde and phenol. The characteristic methoxy groups are observed at ~ 3.7 ppm, while aromatic protons are found in the range of 6.3−6.9 ppm. For the carbon NMR, the triphenylmethyl and methoxy groups are observed in the range 50.6−55.7 ppm. While the *para* position of phenol is the main site for aldehyde coupling, it is noteworthy that certain amount of *ortho* or *meta* coupled byproducts are also observed in the proton spectra, with molar ratio below 8 % of the product mixture. The dominant *para*−coupled products were previously observed, which was related to their higher reactivity and less steric hindrance of their *para* site.[59] Proton NMR spectra of the corresponding glycidyl ethers (GEM_0 to GEM_6) are given in Figure S5.10−S5.18. Compared to TPs, new characteristic peaks are identified at 3.91−4.19 ppm (−CH_2−, b and b'), 3.35 ppm (−CH−, c) and 2.61−2.87 ppm (−CH_2− in epoxy ring, d and d'), which are indicative of formation of epoxy groups.

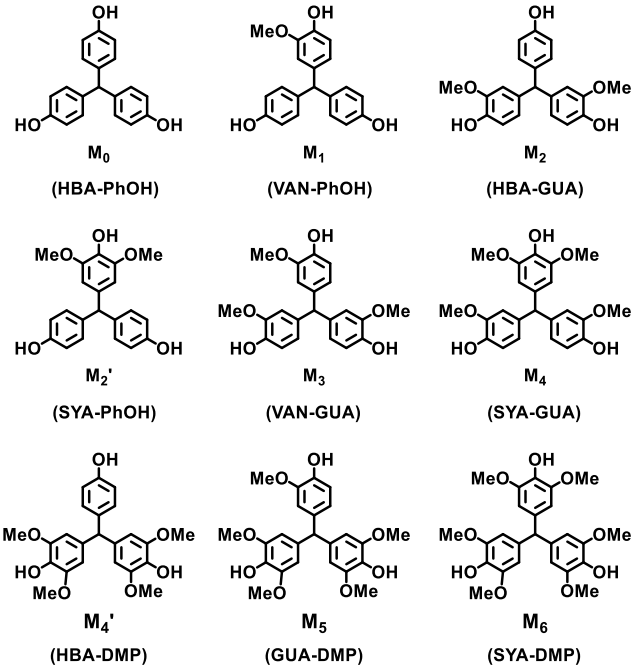

Figure 5.2 List of TPs with different number of methoxy groups. TPs are abbreviated as M_n, while n indicates the number of methoxy groups. The starting aldehyde and phenol for each TP are also listed in parentheses.

Because of the structural similarity of TPs, only one crystal structure (M_6, prepared from syringaldehyde and dimethoxyphenol) was collected to confirm the structure and determine the main coupling sites. Figure 5.3 reveals syringaldehyde couples exclusively at the *para* sites of both dimethoxyphenol. Coupling at *para* sites provides TPs with stretched orientation of hydroxyl groups (Figure 5.3). Together with its rigid architecture and high number of hydroxyl groups (n= 3), TP−based polymers are supposed to exhibit satisfactory mechanical properties.

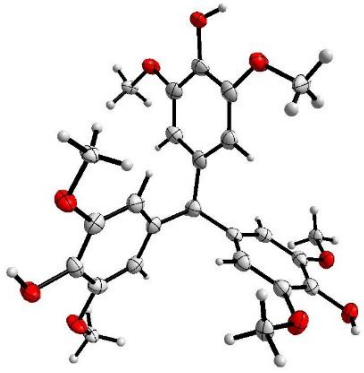

Figure 5.3 Crystal structure of M_6. Crystal was collected from the slow evaporation of an ethyl acetate solution at room temperature.

Structure of TPs is further confirmed by IR spectra in Figures S5.19−S5.27. Starting aldehydes (HBA, VAN and SYA) have an aldehyde peak around 1672 cm^{-1}. After they are condensed with phenols, the aldehyde group becomes triphenylmethyl group. This is consistent with the IR spectra of TPs in which the aldehyde peak disappears (Figure S5.19−S5.27, panel a). Other characteristic bands comprise 3058−3586 cm^{-1} (O−H stretching), and 1608, 1510 and 1437 cm^{-1} (aromatic C−C bond). When TPs are converted to glycidyl ethers, the broad hydroxyl band diminishes significantly, while a new epoxy ring band at 912 cm^{-1} emerges (Figure S5.19−S5.27, panel b). This is consistent with the NMR analysis confirming the formation of epoxy ring. This conclusion is further supported by the IR spectrum of the cured thermosets in Figure S5.19−S5.27, panel c. When epoxy monomers are cured with DETA, epoxy groups are opened by amine while hydroxyl groups are created concurrently. This process is reflected by the IR results, in which the epoxy band at 912 cm^{-1} disappears while the OH band around 3355 cm^{-1} increases. The absence of epoxy bond is indicative of significant conversion of epoxy groups in our investigated networks. Meanwhile, high reactivity of epoxy/DETA system is confirmed by two cycles of heating−cooling using DSC analysis (Figure S5.28), as supported by the lack of exotherm on the second heating.

5.2.2 Effect of Methoxy Substituents on Yields of TPs

To study the conversion of TPs, aldehyde and phenol were reacted under the following conditions: molar ratio of aldehyde: phenol = 1:4, aldehyde: H_2SO_4 = 1:3, absolute ethanol was used as solvent and the mixture was stirred at 65 °C for 2 days. Conversions were calculated

based on integrals of aldehyde and triphenylmethyl peaks in the proton spectra. Table 5.1 lists the conversion of TPs prepared from different aldehydes and phenols. Generally, conversion decreases with increased number of methoxy groups (from 82.5% for M_0 to 35.2% for M_6). Comparisons between starting aldehydes and phenols reveal reactivity of aldehydes (HBA > VAN > SYA) and phenols (PhOH > GUA > DMP) decreases with increased number of methoxy substituents (Table 5.1). The negative effects of methoxy group on conversion could be attributed to: 1) steric effect of methoxy decreases the reactivity of aldehydes and phenols, and 2) as the number of electron−donating groups (methoxy) increases, the electrophilicity decreases, which reduces their reactivity in electrophilic substitution reactions.

Table 5.1. Conversion (%) of TPs Prepared from Lignin−Derived Aldehydes and Phenols with Different Number of Methoxy Groups [a]

Aldehyde / Phenol	HBA (0)	VAN (1)	SYA (2)
PhOH (0) [b]	83 [c]	72	64
GUA (1)	81	68	64
DMP (2)	49	42	35

[a] Reaction conditions: molar ratio of aldehyde: phenol = 1:4, aldehyde: H_2SO_4 = 1:3, 65 °C for 2 days. Absolute ethanol is used as solvent. [b] Numbers (in parentheses) next to starting aldehydes or phenols indicate the number of methoxy groups situated on these reagents. [c] Numbers in the table means conversion (%) of TPs prepared from different aldehydes and phenols. For example, 83% is the conversion of TP synthesized from HBA and PhOH.

Compared to conversion, methoxy groups have even greater negative impact on isolated yields. For TPs (M_0 to M_4) that were prepared from aldehydes (HBA, VAN and SYA) and phenols (PhOH and GUA), satisfactory isolated yields of 46−69% were achieved. However,

when 2,6−dimethoxyphenol (DMP) was reacted with aldehydes, only 18%, 7% and 5% isolated yields were obtained for M_4', M_5 and M_6, respectively. Low isolated yields of DMP−based TPs could be attributed to two reasons. On one hand, conversions of these TPs are relatively low (35.2−48.8%). On the other hand, the aldehyde/phenol reaction can be divided to two steps: in the first step, aldehyde reacts with phenol to yield a diphenylmethyl alcohol derivative intermediate. In the second step, methyl alcohol group of the intermediate couples to another phenol to form the triphenylmethane product. However, because of the steric hindrance of the intermediate and especially the lower reactivity of DMP, the second step could occur very slowly. As a result, the reaction mixtures contain certain amount of dimer intermediate (proton NMR spectrum of the intermediate exhibits no triphenylmethyl peak at 5.3 ppm). These undesired intermediates exhibit similar polarity with TP products and impair the yields of flash column purification. The low yield of DMP−based TPs makes them unreasonable for preparing renewable polymer materials.

5.2.3 Effect of Methoxy Substituents on Melting Point

Melting points of TPs with various number of methoxys are listed in Table 5.2. The highest melting point is found to be 241 °C (M_0), while the lowest is 125 °C (M_3). This obvious difference highlights the role of methoxy. Melting points of TPs from different aldehydes follows the order: HBA > SYA > VAN, while phenols follow the order: PhOH > DMP > GUA (Table 5.2). The lower melting points of TPs prepared from di−methoxy substituents (SYA and DMP) than corresponding non−methoxy compounds (HBA and PhOH) could be explained by the electron donating effect of methoxy. As for the mono−methoxy derivatives (VAN and GUA) that exhibit the lowest TP melting points, influence of methoxy may be reflected by its impact

on the symmetry of TP units. Symmetric TPs like M_0, M_2', M_4' and M_6 exhibit melting points above 190 °C. By comparison, when asymmetric units VAN and GUA (only one methoxy at *ortho* site) are incorporated, melting points of TPs significantly decrease. Especially, M_3 with three asymmetric guaiacol units shows the lowest melting point (125 °C) among all TPs. Moreover, impact of unit symmetry can be highlighted when TPs with same number of methoxy group are compared. For example, melting point of M_2' (SYA−PhOH, 191 °C) is 27 °C higher than M_2 (HBA−GUA, 164 °C), while M_4' (HBA−DMP, 204 °C) is 131 °C higher than M_4 (SYA−GUA, 73 °C).

Table 5.2. Melting Point (°C) of TPs with Different Number of Methoxy Groups [a]

Aldehyde / Phenol	HBA (0)	VAN (1)	SYA (2)
PhOH (0) [b]	241 [c]	188	191
GUA (1)	164	125	146
DMP (2)	204	133	190

[a] Melting points were measured using a capillary melting point apparatus (MEL−TEMP) with a heating rate of 5 °C/min. [b] Numbers (in parentheses) next to starting aldehydes or phenols indicate the number of methoxy groups situated on these reagents. [c] Numbers in the table mean melting points (°C) of TPs prepared from corresponding aldehydes and phenols. For example, 241 °C is the melting point of TP synthesized from HBA and PhOH.

5.2.4 Effect of Methoxy on Properties of TP−Based Epoxy Thermosets

Differential Scanning Calorimetry Analysis.

Effect of methoxy group on curing behavior is studied via DSC tests. Table 5.3 exhibits enthalpy (ΔH) values of all curing systems fall in the range (91.5 to 96.4 kJ/ee), which is in accordance with the typical value of 90−100 kJ/ee for epoxy/amine reactions. Table 5.3

demonstrates peak curing temperatures are not significantly different for studied monomers: GEM_0 (81 °C), GEM_2' (80 °C), GEM_2 (78 °C) and GEM_4 (77 °C), which indicates methoxy group has no impact on the epoxy/amine curing process. This could be attributed to the inert nature of methoxy, which cannot catalyze the epoxy/amine reaction.[62] Degrees of cure were determined through two cycles of curing. As demonstrated in Figure S5.28, all epoxy monomers are most cured as supported by the lack of exotherm on the second heating.

Table 5.3. DSC Curing Data for Epoxy/DETA Systems Exhibiting Onset Curing Temperature (T_i), Peak Curing Temperature (T_p) and Enthalpy of Reaction (ΔH).

sample	T_i (°C)	T_p (°C)	ΔH (kJ/ee)	Theoretic EEW (g/eq.)	Measured EEW (g/eq.)
GEM_0	47	81	96	154	160
GEM_2	43	78	94	174	179
GEM_2'	45	80	95	174	181
GEM_4	44	77	92	194	199

Dynamic Mechanical Analysis.

Figure 5.4 and Table 5.4 illustrates T_α (α−relaxation temperature, related to T_g) of thermosets decreases gradually with increased contents of methoxy group, i.e., ENM_0 (132 °C) > ENM_2' (125 °C) > ENM_2 (120 °C) > ENM_4 (118 °C). Similar negative effects of methoxy on mechanical performance was also reported for cyanate ester resins.[60] Even though some methoxys could form hydrogen bonds with hydroxyls that improves the network constraint, increased void volume created by methoxy groups seems to play a more important role that decreases the T_α. Storage modulus (E') curves of TP−based thermosets are also exhibited in Figure 5.4 and Table 5.4. Similar with T_α, increasing the content of methoxy generally leads to

reduced modulus from ENM_0 to ENM_4. It is noteworthy that glassy modulus (E_{30}', storage modulus at 30 °C) values are in the range of 2.2 to 2.6 GPa. To compare the mechanical performance of TP−based polymers with BPA–based materials, diglycidyl ether of BPA (DGEBA) and diethylenetriamine were cured using the same profiles with TP−based networks. The E_{30}' and T_α of DGEBA/DETA system (ENBPA) were measured to be 2.0 GPa and 103 °C (Figure 5.4 and Table 5.4), which is lower than TP−based thermosets. This result could be explained by the more rigid structure and higher functionality of TPs over BPA. Moreover, this result highlights TP−based epoxy networks possess marked mechanical performance that can replace or supplement BPA−based analogues.

Table 5.4. Thermomechanical Data of T_α, E_{30}' (Glassy Modulus), T_{d5}, T_{d30} (Temperature at 5% and 30% Weight Loss), T_s (Statistic Heat−Resistant Index Temperature) and $Char_{600}$ (Char Residue at 600 °C) of Epoxy Networks Derived from TPs and BPA.

sample	T_α (°C)	E_{30}' (MPa)	T_{d5} (°C)	T_{d30} (°C)	T_s (°C)	$Char_{600}$ (%)
ENM_0	132	2745	257	341	151	20
ENM_2	125	2598	206	321	135	17
ENM_2'	120	2249	218	324	138	18
ENM_4	118	2477	184	296	123	14
ENBPA	100	2042	305	371	169	8

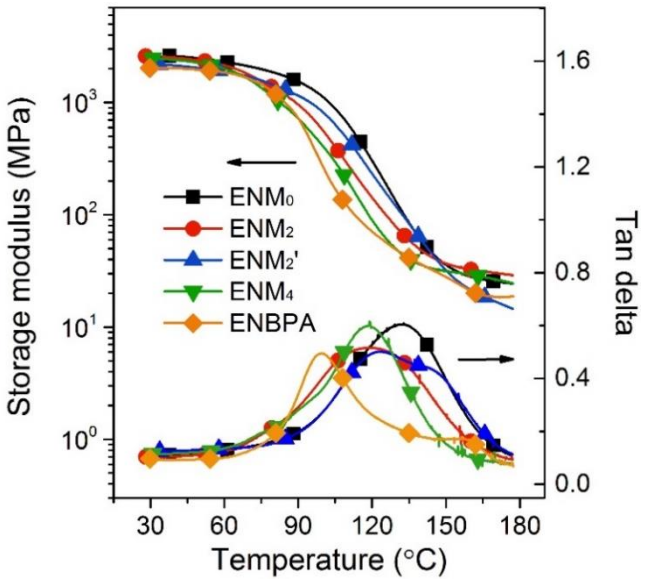

Figure 5.4 DMA curve of epoxy networks derived from TPs with different number of methoxy groups. Temperature at the maximum in tan δ curve is taken as T_α (related to T_g).

Thermogravimetric Analysis.

Figure 5.5 reveals a one−step degradation curve for all TP−based epoxy networks. Figure 5.5 and Table 5.4 illustrate thermal stability of cured networks decreases with increased content of methoxy (i.e., ENM_0 > ENM_2' > ENM_2 > ENM_4). This is reflected from the significant shift of onset degradation temperature (defined as T_{d5}, temperature at 5% weight loss) from ENM_0 (257 °C) to ENM_2' (218 °C), ENM_2 (206 °C) and ENM_4 (184 °C), respectively. The effects of methoxy could be attributed to its electron donation ability.[60] Meanwhile, as methoxy groups increase, content of oxygen within the polymers increases, which accelerates the thermal decomposition. T_{d30} (temperature at 30% weight loss) of cured samples reveal the same trend with T_{d5}, which confirms the effects of methoxy. Besides, for M_2 and M_2' that have similar methoxy contents, they exhibit close values of T_{d5}, T_{d30} and T_s (statistic heat−resistant index temperature). This further supports the relationship between methoxy substituents number and thermal performance of epoxy networks. As for the BPA−based network, it exhibits higher

thermal stability than TP−based thermosets when temperature is relatively low, as reflected by T_{d5} (305 °C), T_{d30} (371 °C) and T_s (169 °C). This could be attributed to the triphenylmethane architecture of TP that is easily oxidized, as well as the electron donating effects of methoxy groups. When temperature reaches 330 °C, ENBPA exhibits a fast degradation behavior and only 8 wt % char was left when the temperature reaches 600 °C. As for the TP−based networks, they start to exhibit higher stability over ENBPA above 391 °C, with 17−23 wt % char formed at 600 °C.

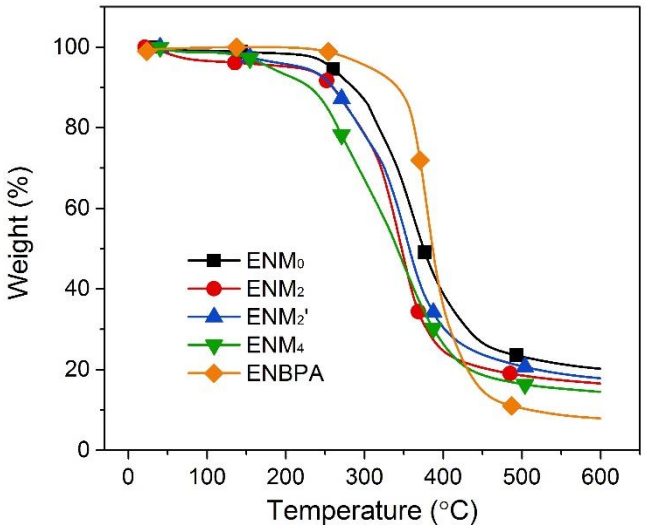

Figure 5.5 Thermogravimetric analysis thermograms of epoxy networks derived from TPs with different number of methoxy groups.

5.3 Conclusions

Preparation of renewable TPs with 0−6 methoxy substituents is described. While the rigid architecture and improved number of hydroxyl of the TP backbone afford epoxy networks with marked properties, the dangling methoxy groups are found to have different levels of impacts on the resulting networks. Because of its chemical inertness, the methoxy group has no impact on the curing process (curing temperature and enthalpy). By comparison, increasing methoxy content results in a decrease in mechanical properties (T_α decreases from 132 to 118 °C, and

glassy modulus decreases from 2.6 to 2.2 GPa). The greater impact of methoxy substitution is related to thermal performance, in which onset degradation temperature decreases significantly from 257 °C for ENM_0 (no methoxy substituents) to 184 °C for ENM_4 (four methoxy substituents). The greatest impact is on the conversion and especially isolated yields of TPs, which determines the feasibility of using these monomers in the manufacture of renewable polymers. The different impacts of methoxy substitution can guide the selection and/or modification (e.g. deoxygenation) of lignin−derived monomers for making epoxy polymers with desirable properies.

5.4 Experimental Section

General. 4−Hydroxybenzaldehyde, vanillin, syringaldehyde, phenol, guaiacol, 2,6−dimethoxyphenol, epichlorohydrin, tetrabutylammonium bromide, diethylenetriamine (DETA) and diglycidyl ether of bisphenol A (DGEBA) were purchased from Aldrich Chemical Co. Ethanol (200 proof) was purchased from Decon Labs, Inc. Sulfuric acid (98%) was obtained from Fisher Scientific. All chemicals were used as received without further purification.

5.4.1 General Procedure for TPs (M_0 to M_6).

4−Hydroxybenzaldehyde (2.44 g, 20 mmol) and phenol (7.52 g, 80 mmol) were dissolved in 30 mL absolute ethanol. To this solution, 5.7 g of concentrated sulfuric acid, dissolved in 5 mL of absolute ethanol, were dropwise added while stirred. An ice bath was used to control the temperature below 10 °C. After the addition of sulfuric acid, the temperature was increased to 65 °C and the mixture was gently stirred for 2 days. Then, 100 mL of brine was poured into the mixture prior to the addition of 3 × 20 mL of ethyl acetate to extract the product. The extract

was dried with $MgSO_4$ and concentrated using a rotary evaporator. Purification of the product using silica gel chromatography (hexane/ethyl acetate, 3:1 to 1:1) gave M_0 as an orange solid (4.26 g, 69% isolated yield). ^{1}H NMR (acetone−d_6, 400 MHz) δ: 6.91 (d, *J* = 8.4, 6H, Ar−H), 6.73 (d, *J* = 8.4, 6H, Ar−H), 5.30 (s, 1H, Ar_3−CH). ^{13}C NMR (acetone−d_6, 400 MHz) δ: 155.4, 135.9, 130.0, 114.7, 54.26 (Ar_3−CH). Other TPs (M_1 to M_6) were prepared using the same methods as M_0. Their structures are listed in Figure 5.2.

M_1, orange solid (3.93 g, 61 % isolated yield). ^{1}H NMR (acetone−d_6, 400 MHz) δ: 6.93 (d, *J* = 5.6, 4H, Ar−H), 6.74−6.71 (m, 6H, Ar−H), 6.51 (dd, *J* = 5.4, 1.2, 1H, Ar−H), 5.31 (s, 1H, Ar_3−CH), 3.71 (s, 3H, −OCH_3). ^{13}C NMR (acetone−d_6, 400 MHz) δ: 155.5, 147.1, 144.7, 136.5, 135.9, 130.0, 121.6, 114.8, 114.4, 112.7, 55.24 (−OCH_3), 54.67 (Ar_3−CH).

M_2, orange solid (3.66 g, 52% isolated yield). ^{1}H NMR (acetone−d_6, 400 MHz) δ: 6.93 (dd, *J* = 15.3, 8.5, 2H, Ar−H), 6.73 (t, *J* = 7.8, 6H, Ar−H), 6.53 (dd, *J* = 8.1, 1.7, 2H, Ar−H), 5.32 (s, 1H, Ar_3−CH), 3.71 (s, 6H, −OCH_3). ^{13}C NMR (acetone−d_6, 400 MHz) δ: 155.5, 147.1, 144.7, 136.4, 135.8, 130.0, 121.6, 114.7, 114.4, 112.7, 55.25 (−OCH_3), 55.05 (Ar_3−CH).

M_2', orange solid (4.51 g, 64% isolated yield). ^{1}H NMR (acetone−d_6, 400 MHz) δ: 6.94 (d, *J* = 8.5, 4H, Ar−H), 6.73 (d, *J* = 8.5, 4H, Ar−H), 6.38 (s, 2H, Ar−H), 5.32 (s, 1H, Ar_3−CH), 3.71 (s, 6H, −OCH_3). ^{13}C NMR (acetone−d_6, 400 MHz) δ: 151.2, 143.2, 132.5, 131.4, 129.9, 125.7, 110.4, 102.5, 51.34 (−OCH_3), 50.68 (Ar_3−CH).

M_3, orange solid (3.90 g, 51% isolated yield). ^{1}H NMR (acetone−d_6, 400 MHz) δ: 6.77−6.71 (m, 6H, Ar−H), 6.54 (m, *J* = 8.1, 1.7, 3H, Ar−H), 5.32 (s, 1H, Ar_3−CH), 3.71 (s, 9H, −OCH_3). ^{13}C NMR (acetone−d_6, 400 MHz) δ: 147.1, 144.7, 136.4, 121.6, 114.4, 112.7, 55.44 (Ar_3−CH), 55.29 (−OCH_3).

M_4, orange solid (3.79 g, 46% isolated yield). ^{1}H NMR (acetone−d_6, 400 MHz) δ: 6.78 – 6.69 (m, 4H, Ar−H), 6.56 (dd, *J* = 5.4, 1.1, 2H, Ar−H), 6.43 (s, 2H, Ar−H), 5.32 (s, 1H, Ar_3−CH), 3.71 (s, 6H, −OCH_3), 3.69 (s, 6H, −OCH_3). ^{13}C NMR (acetone−d_6, 400 MHz) δ: 147.4, 146.9, 144.7, 136.2, 135.5, 121.6, 114.3, 112.7, 106.9, 55.76 (Ar_3−CH), 55.67 (−OCH_3), 55.28 (−OCH_3).

M_4', orange solid (1.74 g, 18% isolated yield). ^{1}H NMR (acetone−d_6, 400 MHz) δ: 6.95 (d, *J* = 8.4, 2H, Ar−H), 6.74 (d, *J* = 8.4, 2H, Ar−H), 6.43 (s, 4H, Ar−H), 5.32 (s, 1H, Ar_3−CH), 3.71 (s, 12H, −OCH_3). ^{13}C NMR (acetone−d_6, 400 MHz) δ: 151.2, 143.2, 131.3, 130.9, 129.9, 125.7, 110.4, 102.5, 51.38 (−OCH_3 and Ar_3−CH).

M_5, orange solid (0.62 g, 7% isolated yield). ^{1}H NMR (acetone−d_6, 400 MHz) δ: 6.77 (d, *J* = 1.2, 1H, Ar−H), 6.72 (dd, *J* = 5.3, 2.7, 1H, Ar−H), 6.57 (dd, *J* = 5.4, 1.2, 1H, Ar−H), 6.45 (s, 4H, Ar−H), 5.32 (s, 1H, Ar_3−CH), 3.72 (s, 3H, −OCH_3), 3.70 (s, 12H, −OCH_3). ^{13}C NMR (acetone−d_6, 400 MHz) δ: 143.1, 131.7, 130.8, 129.9, 117.2, 110.0, 108.3, 102.5, 51.71 (−OCH_3), 51.33 (−OCH_3), 50.93 (Ar_3−CH).

M_6, orange solid (0.47 g, 5% isolated yield). ^{1}H NMR (acetone−d_6, 400 MHz) δ: 6.46 (s, 6H, Ar−H), 5.32 (s, 1H, Ar_3−CH), 3.71 (s, 18H, −OCH_3). ^{13}C NMR (acetone−d_6, 400 MHz) δ: 147.5, 135.1, 106.8, 56.40 (Ar_3−CH), 55.72(−OCH_3).

5.4.2 General Procedure for Glycidyl Ethers of TPs (GEM_0 to GEM_6).

GEM_0 was prepared by reaction of M_0 (2.92 g, 10 mmol) and epichlorohydrin (30 g, 320 mmol). Tetrabutylammonium bromide (0.34 g, 1.1 mmol) was used as a phase transfer catalyst. The mixture was heated at 85 °C for 3 h and followed by a dropwise addition of 6 g of 20% w/w NaOH solution. The reaction was kept for another 1.5 h, and the mixture was washed with

acetone, filtrated to remove formed NaCl and concentrated with a rotary evaporator to yield GEM_0 as a yellowish oil (4.33 g, 94% isolated yield). ^{1}H NMR ($CDCl_3$, 600 MHz) δ: 6.96−6.82 (12H, Ar−H), 5.37 (1H, a), 4.15−3.91 (6H, b + b'), 3.32 (3H, c), 2.87−2.71 (6H, d + d'). Other glycidyl ethers (GEM_1 to GEM_6) were prepared using the same method with 87−96% yields of glycidylation. Epoxy equivalent weights (EEW) of obtained epoxy monomers were determined to be 162−218 g/eq. using the HCl/acetone titration method.[61]

GEM_1, yellowish oil, 94 % isolated yield. ^{1}H NMR ($CDCl_3$, 600 MHz) δ: 6.96−6.58 (11H, Ar−H), 5.36 (1H, a), 4.17−3.91 (6H, b + b'), 3.71 (3H, e), 3.35 (3H, c), 2.88−2.71 (6H, d + d'). GEM_2, yellowish oil, 91 % isolated yield. ^{1}H NMR ($CDCl_3$, 600 MHz) δ: 6.99−6.54 (10H, Ar−H), 5.36 (1H, a), 4.18−3.91 (6H, b + b'), 3.73 (6H, e), 3.35 (3H, c), 2.86−2.71 (6H, d + d'). GEM_2', yellowish oil, 96 % isolated yield. ^{1}H NMR ($CDCl_3$, 600 MHz) δ: 6.98−6.28 (10H, Ar−H), 5.33 (1H, a), 4.18−3.97 (6H, b + b'), 3.73 (6H, e), 3.31 (3H, c), 2.86−2.61 (6H, d + d'). GEM_3, white solid, 87 % isolated yield (melting point 115 °C). ^{1}H NMR ($CDCl_3$, 600 MHz) δ: 6.85−6.54 (9H, Ar−H), 5.34 (1H, a), 4.18−3.99 (6H, b + b'), 3.73 (9H, e), 3.36 (3H, c), 2.86−2.71 (6H, d + d'). GEM_4, yellowish oil, 89 % isolated yield. ^{1}H NMR ($CDCl_3$, 600 MHz) δ: 6.81−6.28 (8H, Ar−H), 5.33 (1H, a), 4.18−3.96 (6H, b + b'), 3.73 (9H, e), 3.69 (9H, f), 3.36 (3H, c), 2.87−2.61 (6H, d + d'). GEM_4', yellowish oil, 91 % isolated yield. ^{1}H NMR ($CDCl_3$, 600 MHz) δ: 6.99−6.28 (8H, Ar−H), 5.33 (1H, a), 4.28−3.96 (6H, b + b'), 3.73 (12H, e), 3.32 (3H, c), 2.88−2.61 (6H, d + d'). GEM_5, yellowish oil, 89 % isolated yield. ^{1}H NMR ($CDCl_3$, 600 MHz) δ: 6.81−6.28 (7H, Ar−H), 5.31 (1H, a), 4.19−3.96 (6H, b + b'), 3.73 (3H, e), 3.66 (12H, f), 3.35 (3H, c), 2.87−2.61 (6H, d + d'). GEM_6, yellowish oil, 87 % isolated yield. ^{1}H NMR ($CDCl_3$, 600 MHz) δ: 6.29 (6H, Ar−H), 5.31 (1H, a), 4.16−3.96 (6H, b + b'), 3.73 (18H,

e), 3.36 (3H, c), 2.77−2.61 (6H, d + d').

5.4.3 Formation of Epoxy Networks.

Four epoxy monomers (GEM_0, GEM_2, GEM_2' and GEM_4) with 0−4 methoxy groups were used to make epoxy networks. GEM_6 was not used because of the low isolated yield of M_6 (5%), which makes it unreasonable for preparing renewable materials. The monomers were respectively mixed with diethylenetriamine (DETA) with 1:1 molar ratio of epoxy vs. −NH for curing. The mixtures were stirred for 10 min, degassed under vacuum to remove entrapped air and poured into silicone molds for curing with the profile: 65 °C for 8 h, 90 °C for 2 h and 120 °C for 2 h. Cured epoxy networks were expressed as ENM_0, ENM_2, ENM_2' and ENM_4, respectively. Degree of cure were monitored using Fourier transform infrared (FTIR). Conventional BPA−based epoxy network (ENBPA) was prepared from DGEBA and DETA using the same method with TP−based materials.

5.4.4 Analysis Methods.

Analysis methods are similar to Chapter 2.

5.5 References

(1) Auvergne, R.; Caillol, S.; David, G.; Boutevin, B.; Pascault, J. P. *Chem. Rev.* **2013**, *114* (2), 1082−1115.

(2) Faye, I.; Decostanzi, M.; Ecochard, Y.; Caillol, S. *Green Chem*. **2017**, *19* (21), 5236−5242.

(3) Pan, X.; Sengupta, P.; Webster, D. C. *Green Chem.* **2011**, *13* (4), 965−975.

(4) Kovash, C. S.; Pavlacky, E.; Selvakumar, S.; Sibi, M. P.; Webster, D. C. *ChemSusChem* **2014**, *7* (8), 2289−2294.

(5) Ma, S.; Webster, D. C. *Macromolecules* **2015**, *48* (19), 7127−7137.

(6) Ma, S.; Webster, D. C.; Jabeen, F. *Macromolecules* **2016**, *49* (10), 3780−3788.

(7) Baroncini, E. A.; Kumar Yadav, S.; Palmese, G. R.; Stanzione, J. F. *J. Appl. Polym. Sci.* **2016**, DOI: 10.1002/app.44103.

(8) Wang, X.; Zhou, S.; Guo, W. W.; Wang, P. L.; Xing, W.; Song, L.; Hu, Y. *ACS Sustainable Chem. Eng.* **2017**, *5* (4), 3409−3416.

(9) Zhang, Q.; Molenda, M.; Reineke, T. M. *Macromolecules* **2016**, *49* (22), 8397−8406.

(10) Hu, F.; La Scala, J. J.; Sadler, J. M.; Palmese, G. R. *Macromolecules* **2014**, *47* (10), 3332−3342.

(11) Liu, R.; Zhang, X.; Gao, S.; Liu, X.; Wang, Z.; Yan, J. *RSC Adv.* **2016**, *6* (58), 52549−52555.

(12) Basnet, S.; Otsuka, M.; Sasaki, C.; Asada, C.; Nakamura, Y. *Ind. Crops Prod.* **2015**, *73*, 63−72.

(13) van de Pas, D. J.; Torr, K. M. *Biomacromolecules* **2017**, *18* (8), 2640−2648.

(14) Janvier, M.; Hollande, L.; Jaufurally, A. S.; Pernes, M.; Ménard, R.; Grimaldi, M.; Beaugrand, J.; Balaguer, P.; Ducrot, P. H.; Allais, F. *ChemSusChem* **2017**, *10* (4), 738−746.

(15) Pin, J. M.; Guigo, N.; Vincent, L.; Sbirrazzuoli, N.; Mija, A. *ChemSusChem* **2015**, *8* (24), 4149−4161.

(16) Maiorana, A.; Spinella, S.; Gross, R. A. *Biomacromolecules* **2015**, *16* (3), 1021−1031.

(17) Eksik, O.; Maiorana, A.; Spinella, S.; Krishnamurthy, A.; Weiss, S.; Gross, R. A.; Koratkar, N. *ACS Sustainable Chem. Eng.* **2016**, *4* (3), 1715−1721.

(18) Miao, J. T.; Yuan, L.; Guan, Q.; Liang, G.; Gu, A. *ACS Sustainable Chem. Eng.* **2017**, *5* (8), 7003−7011.

(19) Ma, S.; Liu, X.; Fan, L.; Jiang, Y.; Cao, L.; Tang, Z.; Zhu, J. *ChemSusChem* **2014**, *7* (2),

555−562.

(20) Sadler, J. M.; Toulan, F. R.; Nguyen, A. P. T.; Kayea, R. V.; Ziaee, S.; Palmese, G. R.; La Scala, J. J. *Carbohydr. Polym.* **2014**, *100*, 97−106.

(21) Jian, X. Y.; An, X. P.; Li, Y. D.; Chen, J. H.; Wang, M.; Zeng, J. B. *Macromolecules* **2017**, *50* (15), 5729−5738.

(22) Liu, W.; Zhou, R.; Goh, H. L. S.; Huang, S.; Lu, X. *ACS Appl. Mater. Interfaces* **2014**, *6* (8), 5810−5817.

(23) Garrison, M. D.; Harvey, B. G. *J. Appl. Polym. Sci.* **2016**, *133* (45), DOI: 10.1002/app.43621.

(24) Kaiho, A.; Mazzarella, D.; Satake, M.; Kogo, M.; Sakai, R.; Watanabe, T. *Green Chem.* **2016**, *18* (24), 6526−6535.

(25) Zhao, S.; Abu−Omar, M. M. *ACS Sustainable Chem. Eng.* **2017**, *5* (6), 5059−5066.

(26) Stärk, K.; Taccardi, N.; Bösmann, A.; Wasserscheid, P. *ChemSusChem* **2010**, *3* (6), 719−723.

(27) Mialon, L.; Pemba, A. G.; Miller, S. A. *Green Chem.* **2010**, *12* (10), 1704−1706.

(28) Parsell, T. H.; Owen, B. C.; Klein, I.; Jarrell, T. M.; Marcum, C. L.; Haupert, L. J.; Amundson, L. M.; Kenttämaa, H. I.; Ribeiro, F.; Miller, J. T.; Abu−Omar, M. M. *Chem. Sci.* **2013**, *4* (2), 806−813.

(29) Luo, H.; Klein, I. M.; Jiang, Y.; Zhu, H.; Liu, B.; Kenttämaa, H. I.; Abu−Omar, M. M. *ACS Sustainable Chem. Eng.* **2016**, *4* (4), 2316−2322.

(30) Huang, X.; Zhao, S.; Abu−Omar, M.; Whelton, A. J. *J. Environ. Chem. Eng.* **2017**, *5* (4), 3622−3631.

(31) Parsell, T.; Yohe, S.; Degenstein, J.; Jarrell, T.; Klein, I.; Gencer, E.; Hewetson, B.; Hurt, M.; Im Kim, J.; Choudhari, H.; Saha, B.; Meilan R.; MosierN.; Ribeiro F.; Delgass W. N.; Chapple C.; Kenttämaa H.I.; Agrawal R.; Abu−Omar M. M. *Green Chem.* **2015**, *17* (3), 1492−1499.

(32) Zhao, S.; Abu−Omar, M. M. *Biomacromolecules* **2015**, *16* (7), 2025−2031.

(33) Fache, M.; Darroman, E.; Besse, V.; Auvergne, R.; Caillol, S.; Boutevin, B. *Green Chem.* **2014**, *16* (4), 1987−1998.

(34) Qin, J.; Liu, H.; Zhang, P.; Wolcott, M.; Zhang, J. *Polym. Int.* **2014**, *63* (4), 760−765.

(35) Fache, M.; Auvergne, R.; Boutevin, B.; Caillol, S. *Eur. Polym. J.* **2015**, *67*, 527−538.

(36) François, C.; Pourchet, S.; Boni, G.; Fontaine, S.; Gaillard, Y.; Placet, V.; Galkin, M. V.; Orebom, A.; Samec, J.; Plasseraud, L. *RSC Adv*. **2016**, *6* (73), 68732−68738.

(37) Guzmán, D.; Ramis, X.; Fernández−Francos, X.; De la Flor, S.; Serra, A. *Prog. Org. Coat.* **2018**, *114*, 259−267.

(38) Enjoji, M.; Yamamoto, A.; Shibata, M. *J. Appl. Polym. Sci.* **2015**, *132* (4), 41347.

(39) Schutyser, W.; Koelewijn, S. F.; Dusselier, M.; Van de Vyver, S.; Thomas, J.; Yu, F.; Carbone, M. J.; Smet, M.; Van Puyvelde, P.; Dehaen, W. *Green Chem*. **2014**, *16* (4), 1999−2007.

(40) Meylemans, H. A.; Groshens, T. J.; Harvey, B. G. *ChemSusChem* **2012**, *5* (1), 206−210.

(41) Ménard, R.; Caillol, S.; Allais, F. *Ind. Crops Prod.* **2017**, *95*, 83−95.

(42) Maiorana, A.; Reano, A. F.; Centore, R.; Grimaldi, M.; Balaguer, P.; Allais, F.; Gross, R. A. *Green Chem.* **2016**, *18* (18), 4961−4973.

(43) Zhao, S.; Abu−Omar, M. M. *ACS Sustainable Chem. Eng.* **2016**, *4* (11), 6082−6089.

(44) Wang, S.; Ma, S.; Xu, C.; Liu, Y.; Dai, J.; Wang, Z.; Liu, X.; Chen, J.; Shen, X.; Wei, J.

Macromolecules **2017**, *50* (5), 1892−1901.

(45) Hitce, J.; Crutizat, M.; Bourdon, C.; Vivès, A.; Marat, X.; Dalko−Csiba, M. *Green Chem.* **2015**, *17* (7), 3756−3761.

(46) Shibata, M.; Tetramoto, N.; Imada, A.; Neda, M.; Sugimoto, S. *React. Funct. Polym.* **2013**, *73* (8), 1086−1095.

(47) Liu, T.; Hao, C.; Wang, L.; Li, Y.; Liu, W.; Xin, J.; Zhang, J. *Macromolecules* **2017**, *50* (21), 8588–8597.

(48) Wan, J.; Zhao, J.; Gan, B.; Li, C.; Molina−Aldareguia, J.; Zhao, Y.; Pan, Y. T.; Wang, D. Y. *ACS Sustainable Chem. Eng.* **2016**, *4* (5), 2869−2880.

(49) Foyer, G.; Chanfi, B. H.; Boutevin, B.; Caillol, S.; David, G. *Eur. Polym. J.* **2016**, *74*, 296−309.

(50) Foyer, G.; Chanfi, B. H.; Virieux, D.; David, G.; Caillol, S. *Eur. Polym. J.* **2016**, *77*, 65−74.

(51) Zhao, S.; Abu−Omar, M. M. *Macromolecules* **2017**, *50* (9), 3573−3581.

(52) Laurichesse, S.; Avérous, L. *Prog. Polym. Sci.* **2014**, *39* (7), 1266−1290.

(53) Upton, B. M.; Kasko, A. M. *Chem. Rev.* **2015**, *116* (4), 2275−2306.

(54) Hosoya, T.; Kawamoto, H.; Saka, S. *J. Anal. Appl. Pyrolysis* **2009**, *84* (1), 79−83.

(55) Zhao, J.; Xiuwen, W.; Hu, J.; Liu, Q.; Shen, D.; Xiao, R. *Polym. Degrad. Stab.* **2014**, *108*, 133−138.

(56) Beste, A.; Buchanan III, A. *J. Org. Chem.* **2009**, *74* (7), 2837−2841.

(57) Britt, P. F.; Buchanan, A.; Cooney, M. J.; Martineau, D. R. *J. Org. Chem.* **2000**, *65* (5), 1376−1389.

(58) Kim, S.; Chmely, S. C.; Nimlos, M. R.; Bomble, Y. J.; Foust, T. D.; Paton, R. S.; Beckham,

G. T. *J. Phys. Chem. Lett.* **2011**, *2* (22), 2846−2852.

(59) Hernandez, E. D.; Bassett, A. W.; Sadler, J. M.; La Scala, J. J.; Stanzione III, J. F. *ACS Sustainable Chem. Eng.* **2016**, *4* (8), 4328−4339.

(60) Harvey, B. G.; Guenthner, A. J.; Lai, W. W.; Meylemans, H. A.; Davis, M. C.; Cambrea, L. R.; Reams, J. T.; Lamison, K. R. *Macromolecules* **2015**, *48* (10), 3173−3179.

(61) Bo C.; Hu L.; Jia P.; Liang B.; Zhou J.; Zhou Y. *RSC Adv.*, **2015**, *5*, 106651−106660

(62) Alzina, C.; Mija, A.; Vincent, L.; Sbirrazzuoli, N. *J. Phys. Chem. B* **2012**, *116* (19), 5786−5794.

Chapter 6

Synthesis of Lignin Incorporated Thermosets through Successive Lignin Modification Using LDPMs

ABSTRACT: An approach to lignin−based epoxy networks from both organosolv lignin and lignin derived phenol monomer (DHE) are developed using multiple chemical modifications including demethylation, phenolation and phenol−formaldehyde reaction. Structures of lignin incorporated novolac polyphenols (LINPs) and epoxy networks (LINENs) were characterized using proton nuclear magnetic resonance (NMR) and infrared (IR) spectroscopy. Compared to a common synthesis route in which lignin was epoxidized prior to blend with comonomers (LBEN), LINEN derivatives exhibited improved cross−link density (ν_e), α−relaxation temperature (T_α) and storage modulus in glassy region (E_g') as obtained from dynamic mechanical analysis (DMA), and increased thermal stability measured by thermogravimetric analysis (TGA).

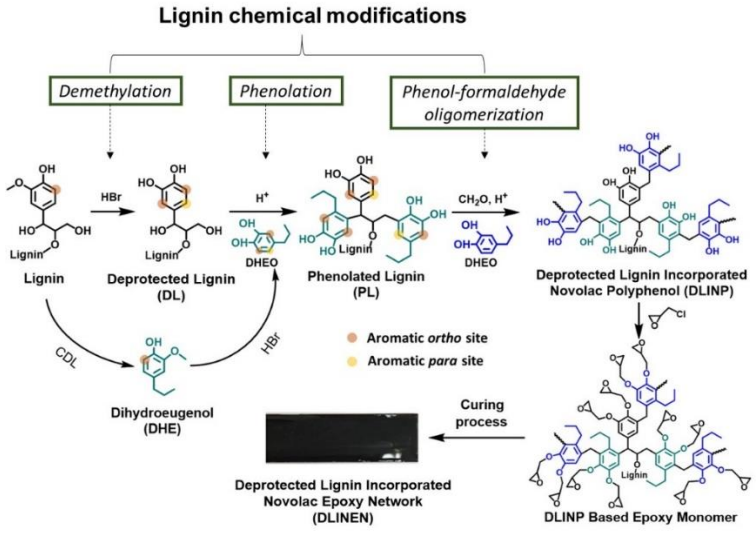

This section is partially adapted from: Shou Zhao and Mahdi M. Abu−Omar, *ACS Sustain. Chem. Eng.* **2017**, *5* (6), 5059−5066.

6.1 Introduction

Epoxy resins are among the versatile thermoset materials because of their excellent thermal and mechanical properties.[1] More than 90 % of epoxy cross−linked polymers are derived from bisphenol A (BPA).[2] However, there is a growing demand to develop renewable aromatic compounds to replace the petroleum−based BPA. Lignin represents an attractive source for large−volume renewable feedstock of aromatics.[3] With structural modifications, lignin can be transformed to have synthetic value for making epoxy resin.[4]

Several lignin−based epoxy networks have already been developed based on either lignin derived phenols (LDPMs, e.g. eugenol,[5] dihydroeugenol[6, 7] and vanillin[8–10]) or direct use of bulk lignin.[11–13] LDPMs are preferred because they are reactive, can be easily modified, and give predictable properties in their product resins. However, LDPMs need to be isolated from lignin biomass through chemical transformations such as catalytic reduction, oxidation and cracking processes, which are energy intensive and require separation and purification steps.[14] In contrast, bulk lignin is low−cost and abundant. Its total availability in the biosphere exceeds 300 billion tons and annually increases by 20 billion tons,[15] while its price is 20 times cheaper than phenol.[16] However, only 2 % of technical grade lignin is being utilized for value−added products.[17] Lignin is incompatible with polymeric compounds and its incorporation often leads to deterioration in the material's mechanical properties.[18, 19] The combination of lignin and LDPMs provides both economic and practical benefits.

Chemical modifications can improve the compatibility of lignin by increasing intermolecular covalent bonds. A common modification method is direct epoxidation of lignin prior to blending with LDP−based epoxy comonomers.[20, 21] The epoxy group of lignin can be

cured with other components. However, steric hindrance and poor dispersion of modified lignin impair covalent cross−link.[12, 20] Another chemical modification is to make covalent links prior to epoxidation and curing. For example, LDPMs can be grafted onto lignin through phenolation, substituting lignin aliphatic hydroxyl by *ortho*/*para*−bound LDPMs. The grafted LDPMs do not only improve lignin's compatibility, they also introduce additional sites (*ortho* and *para*), which can be used in building up cross−linked networks.

In this study, organosolv lignin and LDPMs are deployed through chemical modifications as illustrated in Figure 6.1. First, lignin's aromatic methoxy groups are deprotected,[21] followed by addition of deprotected dihydroeugenol (DHEO), which can be obtained from catalytic depolymerization of lignin (CDL).[22] As depicted in Figure 6.1, deprotected lignin (DL) is reacted with excess amount of DHEO under acid catalysis to yield phenolated lignin (PL). Formaldehyde solution is subsequently added to make a deprotected lignin incorporated novolac polyphenol (DLINP). The latter is reacted with epichlorohydrin to yield epoxy monomer that can be cured with diethylenetriamine (DETA) to make deprotected lignin incorporated novolac epoxy network (DLINEN). A comparison between the proposed synthesis routes with direct epoxidation of lignin (or deprotected lignin, DL) followed by blending with epoxidized DHEO novolac oligomer (DLBEN) is presented in Figure 6.2.

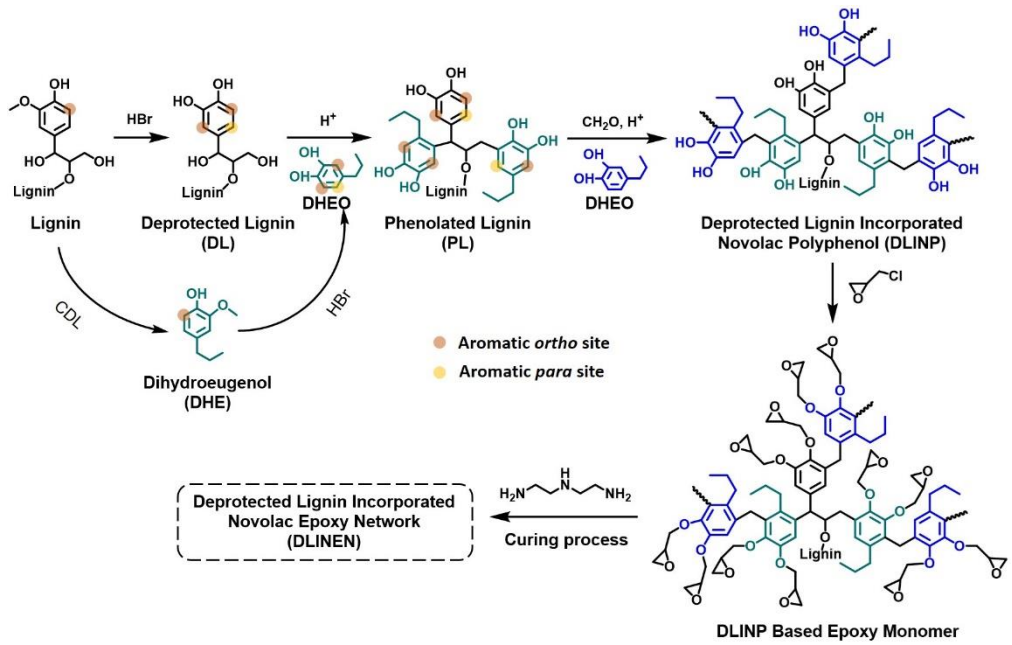

Figure 10 Synthesis route of deprotected lignin incorporated novolac epoxy network (DLINEN). Lignin is chemically modified through demethylation, phenolation and phenol−formaldehyde reactions to yield deprotected lignin incorporate novolac polyphenol (DLINP). DLINP is then epoxidized and cured with diethylenetriamine to make DLINEN. The modifying phenol (DHEO) is obtained via o−demethylation of DHE, a molecule that can be yielded through catalytic decomposition of lignocellulosic biomass. The aromatic *ortho*/*para* sites obtained via chemical modifications are highlighted. Benzodioxane derivatives produced during the glycidylation of DLINP are not shown.

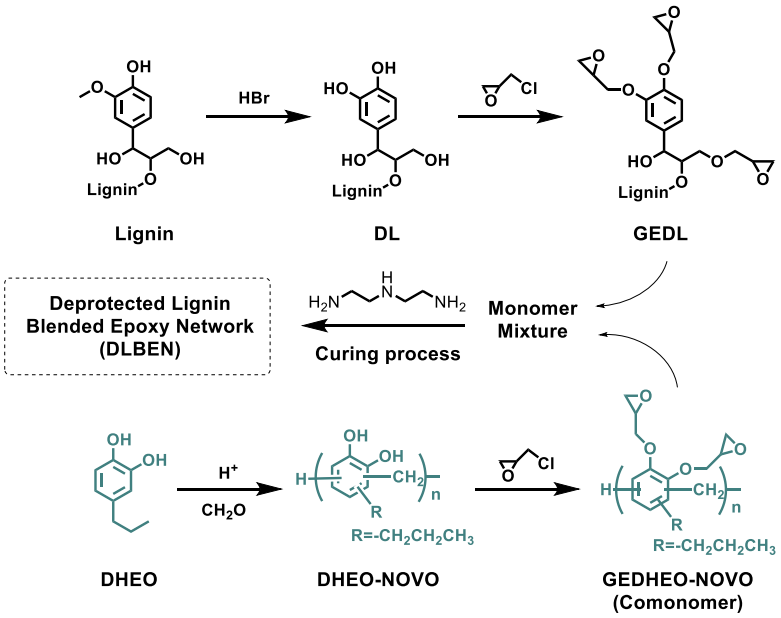

Figure 6.211 Synthesis route of deprotected lignin blended epoxy network (DLBEN), in which DL is epoxidized prior to blend with epoxidized DHEO−NOVO for curing. Benzodioxane derivatives produced during the glycidylation of DL and DHEO−NOVO are not shown.

6.2 Results and Discussion

6.2.1 Characterization of Modified Lignin

6.2.1.1 Deprotection of Lignin through Lewis−Acid−Catalyzed Modification

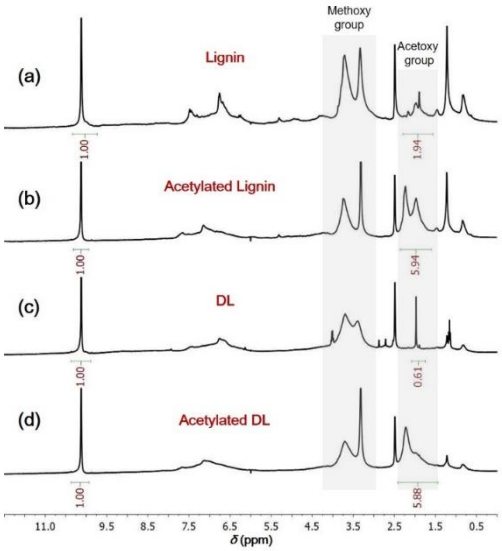

Figure 6.3 ^{1}H NMR spectra of (a) lignin, (b) acetylated lignin, (c) demethylated lignin (DL) and (d) acetylated DL. Solvent: DMSO−d_6.

^{1}H NMR spectra of lignin and DL are illustrated in Figure 6.3 (panels a and c, respectively). The resonance peaks at δ 6.0−7.8 are assigned to aromatic protons while δ 3.0−4.2 are attributed to methoxy groups. Since the NMR peak of hydroxyl is easily affected by hydrogen bonding, acetylation reaction between lignin/DL and acetic anhydride are conducted to determine the hydroxyl content. By calculating the increased integrals of acetoxy groups at δ 1.5−2.4 (Figure 6.3, panel a vs. b), and comparing it to the internal standard of pentafluorobenzaldehyde at δ 10.14, the hydroxyl content of lignin is found to be 4.32 mmol/g. This value is comparable to previously reported values.[23] By comparison, after demethylation the hydroxyl concentration of DL increased to 5.69 mmol/g (Figure 6.3, panel c vs. d). The 32% increase in hydroxyl content is consistent with a previous report in which aqueous HBr was used for demethylation of softwood lignin.[21]

6.2.1.2 Lignin−Based Polyphenols through Phenolation and Phenol−Formaldehyde Reaction

^{1}H NMR spectra of DHEO−NOVO in Figure 6.4, panel a exhibits an intramolecular methylene linkage in the region of δ 3.5−4.6. The integration ratio of H_d/H_b is around 0.57, indicating the novolac oligomer contains mainly dimer and trimer. This is in agreement with the novolac product of wood−tar creosote,[24] which has similar structure with DHEO. Using H_b as an internal standard, the integration ratio of H_d/H_b of LINP−5 (Figure 6.4, panel b) increased compared to DHEO−NOVO. Considering the lignin methoxy group also lies in the H_d region, it points to the integration of lignin with DHEO novolac oligomer. Similarly, other lignin incorporated polyphenols (DLINP−5, LINP−12 and DLINP−12) also exhibit increased H_d/H_b ratios as seen in Figures S7.1−S7.3.

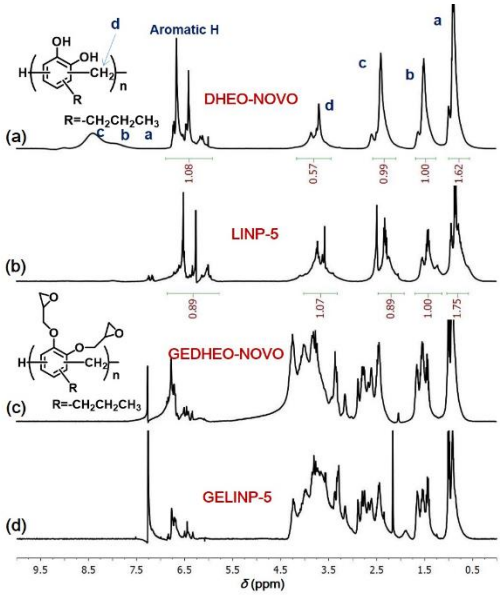

Figure 6.4 ^{1}H NMR spectra of polyphenols (a) DHEO−NOVO and (b) LINP−5, and their glycidylation products (c) GEDHEO−NOVO and (d) GELINP−5.

The structures of DHEO−NOVO and LINP−5 were also examined using IR. Figure 6.5, panel a reveals characteristic absorption bands of DHEO−NOVO appear at around 3383 cm^{-1} (O−H stretching), 2864 cm^{-1}, 2936 cm^{-1} and 2960 cm^{-1} (alkyl C−H stretch), and 1604 cm^{-1}, 1502 cm^{-1}, and 1445 cm^{-1} (aromatic C−C bond). The IR patterns of LINP−5 in Figure 6.5, panel b and DLINP−5, LINP−12 and DLINP−12 in Figure S6.1−S6.3 are also similar to DHEO−NOVO.

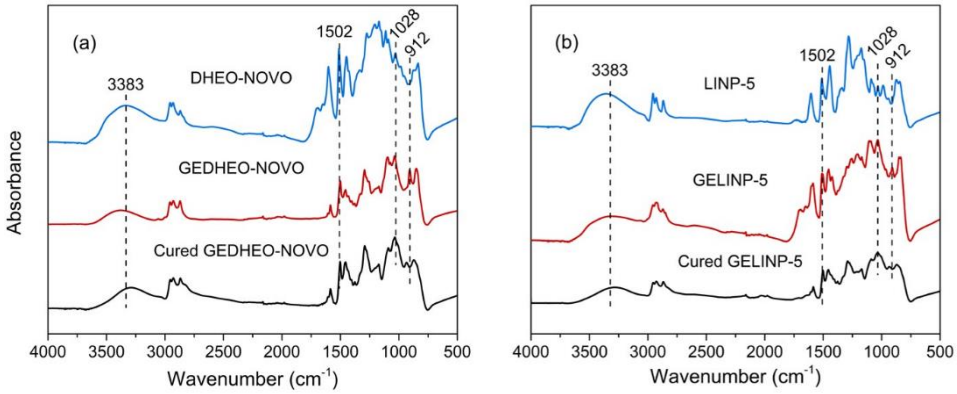

Figure 6.5 FTIR spectra of (a) DHEO−NOVO, GEDHEO−NOVO and cured

GEDHEO−NOVO, and (b) LINP−5, GELINP−5 and cured GELINP−5.

6.2.1.3 Glycidyl Ether of Lignin−Based Polyphenols

Figure 6.4, panel c is the NMR spectrum of glycidyl ether of DHEO−NOVO (GEDHEO−NOVO). The epoxy peaks are difficult to assign since they overlap with the novolac methylene bonds as well as the benzodioxane formed by intramolecular cyclization of catechol−like DHEO with epichlorohydrin. By comparison to the spectrum of DHEO−NOVO in Figure 6.4, panel a, as well as to our previous study on glycidylation of DHEO,[6] the characteristic protons of epoxy and benzodioxane are assigned in the regions of δ 2.6−2.9, δ 3.1−3.4 and δ 3.7−4.4.

The formation of epoxy groups is further supported by IR analysis. As seen in Figure 6.5, panel a, GEDHEO−NOVO exhibits an epoxy ring band at 912 cm^{-1} and a C−O−C ether linkage at 1028 cm^{-1}. GELINP−5, GEDLINP−5, GELINP−12 and GEDLINP−12 reveal similar NMR and IR pattern as GEDHEO−NOVO (Figure 6.4 panel d, Figure 6.5 panel b and Figures S6.4−S6.6). This conclusion is further supported by the IR spectra of cured GEDHEO−NOVO and GELINP−5 (Figure 6.5 and Figure S6.7−S6.8), in which the epoxy band at 912 cm^{-1} disappears. IR spectra of GEL and GEDL are depicted in Figure 6.6. Compared to lignin and DL, GEL and GEDL exhibit new peaks at 912 cm^{-1}, which indicates epoxidation of lignin.

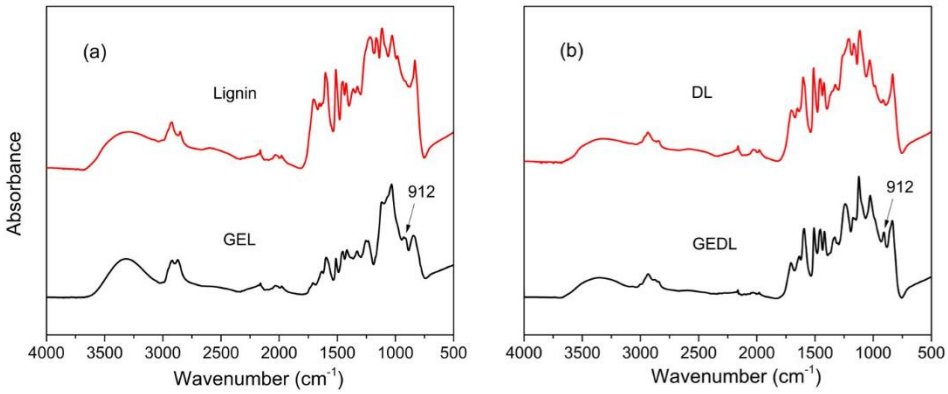

Figure 6.6 FTIR spectra of (a) lignin and glycidyl ether of lignin (GEL), and (b) demethylated lignin (DL) and glycidyl ether of DL (GEDL).

6.2.2 Effects of Lignin on Cross−link Density

Table 6.1 reports the cross−link densities of LINENs and LBENs. Lignin loading, demethylation and preparation approach (LINEN vs LBEN) are found to influence the cross−link density. Compared to the neat network (solely derived from GEDHEO−NOVO), the introduction of lignin is observed to decrease the cross−link density of all networks. The negative impact of lignin could be attributed to its reactivity and incompatibility. Besides, the steric hindrance of lignin restricts the development of cross−links. The role of lignin loading is further supported in the cases of LBENs, LINENs and DLINENs, as the network with 5 wt % lignin loading exhibits higher cross−link density than its 12 wt % counterpart.

Table 6.1. Dynamic mechanical properties and cross−link density (v_e) of LBENs and LINENs. T_α is α−relaxation temperature and E_g' is the storage modulus at glassy region.

Sample	T_α (°C)	E_g' (MPa)	*E' at* T_α*+30°C* (MPa)	v_e (10^{-3} mol/cm^3)
Neat[a]	139	1669	36	9.77
LBEN−5	133	1009	23	6.32
LBEN−12	134	866	21	5.76
DLBEN−5	132	1260	24	6.61
DLBEN−12	135	1142	30	8.21
LINEN−5	130	1128	28	7.75
LINEN−12	136	908	23	6.28
DLINEN−5	141	1420	35	9.45
DLINEN−12	137	1335	32	8.72

[a] "Neat" represents the epoxy network prepared from GEDHEO−NOVO and DETA, with no addition of organosolv lignin.

Unlike lignin loading, demethylation of lignin exhibits a positive role on the cross−link density. Table 6.1 shows epoxy networks from DL (DLBEN−5, DLBEN−12, DLINEN−5 and DLINEN−12) uniformly possess higher cross−link density than the corresponding protected (methoxy containing) LBEN−5, LBEN−12, LINEN−5 and LINEN−12. Improved cross−link density of DL−based polymers is explained as follows: (1) deprotection increases the number of functionality by turning unreactive methoxy groups into functional hydroxyl groups; (2) deprotection produces more *ortho and para* positions for link with DHEO via novolac chemistry; (3) acid treatment of lignin causes the cleavage of lignin intermolecular bonds, which decreases the molecular weight.[25] As a result, steric hindrance of the lignin substrate is reduced.

Cross−link density of lignin−based epoxy resins is dependent on the nature of chemical modification. Table 6.1 shows LINENs exhibit improved cross−link density when compared to the corresponding LBENs. Within the LBENs, GEL links with GEDHEO−NOVO and DETA

mainly via the epoxy groups. However, these linkages are often compromised by the poor reactivity of lignin because of sterics. Moreover, GEL (in the solid state) needs to be blended into oily GEDHEO−NOVO before curing. Compatibility issues of lignin and comonomer means the existence of even small amount of insoluble material defects in the network can give rise to negative effects on cross−link and hence mechanical properties.[26, 27] By comparison, the most obvious merits of the LINEN approach are the improved solubility through phenolation and phenol−formaldehyde reactions. Meanwhile, increased solubility of modified lignin results in a better degree of glycidylation than direct epoxidation of lignin. The homogenous oily mixture of GELINPs exhibits better compatibility with curing agents, which is also beneficial for cross−linking. The improved uniformity of LINEN is demonstrated pictorially in Figure 6.7, which compares LBEN−5 and LINEN−5 with neat polymer without lignin addition. Compared to the homogenous texture of LINEN−5 and neat polymer, LBEN−5 exhibits lignin particles "suspended" in the polymer.

Figure 6.7 Image of LBEN−5, LINEN−5 and neat network. Neat network represents the epoxy network prepared from GEDHEO−NOVO and DETA, with no addition of organosolv lignin.

The α−relaxation temperature (T_α, related to glass transition) is often related to cross−link density. Increased cross−links restrict the mobility of the polymer, resulting in higher T_α.[28, 29] As illustrated in Table 6.1 and Figure 6.8, LINENs and LBENs show a slight T_α decrease

(130−137 °C, except the 141 °C of DLINEN−5) as compared to the neat polymer (139 °C). Despite the negative effect of lignin, it is worth noting that all lignin−based polymers have T_α > 130 °C. Since T_α of traditional DGEBA/DETA epoxy resin is 137 °C,[30] LINENs and LBENs synthesized herein highlight the potential to replace petroleum−based thermosets. Storage modulus in the glassy region (E_g') of neat polymer, LBENs and LINENs are reported in Table 6.1 and Figure 6.8. The results suggest lignin introduction compromises the storage modulus but the lignin deprotection (removal of aromatic methoxy groups) and LINEN approach result in improvements and closer behavior to neat thermoset polymers.

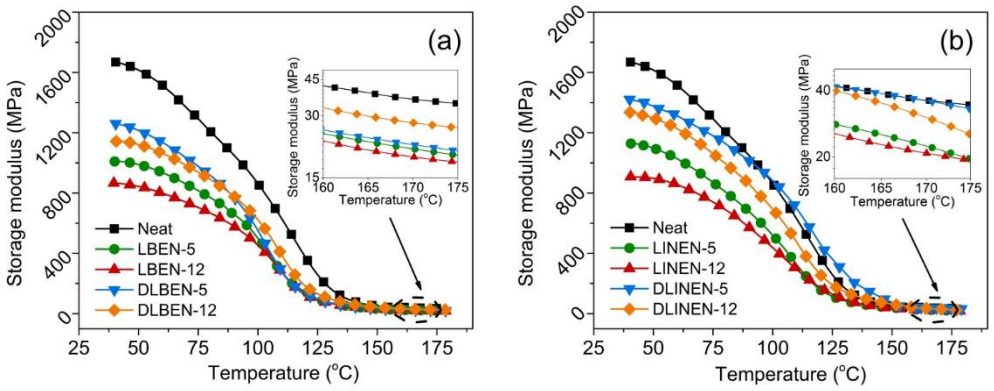

Figure 6.8 Storage modulus values of (a) LBENs and (b) LINENs as a function of temperature. Insets show the storage modulus of LBENs and LINENs at rubbery region. "Neat" represents the epoxy network prepared from GEDHEO−NOVO and DETA, with no addition of organosolv lignin.

The effects of lignin on curing are further investigated through DSC analysis. Figure 6.9 and Table 6.2 show the total enthalpy (ΔH) of lignin−loaded systems is relatively lower than the neat polymer (449 J/g). The exotherm peak shows no obvious change compared to the neat system (70.6−75.4 °C versus 72.6 °C). This phenomenon indicates the addition of lignin does not have significant effect on the activation energy of the curing processes.[31, 32]

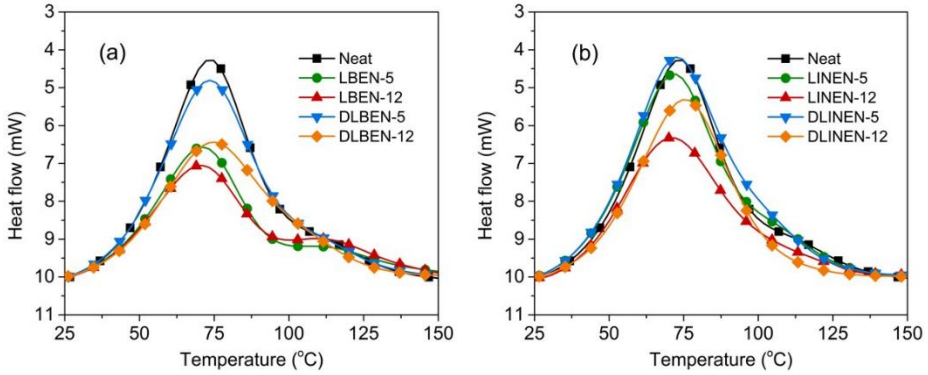

Figure 6.9 DSC curves of heat release during nonisothermal curing of (a) LBENs and (b) LINENs at 10 °C/min. "Neat" represents the epoxy network prepared from GEDHEO−NOVO and DETA, with no addition of organosolv lignin.

Table 6.2. DSC data for LBENs and LINENs exhibiting onset curing temperature (T_i), peak curing temperature (T_p) and enthalpy of reaction (ΔH).

Sample	T_i (°C)	T_p (°C)	ΔH (J/g)
Neat[a]	37.5	72.6	449
LBEN−5	32.6	71.2	284
LBEN−12	26.8	70.6	247
DLBEN−5	34.7	73.5	433
DLBEN−12	31.8	74.7	298
LINEN−5	35.1	71.6	438
LINEN−12	30.9	70.9	316
DLINEN−5	39.6	72.7	484
DLINEN−12	36.7	75.4	380

[a] "Neat" represents the epoxy network prepared from GEDHEO−NOVO and DETA, with no addition of organosolv lignin.

6.2.3 Effects of Lignin on Thermal Properties

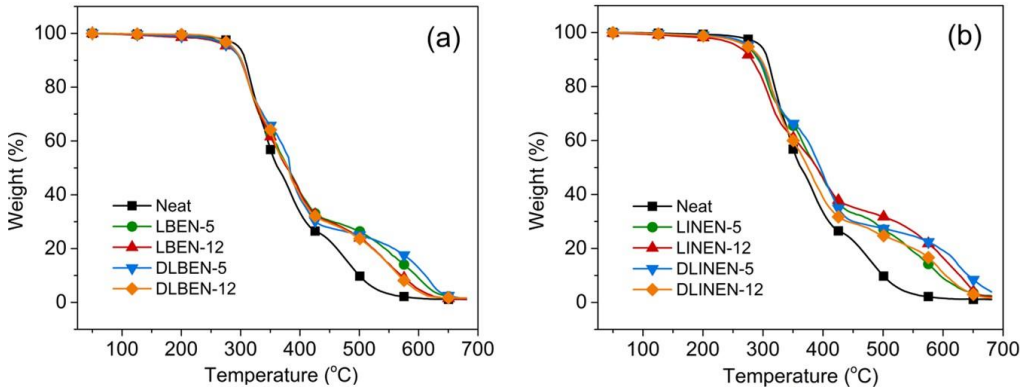

Figure 6.10 Thermogravimetric analysis thermograms of (a) LBENs and (b) LINENs as a function of temperature. "Neat" represents the epoxy network prepared from GEDHEO−NOVO and DETA, with no addition of organosolv lignin.

Figure 6.10 demonstrates all lignin−modified polymers show a two−step degradation profile in the range of 250−425 °C and 425−650 °C. The first degradation is associated with the breaking of aliphatic chains while the second broad mass loss is the rupture of aromatic carbon−carbon bonds.[33] By comparison, the neat polymer exhibits a one−step degradation. It is clear from Figure 6.10 and Table 6.3 that the neat polymer possesses higher thermal stability than the lignin−loaded thermosets, as reflected from the onset degradation temperature (expressed as T_{d5}, temperature at 5% weight loss) of neat (297 °C) and other networks (256−287 °C). As the temperature is increased to > 325 °C, the lignin−loaded polymers start to show higher thermal stability than the neat polymer as indicated by the T_{d50} (temperature at 50% weight loss) and $Char_{500}$ (char formed at 500 °C). The improved thermal stability (especially at relatively high temperature) of lignin−based networks have been previously reported,[34] which could be attributed to the lignin matrix that serves as a thermal barrier preventing the degraded compounds to diffuse out and heat to flow into the underlying

materials. All samples are decomposed with a negligible amount of residue (1.0−2.3 %) above 650 °C.

Table 6.3. Thermogravimetric data of T_{d5}, T_{d50} (temperature at 5% and 50% weight loss), and $Char_{500}$ and $Char_{650}$ (char residue at 500 and 650 °C) of LBENs and LINENs.

Sample	T_{d5} (°C)	T_{d50} (°C)	$Char_{500}$ (%)	$Char_{650}$ (%)
Neat[a]	297	362	10.1	1.0
LBEN−5	282	380	26.2	1.4
LBEN−12	279	377	23.9	1.3
DLBEN−5	282	383	25.0	1.7
DLBEN−12	287	379	23.4	1.6
LINEN−5	273	391	26.7	2.3
LINEN−12	256	389	31.8	2.0
DLINEN−5	277	395	27.4	2.1
DLINEN−12	274	373	24.8	1.3

[a] "Neat" represents the epoxy network prepared from GEDHEO−NOVO and DETA, with no addition of organosolv lignin.

6.3 Conclusions

Renewable epoxy thermosets were synthesized by incorporation of lignin with LDPMs (lignin derived phenol monomers). Materials with a maximum lignin loading of 12 wt % in starting phenols were prepared by successive deprotection of aromatic methoxy groups, phenolation, and phenol−formaldehyde reactions. The obtained DLINENs (deprotected lignin incorporated novolac epoxy network) exhibited thermal and mechanical properties comparable to the neat polymer prepared exclusively with LDPMs and without inclusion of bulk lignin. Overall, DLINENs showed improved performance when compared to LBENs (lignin blended epoxy network), which can be rationalized on the basis of enhanced reactivity, compatibility and covalent linkage of lignin in the networks formed with deprotected groups. The DLINEN approach represents a promising route for making sustainable materials to replace

BPA−derived materials. Further work on increasing lignin content in polymer materials is ongoing.

6.4 Experimental Section

General. Organosolv lignin was provided by Archer Daniels Midland Co. Lignin was used after washing 5 times with 2 M HCl solution to remove water−soluble impurities and ash. The resulting solid was washed with water and dried under vacuum overnight. DHEO was prepared through demethylation of DHE as described previously.[6] DHE, epichlorohydrin, 48% aqueous hydrobromic acid, tetrabutylammonium bromide, pentafluorobenzaldehyde and diethylenetriamine (DETA) were purchased from Aldrich Chemical Co. Formaldehyde solution (37%) and pyridine were obtained from Macron Fine Chemicals. All chemicals were used without further purification.

6.4.1 Synthesis of Lignin Incorporated Novolac Polyphenols (LINP)

6.4.1.1 Preparation of Deprotected Lignin (DL)

Demethylation of lignin was conducted according to a previous study.[21] In brief, 5 g lignin was dissolved in 20 mL of DMF prior to addition of 48% HBr solution (25 g). The reaction mixture was stirred at 120 °C for 20 h, cooled to ambient temperature and added dropwise into 2.5 L of HCl solution (2 M). Precipitate was formed immediately and the mixture was vigorously stirred for 4 h before centrifugation at 10,000 rpm for 15 min. The obtained solid was washed with water and diethyl ether, and dried under vacuum overnight to yield 3.56 g of DL as dark powder.

6.4.1.2 One−Pot Synthesis of Phenolated Lignin (PL) and Condensation with DHEO via Phenol−Formaldehyde Reaction to make LINP

Phenolation of lignin was performed by dissolving 0.6 g lignin in 4.4 g DHEO to obtain a lignin loading of 12 wt %. This is considered the maximum loading, determined by the solubility of lignin in DHEO. The homogenous mixtures were stirred at 110 °C for 30 min catalyzed by 6.7 wt % H_2SO_4, an optimized condition for phenolation as reported previously.[23] Since the content of OH groups in lignin was measured to be 4.32 mmol/g, the amount of DHEO (28.9 mmol) used in phenolation was in excess. 2.34 g (28.9 mmol) of 37% formaldehyde solution and 20 mL H_2O was introduced to make LINP at 100 °C. The resulting mixture was washed with toluene 3 times to remove unreacted DHEO. Toluene was isolated from the mixture through a separatory funnel and solvent removed under vacuum to yield lignin incorporated novolac polyphenol (LINP−12) as a homogeneous viscous oil (4.6 g, 78% yield, based on total mass input including lignin, DHEO and formaldehyde). LINP with lignin loading of 5 wt % (LINP−5) was synthesized following the same procedure.

6.4.2 Synthesis of DHEO Novolac Oligomer (DHEO−NOVO)

DHEO (1.52 g, 0.01 mol), 37% formaldehyde solution (0.81 g, 0.01 mol), hydrochloric acid (4 mg) and H_2O (8 mL) were refluxed at 100 °C for 6 h. Water and hydrogenchloride were evaporated under reduced pressure at 80 °C. The unreacted DHEO was removed by washing with toluene 3 times and toluene removal at 40 °C under vacuum yielded DHEO−NOVO as a viscous oil (1.46 g, 89% yield, based on an assumption that the novolac with an infinite molecular weight was obtained).

6.4.3 Preparation of Glycidyl Ether of Lignin−Based Polyphenols

6.4.3.1 Glycidyl Ether of Lignin (GEL) and Demethylated Lignin (GEDL)

GEL was prepared by dissolving 3.0 g lignin in 15 mL of DMF, followed by addition of

32.0 g epichlorohydrin and 0.28 g of tetrabutylammonium bromide as a phase transfer catalyst. The mixture was heated at 70 °C for 3 h. 3.2 g of 50% w/w NaOH solution was added dropwise. The reaction was kept for an additional 3 h at 70 °C, cooled to ambient temperature and added to 1 L H_2O. GEL precipitated immediately. Isolation was accomplished via centrifugation at 10,000 rpm for 15 min. The isolated solid was washed twice with water and dried under vacuum to afford 1.76 g of GEL as a black powder. Glycidyl ether of deprotected lignin (GEDL) was prepared following the same procedure.

6.4.3.2 Glycidyl Ether of DHEO−NOVO (GEDHEO−NOVO), LINP (GELINP) and DLINP (GEDLINP)

GEDHEO−NOVO was prepared by reaction of DHEO−NOVO (1.72 g) and epichlorohydrin (17 g). Excess epichlorohydrin was used as solvent and could reduce the viscosity and hydrolyzable chlorine content in epoxy monomers. Tetrabutylammonium bromide (0.16 g) was used as a phase transfer catalyst. The mixture was heated at 60 °C for 3 h. 1.8 g of 50% w/w NaOH solution was added dropwise. The reaction was kept for an additional 3 h. The reaction mixture was washed with acetone and filtered to remove salt. The mixture was concentrated under vacuum to yield 2.56 g of GEDHEO−NOVO as a viscous oil. Compared to the LBEN/DLBEN approach in which DMF had to be used to dissolve lignin for glycidylation (GEL/GEDL), LINEN/DLINEN approach was more advantageous since LINP and DLINP could be easily dissolved in epichlorohydrin. Thus, unreacted epichlorohydrin can be easily collected and purified by distillation and reused. Glycidyl ether of LINP (GELINP−5 and GELINP−12) and DLINP (GEDLINP−5 and GEDLINP−12) were obtained according to the same procedure.

6.4.4 Formation of Lignin−Based Epoxy Networks

GELINP−5, GELINP−12, GEDLINP−5 and GEDLINP−12 were respectively introduced to diethylenetriamine (DETA) with stoichiometric ratio of epoxy vs. −NH groups for curing. The mixtures were stirred for 10 min, degassed under vacuum to remove entrapped air and poured into molds for curing according to the profile: 55 °C for 2 h, 75 °C for 2 h and 95 °C for 2 h. The obtained cured lignin incorporated novolac epoxy thermosets were expressed as LINEN−5, LINEN−12, DLINEN−5 and DLINEN−12, respectively.

Epoxy thermoset polymers were also prepared through blending epoxidized lignin (GEL or GEDL) into comonomer (GEDHEO−NOVO) to yield lignin loading of 5 and 12 wt %. The mixtures were cured with DETA according to the above procedure to yield lignin blended epoxy networks (LBEN−5, LBEN−12, DLBEN−5 and DLBEN−12).

6.4.5 Analysis methods

The structural evolution from lignin to lignin−based epoxy monomers was followed by ^{1}H NMR spectroscopy (Bruker Avance ARX−400 spectrometer) using deuterated chloroform or DMSO as solvent. To determine the content of hydroxyl in lignin and DL, acetylation was performed by dissolving 200 mg of lignin or DL in 4 mL of pyridine to form a homogenous solution. 4 mL of acetic anhydride was added and the solution stirred at room temperature for 48 h. The resulting mixture was added dropwise to cold water, followed by centrifuging at 10000 rpm for 15 min to isolate acetylated lignin. The isolated solid was washed with water and dried overnight under vacuum. ^{1}H NMR spectra of lignin samples (25 mg) were recorded in 0.7 mL DMSO−d_6 containing 10 μL of pentafluorobenzaldehyde as an internal standard.

Other analysis methods are similar to Chapter 2.

6.5 References

(1) Hu, F.; La Scala, J. J.; Sadler, J. M.; Palmese, G. R. *Macromolecules* **2014**, *47*, 3332−3342.

(2) Auvergne, R. M.; Caillol, S.; David, G.; Boutevin, B.; Pascault, J. P. *Chem. Rev.* **2013**, *114*, 1082−1115.

(3) Chatel, G.; Rogers, R. D. *ACS Sustain. Chem. & Eng.* **2014**, *2*, 322−339.

(4) Raquez, R. D.; Deléglise, M.; Lacrampe, M. F.; Krawczak, P. *Prog. Polym. Sci.* **2010**, *35*, 487−509.

(5) Qin, J.; Liu, H.; Zhang, P.; Wolcott, M.; Zhang, J. *Polym. Int.* **2014**, *63*, 760−765.

(6) Zhao, S.; Abu−Omar, M. M. *Biomacromolecules* **2015**, *16*, 2025–2031.

(7) Zhao, S.; Abu−Omar, M. M. *ACS Sustain. Chem. & Eng.* **2016**, *4*, 6082−6089.

(8) Fache, M.; Darroman, E.; Besse, V.; Auvergne, R.; Caillol, S.; Boutevin, B. *Green Chem.* **2014**, *16*, 1987−1998.

(9) Fache, M.; Viola, A.; Auvergne, R.; Boutevin, B.; Caillol, S. *Eur. Polym. J.* **2015**, *68*, 526−535.

(10) Fache, M.; Auvergne, R.; Boutevin, B.; Caillol, S. *Eur. Polym. J.* **2015**, *67*, 527−538.

(11) Yin, Q.; Yang, W.; Sun, C.; Di, M. *BioResources* **2012**, *7*, 5737−5748.

(12) El Mansouri, N. E.; Yuan, Q.; Huang, F. *BioResources* **2011**, *6*, 2492−2503.

(13) Thakur, V. K.; Thakur, M. K.; Raghavan, P.; Kessler, M. R. *ACS Sustain. Chem. & Eng.* **2014**, *2*, 1072−1092.

(14) Parsell, T. H.; Owen, B. C.; Klein, I.; Jarrell, T. M.; Marcum, C. L.; Haupert, L. J.; Amundson, L. M.; Kenttämaa, H. I.; Ribeiro, F.; Miller, J. T.; Abu−Omar, M. M. *Chem. Sci.* **2013**, *4*, 806−813.

(15) Smolarski, M. M. High−value opportunities for lignin: unlocking its potential; Frost & Sullivan: Paris, 2012.

(16) Strassberger, Z.; Tanase, S.; Rothenberg, G. *RSC Adv.* **2014**, *4*, 25310−25318.

(17) Laurichesse S.; Avérous, L. *Prog. Polym. Sci.* **2014**, *39*, 1266−1290.

(18) Chung, Y. L.; Olsson, J. V.; Li, R. J.; Frank, C. W.; Waymouth, R. M.; Billington, S. L.; Sattely, E. S. *ACS Sustain. Chem. & Eng.* **2013**, *1*, 1231−1238.

(19) Wang, C.; Venditti, R. A. *ACS Sustain. Chem. & Eng.* **2015**, *3*, 1839–1845.

(20) Xue, B. L.; Wen, J. L.; Sun, R. C. *ACS Sustain. Chem. & Eng.* **2014**, *2*, 1474−1480.

(21) Chung, H.; Washburn, N. R. *ACS Appl. Mater. & Inter.*, **2012**, *4*, 2840−2846.

(22) Parsell, T.; Yohe, S.; Degenstein, J.; Jarrell, T.; Klein, I.; Gencer, E.; Hewetson, B.; Hurt, M.; Im Kim, J.; Choudhari, H.; Saha, B.; Meilan, R.; Mosier, N.; Ribeiro, F.; Delgass, W. N.; Chapple, C.; Kenttämaa, H. I.; Agrawal, R.; Abu−Omar, M. M. *Green Chem.* **2015**, *17*, 1492−1499.

(23) Podschun, J.; Saake, B.; Lehnen, R. *Eur. Polym. J.* **2015**, *67*, 1−11.

(24) Enjoji, M.; Yamamoto, A.; Shibata, M. *J. Appl. Polym. Sci.* **2015**, *132*, doi: 10.1002/app.41347.

(25) Koike, T. *Polym. Eng. & Sci.* **2012**, *52*, 701−717.

(26) Lu, Y.; Weng, L.; Zhang, L. *Biomacromolecules* **2004**, *5*, 1046−1051.

(27) Hamerton, I.; McNamara, L. T.; Howlin, B. J.; Smith, P. A.; Cross, P.; Ward, S. *Macromolecules* **2014**, *47*, 1946−1958.

(28) Huang, K.; Liu, Z.; Zhang, J.; Li, S.; Li, M.; Xia, J.; Zhou, Y. *Biomacromolecules* **2014**, *15*, 837−843.

(29)Wu, Y.; Guo, Q.; Kraska, M.; Stühn, B.; Mai, Y. W. *Macromolecules* **2013**, *46*, 8190−8202.

(30) Garcia, F. G.; Soares, B. G.; Pita, V. J. R. R.; Sánchez, R.; Rieumont, J. *J. Appl. Polym. Sci.* **2007**, *106*, 2047−2055.

(31)Liu, X.; Xin, W.; Zhang, J. *Green Chem.* **2009**, *11*, 1018−1025.

(32)Alzina, C.; Mija, A.; Vincent, L.; Sbirrazzuoli, N. *J. Phys. Chem. B* **2012**, *116*, 5786−5794.

(33)Griffini, G.; Passoni, V.; Suriano, R.; Levi, M.; Turri, S. *ACS Sustain. Chem. & Eng.* **2015**, *3*, 1145−1154.

(34) Morandim−Giannetti, A. A.; Agnelli, J. A. M.; Lanças, B. Z.; Magnabosco, R.; Casarin, S. A.; Bettini, S. H. P. *Carbohyd. Polym.* **2012**, *87*, 2563−2568.

Chapter 7

Formaldehyde−Free Method for Incorporating Lignin into Epoxy Thermosets

ABSTRACT: A series of liquid and curable lignin−containing epoxy prepolymers were prepared for making renewable epoxy thermosets. First, lignin was modified to phenolated lignin (PL) in a solvent−free reaction. PL was subsequently co−oligomerized with salicyl alcohol (SA) in water without the use of formaldehyde to obtain fully bio−based polyphenols (PL−SA). Unlike most of previous works, glycidylation of lignin−based polyphenols yielded exclusively liquid epoxy prepolymers, with no solid phase produced. The liquid epoxy prepolymers were curable with common hardeners to generate homogenous thermosets, which required no epoxy co−prepolymer. The structural evolution from starting monomers to epoxy thermosets was followed by nuclear magnetic resonance and Fourier transform infrared spectroscopy. Compared to a common synthesis route in which lignin was glycidylated prior to being blended with epoxy co−prepolymers, the proposed approach conferred networks with increased glass transition temperature, storage modulus and cross−link density as measured by dynamic mechanical analysis. Moreover, bio−based thermosets exhibited comparable or superior mechanical properties to conventional BPA−based counterpart. By producing liquid−phase lignin−containing epoxy prepolymers, this study provides a method for incorporating lignin in epoxy thermosets without the need for additional epoxy co−prepolymers.

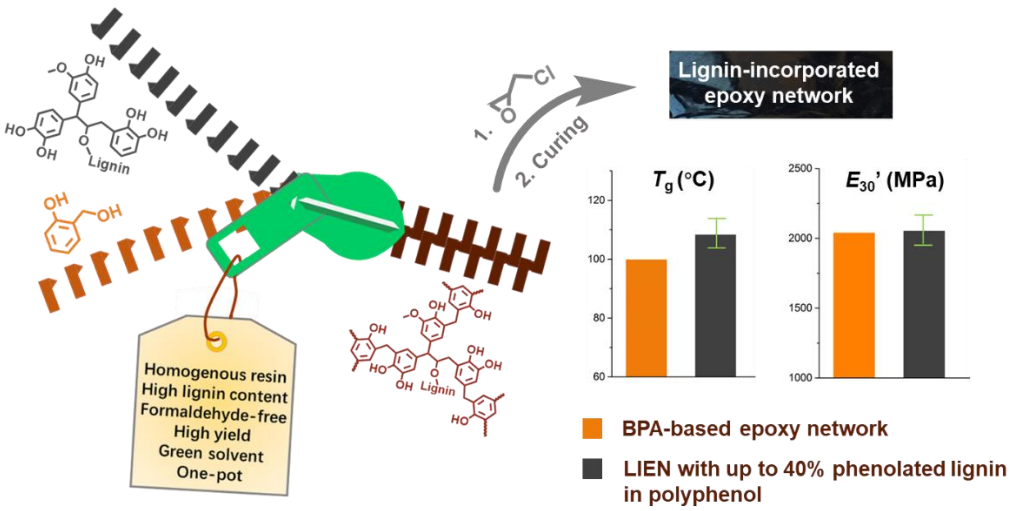

This section is partially adapted from: Shou Zhao, Xiangning Huang, Andrew J. Whelton, and Mahdi M. Abu−Omar, to be submitted.

7.1 Introduction

Recent years have witnessed rapid development of materials made from renewable sources.[1–5] Lignin has been widely viewed as a promising renewable starting material because it is abundant, low−cost and the sole large−volume aromatic feedstock.[6] It is especially reasonable to use lignin−derived chemicals to synthesize thermosetting materials, as the aromatic structure provides good thermal and mechanical performance.[7, 8] Because of the relatively straightforward structure, lignin−derived phenol monomer (LDPM) and partially depolymerized lignin (PDL) are often utilized to make thermosets like epoxy.[8–23] However, LDPM and PDL need to be depolymerized from lignin through chemical transformations including oxidation, catalytic reduction and cracking processes etc., which are associated with intensive energy consumption as well as several separation and purification steps.[24] By comparison, bulk lignin is abundant and cheap. It is reported that the total availability of technical grade lignin in the biosphere exceeds 300 billion tons,[25] while its price is 20 times

cheaper than phenol.[26] Thus, it would be advantageous to replace petroleum−based phenolics (e.g., bisphenol A, BPA) with lignin as prepolymers for thermosets. However, only 2% of lignin is being used for value−added products,[27] which is limited by its low reactivity and incompatibility with polymeric compounds.

Epoxy thermoset is one of the most versatile thermosetting materials that has been utilized in coatings, composites, adhesives and electrical/electronic laminates etc. By far, methods of incorporating bulk lignin into epoxy thermosets can be summarized into three categories[28]: (1) using lignin derivatives as fillers to directly blend into general epoxy thermosets; (2) modifying lignin by direct epoxidation; and (3) modifying lignin derivatives to improve its reactivity, followed by epoxidation. It is noteworthy that epoxy prepolymers (or glycidyl ethers) should be liquid at ambient or elevated temperature for sufficient contacting and reacting with curing agents to form a homogenous cross−linked network. For example, epoxy resins used for encapsulation and potting must melt and flow rather freely to ensure complete filling of the voids prior to cross−linking. Solvents are not preferably used in most instances due to the difficulty of solvent removal before curing.[29] However, most of reported epoxidized lignin are infusible solids, which cannot be directly cured by hardeners and at least one epoxy co−prepolymer needs to be introduced.[30–34] Glycidylation of pre−modified lignin could produce simultaneously solid and liquid phase epoxy prepolymers.[35] However, the liquid phase is often in a small portion and needs to be separated from the mixture sophistically. For example, Hofmann *et al*. prepared epoxy prepolymers using hydroxyalkyl lignin derivatives.[36] Hydroxyalkylation of lignin was conducted by reacting lignin with propylene oxide to improve the solubility and then with ethylene oxide to transform secondary hydroxyls into primary

hydroxyls. Glycidylation of hydroxyalkylated lignin with epichlorohydrin yielded an epoxy prepolymer mixture, while the curable liquid prepolymer had to be collected after several sophisticated solvent fractionation treatments. By reacting methylolated lignin with epichlorohydrin, Mansouri *et al.* synthesized solid and liquid phase of epoxidized lignin simultaneously.[37] Even though the liquid phase could be separated by filtration, its epoxy content only accounted for < 20% in the mixture. Huo *et al.* modified lignin with cardanol−based oligomer and then glycidylated with epichlorohydrin to obtain a viscous liquid.[38] However, only curing kinetics of epoxy−anhydride reactions were reported, while neither the structure of epoxy prepolymer nor the property of obtained thermosets was characterized. By successive demethylation, phenolation, phenol−formaldehyde reaction and glycidylation of organosolv lignin, we reported the synthesis of a liquid lignin−containing epoxy prepolymer.[39] However, lignin content in starting polyphenol could not exceed 12 wt % due to compatibility issue, while the synthesis process involved unfavorable reagents including hydrobromic acid and formaldehyde.

Phenolation has been reported as an effective lignin modification method.[34, 40−42] Acid−catalyzed incorporation of the *ortho* or *para*−phenyl substituent to the α−hydroxyl of lignin increased the reactive phenolic hydroxyl and *ortho*/*para* sites, while the molecular weight of lignin was simultaneously decreased by acid−catalyzed cleavage of the lignin backbone.[40] Direct glycidylation of phenolated lignin (PL) barely produces liquid epoxy prepolymer with decent yield,[43] however, the increased content of phenolic *ortho*/*para* sites in PL enhances its reactivity for phenol−formaldehyde condensation to produce a novolac oligomer, which is a common precursor for liquid epoxy prepolymers.[29] As inspired by these

phenomenon, we reported herein a route to synthesize liquid lignin−containing epoxy prepolymers (Figure 7.1). First, lignin was phenolated by catechol, a renewable building block that is available from lignin through demethylation of lignin−derived guaiacol or by lignin pyrolysis.[44−47] Compared to phenol, catechol is more reactive for phenolation and has increased number of hydroxyl group and phenolic *para*/*ortho* site for condensation.[14] Second, phenolated lignin was condensed with salicyl alcohol (SA, a renewable compound that can be derived from willow bark)[48] to yield lignin−incorporated novolac oligomers (PL−SA), with PL content could reach up to 40 wt %. As SA bears both hydroxymethyl group and reactive phenolic *para*/*ortho* sites, it could simultaneously react with the *para*/*ortho* sites of phenolics in PL and undergo self−condensation without the need for coupling agents like formaldehyde. PL−SA was then glycidylated with epichlorohydrin to generate exclusively liquid epoxy prepolymers with no solid prepolymer obtained. These epoxy prepolymers were curable by diethylenetriamine (DETA) to yield homogenous lignin−incorporated epoxy networks (LIEN). In their liquid phase, lignin−containing epoxy prepolymers would find much wider applications compared to their solid phase counterparts.

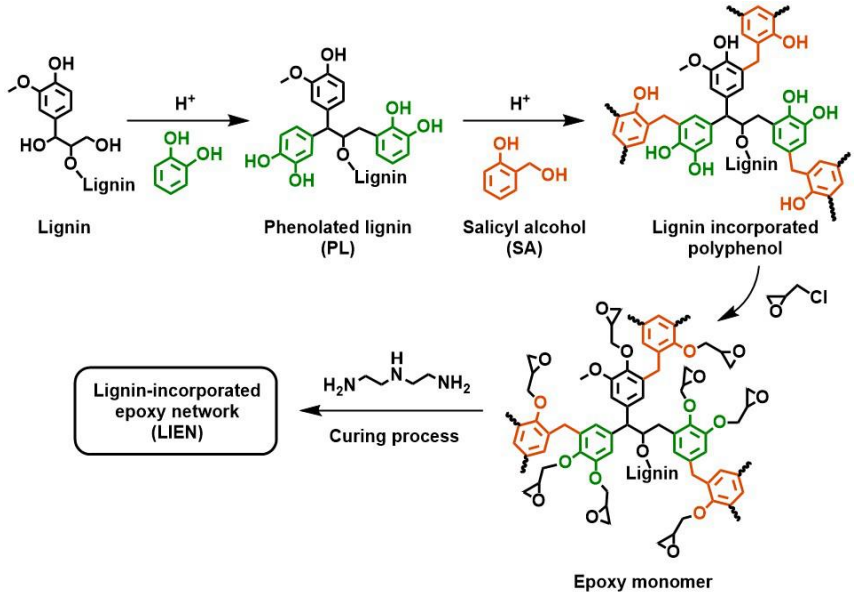

Figure 7.1 Synthesis route of lignin−incorporated epoxy network (LIEN). Lignin is modified through phenolation and formaldehyde−free oligomerization to yield lignin−incorporated polyphenol. Benzodioxane derivatives produced by glycidylation of catechols are not shown for clarity.

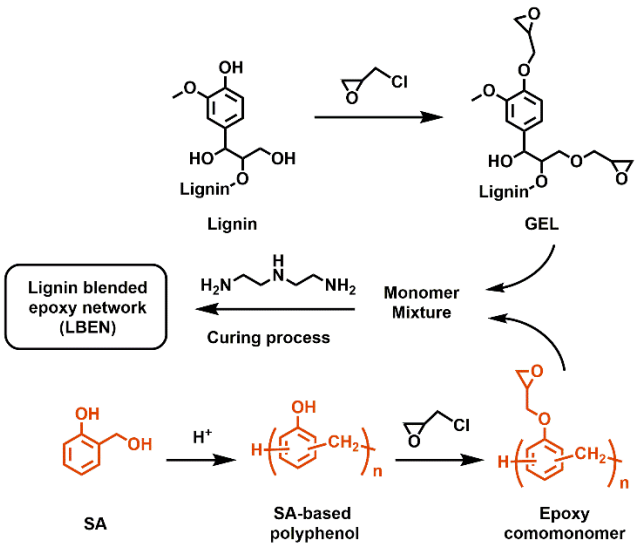

Figure 7.2 Synthesis route of lignin−blended epoxy network (LBEN), which is used to compare with the proposed LIEN route in Figure 7.1. Lignin is glycidylated prior to being blended with glycidyl ether of SA self−condensed oligomer for curing.

7.2 Results and Discussion

7.2.1 Structure of Lignin−Incorporated Polyphenols and Their Glycidyl Ethers

Figure 7.3 shows the ^{1}H NMR spectra of lignin, phenolated lignin, PL_0SA_{100} and PL−incorporated oligomers ($PL_{10}SA_{90}$, $PL_{20}SA_{80}$, $PL_{30}SA_{70}$ and $PL_{40}SA_{60}$). Figure 7.3 panel a exhibits integral ratio of aromatic (6.0−7.3 ppm) vs. aliphatic (3.5−4.1 ppm) protons of lignin is 0.34. When lignin is modified with catechol to make PL, this ratio increases to 1.43 (Figure 7.3 panel b). As there is no catechol residue detected in PL, the enhanced aromatic content indicates the substitution of lignin aliphatic hydroxyls by catechols. Figure 7.3 panel c exhibits

the spectrum of PL_0SA_{100} (oligomer from self−condensation of salicyl alcohol). The peak at 3.8 ppm corresponds to the methylene bridge between repeating phenolic units. Integral ratio of aromatic vs. aliphatic protons of PL_0SA_{100} is 1.7, which is lower than the corresponding ratio of 2 for salicyl alcohol monomer. This indicates the formation of oligomers connected by methylene linkages at the phenolic *para*/*ortho* site. For PL−incorporated polyphenols, the aromatic and aliphatic integrals decrease with increasing percentages of PL from $PL_{10}SA_{90}$ to $PL_{40}SA_{60}$ (Figure 7.3, panel d−g). This is attributed to the lower integrals of PL in aromatic (3.24) and aliphatic (2.26) compared to those of PL_0SA_{100} (8.58 and 5.02, respectively). Moreover, Figure 7.4 reveals the integrals of aromatic and aliphatic regions decrease linearly with PL percentage. This relationship confirms the integration of PL with SA−based oligomers. Glycidyl ethers of PL_0SA_{100} and PL−incorporated polyphenols are shown in Figure 7.5. Compared to polyphenols, glycidyl ethers exhibit new epoxy peaks at 2.67 and 2.88 ppm ($-CH_2-$ in oxirane), 3.22 ppm (−CH− in oxirane) and 3.54 and 3.64 ppm ($-O-CH_2-$).

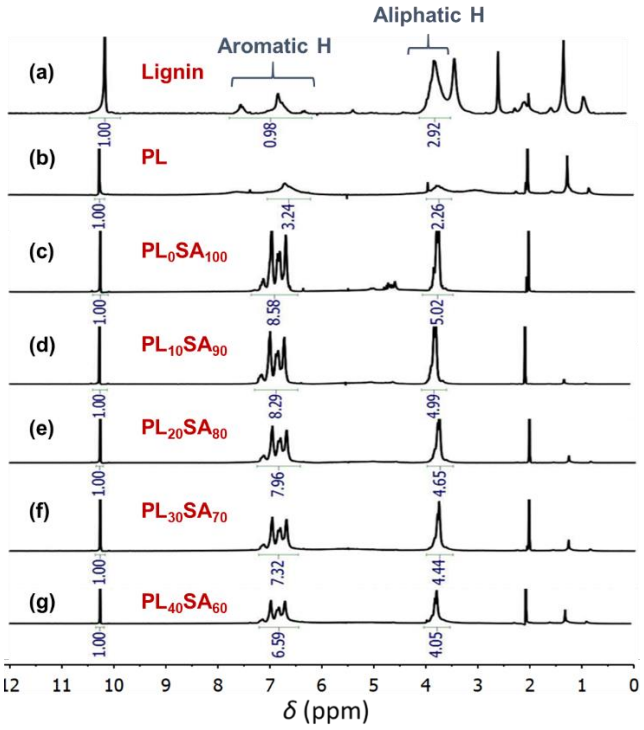

Figure 7.3 ^{1}H NMR spectrum of (a) lignin, (b) phenolated lignin, (c) PL_0SA_{100} (oligomer from self−condensation of SA) and PL−incorporated polyphenols: (d) $PL_{10}SA_{90}$ (e) $PL_{20}SA_{80}$ (f) $PL_{30}SA_{70}$ and (g) $PL_{40}SA_{60}$. Solvent: DMSO−d_6 for lignin and acetone−d_6 for other polyphenols.

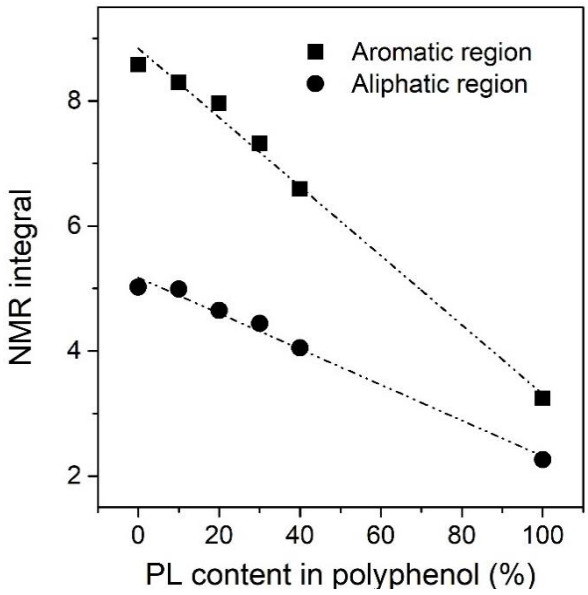

Figure 7.4 Correlations between PL contents and NMR integrals of aromatic and aliphatic regions of different polyphenols. Integrals of aromatic and aliphatic regions were obtained from the ^{1}H NMR spectra in Figure 7.3, in which integrals of internal standard (pentafluorobenzaldehyde) were set as 1.

IR analyses were also conducted to confirm the structure. Figure 7.6, panel a and d illustrate the characteristic absorption bands of PL_0SA_{100} and $PL_{40}SA_{60}$ appear at around 3318 cm^{-1} (O−H stretching), 2857−3005 cm^{-1} (alkyl C−H stretch) and 1602, 1504 and 1457 cm^{-1} (aromatic C−C bond). After polyphenols were reacted with epichlorohydrin, the afforded glycidyl ethers exhibit significantly decreased hydroxyl band and newly−formed C−O−C ether band at 1028 cm^{-1} and epoxy band at 912 cm^{-1}, which confirms the formation of epoxy groups

(Figure 7.6, panels b and e). When these glycidyl ethers were cured with diethylenetriamine, the active amine protons opened epoxies while hydroxyls were created at the same time. As seen in Figure 7.6, panel c and f, cured samples exhibit no epoxy band at 912 cm^{-1}, while the broad hydroxyl band increases. Other lignin−incorporated polyphenols, their glycidyl ethers and cured networks are shown in Figure S7.1−S7.3, which exhibit similar pattern to Figure 7.6.

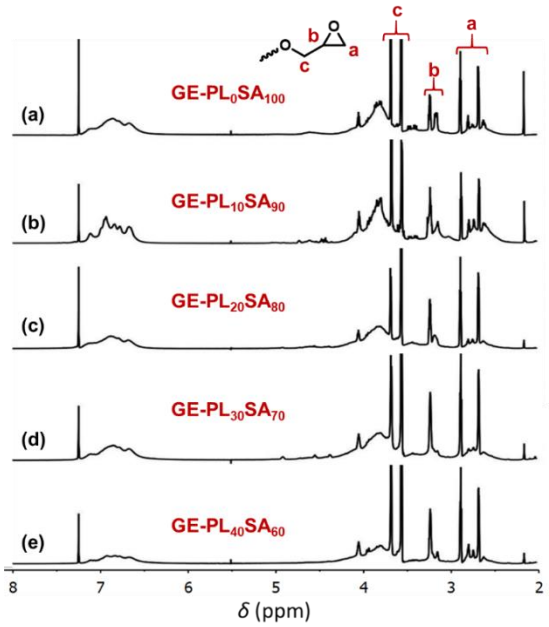

Figure 7.5 ^{1}H NMR spectra of glycidyl ethers of SA−based oligomers with different contents of PL. Solvent: $CDCl_3$.

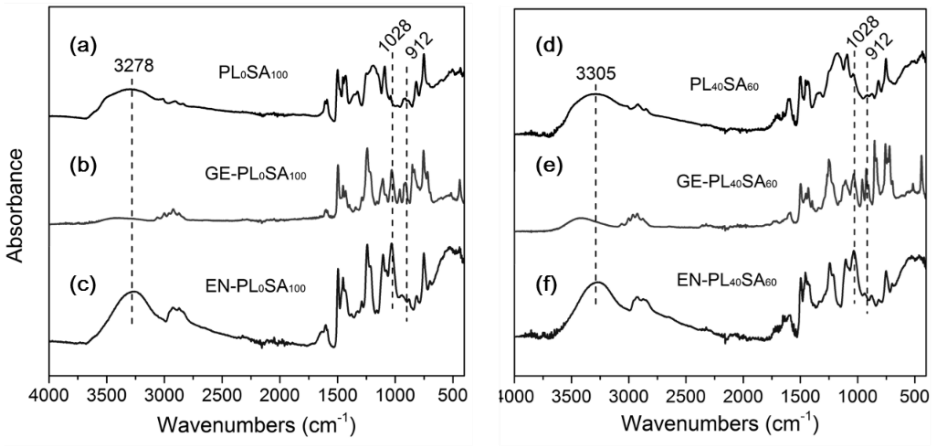

Figure 7.6 FTIR spectra of PL_0SA_{100} (a) and $PL_{40}SA_{60}$ (d), their glycidyl ethers (b and e) and

cured epoxy networks (c and f).

7.2.2 Effect of Lignin on Curing Behavior

The effect of lignin on curing behavior was studied via DSC analysis. Table 7.1 exhibits enthalpy (ΔH) values gradually decreased as lignin content increased. This trend was expected because PL−incorporated polyphenols have relatively more complicated structure, lower reactivity and possibly yield non−curable benzodioxane byproduct caused by the catechol moiety.[12, 39] Thus, PL−incorporated epoxy prepolymers could have less epoxy content and release lower heat compared to neat sample (GE−PL_0SA_{100}). Table 7.1 demonstrates peak curing temperatures of lignin−incorporated samples (GE−$PL_{10}SA_{90}$ to GE−$PL_{40}SA_{60}$) exhibit no obvious change compared to GE−PL_0SA_{100} (72.7−74.9 °C versus 75.6 °C). Meanwhile, epoxy prepolymer prepared from the LBEN route (GE−BL−$GEL_{20}SA_{80}$) exhibits similar peak temperature of 73.4 °C. These observations indicate lignin does not have an impact on the curing process, which is consistent with previous studies.[39] Extent of curing was determined using two cycles of heating/cooling. As shown in Figure S7.4−S7.9, all epoxy prepolymers were most cured as reflected by the lack of exotherm on the second heating.

Table 7.1. DSC curing data for epoxy/amine systems exhibiting onset curing temperature (T_i), peak curing temperature (T_p) and enthalpy of reaction (ΔH).

entry	epoxy prepolymer	T_i (°C)	T_p (°C)	ΔH (J/g)
1	GE−PL_0SA_{100}	42.7	75.6	449
2	GE−$PL_{10}SA_{90}$	39.4	74.9	464
3	GE−$PL_{20}SA_{80}$	34.9	72.7	445
4	GE−$PL_{30}SA_{70}$	36.1	73.9	432
5	GE−$PL_{40}SA_{60}$	36.0	74.1	420
6	GE−BL−$GEL_{20}SA_{80}$	39.2	73.4	431

7.2.3 Effect of Lignin on Mechanical Properties

Table 7.2, Figure 7.7 and Figure S7.10 illustrate α−relaxation temperature (T_α, related to glass transition temperature) and storage modulus of biobased epoxy networks. Lignin loading is found to affect the mechanical performance. Compared to the neat network (EN−PL_0SA_{100}, exclusively prepared from GE−PL_0SA_{100} and DETA, T_α =114 °C), lignin incorporation diminished the glass transition temperatures of all networks (96.0−112 °C). This could be related to the relatively lower reactivity and incompatibility of lignin. Meanwhile, steric hindrance of lignin limits the development of polymer networks. Impacts of lignin are especially evident when higher contents of PL are incorporated, as T_α decreases gradually from EN−PL_0SA_{100} to EN−$PL_{40}SA_{60}$ (entry 1−5).

Table 7.2. α−Relaxation temperature (T_α), glassy storage modulus at 30 °C (E_{30}') and cross−link density (ν_e) of epoxy networks prepared from LIEN and LBEN approaches. BPA−based epoxy network (EN−BPA) was also prepared using the same curing profile as other networks for comparison.

entry	epoxy networks	T_α (°C)	E_{30}' (MPa)	E' at T_α + 30 °C (MPa)	ν_e (10^{-3} mol/cm^3)
1	EN−PL_0SA_{100}	114	2151	50	16.0
2	EN−$PL_{10}SA_{90}$	112	2146	38	11.1
3	EN−$PL_{20}SA_{80}$	106	2118	52	15.4
4	EN−$PL_{30}SA_{70}$	106	2024	68	19.9
5	EN−$PL_{40}SA_{60}$	106	1843	28	8.2
6	EN−BL−$GEL_{20}SA_{80}$	96	1828	18	5.4
7	EN−BPA	100	2042	48	14.4

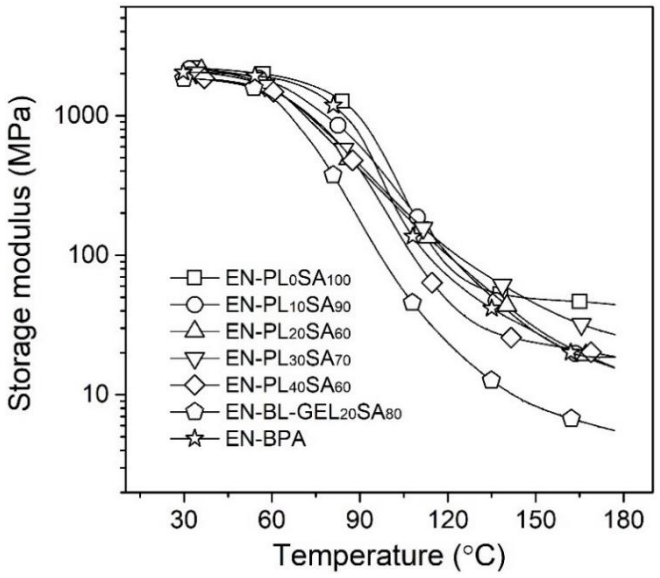

Figure 7.7 Storage modulus of epoxy networks as a function of temperature.

The synthesis route also impacts thermoset properties. As shown in Table 7.2 and Figure 7.7, T_α and E_{30}' of EN−BL−$GEL_{20}SA_{80}$ (LBEN route) are 96.0 °C and 1828 MPa respectively, which are lower than the LIEN−derived networks. As illustrated in Figure 7.2, linkages between GEL and GE−PL_0SA_{100} in LBEN are mainly realized via connecting with the amine hardener. However, these linkages are often compromised by the poor reactivity of lignin. Besides, compatibility between GEL (in solid state) and GE−PL_0SA_{100} (in oily state) is low and the mixture was heterogeneous after blending. The poor compatibility causes insoluble defects within the network, which result in decrease in cross−link. As seen in Table 7.2, cross−link density (ν_e) of the LIEN samples is in the range of 8.2−19.9 × 10^{-3} mol/cm^3, which is much higher than the EN−BL−$GEL_{20}SA_{80}$ (5.4 × 10^{-3} mol/cm^3). This phenomenon highlights the merits of the LIEN approach: (1) as sulfuric acid was used in the phenolation and condensation process, the backbone of lignin was cleaved and the compatibility of lignin with polymeric compounds improved. Meanwhile, intermolecular hydrogen bonds, van der Waals interactions between polymer chains, and π−π stacking of aromatic groups of lignin were

reduced during the modifications, which prevented lignin from aggregating.[49] (2) covalent cross−links between lignin and SA−based oligomers have been established through condensation before curing, (3) improved solubility of lignin−incorporated polyphenols, which leads to improved degree of glycidylation than direct epoxidation of lignin, and (4) the afforded epoxy prepolymers are homogenous liquid, which shows improved compatibility with amine hardener. The enhanced uniformity of LIEN is depicted pictorially in Figure 7.8, pictures of EN−BL−GEL_5SA_{95}, EN−PL_5SA_{95}, and EN−PL_0SA_{100} (neat sample with no lignin addition). Reduced amount of lignin (5 wt %) was employed to illustrate clearly the interactions of lignin with the polymer network. Compared to the homogenous texture of EN−PL_5SA_{95} and EN−PL_0SA_{100}, it is easy to see lignin particles unevenly dispersed in EN−BL−GEL_5SA_{95}. Traditional DGEBA/DETA epoxy network was also prepared using the same curing profile. Table 7.2 compares T_α, E_{30}' and ν_e of biobased epoxy networks with the BPA−based counterpart. It is found that LIEN−derived polymers have T_α, modulus and cross−link density that are comparable or superior to the BPA−based materials (T_α of 100 °C, E_{30}' of 2042 MPa and ν_e of 14.4 × 10^{-3} mol/cm^3). This highlights the potential of replacing or supplementing petroleum−based thermosets with lignin−containing materials.

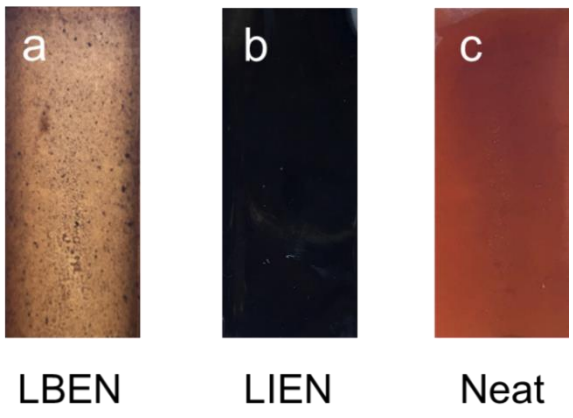

Figure 7.8 Image of epoxy networks prepared using (a) LBEN and (b) LIEN approaches (5 wt %

of GEL or PL in epoxy prepolymers were employed for clear illustration). (c) Neat network represents EN−PL_0SA_{100}, with no addition of organosolv lignin.

7.2.4 Effect of Lignin on Thermal Stability

Figure 7.9 demonstrates thermal degradation of neat and lignin−loaded thermosets in the range of 40 to 600 °C. It is observed from Figure 7.9 and Table 7.3 that thermal stability of lignin−loaded samples is clearly higher than the neat networks, which is suggested by the onset degradation temperature (expressed as T_{d5}, temperature at 5% weight loss) of lignin−loaded ones (191−239 °C) and neat sample (136 °C). Meanwhile, T_{d30} (temperature at 30% weight loss) exhibits the same trend with T_{d5}. The improved thermal properties of lignin−loaded thermosets are consistent with previous studies,[50] which is explained by the lignin matrix that acts as a thermal barrier hindering mass exchange. To highlight the barrier role of phenolated lignin, thermal analysis of PL was also conducted and it revealed high stability as indicated by T_{d5} (245 °C), T_{d30} (363 °C) and $Char_{600}$ (46%). The way lignin incorporates into network does not have impact on thermal performance, as EN−BL−$GEL_{20}SA_{80}$ has comparable thermal parameters with thermosets prepared from LIEN. As for the BPA−based network, it exhibits the highest thermal stability when temperature is relatively low, as reflected by T_{d5} (305 °C) and T_{d30} (371 °C). However, when temperature reaches 330 °C, EN−BPA exhibits a fast degradation behavior and only 8 wt % char was left when the temperature reaches 600 °C. As for the lignin−loaded samples, they start to exhibit higher stability over EN−BPA above 374 °C, with 23−39 wt % char formed at 600 °C.

Table 7.3. Thermogravimetric data of T_{d5}, T_{d30} (temperature at 5% and 30% weight loss), and $Char_{600}$ (char residue at 600 °C) of epoxy networks and phenolated lignin.

entry	epoxy networks	T_{d5} (°C)	T_{d30} (°C)	$Char_{600}$ (%)
1	EN−PL_0SA_{100}	136	297	28
2	EN−$PL_{10}SA_{90}$	191	322	23
3	EN−$PL_{20}SA_{80}$	192	301	23
4	EN−$PL_{30}SA_{70}$	239	348	34
5	EN−$PL_{40}SA_{60}$	213	315	29
6	EN−BL−$GEL_{20}SA_{80}$	216	325	39
7	PL	245	363	46
8	EN−BPA	305	371	8

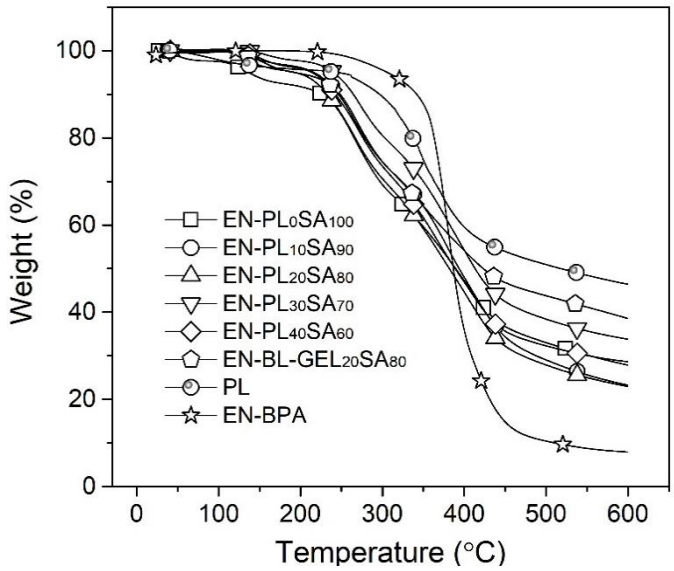

Figure 7.9 Thermogravimetric analysis thermograms of epoxy networks as a function of temperature.

7.2.5 Content of Lignin and Biomass in Thermosets

Table 7.4 lists the weight percentages of lignin, PL and biomass in polyphenols, epoxy prepolymers and thermosets. Considering lignin, catechol and salicyl alcohol are all available from renewable sources as stated above, the starting polyphenol precursors are fully bio−based. As calculated above, lignin content in PL was *ca*. 68 wt %. Thus, lignin content in polyphenol could be up to 27 wt %. When polyphenols are glycidylated to epoxy prepolymers, the biomass content is reduced to the range of 71−77 wt %, while the rest is occupied by the glycidyl ether

groups. These values are consistent with the weight ratio (75 wt %) of 2−methoxy−4−propylphenol (a typical lignin building block) in its glycidylated form. Since reacting with epichlorohydrin is the most commonly method to convert phenol into its glycidyl ether, it is inevitable to dilute the biomass content in the epoxy prepolymers. It is noteworthy that lignin content could reach up to 21 wt % in the homogenous liquid epoxy prepolymer, with no solid phase formed. To our knowledge, this is the highest value and most efficient approach that has ever been reported for a liquid lignin−containing epoxy prepolymer. For the cured epoxy thermosets, the content of biomass decreases slightly to 65−69 wt %, while lignin content is up to 19 wt %. This decrease in biomass content depends on the properties of hardeners and is inevitable unless renewable hardeners like succinic anhydride are employed.

Table 7.4. Weight percentage of bulk lignin, PL and biomass in polyphenols, epoxy prepolymers and thermosets.

samples	polyphenol			epoxy prepolymer			thermoset		
	lignin[a] (wt %)	PL (wt %)	biomass[b] (wt %)	lignin (wt %)	PL (wt %)	biomass[c] (wt %)	Lignin (wt %)	PL (wt %)	biomass[d] (wt %)
EN−PL_0SA_{100}	0	0	100	0	0	71	0	0	65
EN−$PL_{10}SA_{90}$	7	10	100	5	7	72	4	6	66
EN−$PL_{20}SA_{80}$	14	20	100	10	15	73	9	14	66
EN−$PL_{30}SA_{70}$	20	30	100	16	23	75	14	21	67
EN−$PL_{40}SA_{60}$	27	40	100	21	31	77	19	28	69

[a] content of lignin in PL was calculated to be *ca*. 68 wt % as demonstrated in experimental section.

[b] Considering lignin, catechol and salicyl alcohol are all available from bio−based sources, biomass contents in polyphenol for all samples are 100 wt %.

[c] Weight ratio of biomass in epoxy prepolymer (B/EP) is in the range of 71−77 wt %. This ratio is calculated by experiments, for example, 1 g of polyphenol ($PL_{40}SA_{60}$) reacts with epichlorohydrin to yield 1.3 g of GE−$PL_{40}SA_{60}$. Thus, weight ratio of $PL_{40}SA_{60}$ in epoxy prepolymer GE−$PL_{40}SA_{60}$ is calculated to be 1/1.3 = 0.77. Contents of lignin and PL in epoxy prepolymer are calculated by multiplying their contents in polyphenol with corresponding B/EP ratios.

[d] Weight ratio of biomass in thermoset (B/T) is in the range of 65−69 wt %. This ratio is calculated by, for example, 1 g of epoxy prepolymer (GE−$PL_{40}SA_{60}$, EEW=178 g/eq.) is cured with 0.12 g of DETA (1:1 ratio of epoxy/−NH) to yield 1.12 g of thermoset. Thus, weight ratio of $PL_{40}SA_{60}$ in thermoset EN−$PL_{40}SA_{60}$ is calculated to be 0.77×1/1.12 = 0.69. Contents of lignin and PL in thermoset are calculated by multiplying their contents in

polyphenol with corresponding B/T ratios.

7.3 Conclusions

A series of liquid and curable lignin−containing epoxy prepolymers were prepared. Compared to previous lignin−containing prepolymers that are mainly infusible solids, the prepared liquid epoxy prepolymer can yield homogenous thermoset without the need for additional epoxy co−prepolymer. The prepared thermosets have high content of biomass, and they exhibit mechanical properties that are comparable or superior to conventional BPA−based counterpart. Meanwhile, these networks are prepared using several green approaches: solvent−free synthesis of PL; formaldehyde−free preparation of oligomers using water as solvent; one−pot synthesis of epoxy prepolymers; and use of high boiling point sulfuric acid as catalyst. Without lignin formed as the low−reactivity solid phase epoxy prepolymer, the proposed approach represents a promising route for making lignin−containing thermosets with multiple purposes.

7.4 Experimental Section

General. Organosolv lignin was provided by Archer Daniels Midland Co. Lignin was used after washing five times with 2 M HCl solution to remove water−soluble impurities and ash. The resulting solid was washed with water and dried under vacuum overnight. The hydroxyl content of the lignin was measured to be 4.32 mmol/g as previously reported.[39] Catechol, salicyl alcohol (2−hydroxybenzyl alcohol), epichlorohydrin, tetrabutylammonium bromide, diethylenetriamine (DETA), diglycidyl ether of bisphenol A (DGEBA) and pentafluorobenzaldehyde were purchased from Aldrich Chemical Co. Sulfuric acid (98%) was obtained from Fisher Scientific. All chemicals were used as received without further

purification. Glycidyl ethers of lignin (GEL) was prepared according to a previous method.[39]

7.4.1 Preparation of Phenolated Lignin.

Catechol (7.0 g) was heated at 115 °C in a 100 mL round bottomed flask until melting. Then, 3.50 g organosolv lignin and 0.70 g sulfuric acid were subsequently added and a homogenous mixture was obtained. Weight ratio of reagents (catechol/lignin =2, with 6.7 wt % of catalyst) was consistent with previous study, which could produce phenolated lignin with optimal degree of phenolation.[40] The mixture was stirred at 110 °C for 2 h, cooled to room temperature and 100 mL H_2O was added. Phenolated lignin precipitated immediately. The precipitate was collected via filtration and washed with H_2O several times with the help of sonication until no catechol residue was detected as indicated by high−performance liquid chromatography (HPLC). Drying the solid under vacuum afforded PL as a black powder (4.28 g, 83% yield based on a lignin in which hydroxyl groups were completely substituted by catechol). Yield of PL was in accordance with previous study.[40] Lignin content in PL was calculated based on lignin's hydroxyl content (4.32 mmol/g, sum of aliphatic and aromatic hydroxyls). Assuming all hydroxyl groups were substituted by catechol, lignin content in PL was *ca*. 68 wt %. However, considering the aromatic hydroxyls are not reactive with catechol and the aliphatic hydroxyls may not be completely substituted, lignin content in PL should be higher than 68 wt %.

7.4.2 One−Pot Preparation of Glycidyl Ethers.

7.4.2.1 Preparation of Oligomers from PL and Salicyl Alcohol.

Oligomers with various PL weight ratios (10, 20, 30 and 40 wt %) were synthesized using a formaldehyde−free method and water was employed as solvent. $PL_{10}SA_{90}$, a phenolic

oligomer containing 10 wt % of PL and 90 wt % of salicyl alcohol, was prepared as follows: salicyl alcohol (2.0 g, 16.1 mmol) was dissolved in 20 mL H_2O at 100 °C in a 100 mL round bottomed flask. To this mixture was added 0.22 g phenolated lignin, and the powder was dispersed through stirring using a magnetic stirring bar. A mixture of sulfuric acid (1.6 mL) and H_2O (10 mL) was dropwise added to the flask. The mixture was stirred at 110 °C for 30 min. During the period, it was observed that dark viscous oil was gradually formed and accumulated on the magnetic bar. When the reaction was complete, the mixture was cooled to room temperature and the dark oil became solid. The acidic solution was discarded, and the afforded solid was washed with H_2O several times to remove H_2SO_4 residue.

7.4.2.2 Preparation of Glycidyl Ethers.

In the same flask, 30 g epichlorohydrin was introduced to react with $PL_{10}SA_{90}$ to make the glycidyl ether (GE−$PL_{10}SA_{90}$). Excess epichlorohydrin was used as solvent to reduce the viscosity and hydrolyzable chlorine content in epoxy prepolymers.[51] Small amount of leftover water in the flask did not influence the glycidylation reaction. 0.21 g tetrabutylammonium bromide was used as a phase transfer catalyst. The mixture was heated at 85 °C for 3 h, and cooled to room temperature prior to the dropwise addition of 5 g 20% w/w KOH solution. The reaction was then heated to 85 °C and kept for 2 h. When the reaction was complete, the mixture was washed with 30 mL acetone, filtrated to remove KCl, dried with Na_2SO_4 and concentrated with a rotary evaporator to yield GE−$PL_{10}SA_{90}$ as a dark oil (3.06 g).

To measure the yield of polyphenol, in a separate reaction, the oligomer product $PL_{10}SA_{90}$ was scratched from the stirring bar and dried overnight in an oven at 60 °C to give the polyphenol product of 2.11 g, 95% yield based on mass. Other oligomers with various PL

contents (0, 20, 30 and 40 wt %) and their glycidyl ethers (denoted as GE−PL_0SA_{100}, GE−$PL_{20}SA_{80}$, GE−$PL_{30}SA_{70}$ and GE−$PL_{40}SA_{60}$, respectively) were synthesized using the same method as GE−$PL_{10}SA_{90}$, with comparable yields. Epoxy equivalent weight (EEW) was determined to be 178−207 g/eq., using the HCl/acetone titration method.[52]

7.4.3 Formation of Epoxy Networks.

Glycidyl ethers with different weight ratios of PL (GE−PL_0SA_{100} to GE−$PL_{40}SA_{60}$) were respectively mixed with diethylenetriamine with 1:1 molar ratio of epoxy vs. −NH for curing. The mixtures were stirred for 10 min, degassed under vacuum to remove entrapped air and poured into silicone molds for curing with the profile: 65 °C for 12 h, 90 °C for 2 h and 120 °C for 2 h. Cured lignin−incorporated epoxy networks were expressed as EN−PL_0SA_{100}, EN−$PL_{10}SA_{90}$, EN−$PL_{20}SA_{80}$, EN−$PL_{30}SA_{70}$, and EN−$PL_{40}SA_{60}$, respectively. Meanwhile, by blending GEL into GE−PL_0SA_{100} co−prepolymer to form 20 wt % GEL in the mixture (LBEN approach, Figure 7.2), an epoxy network EN−BL−$GEL_{20}SA_{80}$ was also prepared according to the above curing profile and used for comparison.

7.4.4 Analysis Methods.

Analysis methods are similar to Chapter 2.

7.5 References

(1) Schneiderman, D. K.; Hillmyer, M. A. *Macromolecules* **2017**, *50* (10), 3733−3749.

(2) Upton, B. M.; Kasko, A. M. *Chem. Rev.* **2016**, *116* (4), 2275−2306.

(3) Baroncini, E. A.; Kumar Yadav, S.; Palmese, G. R.; Stanzione, J. F. *J. Appl. Polym. Sci.* **2016**, DOI: 10.1002/app.44103.

(4) Saito, T.; Brown, R. H.; Hunt, M. A.; Pickel, D. L.; Pickel, J. M.; Messman, J. M.; Baker,

F. S.; Keller, M.; Naskar, A. K. *Green Chem.* **2012**, *14* (12), 3295−3303.

(5) Gandini, A. *Green Chem.* **2011**, *13* (5), 1061−1083.

(6) Kaiho, A.; Mazzarella, D.; Satake, M.; Kogo, M.; Sakai, R.; Watanabe, T. *Green Chem.* **2016**, *18* (24), 6526−6535.

(7) Griffini, G.; Passoni, V.; Suriano, R.; Levi, M.; Turri, S. *ACS Sustainable Chem. Eng.* **2015**, *3* (6), 1145−1154.

(8) van de Pas, D. J.; Torr, K. M. *Biomacromolecules* **2017**, *18* (8), 2640−2648.

(9) Fache, M.; Boutevin, B.; Caillol, S. *Green Chem.* **2016**, *18* (3), 712−725.

(10) Fache, M.; Auvergne, R.; Boutevin, B.; Caillol, S. *Eur. Polym. J.* **2015**, *67*, 527−538.

(11) Wan, J.; Gan, B.; Li, C.; Molina−Aldareguia, J.; Li, Z.; Wang, X.; Wang, D. Y. *J. Mater. Chem. A* **2015**, *3* (43), 21907−21921.

(12) Zhao, S.; Abu−Omar, M. M. *Biomacromolecules* **2015**, *16* (7), 2025−2031.

(13) Zhao, S.; Abu−Omar, M. M. *ACS Sustainable Chem. Eng.* **2016**, *4* (11), 6082−6089.

(14) Zhao, S.; Abu−Omar, M. M. *Macromolecules* **2017**, *50* (9), 3573−3581.

(15) Faye, I.; Decostanzi, M.; Ecochard, Y.; Caillol, S. *Green Chem*. **2017**, *19* (21), 5236−5242.

(16) Wang, S.; Ma, S.; Xu, C.; Liu, Y.; Dai, J.; Wang, Z.; Liu, X.; Chen, J.; Shen, X.; Wei, J. *Macromolecules* **2017**, *50* (5), 1892−1901.

(17) Hernandez, E. D.; Bassett, A. W.; Sadler, J. M.; La Scala, J. J.; Stanzione III, J. F. *ACS Sustainable Chem. Eng.* **2016**, *4* (8), 4328−4339.

(18) Mauck, J. R.; Yadav, S. K.; Sadler, J. M.; La Scala, J. J.; Palmese, G. R.; Schmalbach, K. M.; Stanzione, J. F. *Macromol. Chem. Phys.* **2017**, *218*, DOI: 10.1002/macp.201700013.

(19) Ferdosian, F.; Yuan, Z.; Anderson, M.; Xu, C. C. *Thermochim. Acta* **2015**, *618*, 48−55.

(20) Sasaki, C.; Wanaka, M.; Takagi, H.; Tamura, S.; Asada, C.; Nakamura, Y. *Ind. Crops Prod.* **2013**, *43*, 757−761.

(21) Asada, C.; Basnet, S.; Otsuka, M.; Sasaki, C.; Nakamura, Y. *Int. J. Biol. Macromol.* **2015**, *74*, 413−419.

(22) Qin, J.; Woloctt, M.; Zhang, J. *ACS Sustainable Chem. Eng.* **2013**, *2* (2), 188−193.

(23) Xin, J.; Li, M.; Li, R.; Wolcott, M. P.; Zhang, J. *ACS Sustainable Chem. Eng.* **2016**, *4* (5), 2754−2761.

(24) Parsell, T. H.; Owen, B. C.; Klein, I.; Jarrell, T. M.; Marcum, C. L.; Haupert, L. J.; Amundson, L. M.; Kenttämaa, H. I.; Ribeiro, F.; Miller, J. T.; Abu−Omar, M. M. *Chem. Sci.* **2013**, *4* (2), 806−813.

(25) Smolarski, N. *High−value opportunities for lignin: unlocking its potential*; Frost & Sullivan, Paris, 2012.

(26) Strassberger, Z.; Tanase, S.; Rothenberg, G. *RSC Adv.* **2014**, *4* (48), 25310−25318.

(27) Laurichesse, S.; Avérous, L. *Prog. Polym. Sci.* **2014**, *39* (7), 1266−1290.

(28) Xu, C.; Ferdosian, F., *Conversion of lignin into bio−based chemicals and materials*; Springer, 2017.

(29) Boozalis, T. S., Low molecular weight epoxidized resorcinol novolac resin having high functionality. Patents, US3406150 A, 1968.

(30) Ghaffar, S. H.; Fan, M. *Int. J. Adhes. Adhes.* **2014**, *48*, 92−101.

(31) Malutan, T.; Nicu, R.; Popa, V. I. *BioResources* **2008**, *3* (4), 1371−13767.

(32) Hirose, S.; Hatakeyama, H. *Mem. Fukui Univ. Technol.* **2000**, *30*, 255–262.

(33) Holsopple, D. B.; Kurple, W. W.; Kurple, W. M.; Kurple, K. R. Method of making

epoxide−lignin resins. Patents, US4265809 A, 1981.

(34) Simionescu, C. I.; Rusan, V.; Macoveanu, M. M.; Cazacu, G.; Lipsa, R.; Vasile, C.; Stoleriu, A.; Ioanid, A. *Compos. Sci. Technol.* **1993**, *48* (1−4), 317−323.

(35) Koike, T. *Polym. Eng. Sci.* **2012**, *52* (4), 701−717.

(36) Hofmann, K.; Glasser, W. G. *J. Wood Chem. Technol.* **1993**, *13* (1), 73−95.

(37) El Mansouri, N.−E.; Yuan, Q.; Huang, F. *BioResources*, **2011**, *6* (3), 2492−2503.

(38) Huo, S. P.; Wu, G. M.; Chen, J.; Liu, G. F.; Kong, Z. W. *Thermochim. Acta* **2014**, *587*, 18−23.

(39) Zhao, S.; Abu−Omar, M. M. *ACS Sustainable Chem. Eng.* **2017**, *5* (6), 5059−5066.

(40) Podschun, J.; Saake, B.; Lehnen, R. *Eur. Polym. J.* **2015**, *67*, 1−11.

(41) Alonso, M. V.; Oliet, M.; Rodrıguez, F.; Garcıa, J.; Gilarranz, M.; Rodrıguez, J. *Bioresour. Technol.* **2005**, *96* (9), 1013−1018.

(42) Funaoka, M. *React. Funct. Polym.* **2013**, *73* (2), 396−404.

(43) Zhao, B.; Chen, G.; Liu, Y.; Hu, K.; Wu, R. *J. Mater. Sci. Lett.* **2001**, *20* (9), 859−862.

(44) Jeenpadiphat, S.; Mongkolpichayarak, I.; Tungasmita, D. N. *J. Anal. Appl. Pyrolysis* **2016**, *121*, 318−328.

(45) Jiang, G.; Nowakowski, D. J.; Bridgwater, A. V. *Energy Fuels* **2010**, *24* (8), 4470−4475.

(46) Hosoya, T.; Kawamoto, H.; Saka, S. *J. Anal. Appl. Pyrolysis* **2009**, *85* (1), 237−246.

(47) Fang, Z.; Sato, T.; Smith, R. L.; Inomata, H.; Arai, K.; Kozinski, J. A. *Bioresour. Technol.* **2008**, *99* (9), 3424−3430.

(48) Karp, A. Willows as a source of renewable fuels and diverse products. In *Challenges and Opportunities for the World's Forests in the 21st Century*, Springer, 2014.

(49) Liu, W.; Zhou, R.; Goh, H. L. S.; Huang, S.; Lu, X. *ACS Appl. Mater. Interfaces* **2014**, *6* (8), 5810−5817.

(50) Morandim−Giannetti, A. A.; Agnelli, J. A. M.; Lanças, B. Z.; Magnabosco, R.; Casarin, S. A.; Bettini, S. H. P. *Carbohydr. Polym.* **2012**, *87* (4), 2563−2568.

(51) Vargiu, S.; Pitzalis, M.; Crespolini, G.; Giuliani, G., Preparation of liquid epoxy resins from bisphenols. Patents, US4132718 A, 1979.

(52) Sun, J.; Wang, C.; Yeo, J. C. C.; Yuan, D.; Li, H.; Stubbs, L. P.; He, C. *Macromol. Mater. Eng.* **2016**, *301* (3), 328−336.

Chapter 8

Synthesis of Recyclable Epoxy Thermosets

ABSTRACT: A process for synthesizing degradable and recyclable epoxy thermosets is presented. The process comprises the synthesis of bisphenol connected by imine bonds, glycidylation of phenols and formation of thermoset. The novel epoxy thermosets possessed comparable properties to ordinary epoxy thermoset (e.g., bisphenol A, BPA, based materials), but when treated by a stimulus like acid and/or temperature, exhibited reprocessiblity. Recycling the thermosets involved breakage and reformation of imine bonds; reshaping and repairing the thermosets were realized through imine exchange reaction. All the described processes required no catalyst or press molding.

8.1 Introduction

Epoxy thermoset is one of the most versatile thermosetting materials owing to its outstanding mechanical strength, chemical and thermal resistance and excellent insulation. However, because of its irreversible covalent cross−links, epoxy thermoset is mostly infusible and insoluble, and cannot be reprocessed or recycled after molding. Recently, increasing efforts have been paid to eliminate the “inertness” of thermosets by incorporating dynamic covalent bonds into the networks. The formed covalent adaptable networks, or CANs, while still covalently cross−linked, can achieve stress relaxation and reversible depolymerization through cross−link exchange and cleavage−reformation.[1−4] Although the abundance of dynamic covalent motifs, epoxy cross−linked CANs were only achieved by the reversible nature of

ester[5–9], Diels–Alder (DA)[10–16] and disulfide bonds.[17–26] For example, Leibler *et al*. developed a malleable thermoset by epoxy–carboxylic acid reaction, while the malleability was realized through metal–catalyzed reversible transesterification at elevated temperature.[5] Zhang *et al*. synthesized an epoxy–amine cross–linked thermoset embedded with DA bonds.[11] The thermoset could be converted to soluble polymers with the aid of sonication and repolymerized via DA reaction. Odriozola *et al.* used diglycidyl ether of bisphenol A (DGEBA) to react with a disulfide–containing amine hardener for making fiber–reinforced polymer composites, while the recyclability of composites was derived from the exchangeable disulfide bonds.[19] However, these studies uniformly suffered issues including: need of hot press molding in reprocessing, requirement of expensive metal catalysts, need of additional monomers or special treatments (e.g., sonication), synthetic difficulty and availability of commodity raw materials. Moreover, bisphenol A (BPA) is still preferably selected as thermoset precursor, although it has long been viewed as a non–sustainable chemical.

CANs are broadly classified into two groups, the dynamic structure of which is obtained either kinetically by bond exchange (associative) or through equilibrium shifts leading to reversible depolymerization (dissociative).[2,3] Among the known dynamic bonds, imine bond is unique since it possesses both associative (imine–amine exchange and imine metathesis) and dissociative (imine hydrolysis and reformation) properties that occur under mild conditions. By embedding imine bonds into epoxy cross–linked networks as intermolecular linkages, we herein report a novel epoxy thermoset that exhibits decomposability, recyclability, malleability and weldability without requiring additional ingredients such as catalyst or additional monomer, or complicated processing like press heating. The recyclable thermoset is amenable to

monomers derived from renewable sources (e.g., vanillin, **VAN**, a lignin−derived compound).[27]

8.2 Results and Discussion

8.2.1 Structural Characterization

Synthetic route of the epoxy network is shown in Figure 8.1, panel A. Imine−embedded bisphenol (**VAN−AP**) was readily prepared by reacting **VAN** with aminophenol (**AP**) in water at room temperature (95% isolated yield). While **VAN−AP** possesses structure like the conventional BPA, the attachment of aryl groups to both nitrogen and carbon atoms of imine bonds is a critical structural characteristic that leads to the complete reaction of aromatic aldehyde and amine,[28] which improves the efficiency at the stage of monomer synthesis and polymer recycling. Structure of **VAN−AP** was characterized by NMR spectroscopy. As seen in Figure S8.1, the proton peak at 8.4 ppm and carbon peak at 153 ppm correspond to the imine group, indicating the coupling of aldehyde and amine. **VAN−AP** was then reacted with epichlorohydrin to obtain a glycidyl ether (**GE−VAN−AP**), which exhibited new epoxy proton peaks at 2.7 and 2.9 ppm (−CH_2− in oxirane), 3.3 ppm (−CH− in oxirane), and 4.0 and 4.2 ppm (−O−CH_2−) in Figure S8.2. No aldehyde peak was observed for **GE−VAN−AP**, suggesting imine was stable during the glycidylation process. IR spectra were collected to confirm the structure. IR spectrum of **VAN−AP** exhibited the characteristic absorption bands of imine at 1630 cm^{-1} (Figure S8.3). **GE−VAN−AP** exhibited new oxirane band at 912 cm^{-1}, while the OH bond at 3265 cm^{-1} decreased significantly, which confirmed the formation of epoxy group. When epoxy groups were reacted with amine hardener to form the epoxy network (**EN−VAN−AP**), the active amine protons opened the epoxides while hydroxyls were created at the same time. This process was reflected by the IR spectrum of **EN−VAN−AP** (Figure S8.3),

which exhibited no epoxy band at 912 cm^{-1}, while the broad hydroxyl band increased compared to **GE−VAN−AP**.

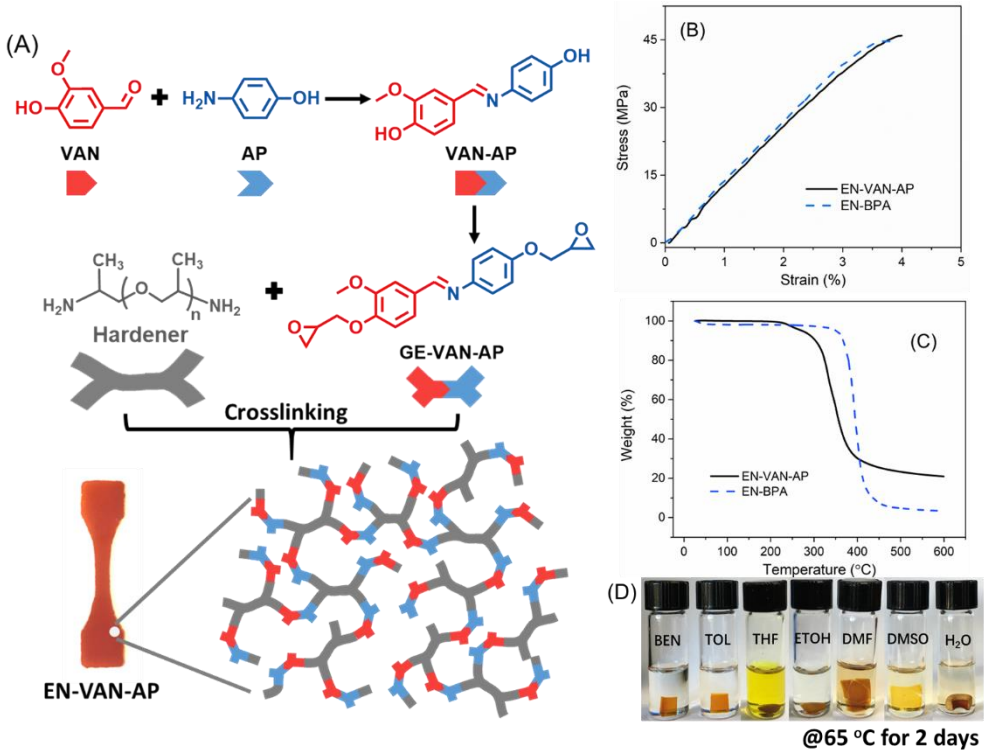

Figure 8.1 Synthesis and properties of **EN−VAN−AP.** Synthesis of **EN−VAN−AP** (A); Tensile (B) and thermal (C) properties of **EN−VAN−AP** and **EN−BPA**, and solvent resistance of **EN−VAN−AP** (D).

8.2.2 Properties of Original Thermoset

EN−VAN−AP was prepared by reacting **GE−VAN−AP** with a commercially available polyamine (Jeffamine D−400, MW= 430) at 120 °C for 24 h. The resulting thermoset exhibited breaking strength and elongation of 46 MPa and 4%. These properties were comparable to BPA−based thermoset (**EN−BPA**, prepared using the same cross−linking conditions as **EN−VAN−AP**) (Figure 8.1, panel B), which was attributed to the structural similarity between **VAN−AP** and BPA. Meanwhile, it suggested the incorporation of dynamic imine bonds did not impair the mechanical properties of epoxy cross−linked thermoset. By comparison, onset

degradation temperature of **EN−VAN−AP** was lower than **EN−BPA** (271 °C vs 350 °C, Figure 8.1, panel C), which was attributed to the increased dissociating tendency of imine bonds at elevated temperature. In addition, **EN−VAN−AP** exhibited good resistance to various solvents including benzene, toluene, THF, ethanol, DMF, DMSO and water. **EN−VAN−AP** exhibited mainly swelling behavior, with limited portion dissolved (< 15 wt %, Figure 8.1, panel D). Overall, **VAN−AP**−derived epoxy thermoset exhibits properties in line with the conventional **BPA** based counterpart when the same hardener and curing conditions are employed, which suggests **VAN−AP** could be a suitable thermoset precursor for a range of applications.

8.2.3 Degradation and Recycling of EN−VAN−AP

By acid−aided hydrolysis of the imine linkages, we then demonstrated **EN−VAN−AP** could be transformed into smaller and soluble oligomers using proper degradation conditions. **EN−VAN−AP** was cut into pieces (*ca*. 4 mm L × 3 mm W × 2 mm T) and immersed (no stirring was applied) in 1.5 mL solvent with various hydrochloric acid concentrations and temperature for two days (Figure S8.4). At room temperature or 65 °C with no HCl added, **EN−VAN−AP** exhibited good resistance to solvents as mentioned above. Concentrated HCl acid was selected to depolymerize the thermosets. This selection was based on its strong acidity, compatibility with hydrophilic solvents and low boiling point that can be readily removed along with solvent during the drying process. At low HCl concentration (0.17 mol/L), limited portion (< 6 wt %) of **EN−VAN−AP** was dissolved in toluene and benzene. This was related to the limited compatibility of HCl solution with toluene and benzene, as reflected by the uneven corrosion on thermoset surface (Figure S8.4). The aggregation of depolymerized thermoset residue in toluene and benzene further confirmed the poor compatibility of decomposed thermoset in

these solvents (Figure S8.4). By comparison, THF, ethanol, DMF, DMSO and water exhibited homogenous solution of the decomposed residue. Especially, 100% **EN−VAN−AP** was dissolved in water at room temperature with HCl concentration as low as 0.17 mol/L, which was significantly higher than other solvents. This could be attributed to the specific sensitivity of imine bonds to water. Increasing the temperature to 65 °C and maintaining the same HCl concentration (0.17 mol/L) accelerated the dissociation of thermosets, which resulted in 100 wt % dissolution of **EN−VAN−AP** in water and DMSO, 79 wt % in DMF, 40 wt % in ethanol, 14 wt % in THF and ~ 7 wt % in toluene and benzene after 2 days. This phenomenon indicated that **EN−VAN−AP** could be readily decomposed when treated by hydrophilic solvents under mild conditions. The affinity of thermoset to solvents followed the order: water > DMSO > DMF > ethanol > THF > benzene ≈ toluene (Figure 8.2, panel B), which was consistent with the polarity of these solvents. Compared to the degradation of conventional epoxy thermosets that involves harsh conditions like high temperature and strong acid/base,[29–33] the facile decomposability and solubility of **EN−VAN−AP** in slightly acidified hydrophilic solvents, especially water, highlights its environmental importance. Meanwhile, it may provide a facile method to recycle the fillers (e.g., carbon fiber) from **EN−VAN−AP** based composites. Moreover, this unique decomposability could distinguish **EN−VAN−AP** from other types of thermosets or thermoplastics, which facilitates the isolation and recycling of plastics.

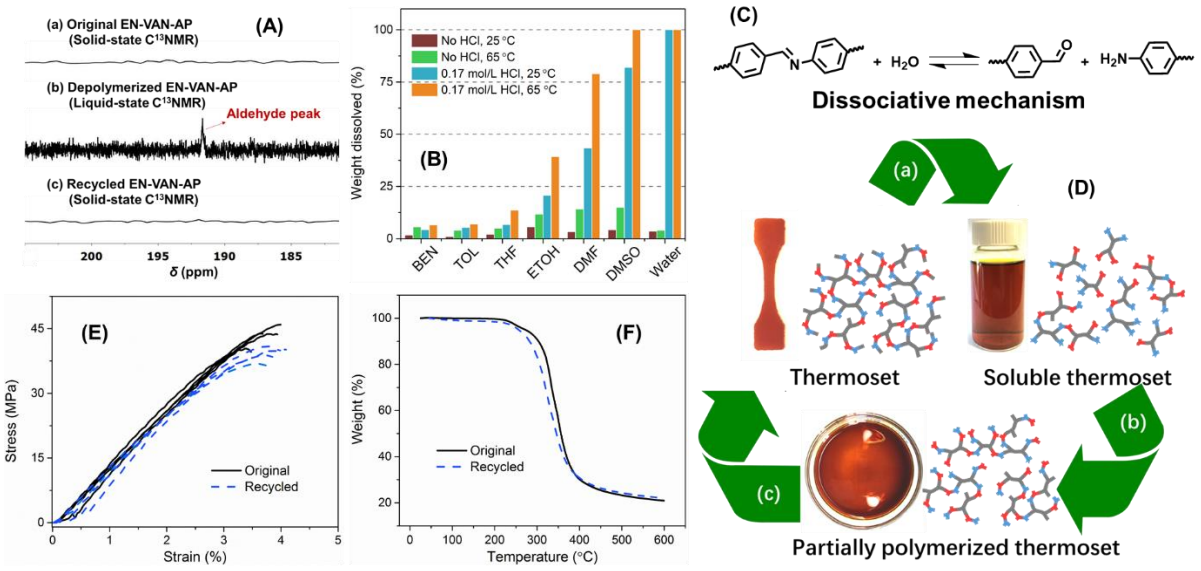

Figure 8.2 Depolymerization and recycling of **EN−VAN−AP** through dissociative mechanism. NMR spectra of solid and depolymerized samples (A); Depolymerization of **EN−VAN−AP** in different solvents and temperature (B); Dissociative mechanism (C); Recycling approaches (D); Tensile (E) and thermal (F) properties of original and recycled **EN−VAN−AP.**

While the original **EN−VAN−AP** was formed through epoxy−amine reaction, formation of the recycled thermoset was realized via aldehyde−amine reaction. The recycling process occurred in two steps: drying the oligomer solution to remove most of the solvent and HCl, and re−cross−linking the oligomers at elevated temperature to recover the thermoset. Solvent used for thermoset degradation was found to be a major factor that determined the efficiency and properties of the recycled thermoset. Optimal solvent should have properties including: 1) high solubility for thermoset, 2) reasonable boiling point that can be readily removed, and 3) properties of recycled thermoset should be comparable to original thermoset. Because of their relatively lower solubility for **EN−VAN−AP,** toluene, benzene, THF and ethanol might not be optimal as compared to DMF, DMSO and water, which exhibited sufficient solubility under mild conditions. From the aspect of solvent removal, DMSO might be problematic due to its

high boiling point (189 °C). In a preliminary experiment, it took more than three times longer for DMSO to be mostly removed under vacuum from polymer solution than when DMF or water was used as solvent. The use of DMSO increased separation difficulty, while the presence of DMSO residue in recycled thermoset might lead to decreased cross−link density, and possibly compromised mechanical and thermal properties. As for water, the thermoset recovered from water solution exhibited significantly poor water resistance. It deformed quickly when immersed in water at room temperature, even though no acid was added (Figure S8.5). This could be related to the high affinity of HCl to water, which made HCl difficult to be completely removed from the polymer mixture. The trapped trace amount of HCl could still lead to significant deformation of recycled thermoset when exposed to water. By comparison, DMF exhibited the highest suitability among studied solvents for recycling, since it demonstrated sufficient solubility and reasonable boiling point, while the properties of recycled thermoset were retained. The recycling process and properties of recycled thermoset are illustrated next.

Using the **EN−VAN−AP**/DMF weight ratio of 1:10, HCl concentration of 0.25 mol/L and stirring, **EN−VAN−AP** could be fully dissolved within 1 h at 65 °C. The solution was dried by two steps: 1) the mixture was heated at 80 °C and dried by an air flow to get rid of *ca*. 60% volume, and 2) the mixture was slowly dried under vacuum at room temperature overnight to remove most of volatile components, leaving the depolymerized **EN−VAN−AP** as a viscous gel. It should be noted that after the acid−aided depolymerization, the DMF solution contained a mixture of oligomer chains with terminal aldehyde and/or amine groups (structural illustration in Figure 8.2, panel D). During the drying processes, as HCl was gradually

evaporated, the rate of imine formation increased, and the molecular weight of polymer chains continuously increased. At the end of the drying processes, the formed polymer gel was heated at 120 °C for 24 h to promote solvent residue evaporation, facilitate the aldehyde−amine reaction and recreate the polymer network. Depolymerization and reformation of **EN−VAN−AP** were confirmed by the NMR spectra of original, depolymerized and recycled samples in Figure 8.2, panel A and Figure S8.6−S8.8. As the imine linkages within the original **EN−VAN−AP** were intact, no aldehyde peak was observed from the solid−state carbon spectrum (imine peak was overlapped with aromatic peaks at 160 ppm). By comparison, depolymerizing the thermoset in acidified DMSO−d_6 revealed the aldehyde group at 9.8 ppm, indicating the cleavage of imine bond. After re−cross−linking, the aldehyde group of recycled thermoset disappeared again, suggesting reformation of network was realized through aldehyde−amine reaction. IR spectrum of recycled thermoset also revealed no aldehyde group, suggesting the aldehyde−amine reaction was complete (Figure S8.9). Moreover, IR spectra of original and recycled thermosets exhibited the same pattern (Figure S8.9), which indicated recycled thermoset retained similar chemical structure to original thermoset. Tensile and thermal properties of the recycled thermoset exhibited no major decrease as compared to original samples (Figure 8.2, panel E and F). The dissociative mechanism (bond cleavage and reformation) of imine bond conferred epoxy thermoset with facile degradation and recycling methods, which required no press heating or catalyst. By comparison, high temperature, press molding and catalyst are often required to convert the rigid networks into viscoelastic liquids when recycling the associative CANs.

8.2.4 Malleability and Weldability

By utilizing the associative mechanisms of imine bonds, we then demonstrated **EN−VAN−AP** was malleable. The malleability came from the imine exchange reactions at elevated temperature, which has been well proved by model compound study and imine−containing thermosets. According to Zhang *et al.*,[34] imine exchange in network was primarily catalyzed by residual unreacted primary amino groups via an associative approach. Considering the high rigidity and T_g of **EN−VAN−AP**, molar ratio of epoxy: $-NH_2$ was set as 2: 1.05 when curing to facilitate the imine exchange reactions. A stress relaxation experiment of **EN−VAN−AP** was carried out. The measurements were conducted at different temperatures in the range from 30 to 60 °C. Thermoset with thickness of 0.22 mm was heated to the test temperature. After the temperature was equilibrated for 5 min, a 1 % strain step was applied, and the stress was recorded over time. A constant normal force of 5 N was applied to maintain a good contact of the sample with the parallel plate. As seen in Figure 8.3, panel A, **EN−VAN−AP** was observed to dissipate almost all stress within 50 s at 60°C, while no catalyst was needed.

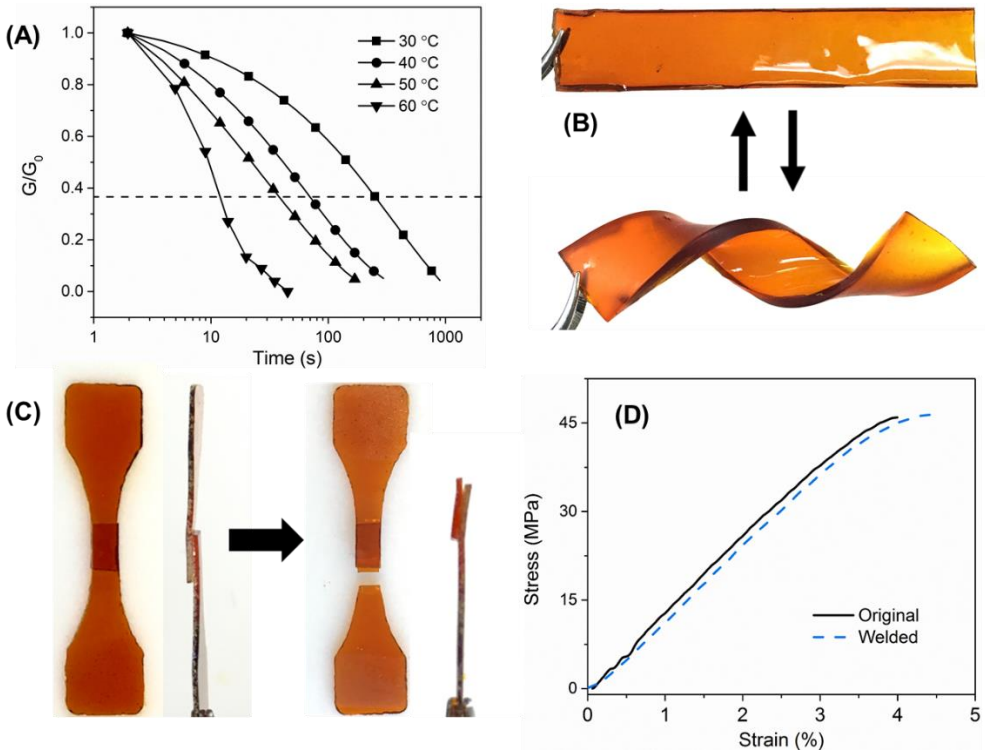

Figure 8.3 Malleability and weldability of **EN−VAN−AP** through associative mechanism. Stress relaxation test of **EN−VAN−AP** (A); Malleability of **EN−VAN−AP** (B); Weldability of **EN−VAN−AP** (C) and mechanical properties of original and welded samples (D).

The shape transformation of thermoset is another evidence supporting the stress relaxation of thermoset at elevated temperature. An **EN−VAN−AP** strip with dimensions of 125 mm L × 12.5 mm W × 2.2 mm T was used for illustration. By heating the strip at 120 °C for 2 min, the rigid thermoset was converted into a viscoelastic state. At this time, the strip was twisted into a helical fusilli−like shape (Figure 8.3, panel B). When the thermoset was cooled to room temperature, the helical fusilli−like shape was retained. Applying a new force and heat could recover the thermoset back to its original flat shape. Conventional permanently cross−linked epoxy thermoset, however, cannot exhibit stress relaxation at elevated temperature and is prone to fracture when additional force is applied.

By utilizing the imine exchange reactions occurred at the interfaces of overlapped

thermoset pieces, **EN−VAN−AP** was also weldable and repairable. To prove this, a rectangular **EN−VAN−AP** film (50 mm L × 25 mm W × 0.4 mm T) was cut into two pieces. The two pieces were overlapped by *ca*. 3.2 mm on a Teflon sheet and preheated at 100 °C for 60 s. During the preheating period, a *ca.* 10 N force was applied to the overlapping area to facilitate the welding. It was observed that the two pieces started to attach to each other. The film was then transferred to an oven and heated at 120 °C for 4 h for welding, which required no additional pressure or amine monomer. After the welding process, a dog−bone shaped sample was punched out, while the overlapped area was left in the middle of the sample (Figure 8.3, panel C). The welded sample, which possessed same dimensions with original samples (prepared using the same punch), was subjected to tensile test. As seen in Figure 8.3, panel C, the welded sample always fractured at a different place rather than the overlapped area, suggesting the overlapped area was not the weakest part of the sample. Meanwhile, tensile strength and elongation at break of welded sample were 46 MPa and 4.4%, respectively, which were comparable to the original sample (Figure 8.3, panel D).

8.2.5 Water Sensitivity

Lastly, we demonstrated that water resistance of imine−containing thermoset may be impacted by the concentration of imine bond and cross−link density of the thermoset. Previously reported imine−containing thermosets were mainly prepared through direct condensation between poly−functionalized aldehydes and aliphatic polyamines[34–39]. In these networks, imine bonds acted as the cross−linking sites. However, because of the water−sensitive nature of imine bonds, strength of thermosets was reported to decrease when exposed to water.[35] In contrast to previous approaches, we embedded imine bonds in the

backbone of diglycidyl ethers, while cross−linking was realized through epoxy−amine reactions. This approach increases the cross−link density (epoxy reacts with $-NH_2$ in 2:1 ratio, while aldehyde reacts with $-NH_2$ in 1:1 ratio) while decreases the content of imine bonds within the network, both of which improve the water resistance of imine−containing thermosets.

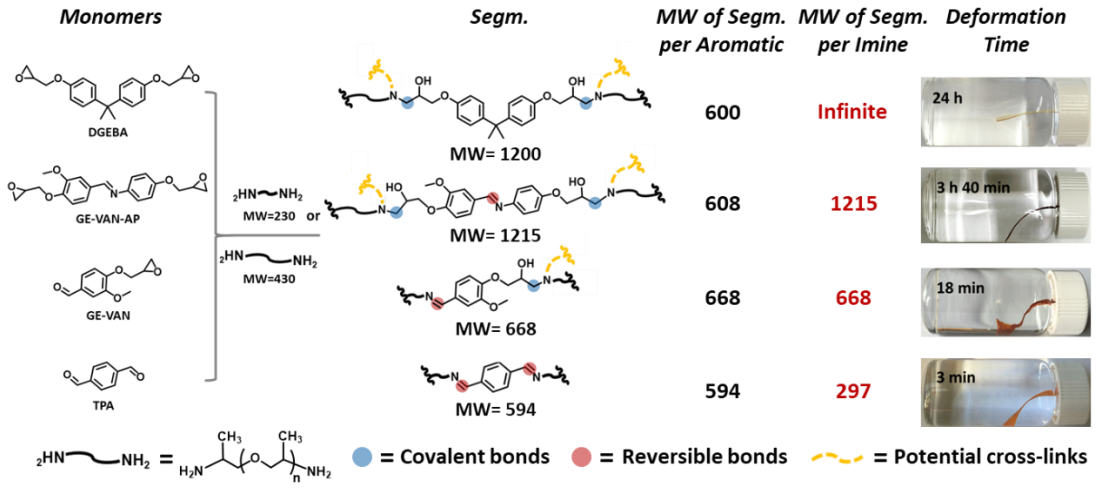

Figure 8.4 Impacts of imine content and cross−link density on water sensitivity of thermosets.

To explore the impacts of cross−link density and content of imine bonds on the water resistance of thermoset, three precursors (**DGEBA**, **GE−VAN** and terephthaldehyde) with various epoxy and aldehyde groups were compared to **GE−VAN−AP**. All precursors were reacted with polyamines to obtain thermosets containing various contents of imine bonds. Since aromatic motif could increase the strength of thermoset, weight ratio of aromatic ring in each thermoset was kept similar by adjusting the molecular weight of polyamines (MW = 230 or 400). All thermosets were cured at 120 °C for 1 to 3 days for complete conversions of epoxy or aldehyde groups as confirmed by IR spectra. Figure S8.10 demonstrates the experimental setup for testing the water sensitivity of thermosets. As seen in Figure 8.4, it took only 3 and 18 min for **EN−TPA** and **EN−VAN** to lose most of their strength when immersed in water at room temperature. By comparison, **EN−VAN−AP** exhibited significantly improved water

resistance, as it took more than 220 min to get the same deformation. As for the conventional **BPA**−based thermoset (**EN−BPA**), it exhibited the highest water resistance, as most of its strength was retained even after immersing in water for 24 h.

Because of the complexity of cross−linked network, a representative polymer segment from each of the four thermosets was illustrated in Figure 8.4 for comparison. The segments were simplified to contain one molecule of precursor and two molecules of amine hardener chains that reacted at each side of the precursor. Covalent (formed through epoxy−amine reactions) and reversible bonds (formed by aldehyde−amine reactions) within the segments were highlighted. The aromatic content in each segment was similar (1 aromatic ring per segmental molecular weight of *ca*. 600). However, the content of reversible imine bonds varied significantly among segments. It was observed that water resistance of thermosets decreased as imine content increased. **EN−BPA** has no reversible bond, and its permanently cross−linked network makes it the most resistant to water. **EN−VAN−AP** has one imine bond per segmental MW of ca. 1215. Although imine bonds were "protected" by adjacent phenyl groups and other covalent cross−links, water molecules could still gradually penetrate the network by hydrolyzing the imine bond and eventually softened the thermoset. When it comes to **EN−VAN** and **EN−TPA**, the imine content is doubled and quadrupled compared to **EN−VAN−AP**, respectively. These increments result in the deformation of thermosets in much shorter time of exposure. While reduced imine content postponed the deformation of network, increased cross−link density, in a similar way, helped decrease the exposure of imine bond to water molecules. It should be noted that, epoxy reacts with amine ($-NH_2$) in 2: 1 molar ratio, while aldehyde reacts with amine ($-NH_2$) in 1:1 molar ratio. Thus, as illustrated in Figure 8.4,

precursors of **EN−BPA** and **EN−VAN−AP** can develop in four directions, while TPA−based polymer is basically linear. Possessing lower imine content while still highly cross−linked, **EN−VAN−AP** exhibits improved water resistance over the straightforward aldehyde−amine cross−linked thermosets.

8.3 Conclusions

In summary, we report a novel epoxy thermoset that exhibits decomposability, recyclability, malleability and weldability without requiring additional ingredients such as catalyst or additional monomer, or complicated processes like press heating. Through breaking and reforming the imine bonds, the epoxy thermosets can be: 1) decomposed and solubilized in organic or aqueous solutions under mild conditions, and 2) reformed from the solutions with the original thermal and mechanical properties retained. Through imine exchange reaction, the epoxy thermosets at sufficient temperature can be: 1) reshaped through bond exchange within polymer networks, and 2) welded through bond exchange at the interface of overlapping thermoset pieces.

8.4 Experimental Section

General. Vanillin (VAN), 4−aminophenol (AP), epichlorohydrin, tetrabutylammonium bromide, diethylenetriamine (DETA), diglycidyl ether of bisphenol A (DGEBA), terephthaldehyde, Jeffamine (poly(propylene glycol) bis(2−aminopropyl ether)) (molecular weight of 230 or 430) were purchased from Aldrich Chemical Co. Concentrated hydrochloric acid (37%) was obtained from Fisher Scientific. All chemicals were used as received without further purification.

8.4.1 Synthesis of VAN−AP.

A mixture of vanillin (6.08 g, 40 mmol) and 4−aminophenol (4.36 g, 40 mmol) was stirred in water (125 mL) at room temperature for 4 h. The afforded powder was collected by filtration, washed with water and dried in a desiccator to give VAN−AP as a yellowish powder (9.23 g, 95% yield).

8.4.2 Synthesis of GE−VAN−AP.

Glycidyl ether of VAN−AP (GE−VAN−AP) was prepared by reacting VAN−AP (2.43 g, 10 mmol) with epichlorohydrin (25 g, 266 mmol). Tetrabutylammonium bromide (0.26 g, 0.85 mmol) was used as a phase transfer catalyst. The mixture was heated at 85 °C for 3 h and followed by a dropwise addition of 5 g of 20% w/w NaOH solution. The reaction was kept for another 2 h, and the mixture was washed with acetone, filtrated to remove formed NaCl and concentrated with a rotary evaporator to yield GE−VAN−AP as a yellowish solid (3.49 g, 94% isolated yield).

8.4.3 Formation of Polymer Networks.

GE−VAN−AP was first melt at 100 °C. Then, Jeffamine 430 with 1:1 molar ratio of epoxy vs. −NH was dropwise added. The mixture was vigorously stirred at 100 °C for 3 min, degassed under vacuum to remove trapped air, poured into silicone mold and cured at 60 °C for 4 h and 120 °C for 20 h. The obtained brownish epoxy network was denoted as EN−VAN−AP.

8.4.4 Remolding Methods.

1.5 g cured thermoset was cut into pieces (*ca*. 12.5 mm × 5mm) and placed in a 20 mL glass vial. To this vial was added successively 15 mL DMF and 12 drops of concentrated HCl. The mixture was then heated up at 60 °C and stirred. Thermoset samples were found to dissolve gradually and a homogenous solution was obtained after 1 h. DMF and HCl in the homogenous

solution were slowly evaporated when stirred at 60 °C with the aid of an air flow. When thin polymer film started to form on the surface of solution (at this point, *ca*. 8 mL solution was left), the solution was transferred to a glass plate. The mixture was then placed in a vacuum desiccator to remove the leftover DMF and HCl. After 16 h, the mixture was put in an oven at 120 °C for 24 h to obtain the remolded thermoset.

8.4.5 Analysis Methods.

Tensile testing was performed on 0.5 mm thick dog bone−shaped specimens according to the ASTM D638 standard, on a custom−built setup on a vertical TwinRail positioning table (Lintech, CA) with a 100−lb load cell.

Other analysis methods are similar to Chapter 2.

8.5. References

(1) Kloxin, C. J.; Scott, T. F.; Adzima, B. J.; Bowman, C. N. *Macromolecules* **2010**, *43*, 2643.

(2) Denissen, W.; Winne, J. M.; Du Prez, F. E. *Chem*. *Sci*. **2016**, *7,* 30.

(3) Bowman, C. N.; Kloxin, C. J. *Angew Chem*. *Inter*. *Edi*. **2012**, *51*, 4272.

(4) Kloxin, C. J.; Bowman, C. N. *Chem*. *Soc*. *Rev*. **2013**, *42*, 7161.

(5) Montarnal, D.; Capelot, M.; Tournilhac, F.; Leibler, L. *Science* **2011**, *334*, 965.

(6) Capelot, M.; Montarnal, D.; Tournilhac, F. o.; Leibler, L. *J. Am. Chem. Soc.* **2012**, 134, 7664.

(7) Pei, Z.; Yang, Y.; Chen, Q.; Terentjev, E. M.; Wei, Y.; Ji, Y. *Nat. Mater*. **2014**, *13*, 36.

(8) Shi, Q.; Yu, K.; Dunn, M. L.; Wang, T.; Qi, H. J. *Macromolecules* **2016**, *49*, 5527.

(9) Shi, Q.; Yu, K.; Kuang, X.; Mu, X.; Dunn, C. K.; Dunn, M. L.; Wang, T.; Qi, H. *J. Mater*. *Hor*. **2017**.

(10) Bai, N.; Saito, K.; Simon, G. P. *Polym*. *Chem*. **2013**, *4*, 724.

(11) Min, Y.; Huang, S.; Wang, Y.; Zhang, Z.; Du, B.; Zhang, X.; Fan, Z. *Macromolecules* **2015**, *48*, 316.

(12) Li, Q.−T.; Jiang, M.−J.; Wu, G.; Chen, L.; Chen, S.−C.; Cao, Y.−X.; Wang, Y.−Z. *ACS Appl*. *Mater*. *Interfaces* **2017**, *9* (24), 20797–20807.

(13) Tian, Q.; Yuan, Y. C.; Rong, M. Z.; Zhang, M. Q. *J. Mater. Chem.* **2009**, *19*, 1289.

(14) Luo, K.; Xie, T.; Rzayev, J. *J. Polym. Sci. Part A: Polym*. *Chem*. **2013**, *51*, 4992.

(15) Marref, M.; Mignard, N.; Jegat, C.; Taha, M.; Belbachir, M.; Meghabar, R. *Polym. Int.* **2013**, *62*, 87.

(16) Fan, M.; Liu, J.; Li, X.; Zhang, J.; Cheng, *J. Ind. Eng. Chem. Res.* **2014**, *53*, 16156.

(17) Tesoro, G.; Sastri, V. *J. Appl. Polym. Sci.* **1990**, *39*, 1425.

(18) Sastri, V.; Tesoro, G. *J. Appl. Polym. Sci.* **1990**, *39*, 1439.

(19) de Luzuriaga, A. R.; Martin, R.; Markaide, N.; Rekondo, A.; Cabañero, G.; Rodríguez, J.; Odriozola, I. *Mater. Hor.* **2016**, *3,* 241.

(20) Azcune, I.; Odriozola, I. *Eur. Polym. J*. **2016**, *84*, 147.

(21) Pepels, M.; Filot, I.; Klumperman, B.; Goossens, H. *Polym. Chem.* **2013**, *4*, 4955.

(22) Canadell, J.; Goossens, H.; Klumperman, B. *Macromolecules* **2011**, *44*, 2536.

(23) Imbernon, L.; Oikonomou, E.; Norvez, S.; Leibler, L. *Polym*. *Chem*. **2015**, *6*, 4271.

(24) Lei, Z. Q.; Xiang, H. P.; Yuan, Y. J.; Rong, M. Z.; Zhang, M. Q. *Chem*. *Mater*. **2014**, *26*, 2038.

(25) Ma, Z.; Wang, Y.; Zhu, J.; Yu, J.; Hu, Z. *J. Polym. Sci. Part A*: *Polym*. *Chem*. **2017**, *55*, 1790.

(26) Takahashi, A.; Ohishi, T.; Goseki, R.; Otsuka, H. *Polymer* **2016**, *82*, 319.

(27) Fache, M.; Boutevin, B.; Caillol, S. *ACS Sustain. Chem. Eng.* **2015**, *4*, 35.

(28) Lei, Z. Q.; Xie, P.; Rong, M. Z.; Zhang, M. Q. *J. Mater. Chem. A* **2015**, *3*, 19662.

(29) Wang, Y.; Cui, X.; Ge, H.; Yang, Y.; Wang, Y.; Zhang, C.; Li, J.; Deng, T.; Qin, Z.; Hou, X. *ACS Sustain. Chem. Eng.* **2015**, *3*, 3332.

(30) Jiang, G.; Pickering, S. J.; Lester, E. H.; Turner, T.; Wong, K.; Warrior, N. *Compos. Sci. Technol.* **2009**, *69*, 192.

(31) Dang, W.; Kubouchi, M.; Yamamoto, S.; Sembokuya, H.; Tsuda, K. *Polymer* **2002**, *43*, 2953.

(32) Dang, W.; Kubouchi, M.; Sembokuya, H.; Tsuda, K. *Polymer* **2005**, *46*, 1905.

(33) Liu, T.; Guo, X.; Liu, W.; Hao, C.; Wang, L.; Hiscox, W. C.; Liu, C.; Jin, C.; Xin, J.; Zhang, J. *Green Chem*. **2017**, *19*, 4364.

(34) Chao, A.; Negulescu, I.; Zhang, D. *Macromolecules* **2016**, *49*, 6277.

(35) Taynton, P.; Yu, K.; Shoemaker, R. K.; Jin, Y.; Qi, H. J.; Zhang, W. *Adv*. *Mater*. **2014**, *26*, 3938.

(36) Taynton, P.; Ni, H.; Zhu, C.; Yu, K.; Loob, S.; Jin, Y.; Qi, H. J.; Zhang, W. *Adv*. *Mater*. **2016**, *28*, 2904.

(37) Taynton, P.; Zhu, C.; Loob, S.; Shoemaker, R.; Pritchard, J.; Jin, Y.; Zhang, W. *Polym. Chem*. **2016**, *7*, 7052.

(38) Lei, X.; Jin, Y.; Sun, H.; Zhang, W. J. *Mater*. *Chem*. *A* **2017**, *5*, 21140.

(39) Zhu, C.; Xi, C.; Doro, W.; Wang, T.; Zhang, X.; Jin, Y.; Zhang, W. *RSC Adv*. **2017**, *7*, 48303.

Chapter 9

Summary and Future Work

The objective of this research project is to develop high−performance lignin−based epoxy thermosets. Lignin−derived phenol monomers and bulk lignin are successfully converted to BPA analogs for thermoset syntheses. For lignin−derived phenol monomers, different modification methods can yield multifunctional phenols with different (1) molecular weight, (2) orientation and (3) number of hydroxyl groups via dimerization and oligomerization reactions. By using different modification strategies, cross−link density and thermomechanical properties of obtained thermosets can be tuned.

According to the above findings, a fully lignin−based triphenol (VAN−M−CAT) is developed, which has rigid framework, high functionality (n = 5) and stretched hydroxyl groups. These advantageous structural properties make VAN−M−CAT excellent precursor to epoxy thermosets. As an example, VAN−M−CAT based network exhibits excellent glassy modulus (12.3 GPa) and glass transition temperature (167 °C). By adjusting the number of methoxy substituents, impacts of methoxy group on properties of thermosets are also investigated. Especially, increasing the content of methoxy significantly decreases the yield of starting phenols and thermal properties of thermosets. This conclusion can guide the selection and/or modification (e.g. deoxygenation) of lignin−derived monomers for making epoxy polymers with desirable properties. For further work, an interesting study includes finding out an approach that could tune the rigidity and modulus of the rigid TP−based thermosets. This could be achieved by adjusting the content of non−curable benzodioxane byproducts in the mixture.

To incorporate bulk lignin into thermosets, an approach that involves successive

demethylation, phenolation and phenol−formaldehyde reactions is proposed. Overall, DLINENs (deprotected lignin incorporated novolac epoxy networks) show improved performance when compared to LBENs (lignin blended epoxy network), which can be rationalized on the basis of enhanced reactivity, compatibility and covalent linkage of lignin in the networks. To avoid the use of formaldehyde, a modified approach is also proposed, which involves the self−condensation of salicyl alcohol. The modified approach also increases the content of lignin in thermoset (up to 20 wt%), which significantly widens the application of bulk lignin. It would be interesting to further increase the content of bulk lignin in thermoset. This could be achieved by using lignin with lower molecular weight, or using partially depolymerized lignin that has less complicated structure.

Lastly, a novel epoxy thermoset that exhibits decomposability, recyclability, malleability and weldability is proposed. Reprocessiblity of the thermoset requires no additional ingredient such as catalyst or additional monomer, or complicated processes like press heating when recycled. Through breaking and reforming the imine bonds (dissociative mechanism), the epoxy thermosets can be decomposed and solubilized in organic or aqueous solutions under mild conditions, and reformed from the solutions while original thermal and mechanical properties are retained. Through imine exchange reaction (associative mechanism), the epoxy thermosets at sufficient temperature can be reshaped and welded. Keeping the malleability and recyclability in mind, potential further study should be focused on increasing the biomass content of the thermosets.

Appendix 1 for Chapter 2

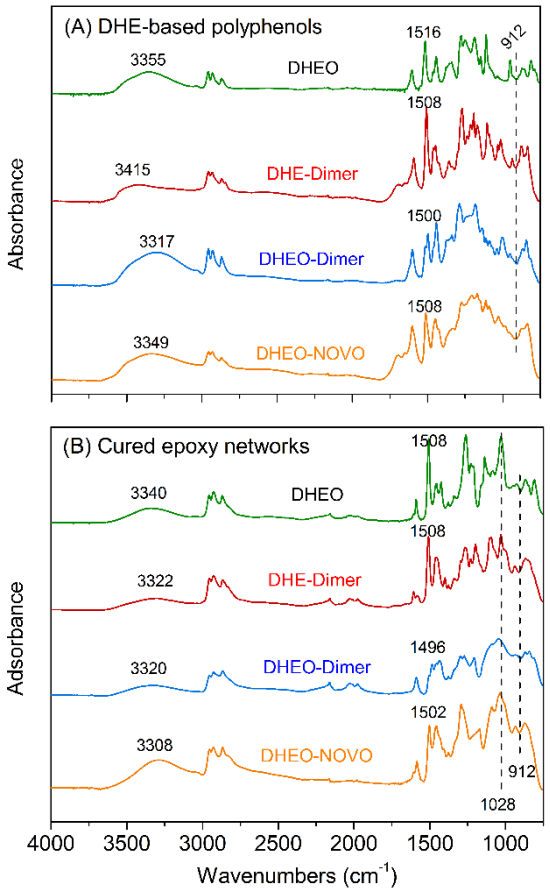

Figure S2.1. FTIR spectra of (A) DHE−based polyphenols and (B) cured DHE−based networks after curing 2 h at 55 °C, 2 h at 75 °C and 2 h at 95 °C using DETA as a hardener.

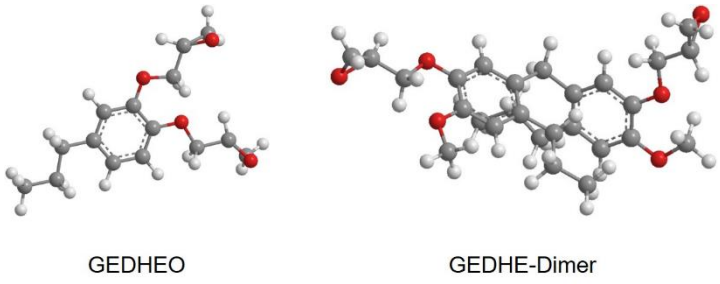

Figure S2.2. 3−D models of GEDHEO and GEDHE−Dimer. The models were generated by ChemBio3D Ultra 14.0.

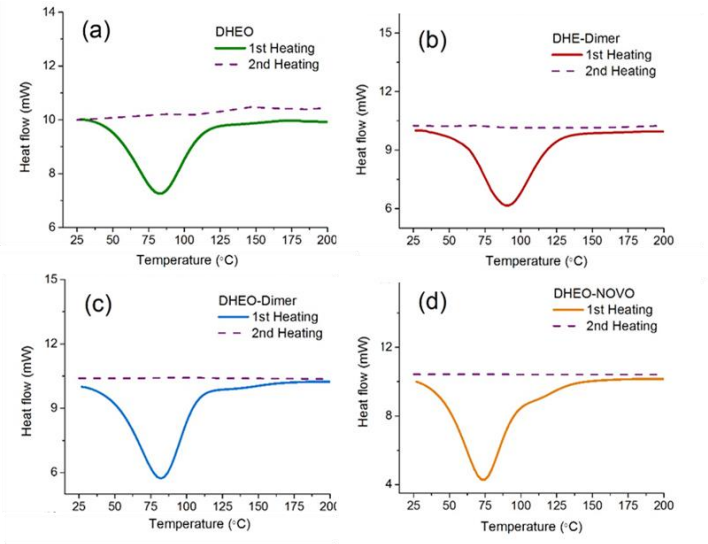

Figure S2.3. Heat release during nonisothermal cures via DSC of different DHE−based epoxy monomers/DETA systems. Degrees of cure were determined through two cycles of heating. Samples were firstly heated from 0 to 200 °C at 10 °C/min, cooled to 0 °C, and reheated to 200 °C at 10 °C/min. All samples were completely cured as supported by the lack of exotherm on the second heating.

Appendix 2 for Chapter 3

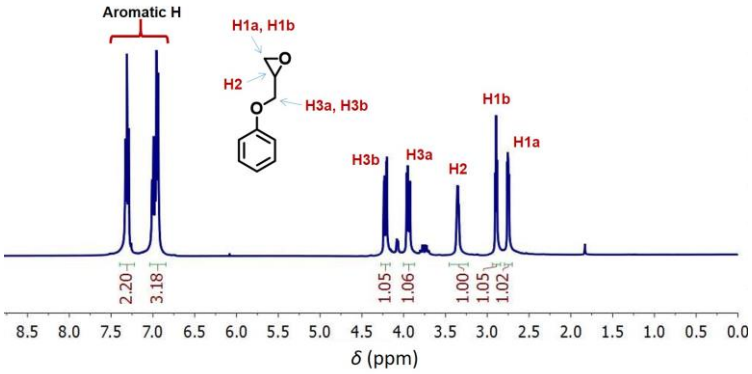

Figure S3.1. Proton NMR spectra of glycidyl ether of phenol. Solvent: $CDCl_3$.

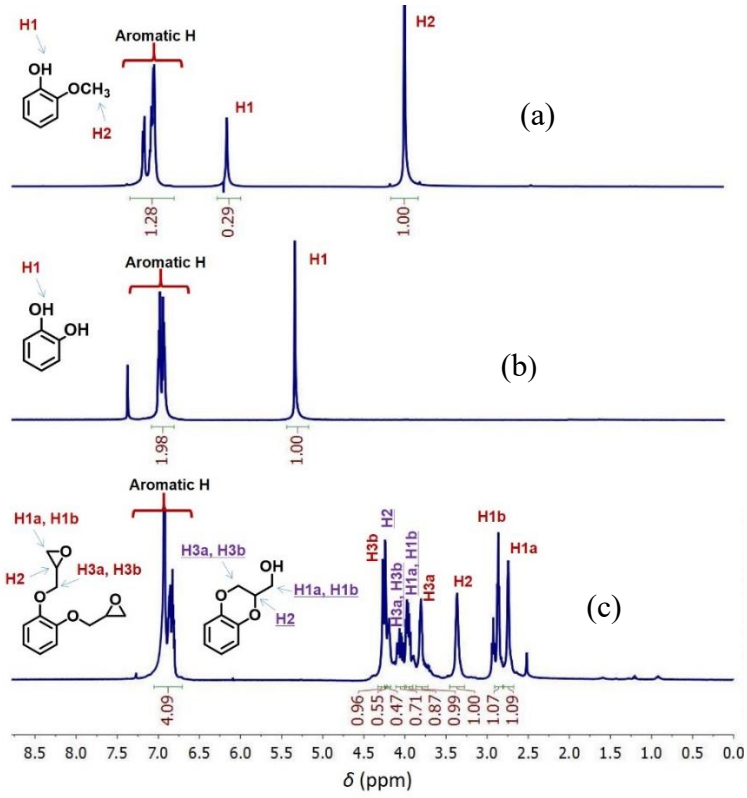

Figure S3.2. Proton NMR spectra of (a) guaiacol, (b) catechol and (c) glycidylation products. Solvent: $CDCl_3$.

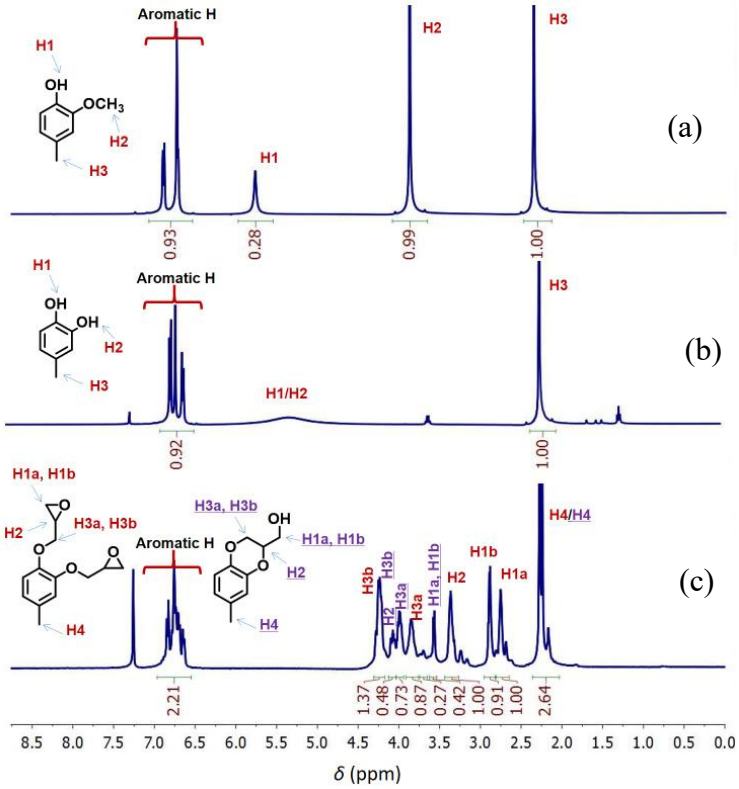

Figure S3.3. Proton NMR spectra of (a) M−GUA, (b) M−CAT and (c) glycidylation products.

Solvent: $CDCl_3$.

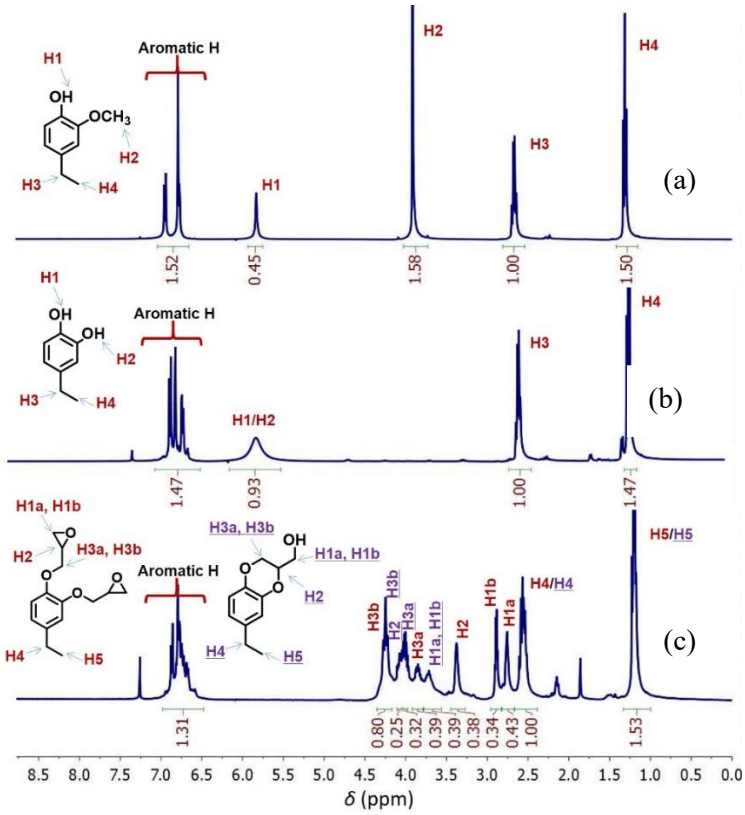

Figure S3.4. Proton NMR spectra of (a) E−GUA, (b) E−CAT and (c) glycidylation products. Solvent: $CDCl_3$.

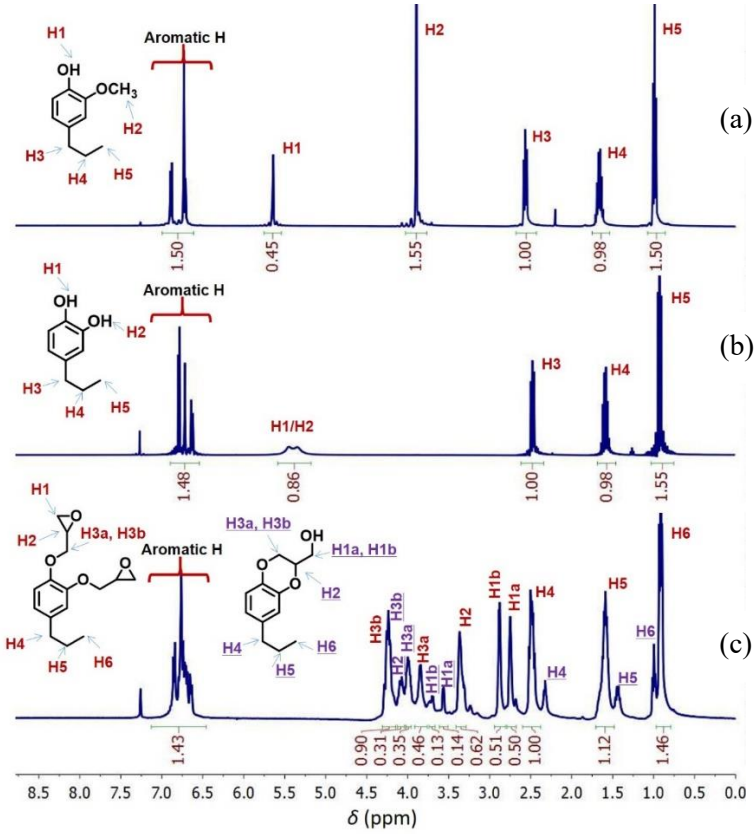

Figure S3.5. Proton NMR spectra of (a) P−GUA, (b) P−CAT and (c) glycidylation products.

Solvent: $CDCl_3$.

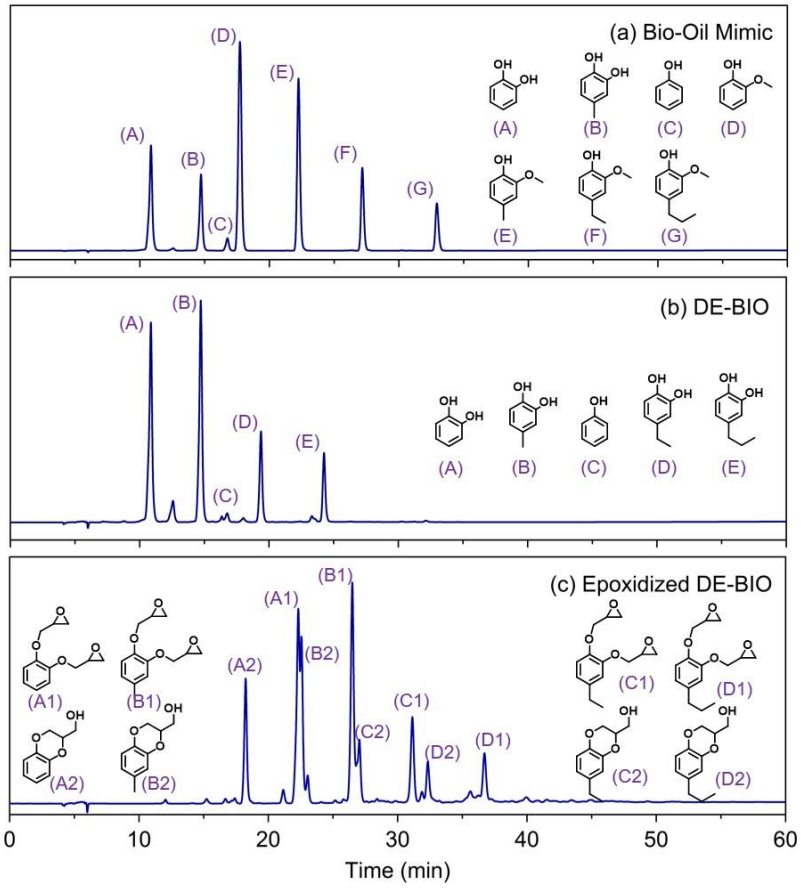

Figure S3.6. HPLC spectra of (a) bio−oil mixture, (b) demethylated bio−oil (DE−BIO) and (c) glycidylation products of DE−BIO.

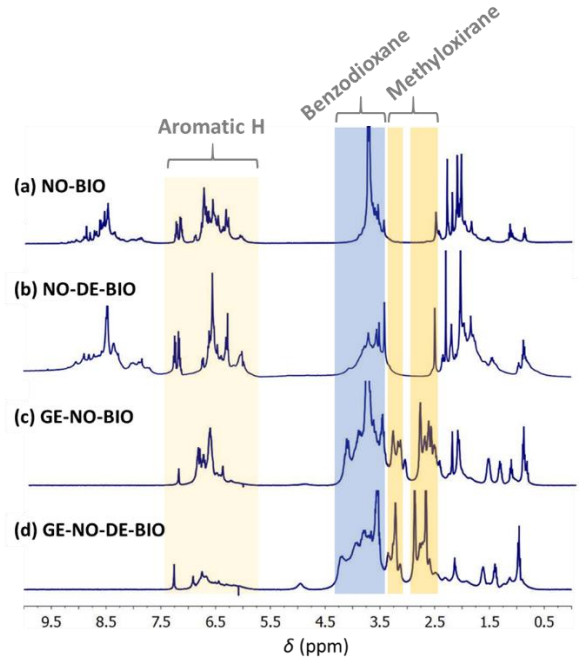

Figure S3.7. Proton NMR spectra of (a) NO−BIO, (b) NO−DE−BIO and glycidylation products (c) GE−NO−BIO and (d) GE−NO−DE−BIO. Solvent: $CDCl_3$.

Appendix 3 for Chapter 4

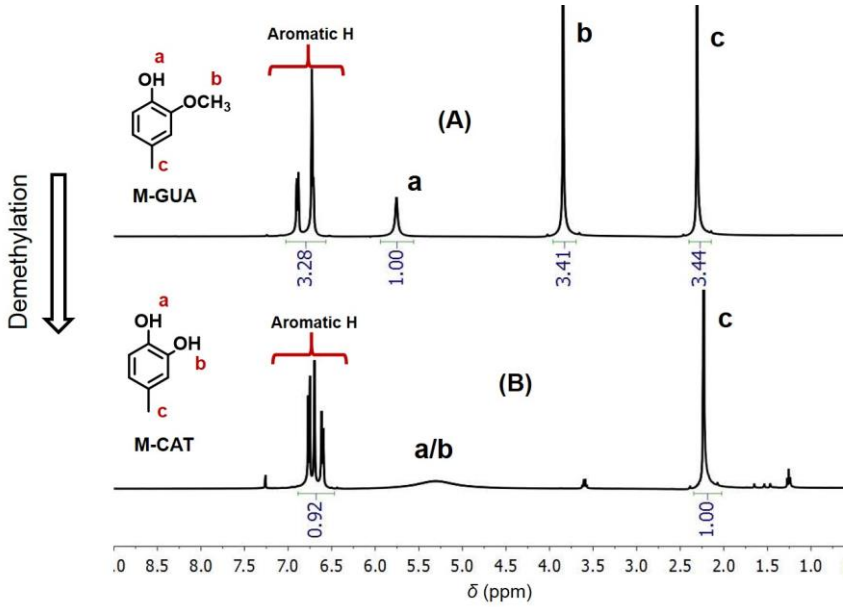

Figure S4.1. Proton NMR spectra of (A) M−GUA and (B) M−CAT. Solvent: $CDCl_3$.

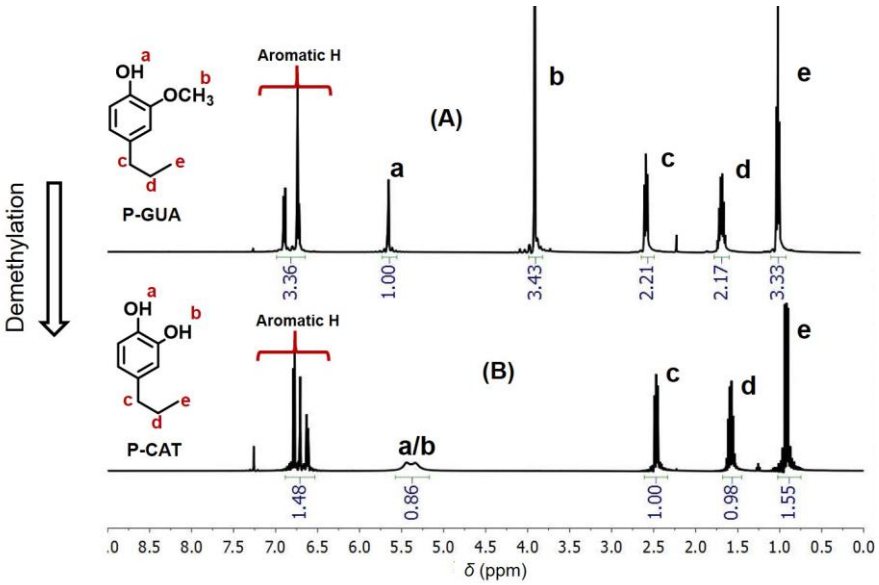

Figure S4.2. Proton NMR spectra of (A) P−GUA and (B) P−CAT. Solvent: $CDCl_3$.

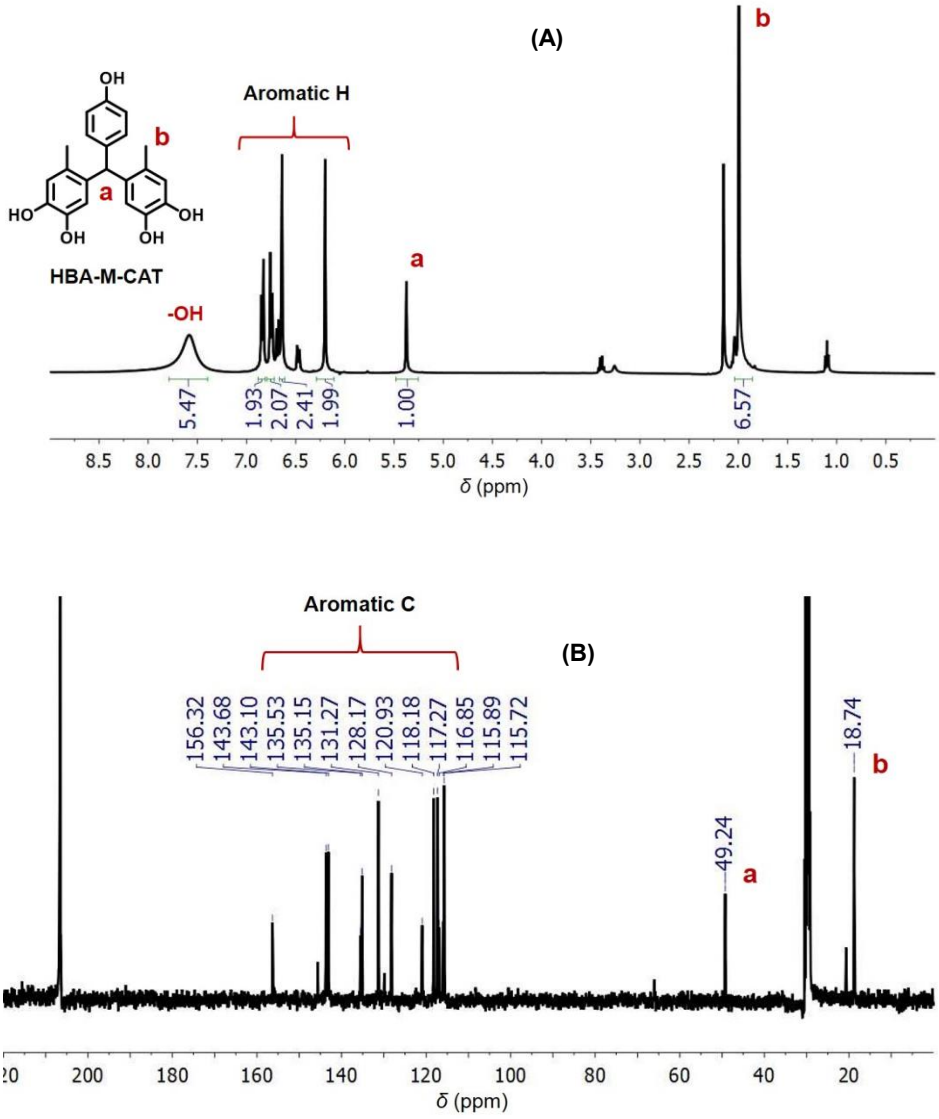

Figure S4.3. Proton (A) and carbon (B) NMR spectra of HBA−M−CAT. Solvent: acetone−d_6.

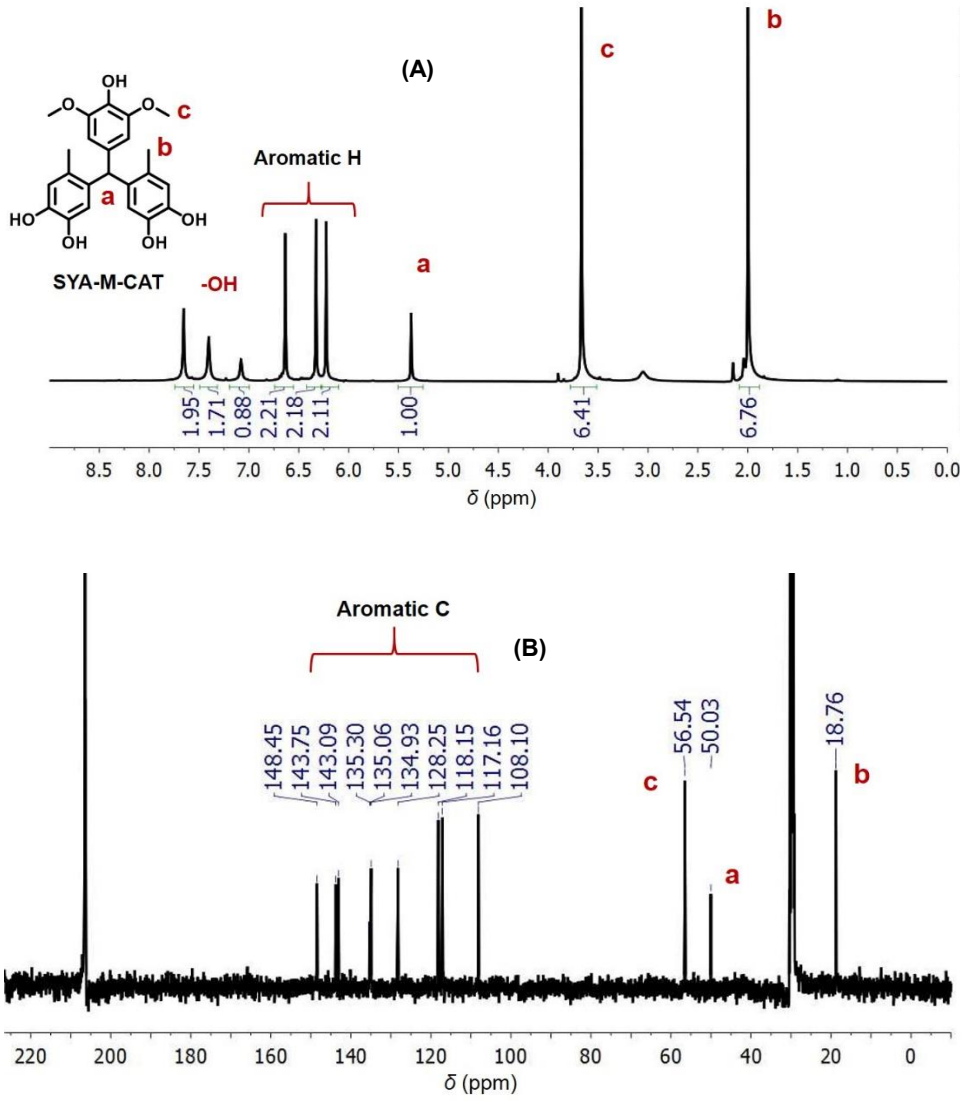

Figure S4.4. Proton (A) and carbon (B) NMR spectra of SYA−M−CAT. Solvent: acetone−d_6.

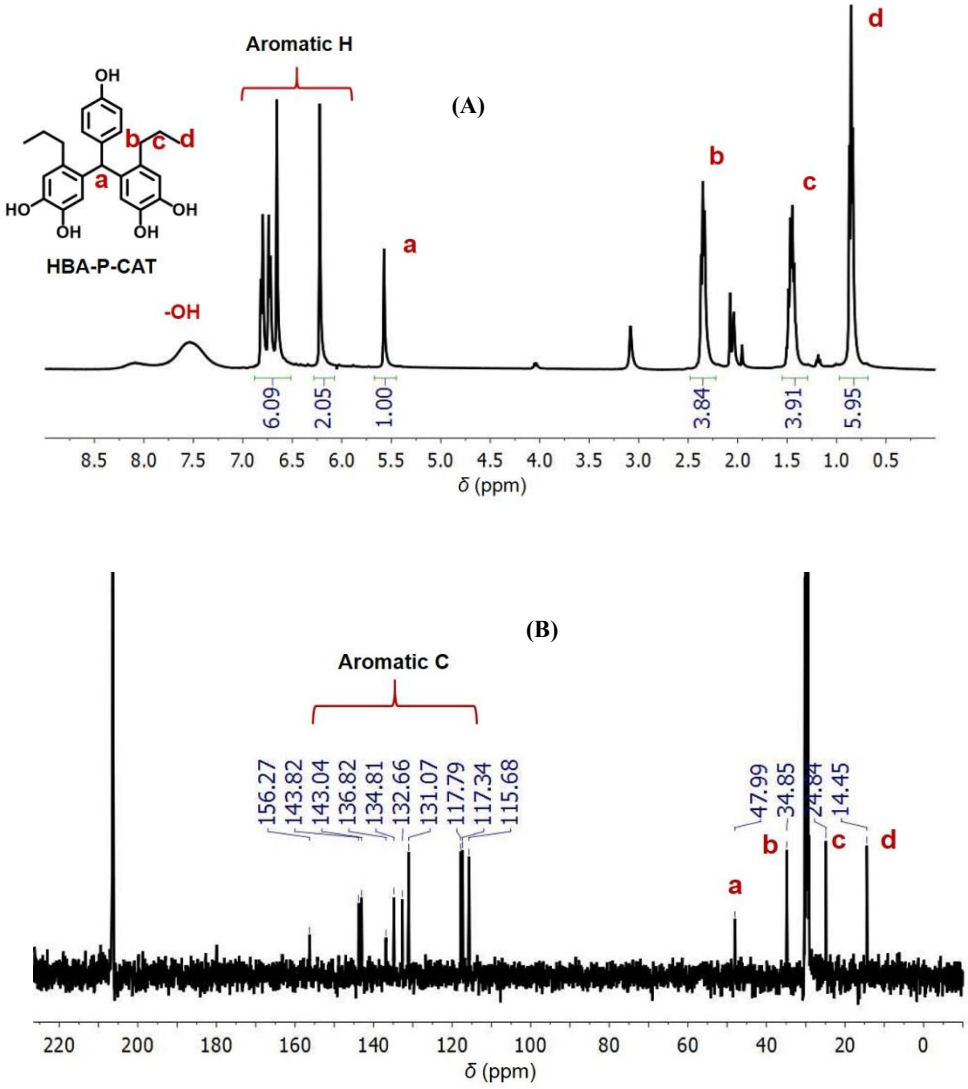

Figure S4.5. Proton (A) and carbon (B) NMR spectra of HBA−P−CAT. Solvent: acetone−d_6.

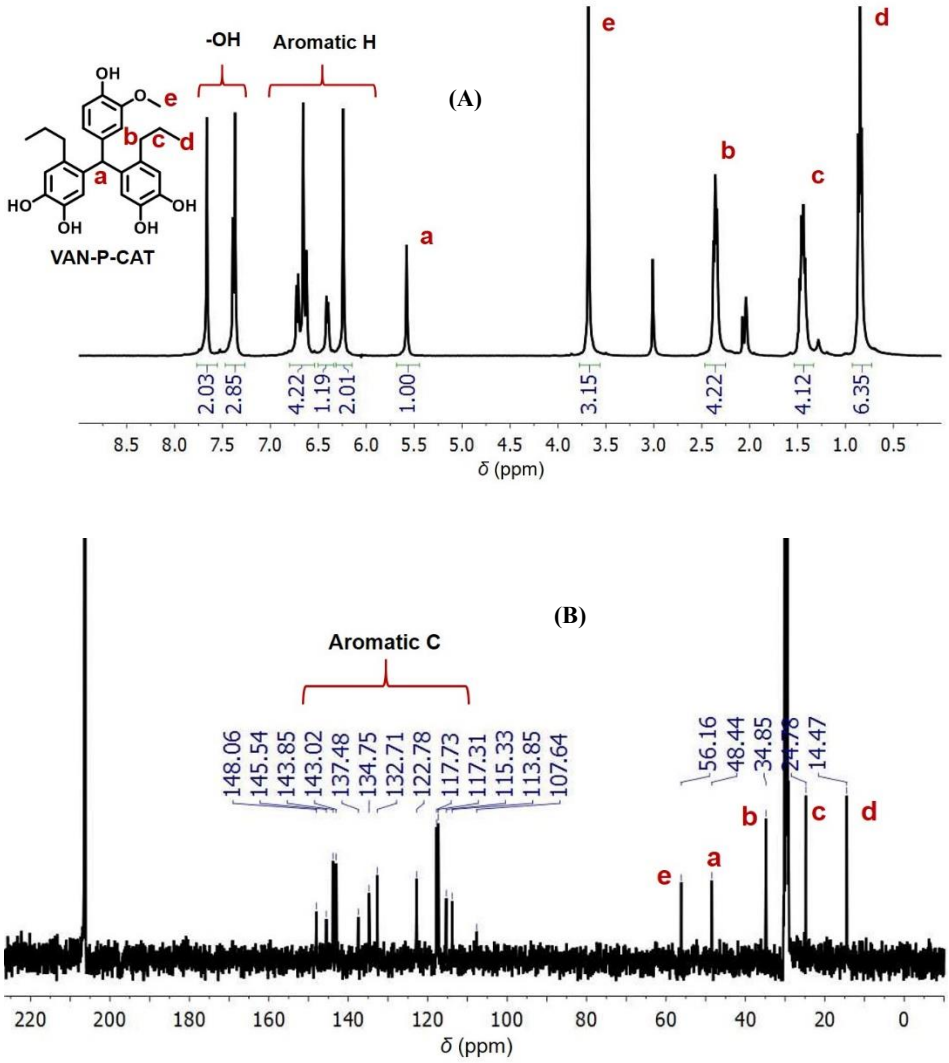

Figure S4.6. Proton (A) and carbon (B) NMR spectra of VAN−P−CAT. Solvent: acetone−d_6.

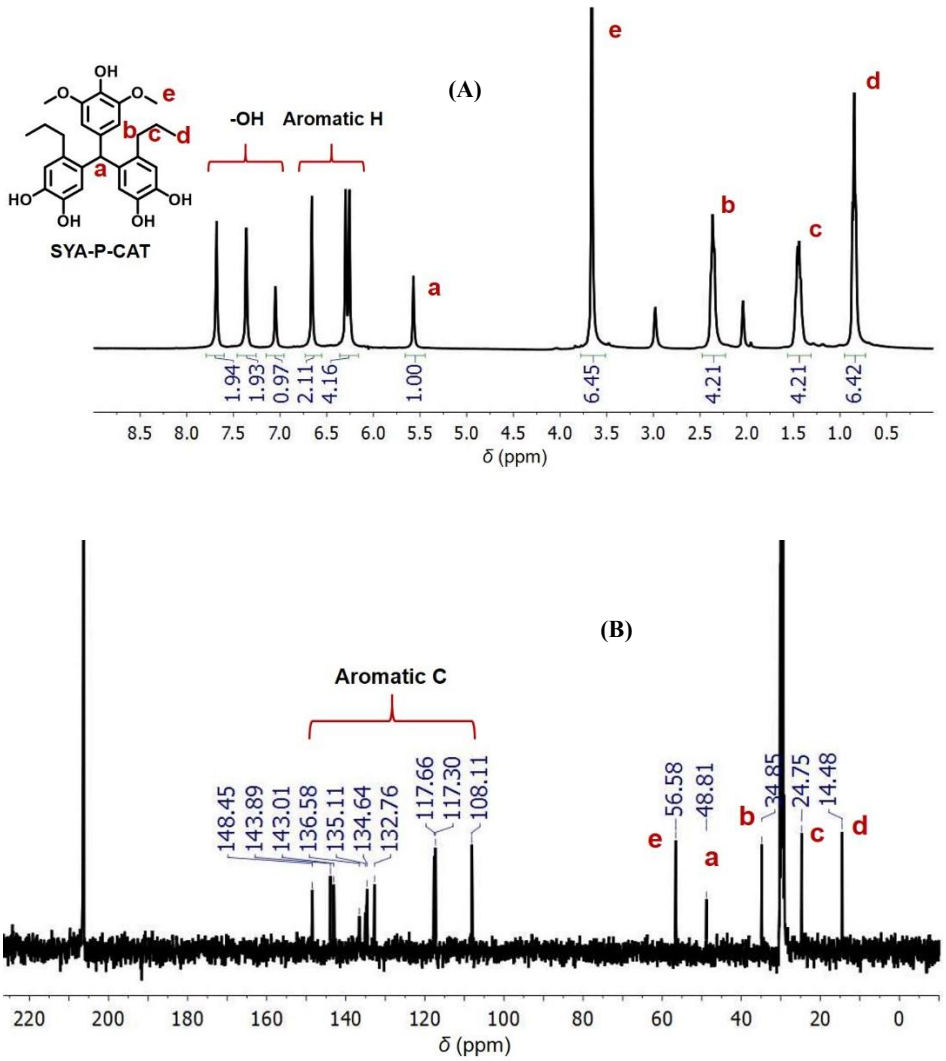

Figure S4.7. Proton (A) and carbon (B) NMR spectra of SYA−P−CAT. Solvent: acetone−d_6.

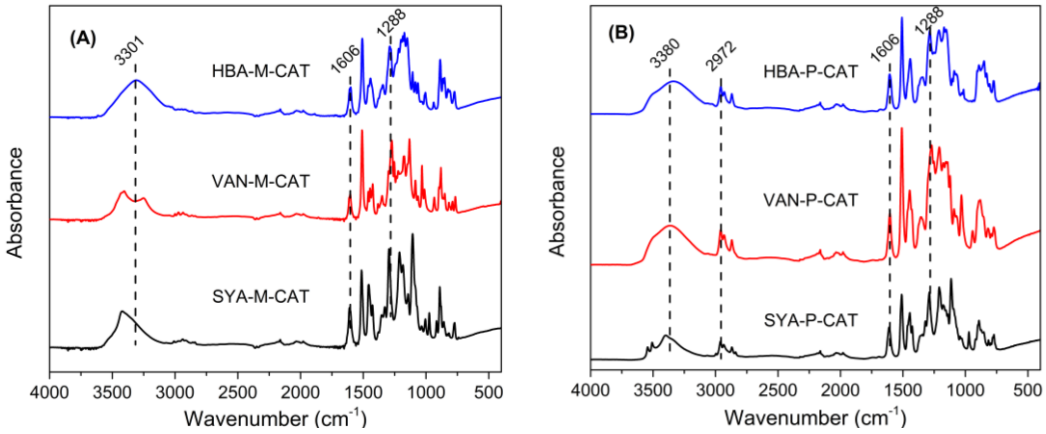

Figure S4.8. FTIR spectra of (A) M−CAT based and (B) P−CAT based TPs.

Vanillin has an aldehyde peak showing up at 1672 cm^{-1}.[1] After it is coupled with methylcatechol, the aldehyde group is converted to triphenyl methyl group. This is consistent with IR spectrum of VAN−M−CAT, in which the aldehyde peak disappears. Other characteristic absorption bands include 3052−3610 cm^{-1} (O−H stretching), 2972, 2927 and 2871 cm^{-1} (alkyl C−H stretch), 1606, 1508 and 1427 cm^{-1} (aromatic C−C bond), and 1288 and 1035 cm^{-1} (asymmetric and symmetric stretching of the C−O−C ether linkage). FTIR pattern of other TPs are similar with VAN−M−CAT.

Reference: Zhang L., Zhu Y., Li D., Wang M., Chen H., Wu J. *RSC Adv.*, 2015, *5*, 96879−96887.

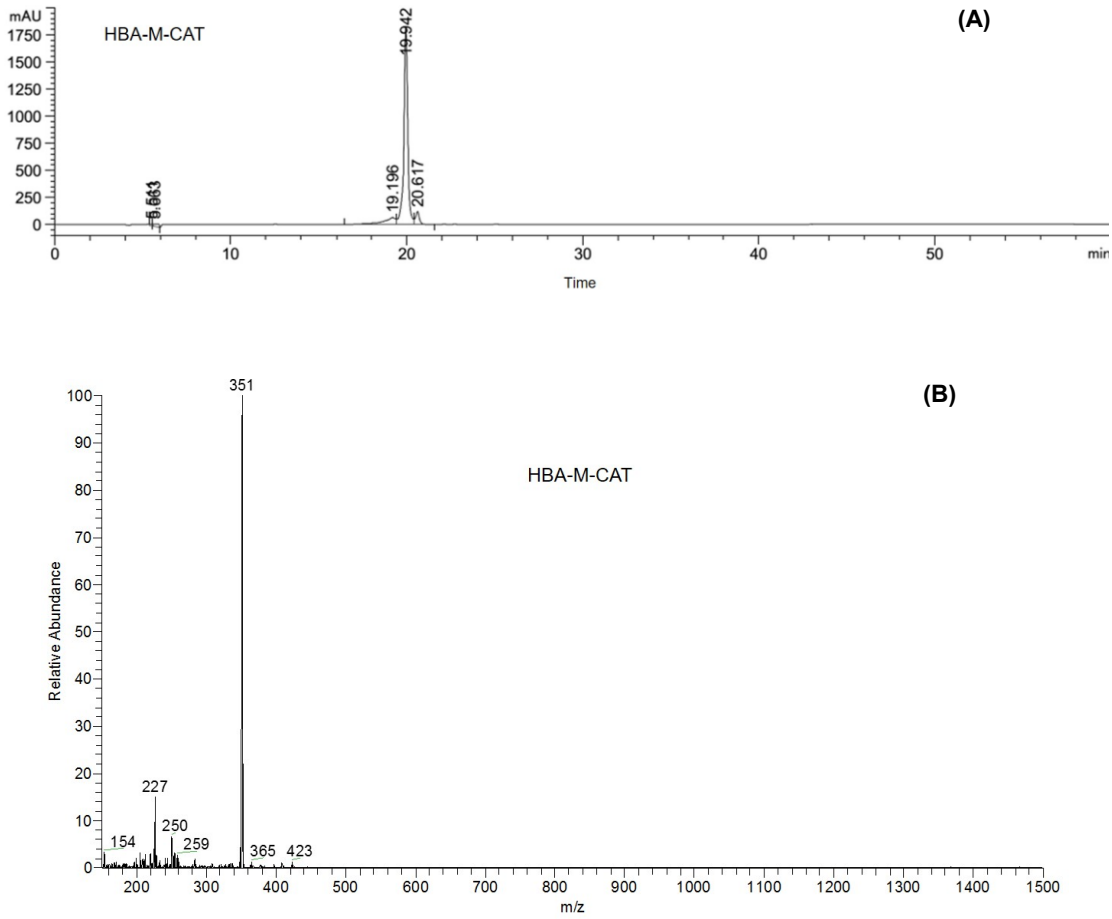

Figure S4.9. HPLC (A) and mass spectra (B) of HBA−M−CAT.

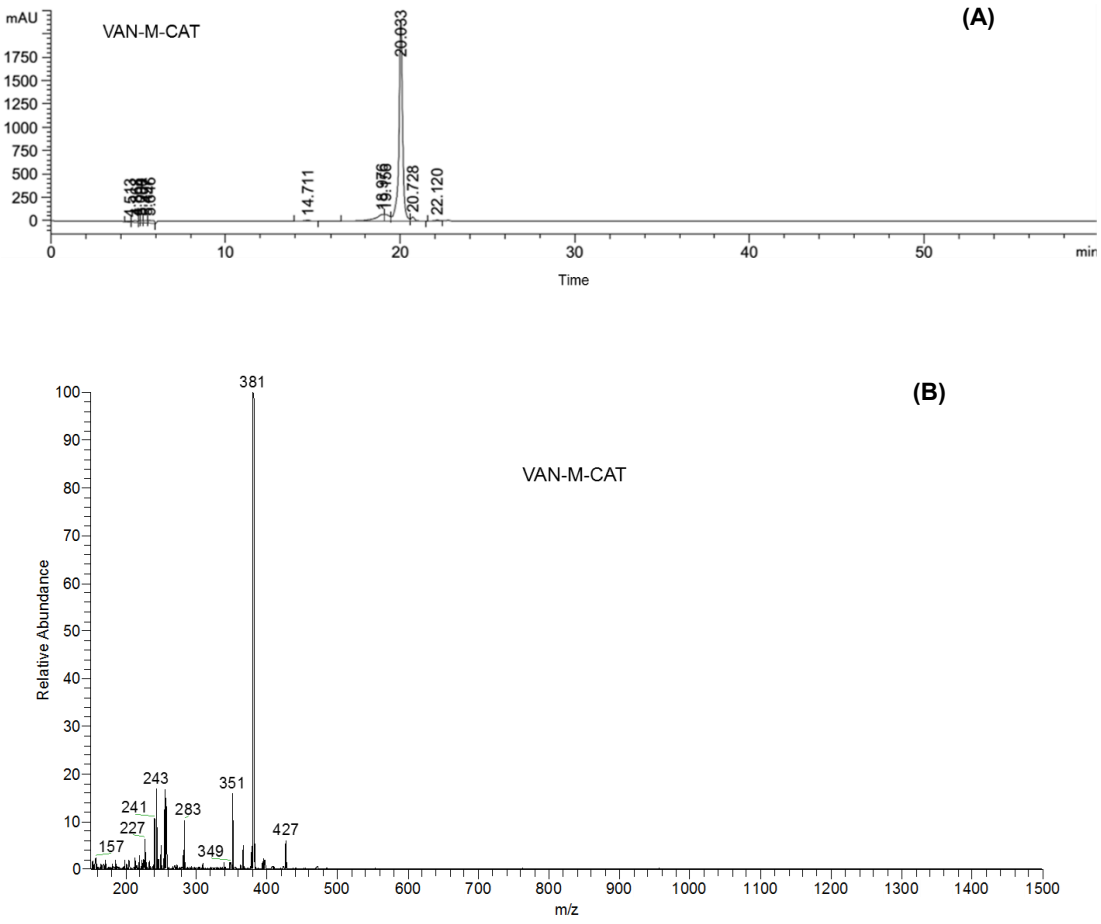

Figure S4.10. HPLC (A) and mass spectra (B) of VAN−M−CAT.

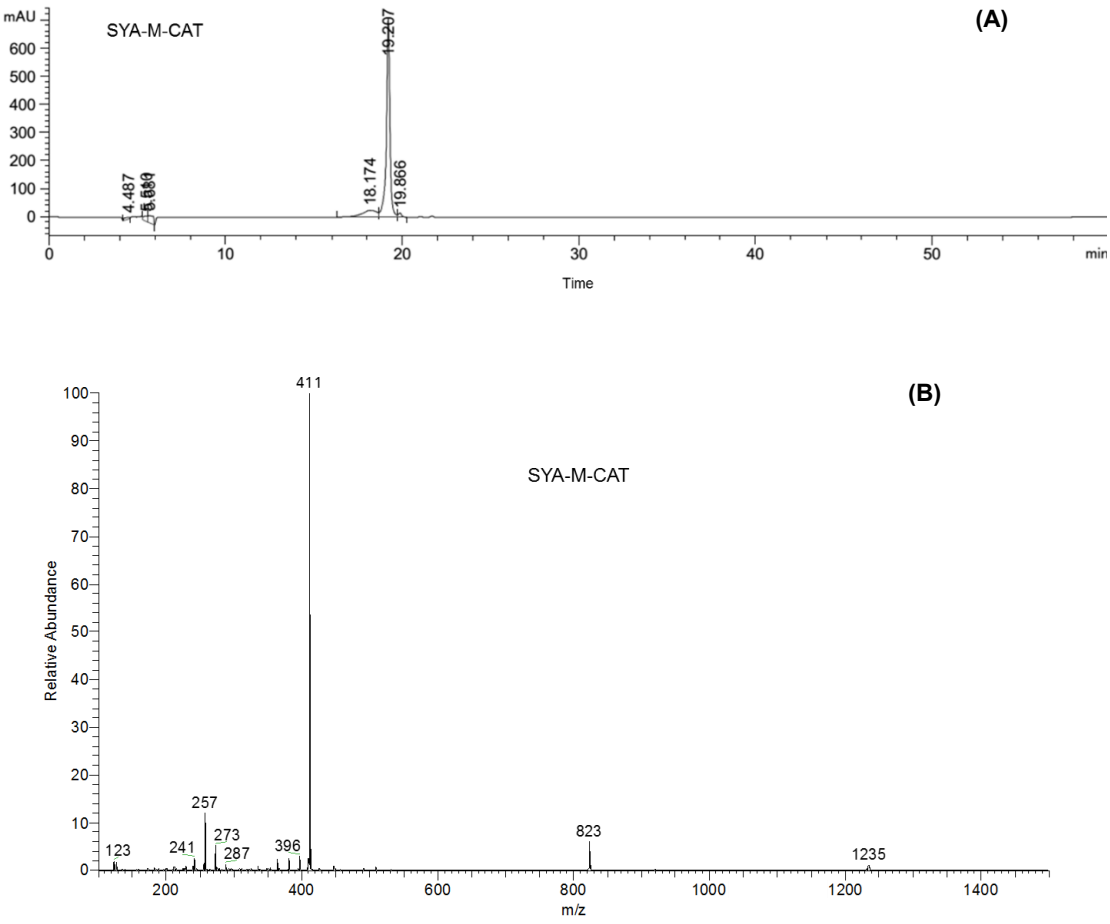

Figure S4.11. HPLC (A) and mass spectra (B) of SYA−M−CAT.

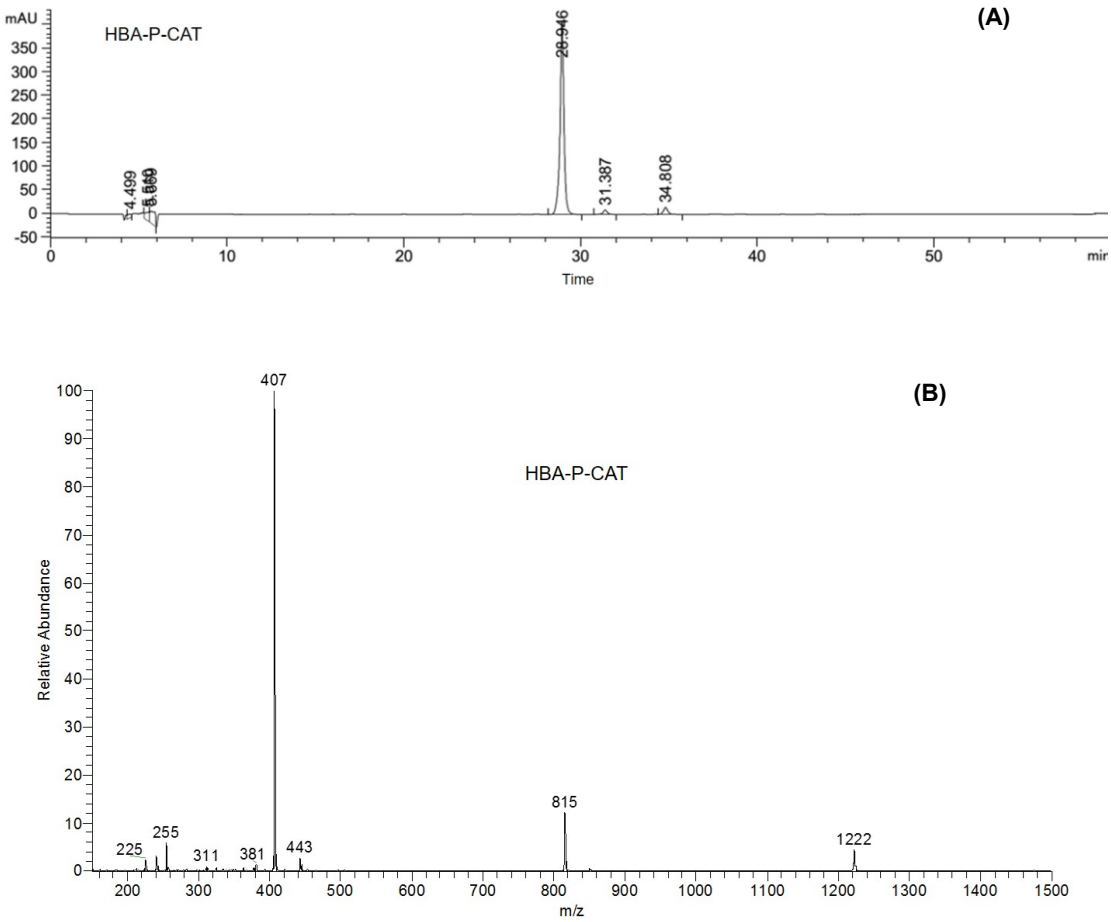

Figure S4.12. HPLC (A) and mass spectra (B) of HBA−P−CAT.

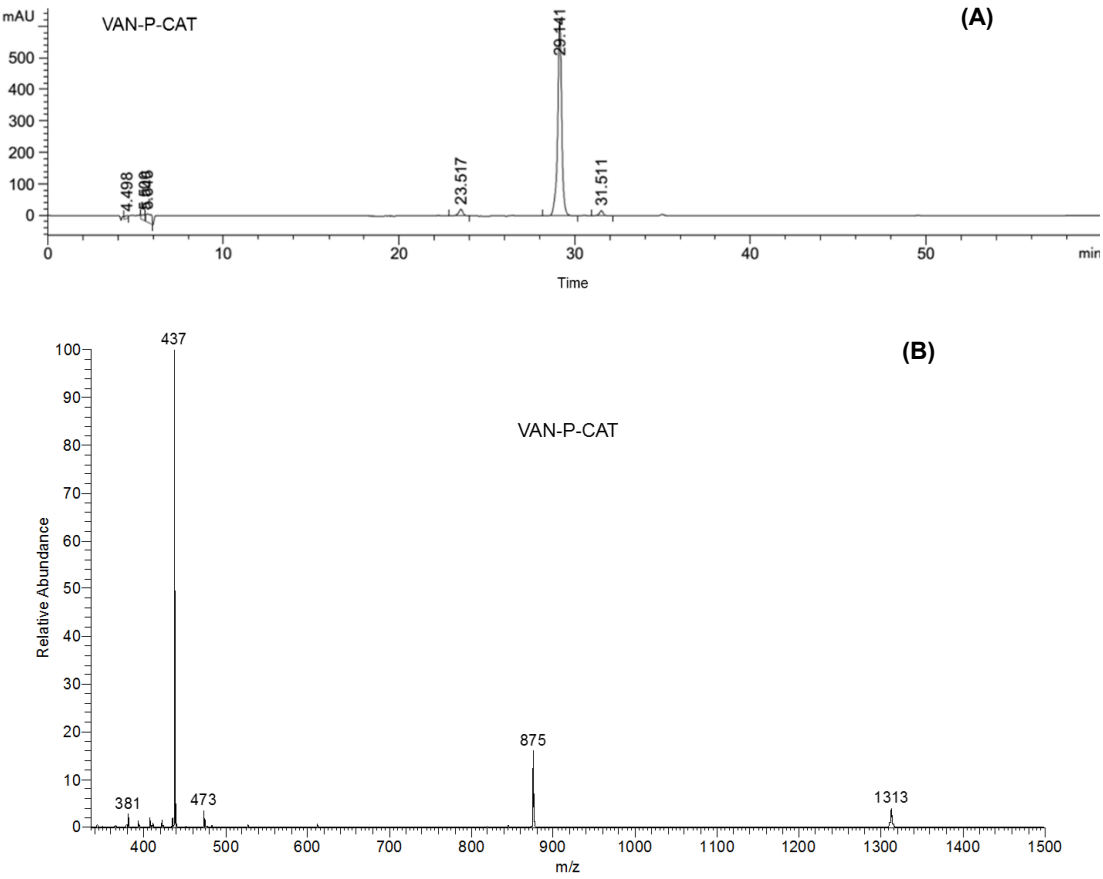

Figure S4.13. HPLC (A) and mass spectra (B) of VAN−P−CAT.

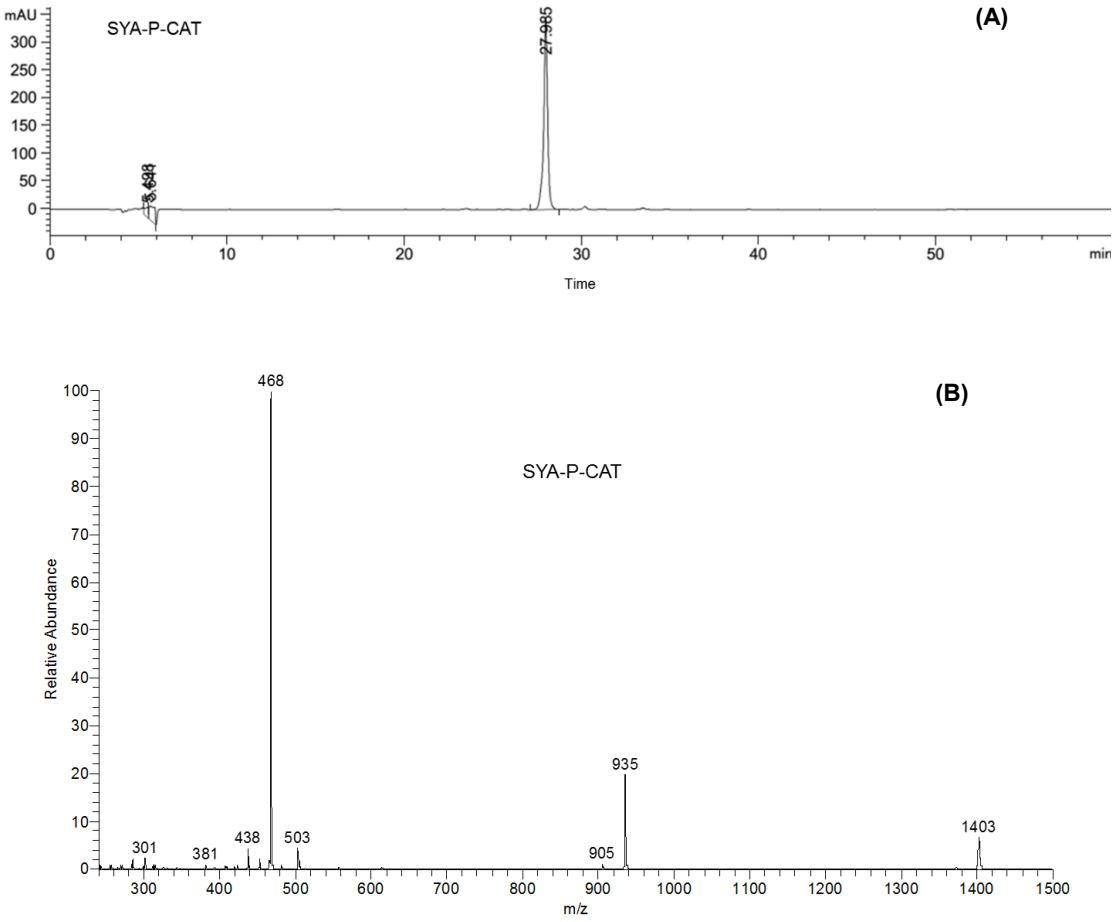

Figure S4.14. HPLC (A) and mass spectra (B) of SYA−P−CAT.

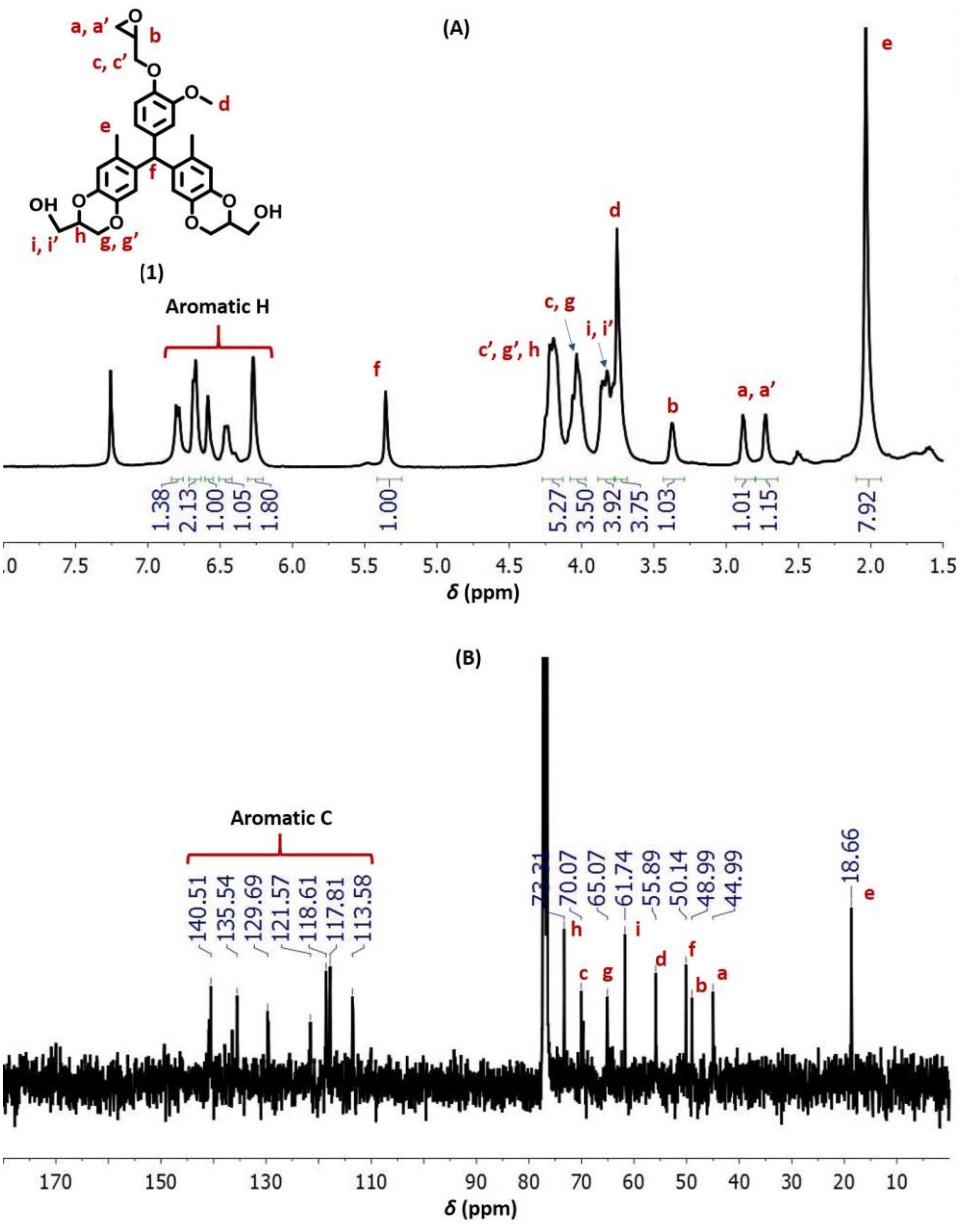

Figure S4.15. Proton (A) and carbon (B) NMR spectra of mono−epoxy substituted product GE−VAN−M−CAT−1. Solvent: $CDCl_3$.

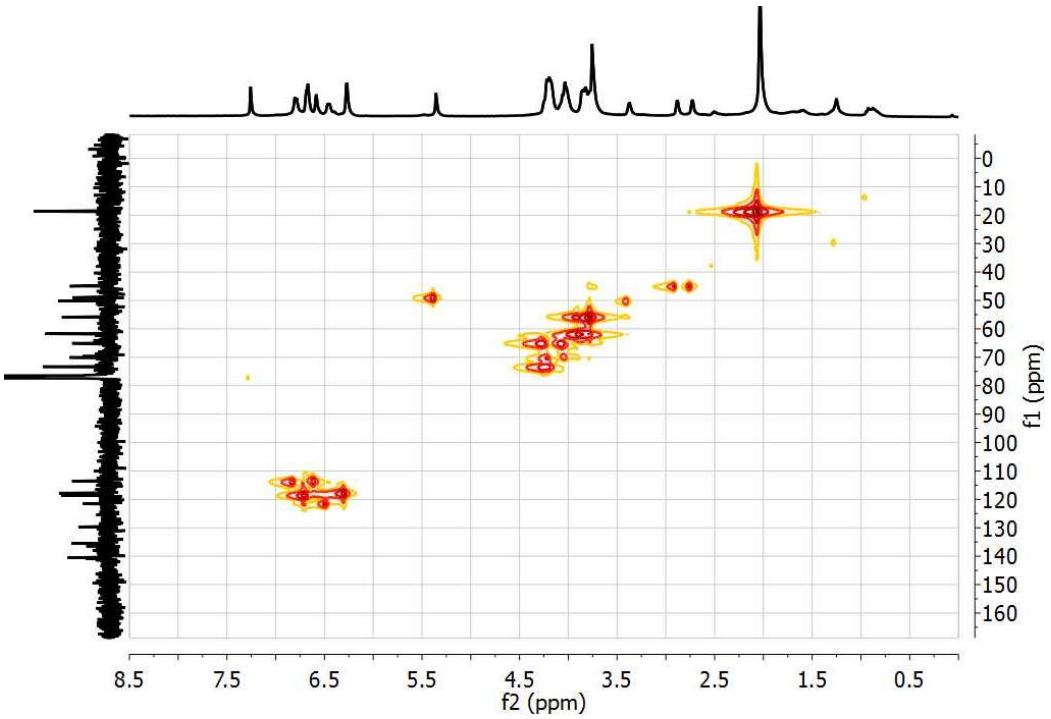

Figure S4.16. HMQC spectra of mono−epoxy substituted product GE−VAN−M−CAT−1.

Solvent: $CDCl_3$.

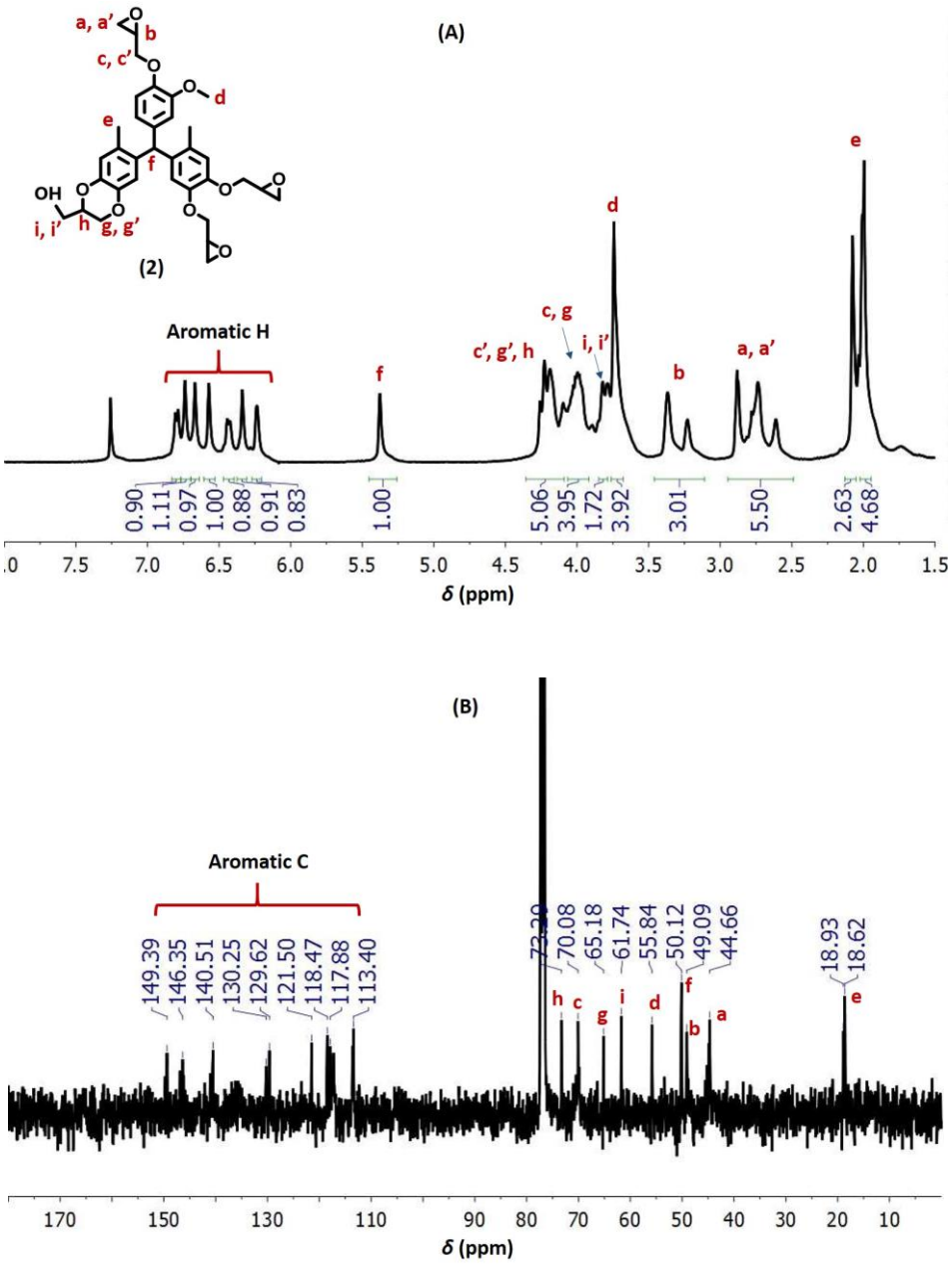

Figure S4.17. Proton (A) and carbon (B) NMR spectra of tri−epoxy substituted product GE−VAN−M−CAT−3. Solvent: $CDCl_3$.

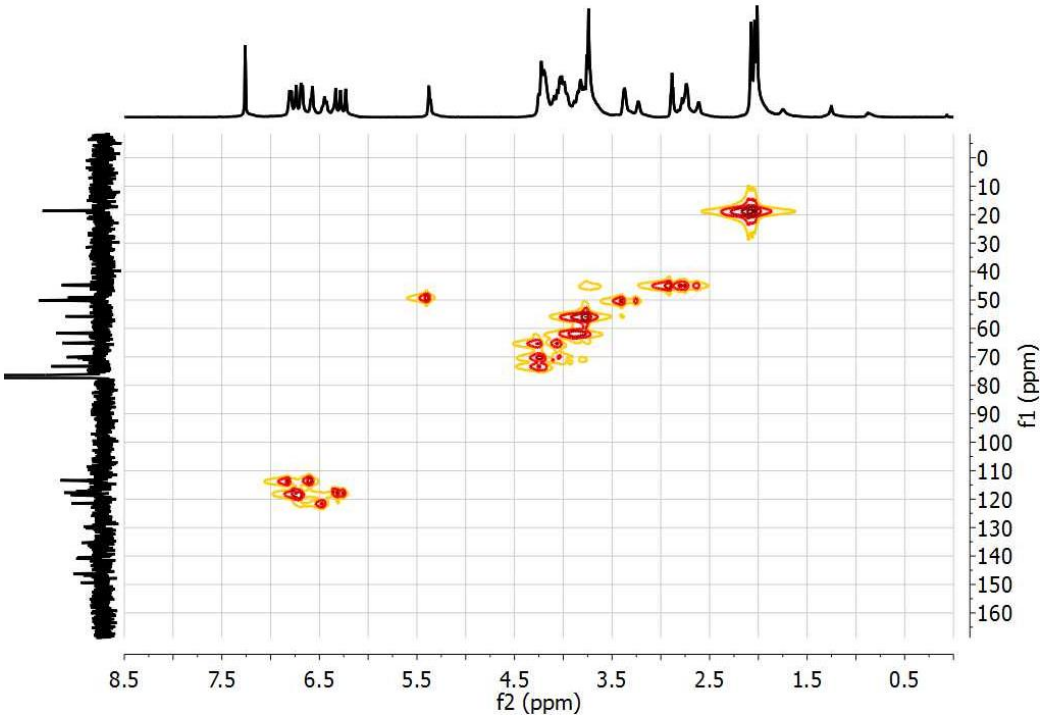

Figure S4.18. HMQC spectra of tri−epoxy substituted product GE−VAN−M−CAT−3.

Solvent: $CDCl_3$.

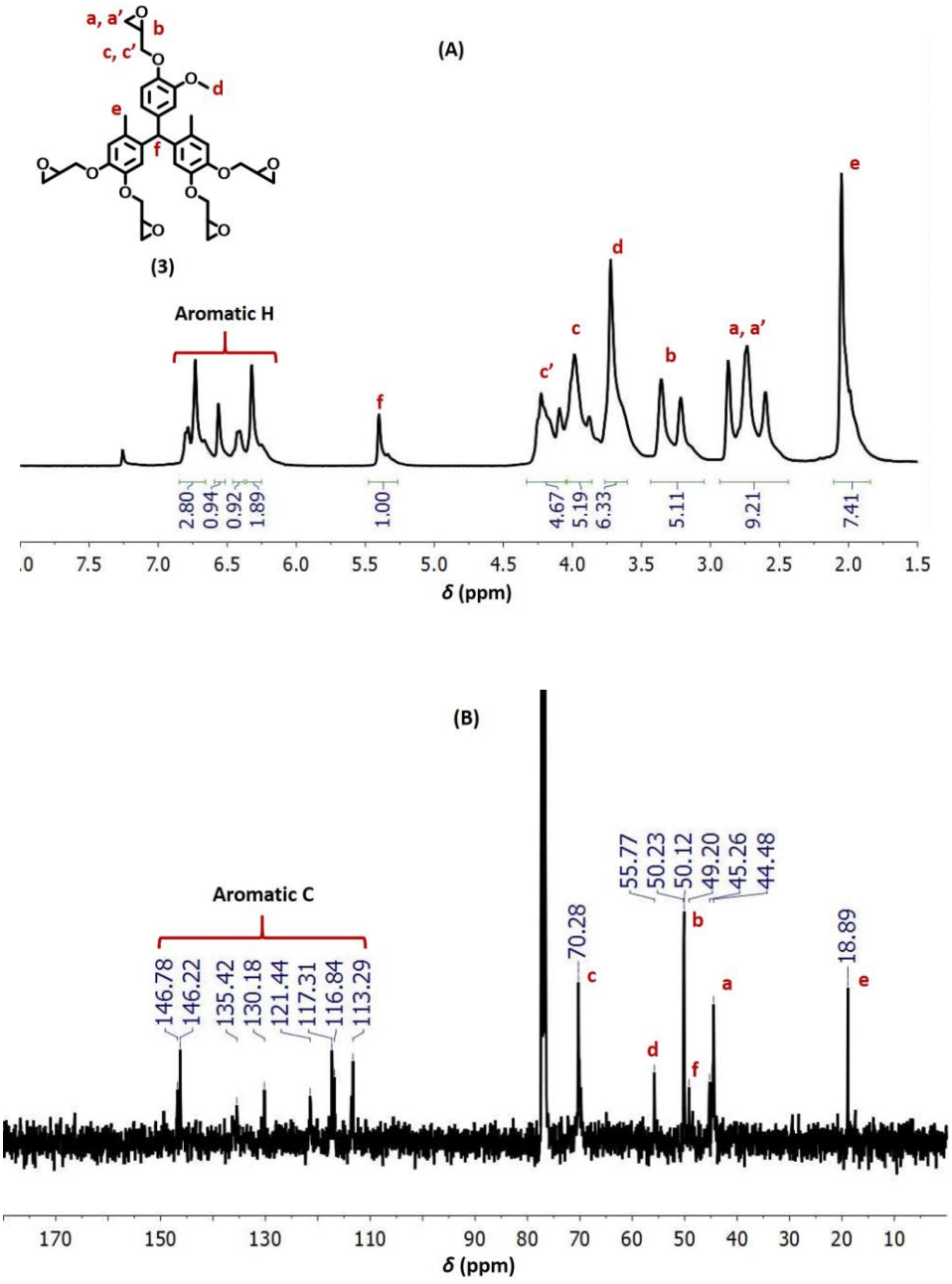

Figure S4.19. Proton (A) and carbon (B) NMR spectra of penta−epoxy substituted product GE−VAN−M−CAT−5. Solvent: $CDCl_3$.

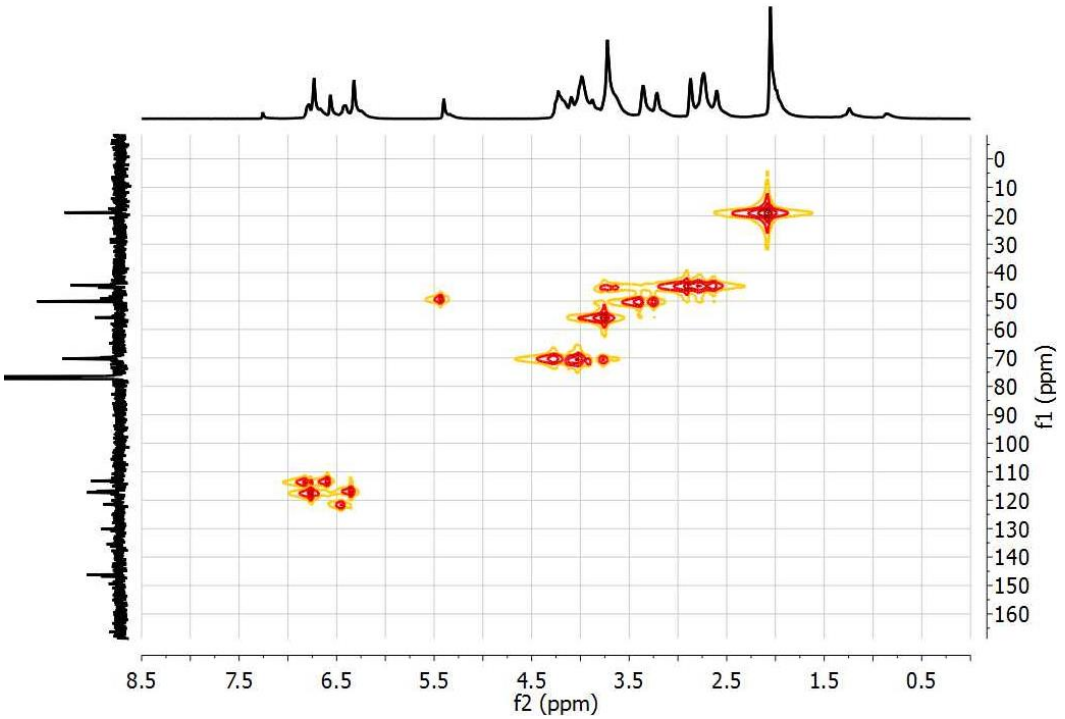

Figure S4.20. HMQC spectra of penta−epoxy substituted product GE−VAN−M−CAT−5.

Solvent: $CDCl_3$.

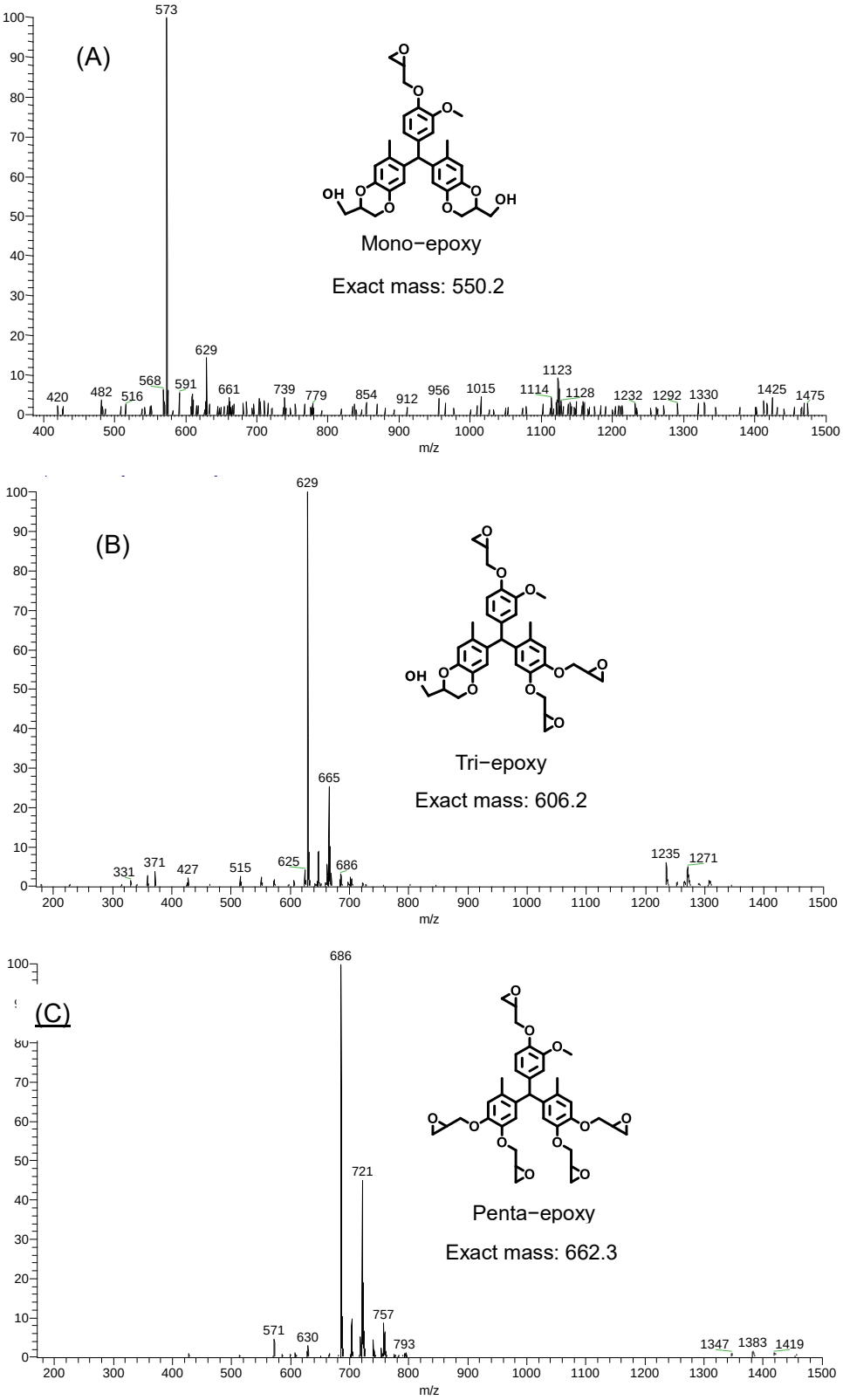

Figure S4.21. Mass spectra of VAN−M−CAT epoxidized products: (A) mono−epoxy substituted GE−VAN−M−CAT−1, (B) tri−epoxy substituted GE−VAN−M−CAT−3 and (C) penta−epoxy substituted GE−VAN−M−CAT−5.

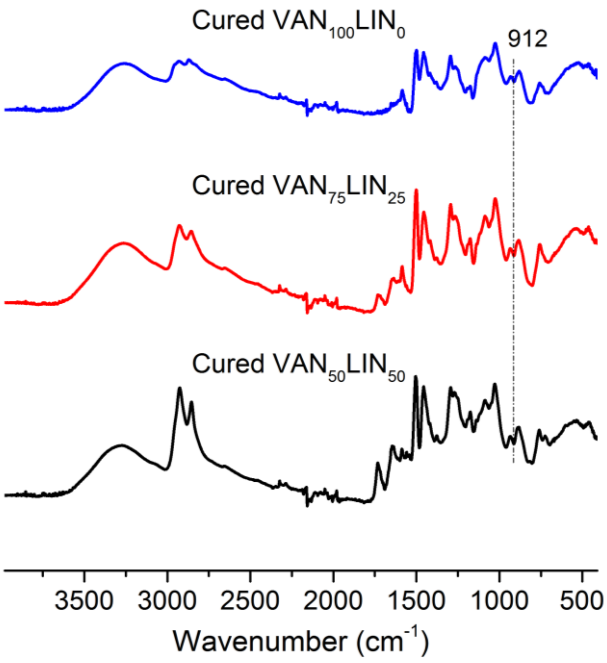

Figure S4.22. FTIR spectra of $VAN_{50}LIN_{50}$, $VAN_{75}LIN_{25}$ and $VAN_{100}LIN_{0}$. Epoxy peak at 912 cm^{-1} disappears after curing, which indicates significant amount of epoxy groups are reacted during the crosslinking process.

Appendix 4 for Chapter 5

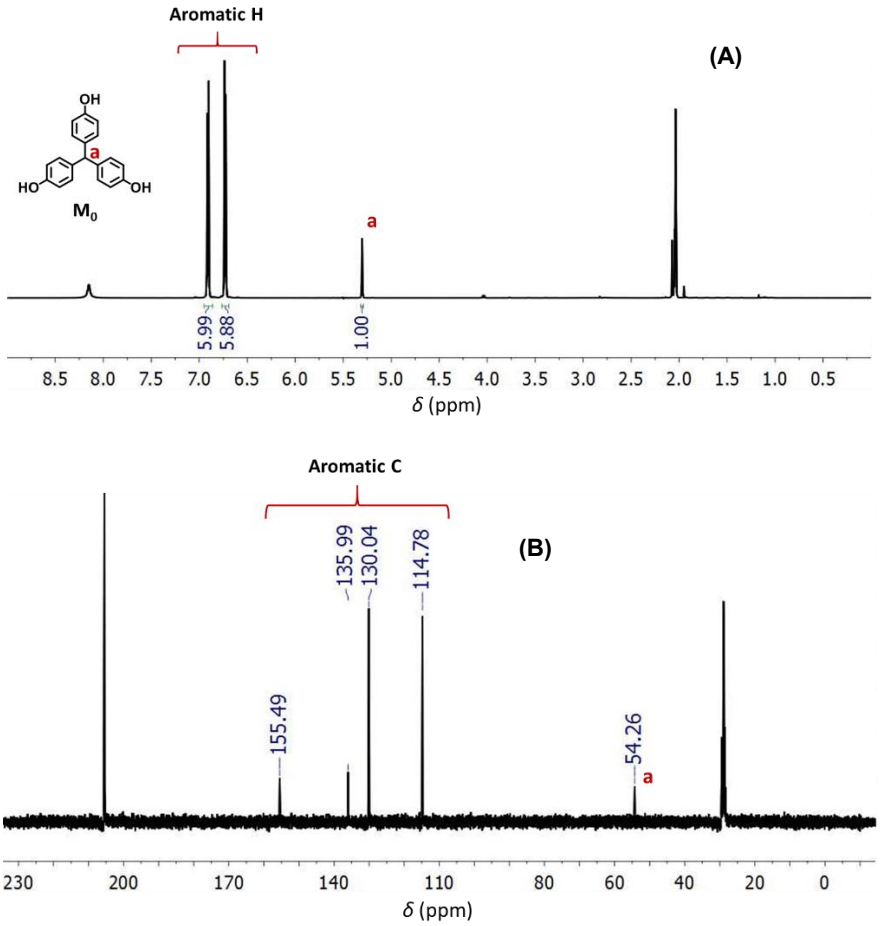

Figure S5.1. Proton (A) and carbon (B) NMR spectra of M_0. Solvent: acetone−d_6.

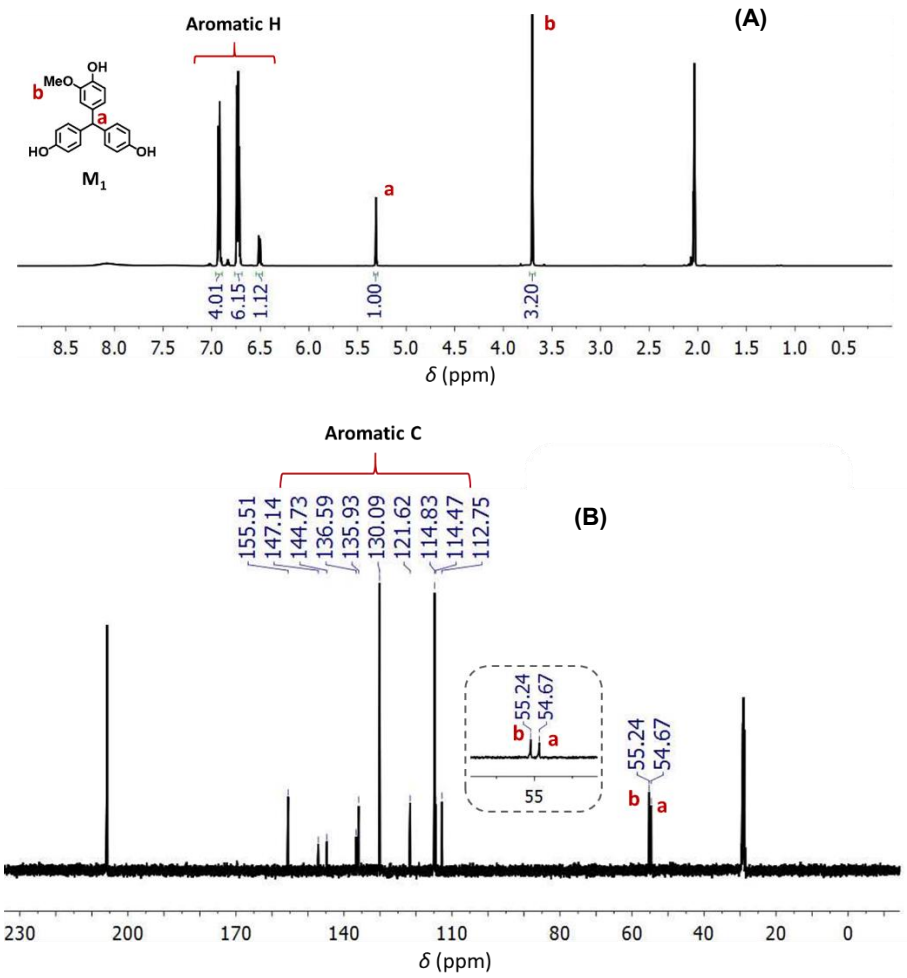

Figure S5.2. Proton (A) and carbon (B) NMR spectra of M_1. Solvent: acetone−d_6.

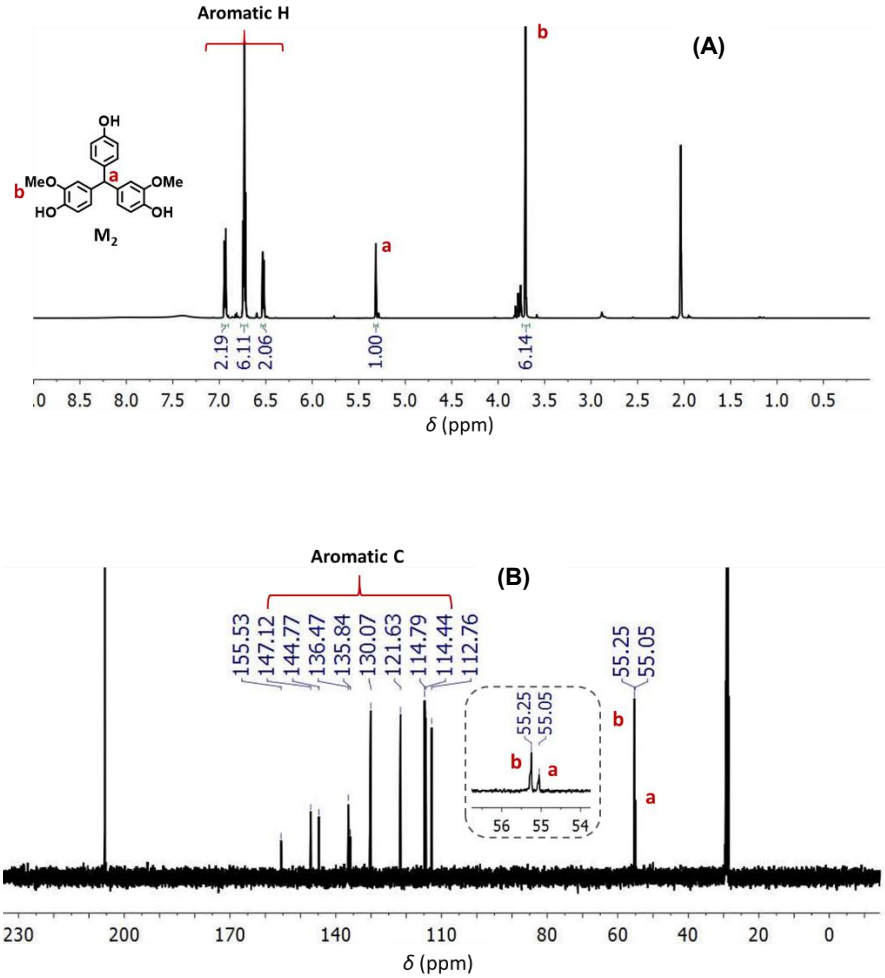

Figure S5.3. Proton (A) and carbon (B) NMR spectra of M_2. Solvent: acetone−d_6.

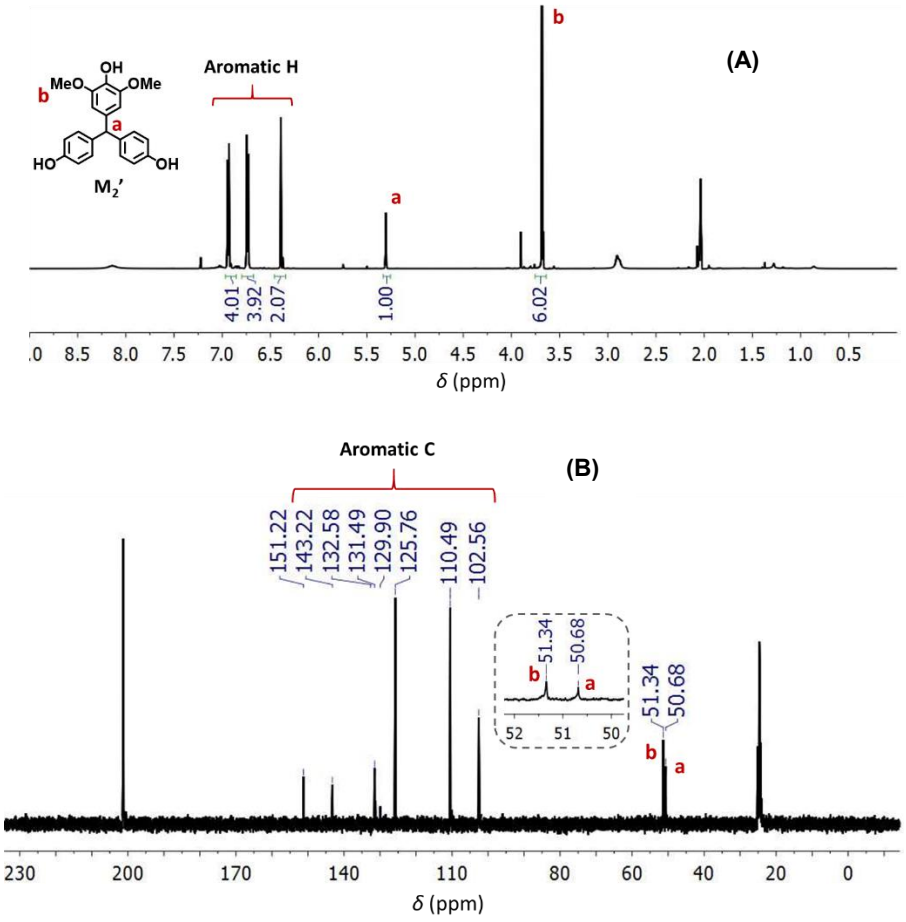

Figure S5.4. Proton (A) and carbon (B) NMR spectra of M_2'. Solvent: acetone−d_6.

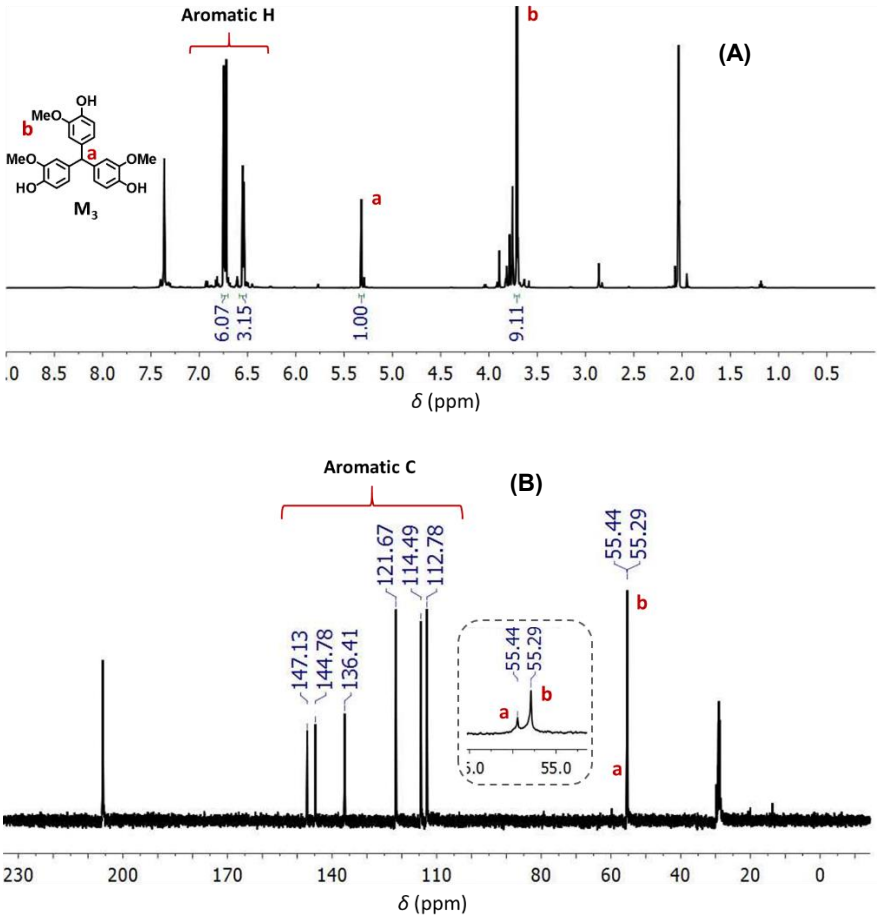

Figure S5.5. Proton (A) and carbon (B) NMR spectra of M_3. Solvent: acetone−d_6.

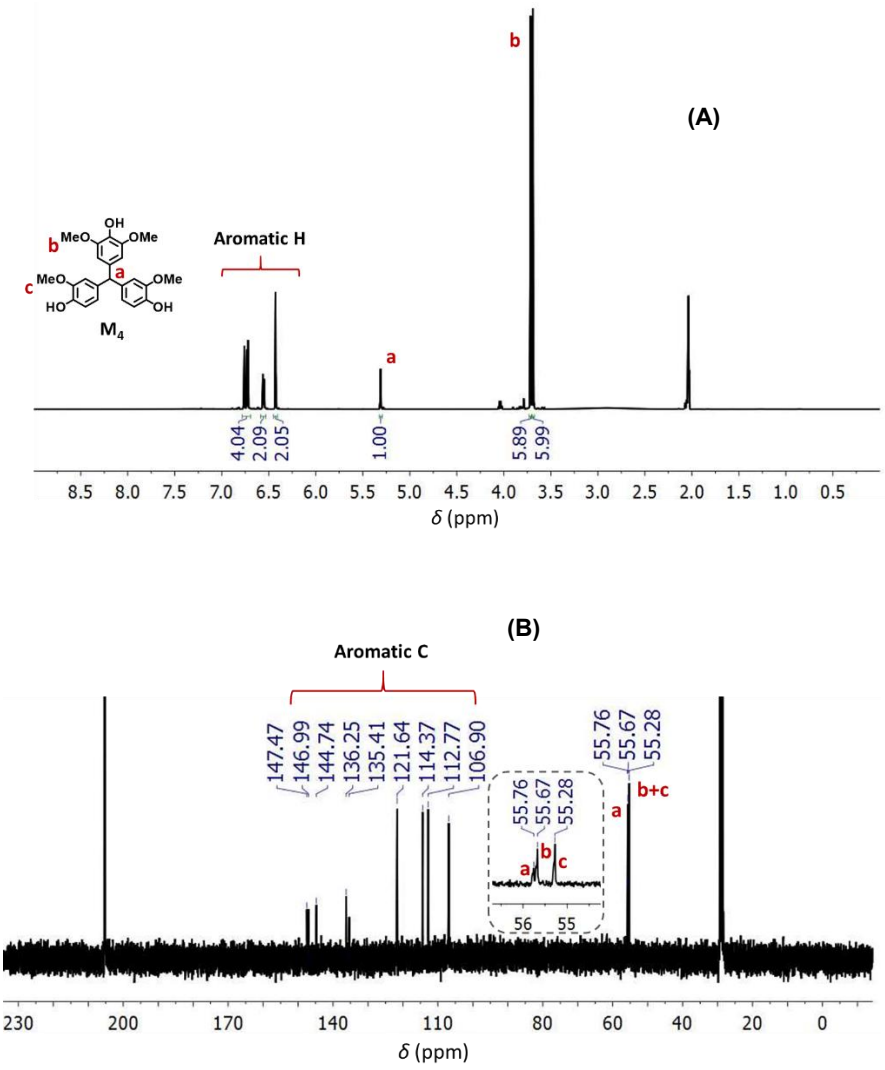

Figure S5.6. Proton (A) and carbon (B) NMR spectra of M_4. Solvent: acetone−d_6.

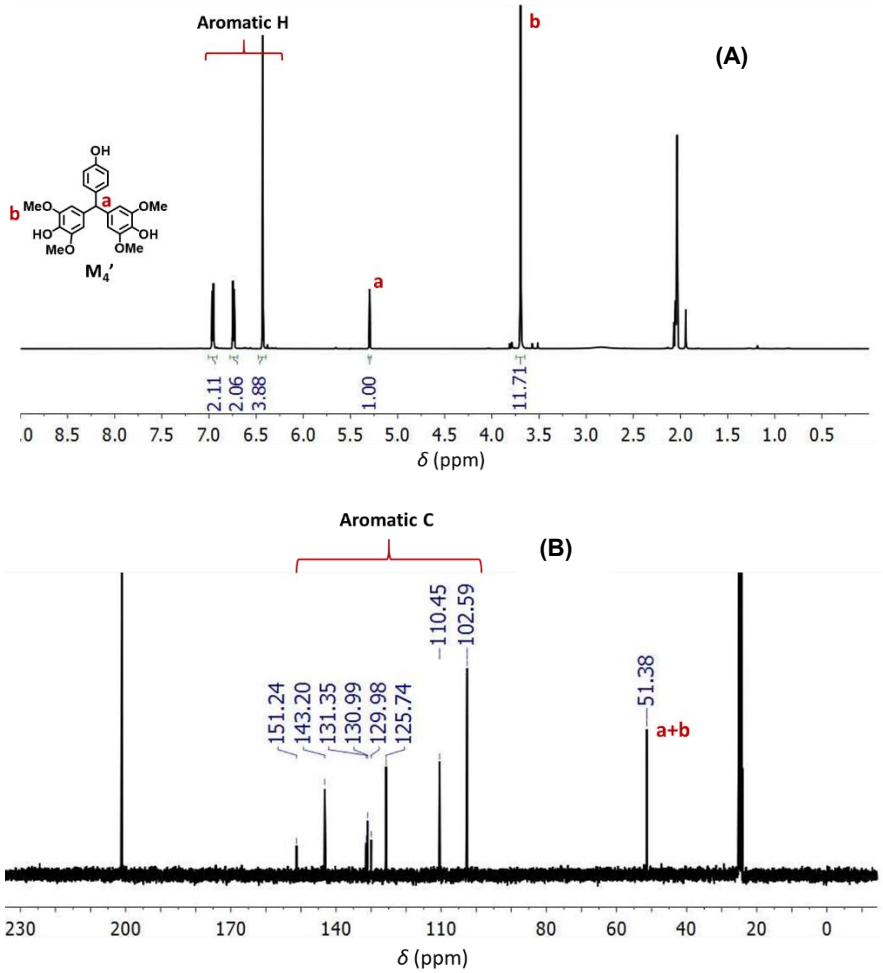

Figure S5.7. Proton (A) and carbon (B) NMR spectra of M_4'. Solvent: acetone−d_6.

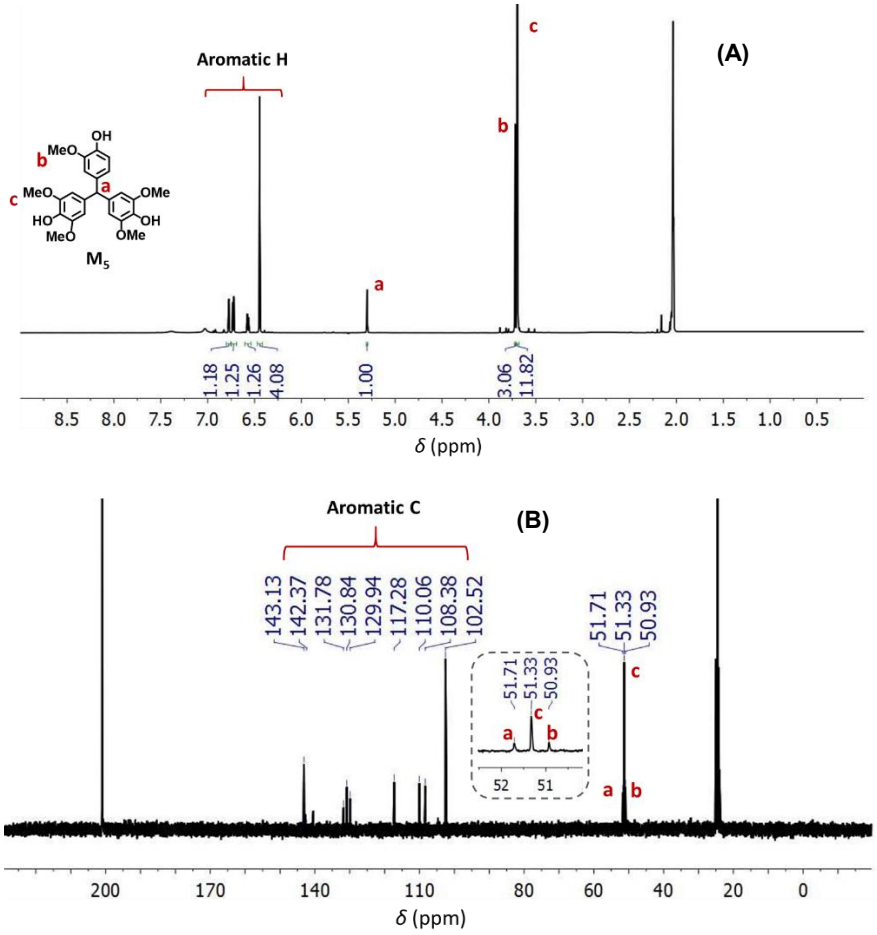

Figure S5.8. Proton (A) and carbon (B) NMR spectra of M_5. Solvent: acetone−d_6.

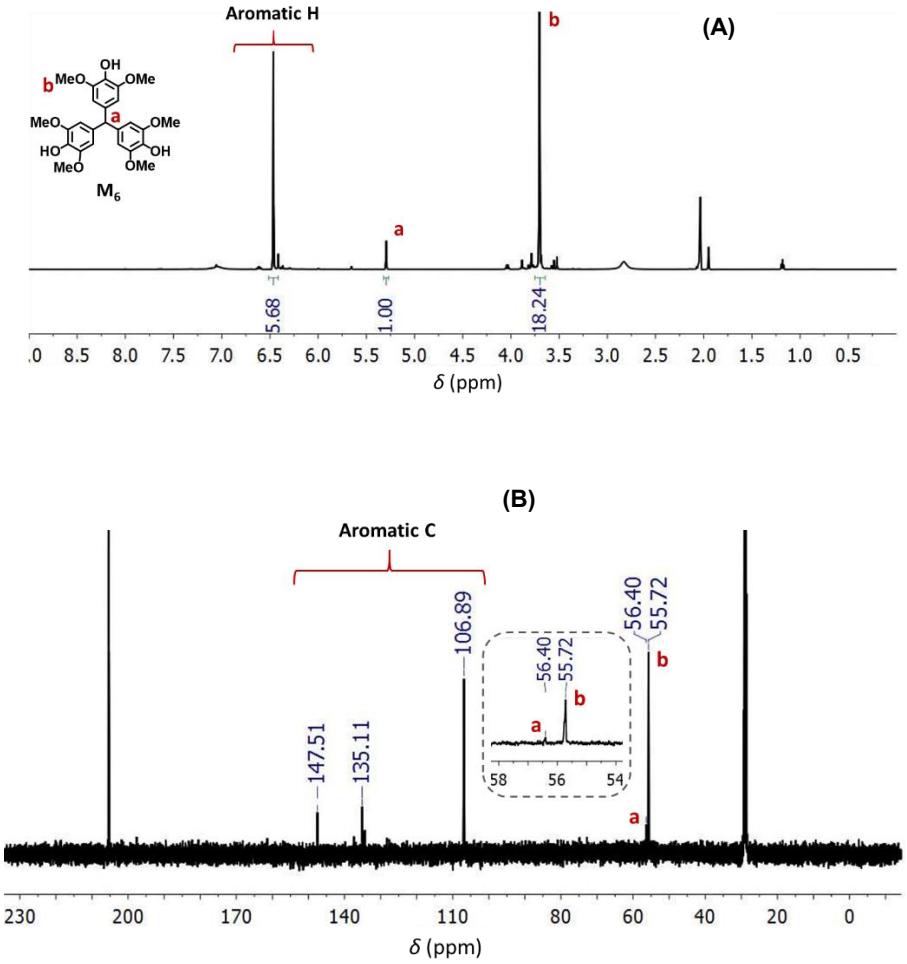

Figure S5.9. Proton (A) and carbon (B) NMR spectra of M_6. Solvent: acetone−d_6.

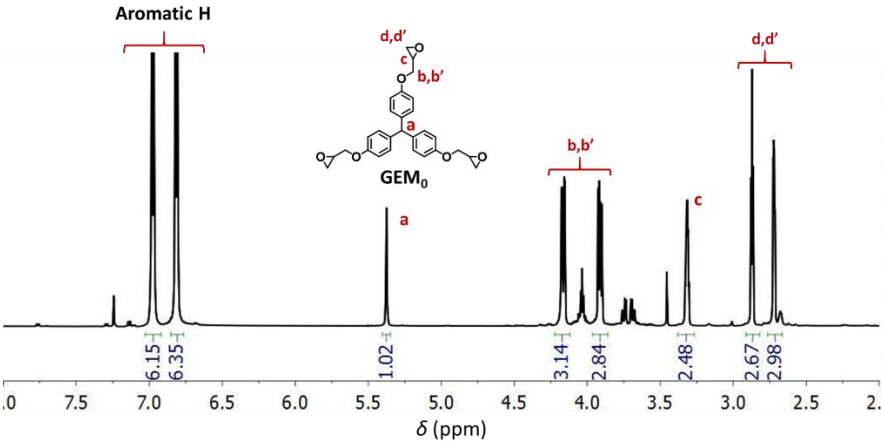

Figure S5.10. Proton NMR spectra of GEM_0. Solvent: $CDCl_3$.

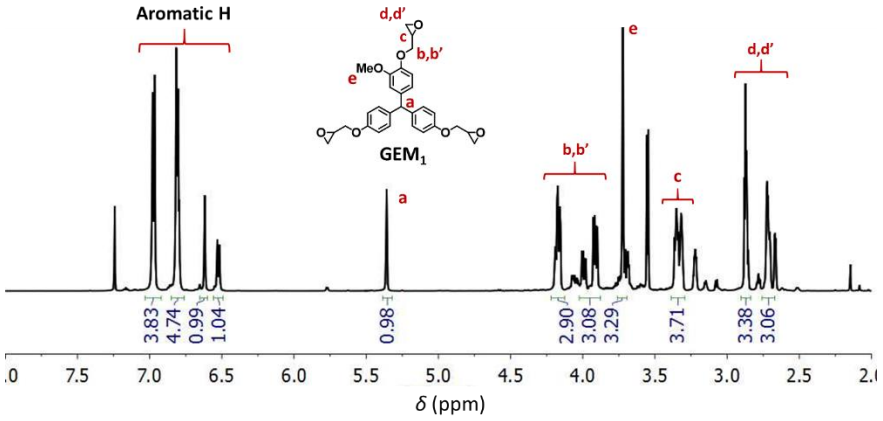

Figure S5.11. Proton NMR spectra of GEM_1. Solvent: $CDCl_3$.

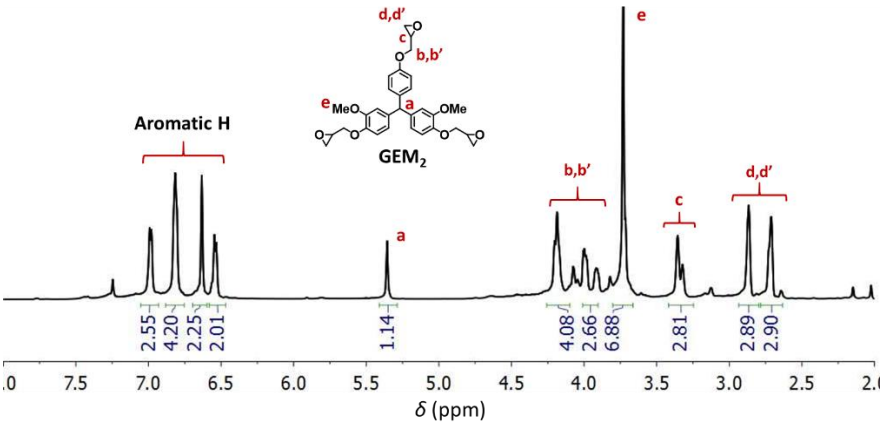

Figure S5.12. Proton NMR spectra of GEM_2. Solvent: $CDCl_3$.

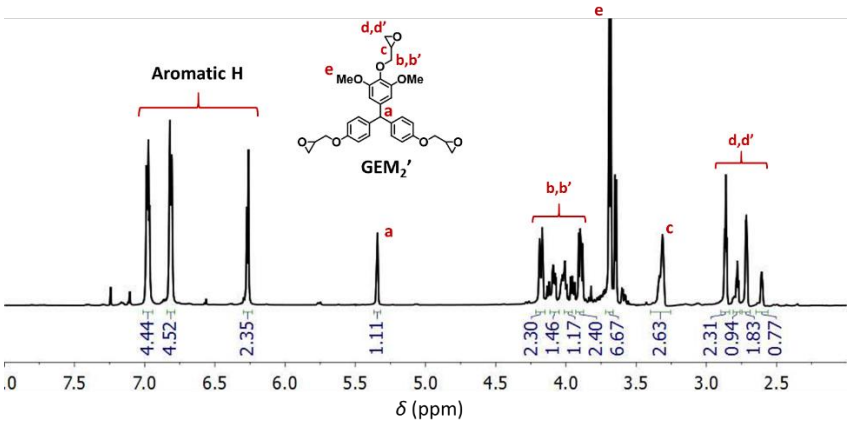

Figure S5.13. Proton NMR spectra of GEM_2'. Solvent: $CDCl_3$.

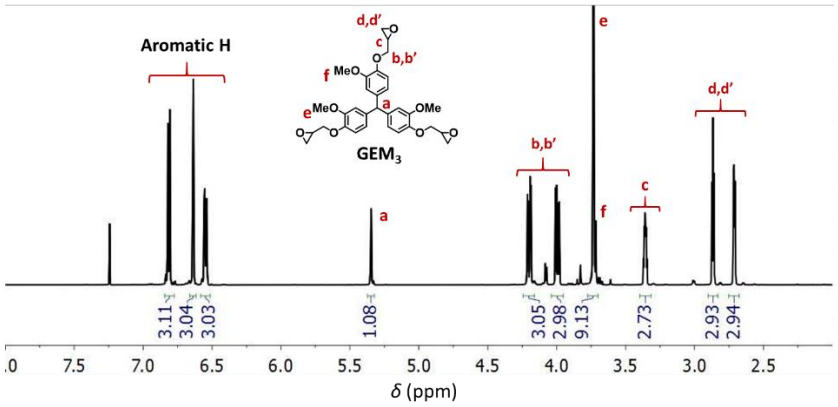

Figure S5.14. Proton NMR spectra of GEM_3. Solvent: $CDCl_3$.

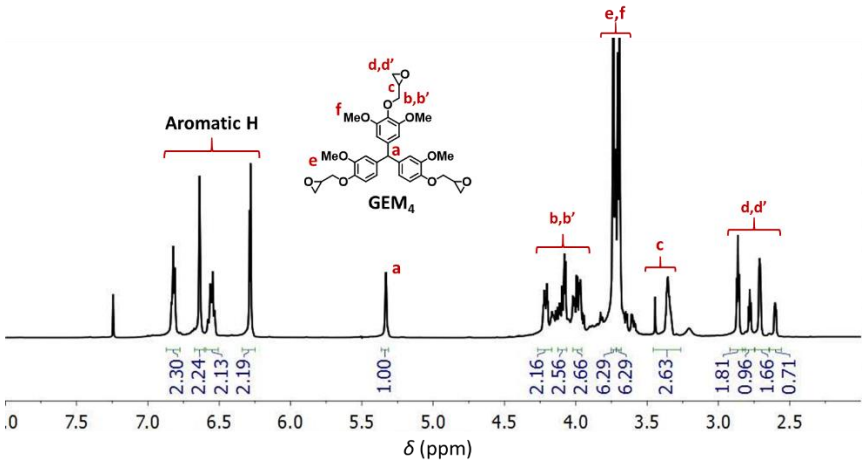

Figure S5.15. Proton NMR spectra of GEM_4. Solvent: $CDCl_3$.

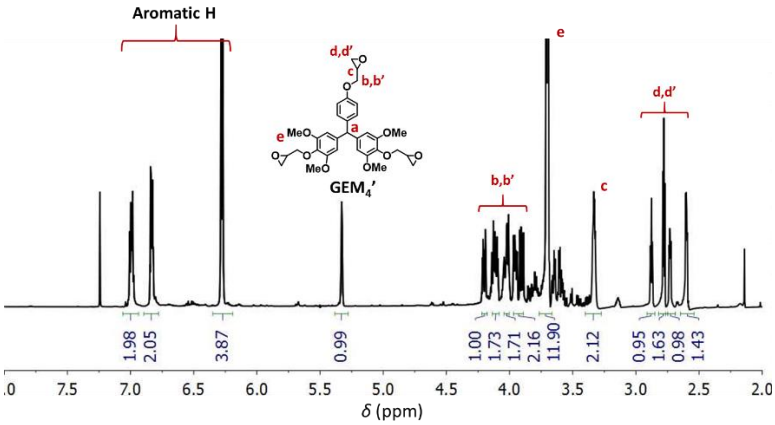

Figure S5.16. Proton NMR spectra of GEM_4'. Solvent: $CDCl_3$.

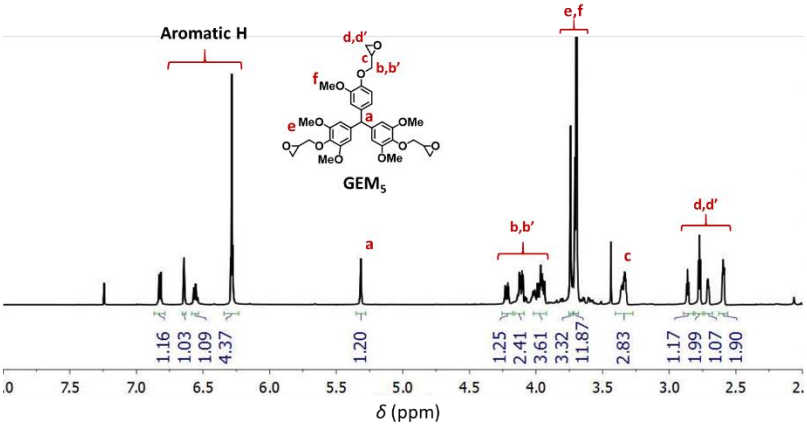

Figure S5.17. Proton NMR spectra of GEM_5. Solvent: $CDCl_3$.

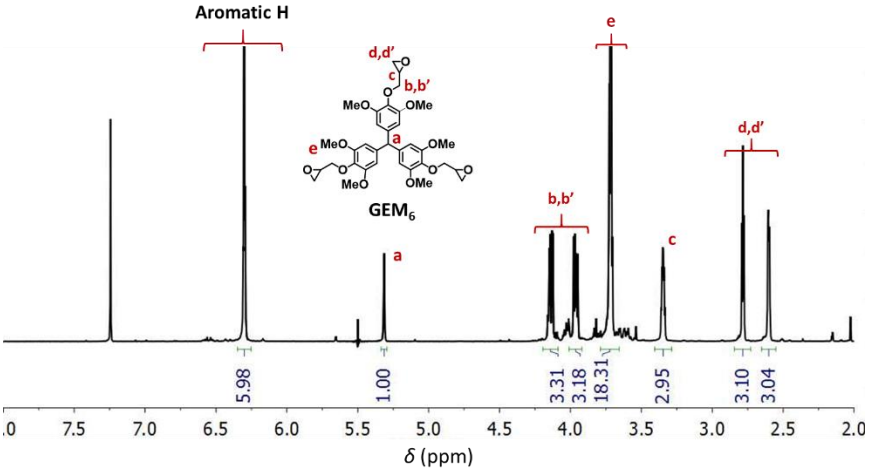

Figure S5.18. Proton NMR spectra of GEM_6. Solvent: $CDCl_3$.

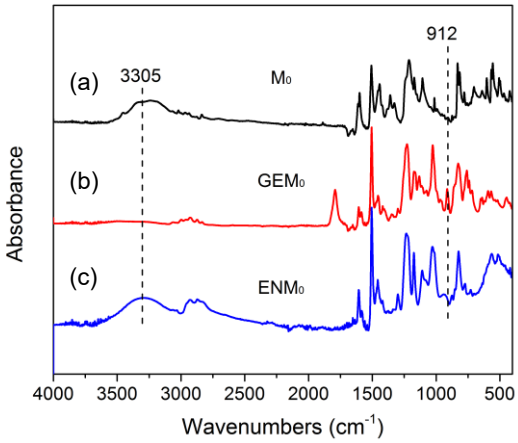

Figure S5.19. FTIR spectra of M_0, GEM_0 and ENM_0.

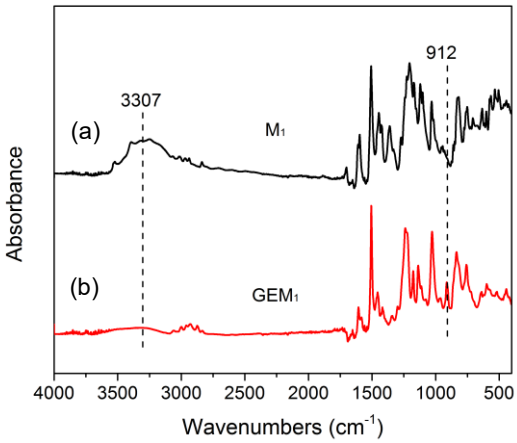

Figure S5.20. FTIR spectra of M_1 and GEM_1.

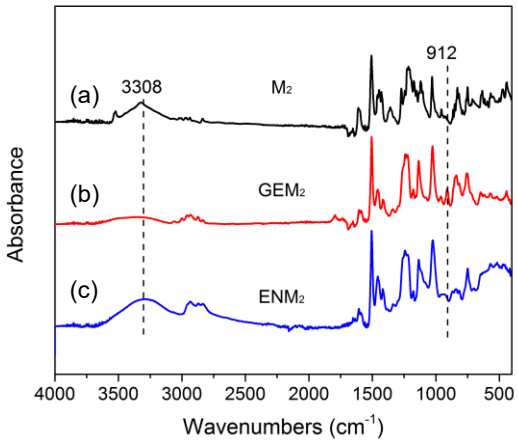

Figure S5.21. FTIR spectra of M_2, GEM_2 and ENM_2.

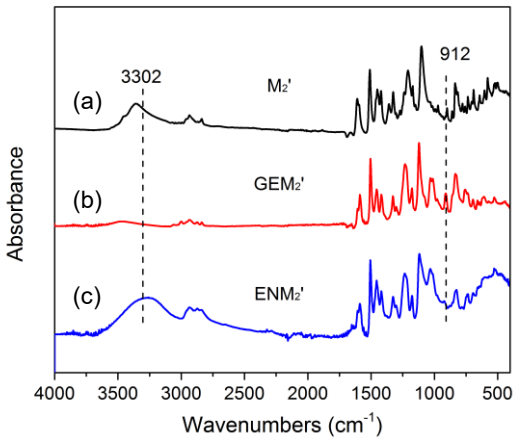

Figure S5.22. FTIR spectra of M_2', GEM_2' and ENM_2'.

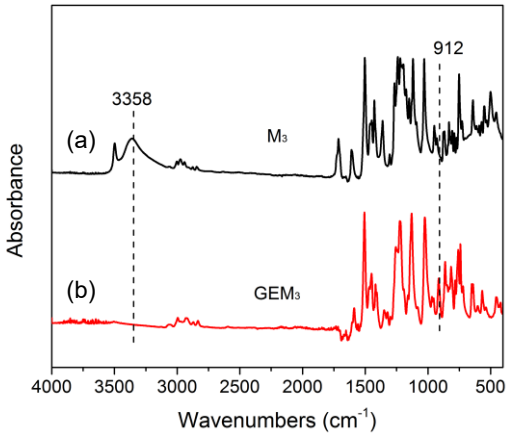

Figure S5.23. FTIR spectra of M_3 and GEM_3.

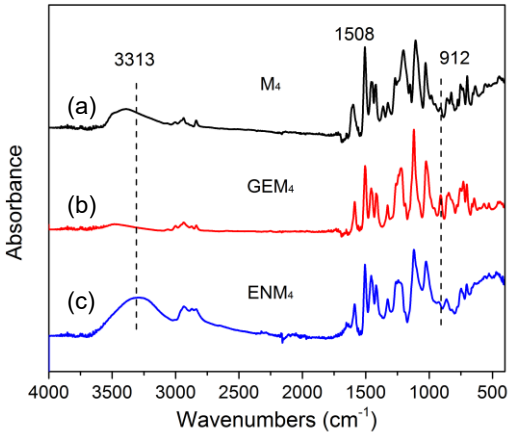

Figure S5.24. FTIR spectra of M_4, GEM_4 and ENM_4.

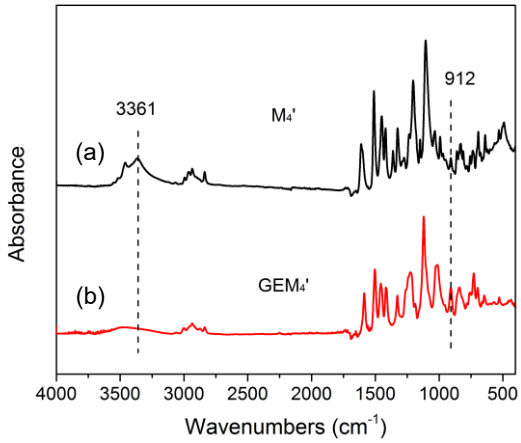

Figure S5.25. FTIR spectra of M_4' and GEM_4'.

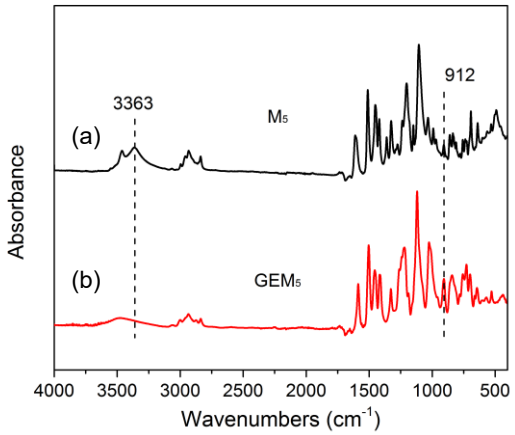

Figure S5.26. FTIR spectra of M_5 and GEM_5.

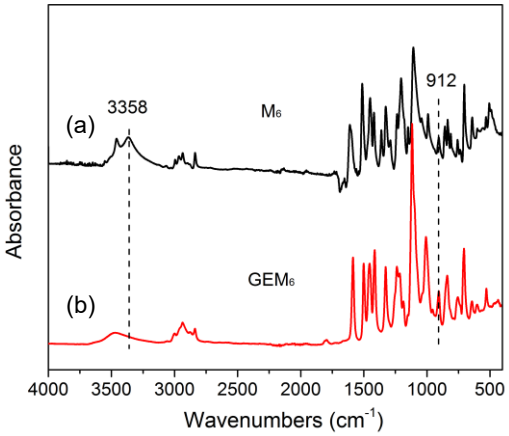

Figure S5.27. FTIR spectra of M_6 and GEM_6.

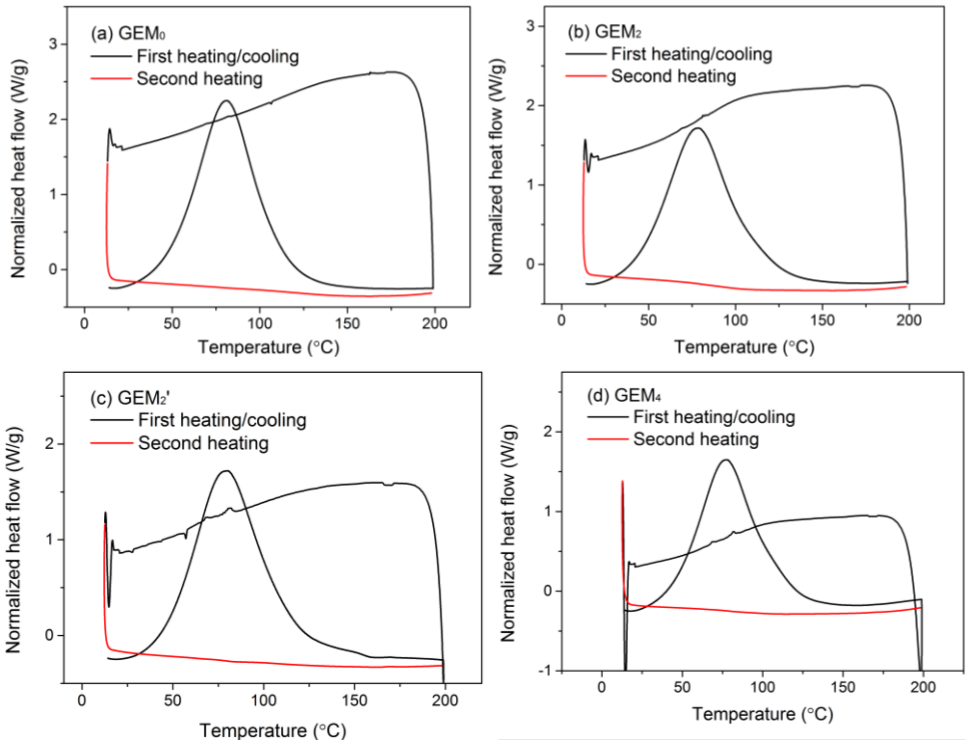

Figure S5.28. Heat release during nonisothermal cures via DSC of epoxy/DETA systems. Degrees of cure were determined through two cycles of heating. Samples were firstly heated from 10 to 200 °C at 10 °C/min, cooled to 10 °C, and reheated to 200 °C at 10 °C/min. All samples were completely cured as supported by the lack of exotherm on the second heating.

Appendix 5 for Chapter 6

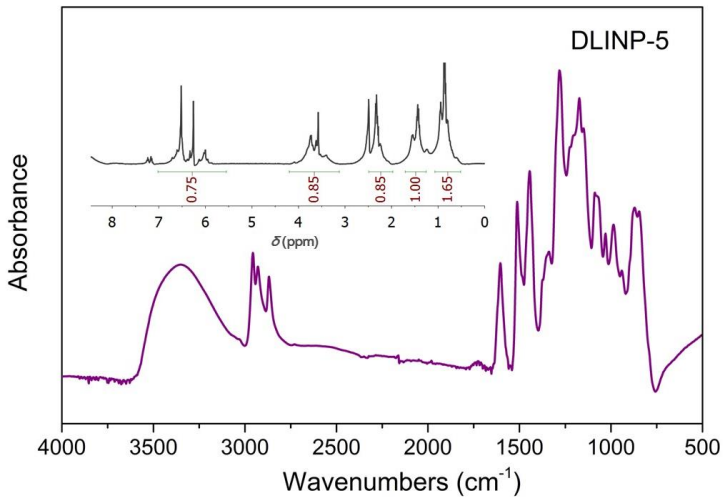

Figure S6.1. ^{1}H NMR and IR spectra of DLINP−5. Solvent: DMSO−d_6.

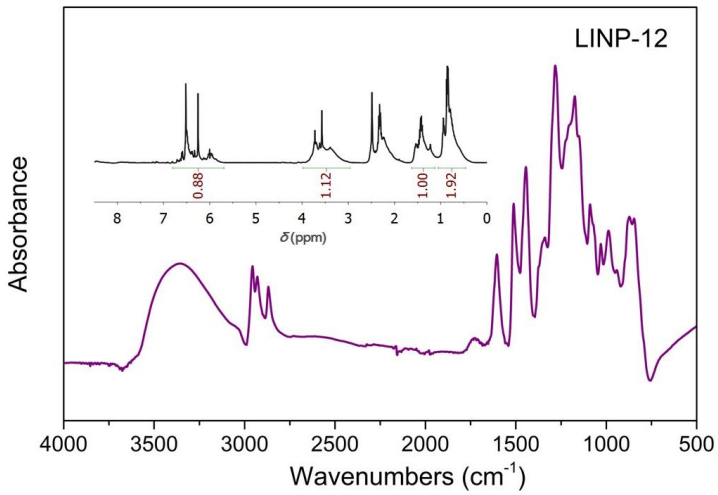

Figure S6.2. ^{1}H NMR and IR spectra of LINP−12. Solvent: DMSO−d_6.

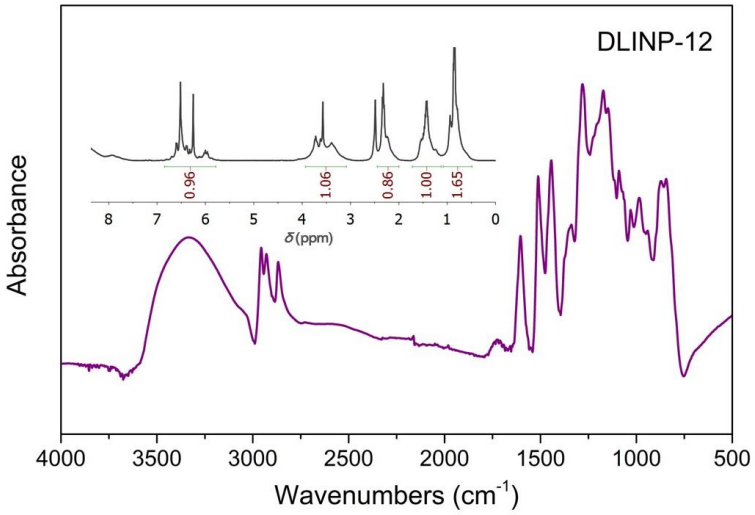

Figure S6.3. ^{1}H NMR and IR spectra of DLINP−12. Solvent: DMSO−d_6.

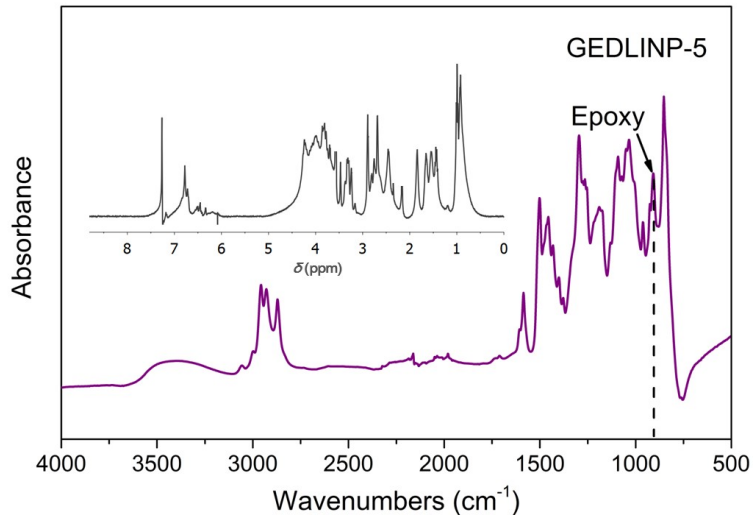

Figure S6.4. ^{1}H NMR and IR spectra of GEDLINP−5. Solvent: DMSO−d_6.

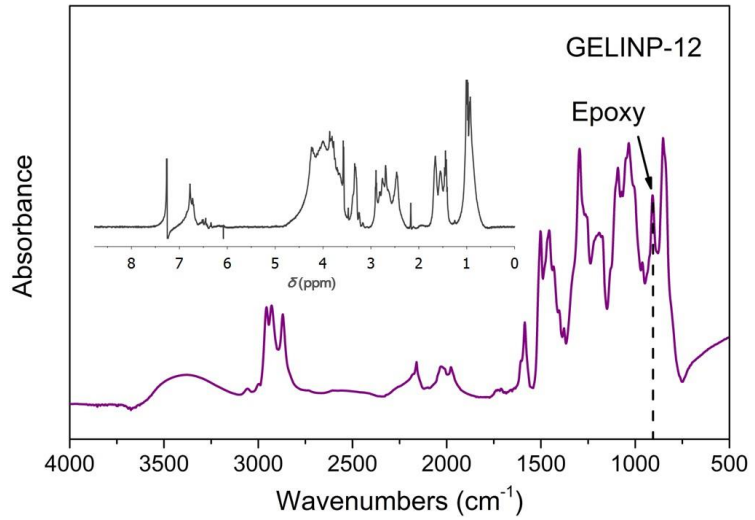

Figure S6.5. ^{1}H NMR and IR spectra of GELINP−12. Solvent: DMSO−d_6.

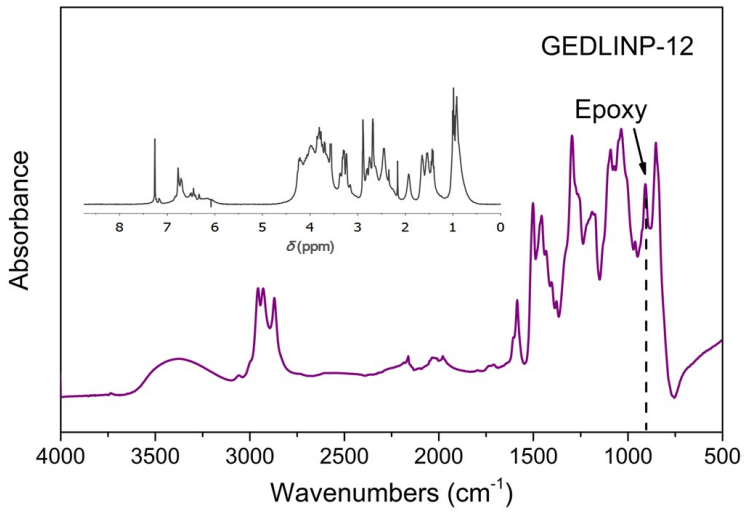

Figure S6.6. ^{1}H NMR and IR spectra of GEDLINP−12. Solvent: DMSO−d_6.

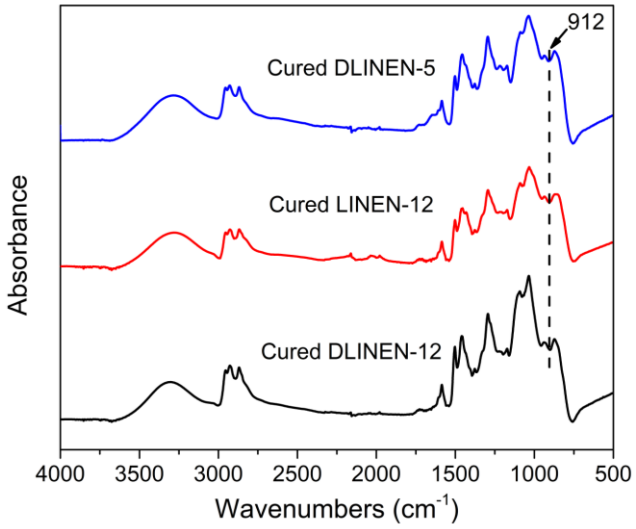

Figure S6.7. IR spectra of cured networks of DLINEN−5, LINEN−12 and DLINEN−12.

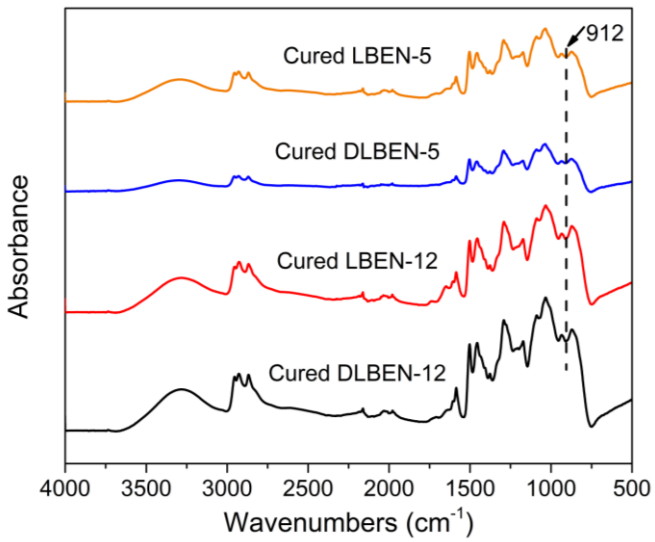

Figure S6.8. FTIR spectra of cured networks of LBEN−5, DLBEN−5, LBEN−12 and DLBEN−12.

Appendix 6 for Chapter 7

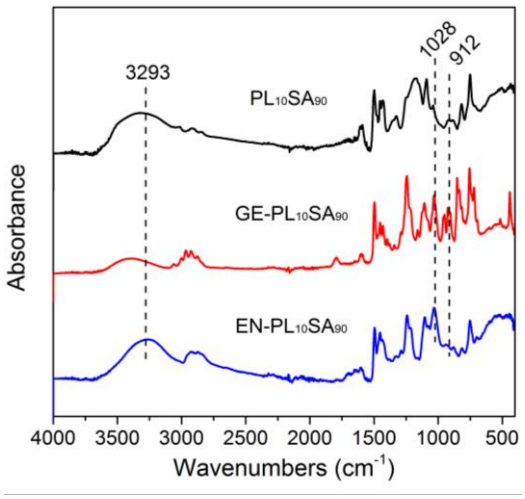

Figure S7.1. FTIR spectra of $PL_{10}SA_{90}$, its glycidyl ethers ($GE{-}PL_{10}SA_{90}$) and cured epoxy networks ($EN{-}PL_{10}SA_{90}$).

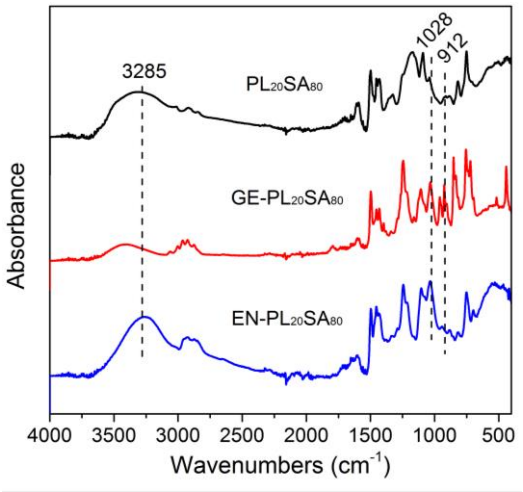

Figure S7.2. FTIR spectra of $PL_{20}SA_{80}$, its glycidyl ethers ($GE{-}PL_{20}SA_{80}$) and cured epoxy networks ($EN{-}PL_{20}SA_{80}$).

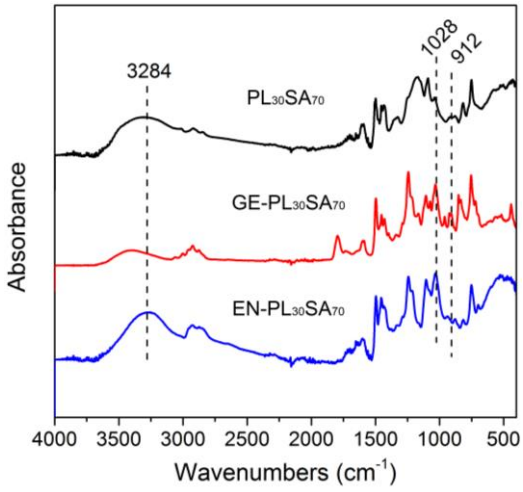

Figure S7.3. FTIR spectra of $PL_{30}SA_{70}$, its glycidyl ethers ($GE{-}PL_{30}SA_{70}$) and cured epoxy networks ($EN{-}PL_{30}SA_{70}$).

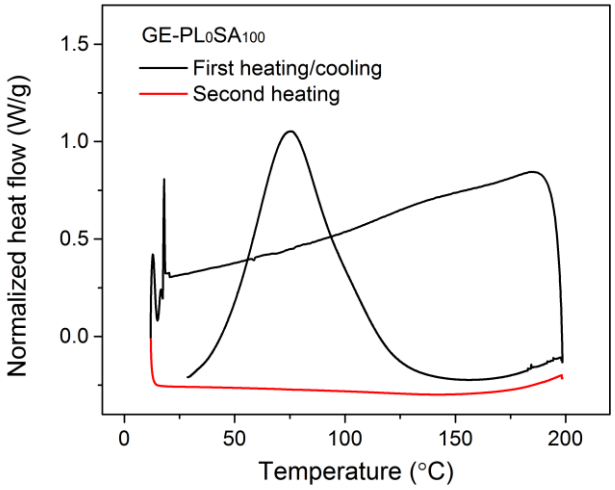

Figure S7.4. Heat release during nonisothermal cures via DSC of $GE{-}PL_0SA_{100}$/DETA systems. Degrees of cure were determined through two cycles of heating. Samples were firstly heated from 10 to 200 °C at 10 °C/min, cooled to 10 °C, and reheated to 200 °C at 10 °C/min. All samples were completely cured as supported by the lack of exotherm on the second heating.

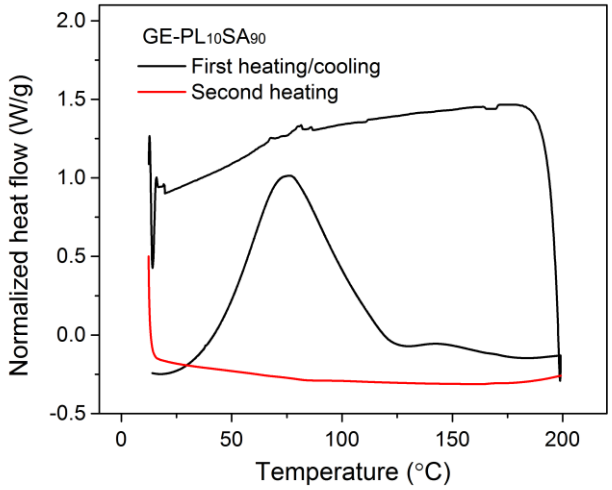

Figure S7.5. Heat release during nonisothermal cures via DSC of GE−$PL_{10}SA_{90}$/DETA systems. Heating and cooling rates are same with Figure S7.4.

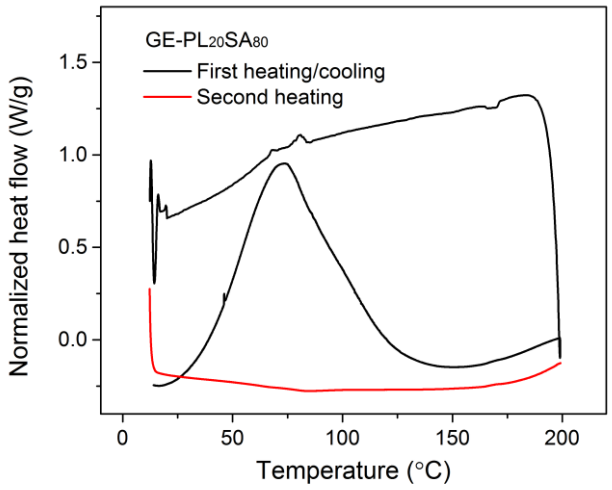

Figure S7.6. Heat release during nonisothermal cures via DSC of GE−$PL_{20}SA_{80}$/DETA systems. Heating and cooling rates are same with Figure S7.4.

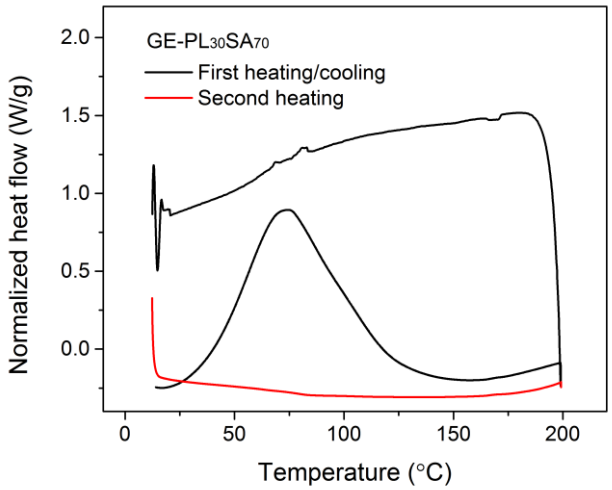

Figure S7.7. Heat release during nonisothermal cures via DSC of GE−$PL_{30}SA_{70}$/DETA systems. Heating and cooling rates are same with Figure S7.4.

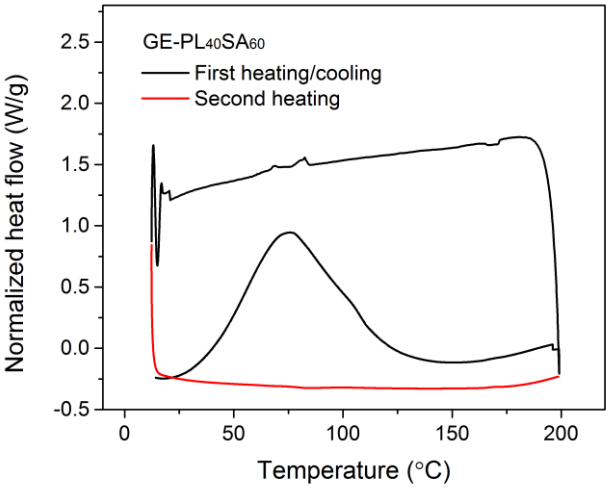

Figure S7.8. Heat release during nonisothermal cures via DSC of GE−$PL_{40}SA_{60}$/DETA systems. Heating and cooling rates are same with Figure S7.4.

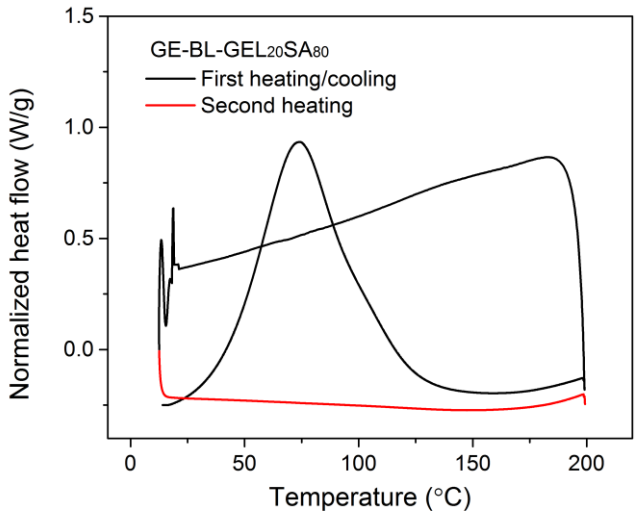

Figure S7.9. Heat release during nonisothermal cures via DSC of GE−BL−$GEL_{20}SA_{80}$/DETA systems. Heating and cooling rates are same with Figure S7.4.

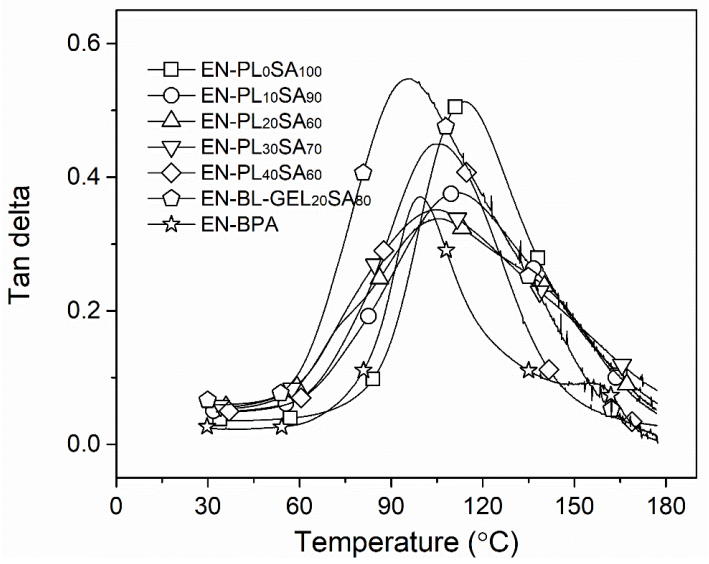

Figure S7.10. DMA tan delta curve of epoxy networks.

Appendix 7 for Chapter 8

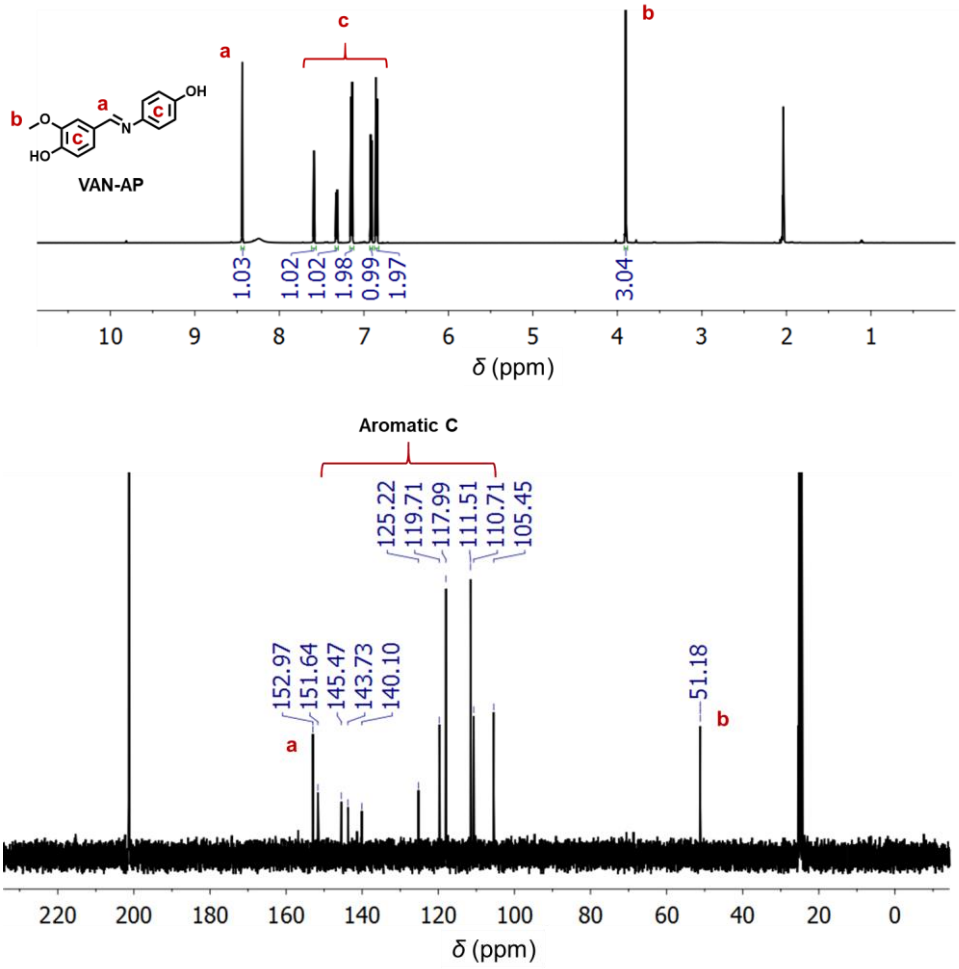

Figure S8.1. (A) Proton and (B) carbon NMR spectra of **VAN−AP**. Solvent: acetone−d_6.

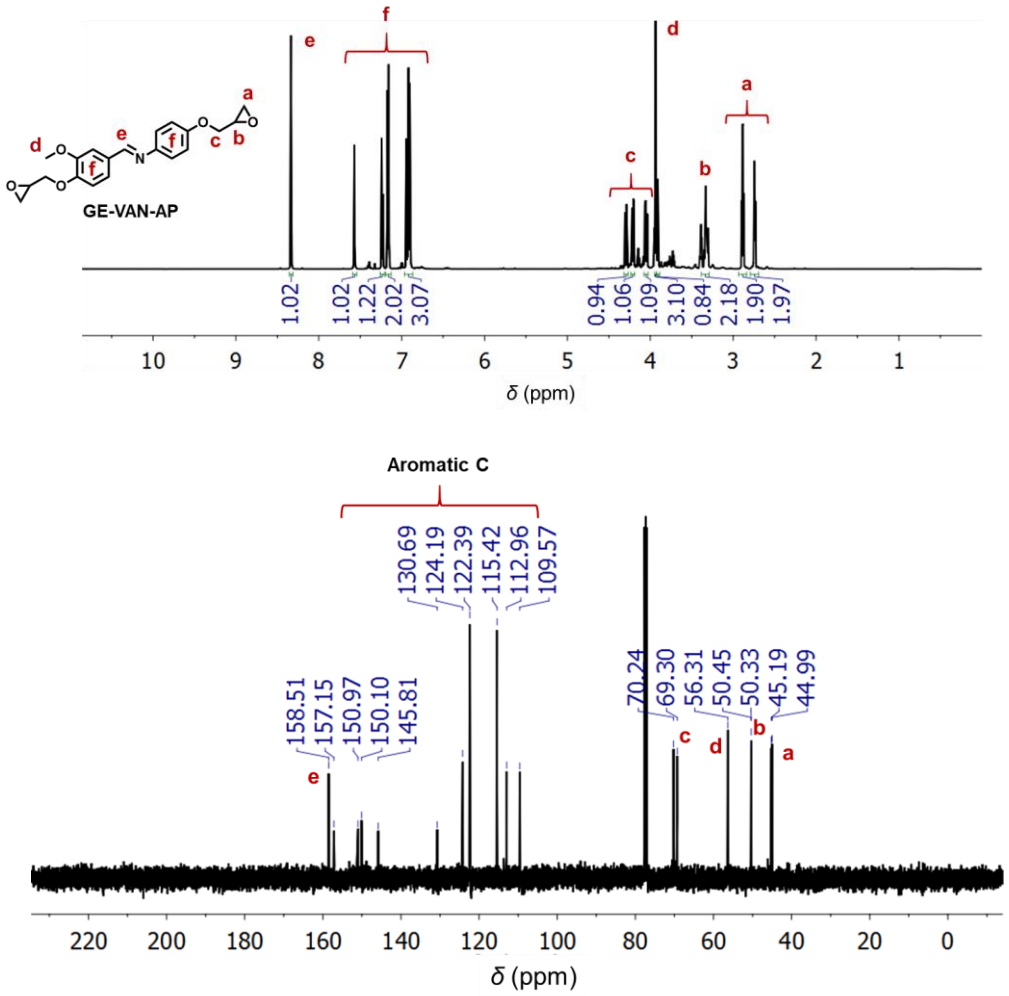

Figure S8.2. (A) Proton and (B) carbon NMR spectra of **GE−VAN−AP**. Solvent: $CDCl_3$.

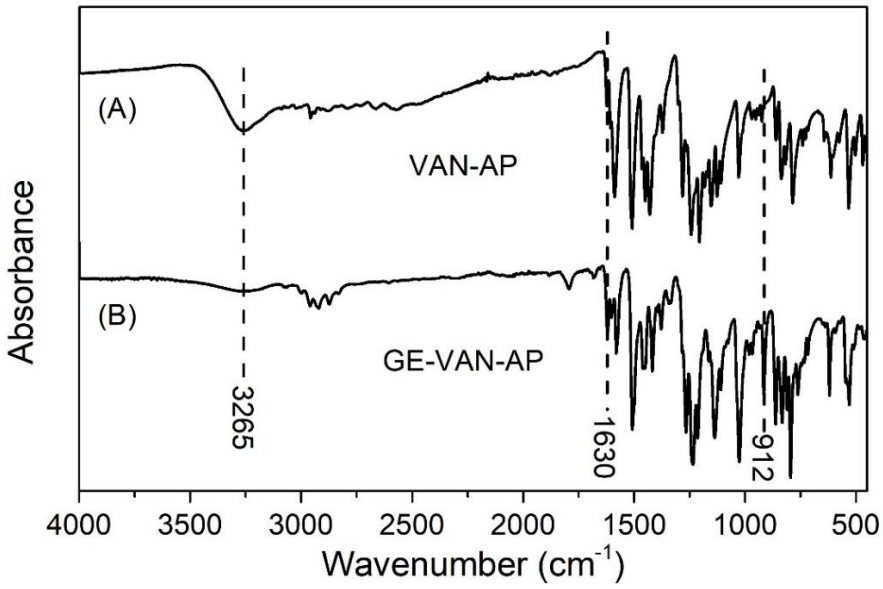

Figure S8.3. IR spectra of (A) **VAN−AP** and (B) **GE−VAN−AP**.

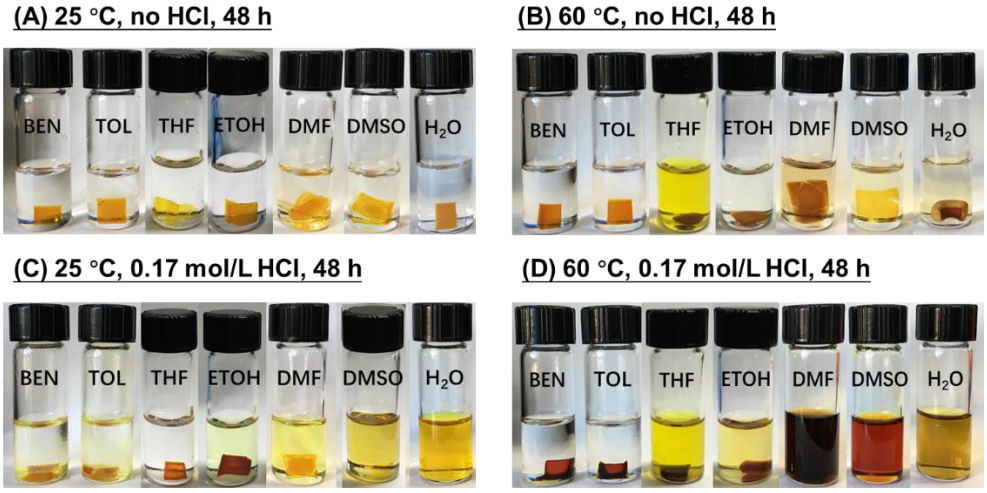

Figure S8.4. Degradation of **EN−VAN−AP** in different solvents.

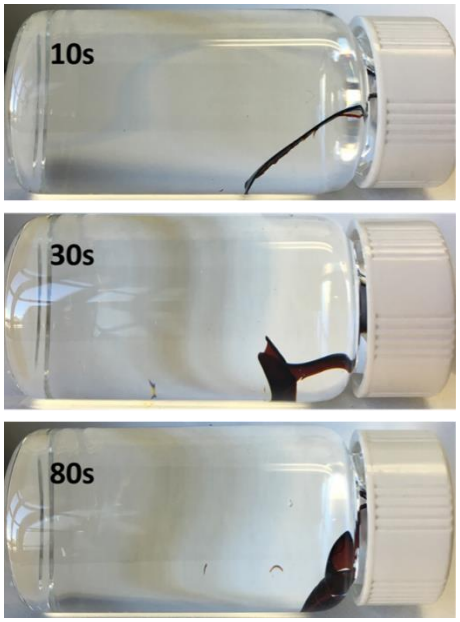

Figure S8.5. **EN−VAN−AP** recycled from water solution exhibited poor water resistance. Recycled thermoset deformed rapidly in water under room temperature.

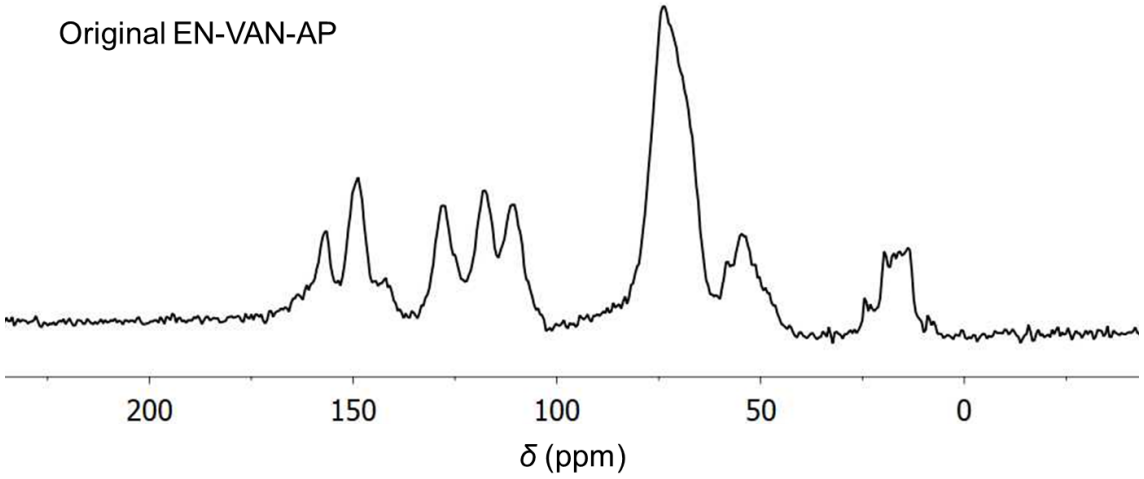

Figure S8.6. Solid−state carbon NMR spectrum of original **EN−VAN−AP**.

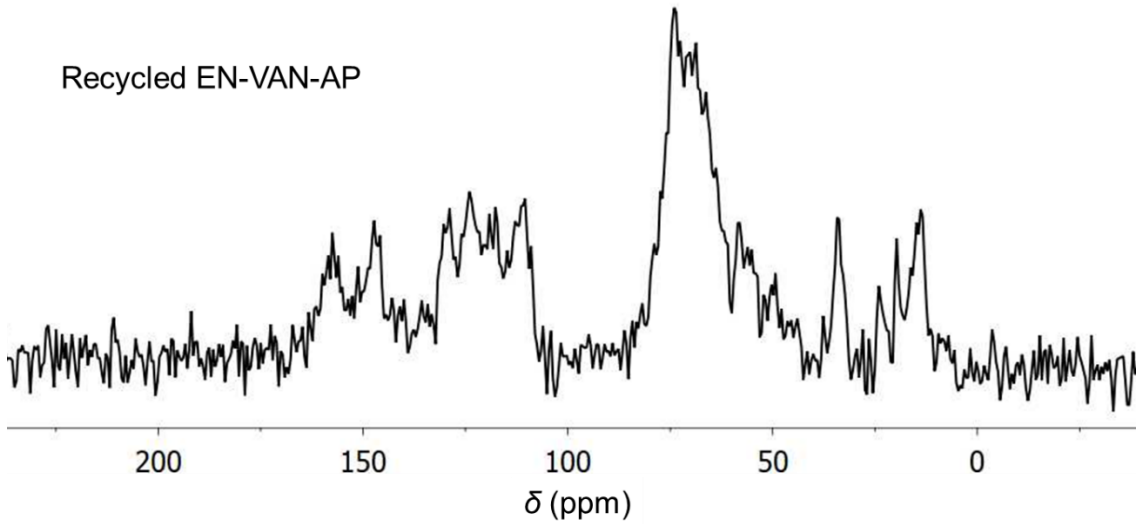

Figure S8.7. Solid−state carbon NMR spectrum of recycled **EN−VAN−AP**.

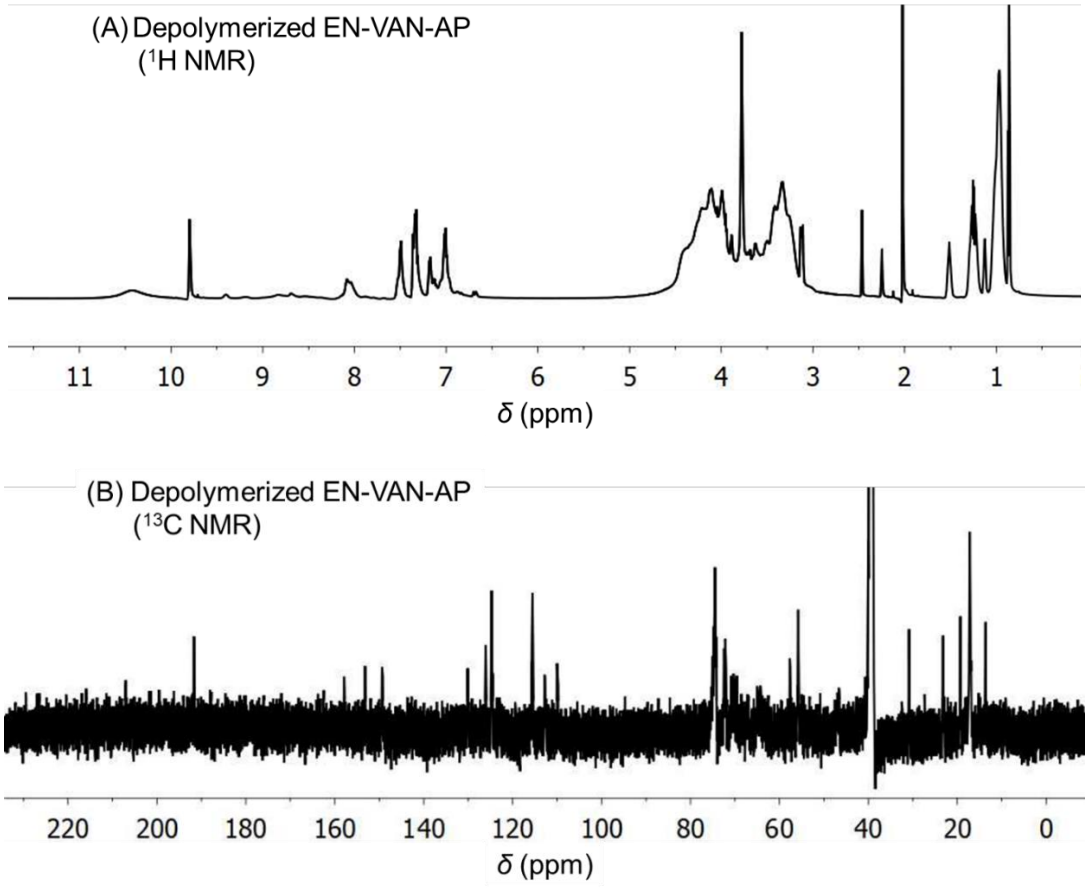

Figure S8.8. Proton and carbon NMR spectra of depolymerized **EN−VAN−AP** (solvent: DSMO−d_6). To collect the NMR spectra, 0.2 g of **EN−VAN−AP** was depolymerized in 2 mL of DMSO−d_6 with the aid of HCl acid (0.25 mol/L in solution). Aldehyde group was observed at 9.8 ppm for proton NMR and 192 ppm for carbon NMR. The presence of free aldehyde groups indicated the depolymerization of **EN−VAN−AP** was realized by acid−catalyzed breakage of the imine bonds.

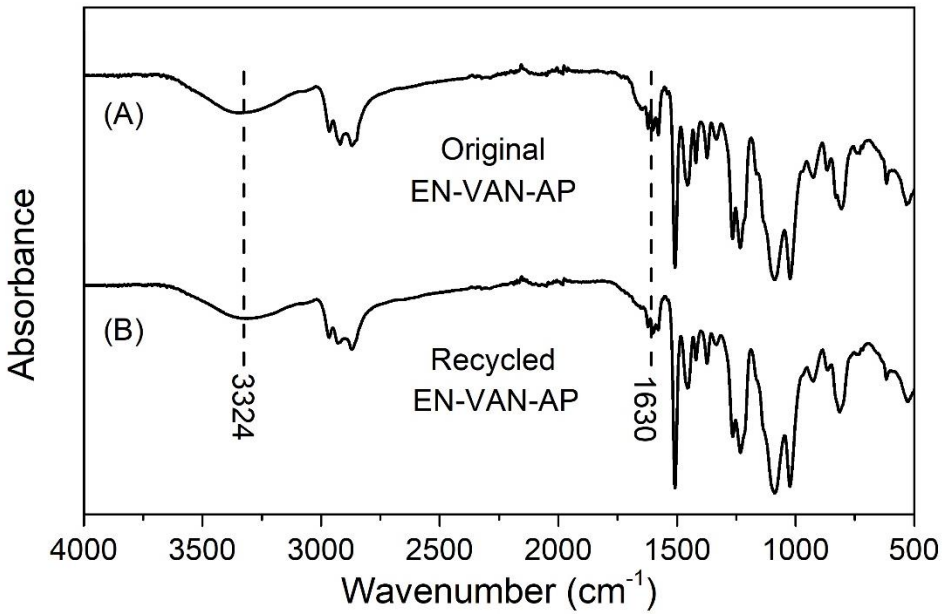

Figure S8.9. IR spectra of (A) original and (B) recycled **EN−VAN−AP**.

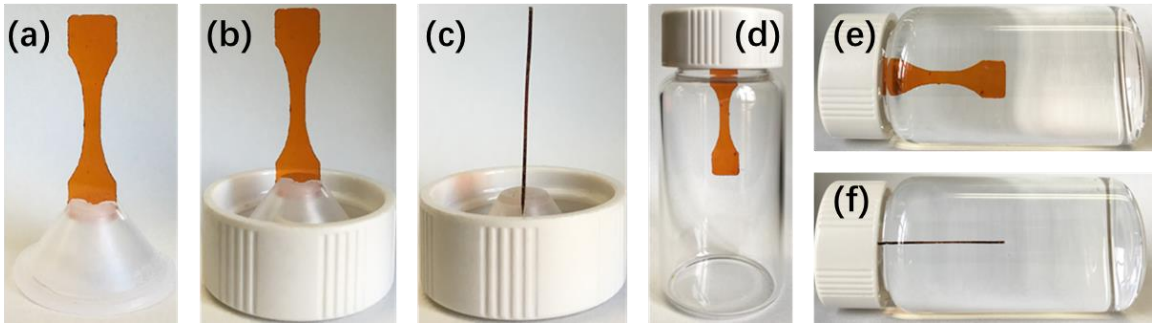

Figure S8.10. Experimental setup for testing water resistance of thermosets. (a) The light plastic part in the cap of a 20 mL vial was cut by a razor at the tip. The thermoset sample was inserted and fixed through the notch. (b) The light plastic part was put back in the cap. (c) Side view of (b). (d) The cap could be screwed up, while thermoset sample was still attached. (e) The vial was filled with water. (f) The water−filled vial was turned to a position where the attached thermoset lied horizontally. The position of the vial was fixed and time for thermoset to obtain certain deformation was recorded. All samples were cut into same shape with same thickness. Samples were dried at 120 °C for 24 h before immersing into water.